CONVOLUTION BACKPROJECTION ALGORITHM IN COMPUTERIZED TOMOGRAPHY: STATISTICAL ERROR ESTIMATES AND OPTIMAL FILTER

A Thesis Submitted
in Partial Fulfilment of the Requirements
for the Degree of

DOCTOR OF PHILOSOPHY

by

TANUJA SRIVASTAVA

to the

DEPARTMENT OF MATHEMATICS

INDIAN INSTITUTE OF TECHNOLOGY KANPUR

JULY 1989

Dedicated to

Dr. R.K.S. Rathore

and

Karishal

CERTIFICATE

This is to certify that the matter embodied in the thesis entitled "CONVOLUTION BACKPROJECTION ALGORITHM IN COMPUTERIZED TOMOGRAPHY: STATISTICAL ERROR ESTIMATES AND OPTIMAL FILTER" submitted by Tanuja Srivastava for the award of the degree of Doctor of Philosophy to the Department of Mathematics, I.I.T. Kanpur, is a record of bonafide research work carried out by her under my supervision. The thesis has, in my opinion, reached the standard fulfilling the requirements for the Ph.D. degree. The results embodied in this thesis have not been submitted elsewhere for the award of any degree or diploma.

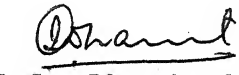

(I.D. Dhariyal)
Assistant Professor
Department of Mathematics
Indian Institute of Technology
Kanpur

July, 1989

ACKNOWLEDGEMENTS

I would like to express my deep gratitude to my supervisor Dr. I.D. Dhariyal for his advice, encouragement and guidence throughout the course of this research. I am also indebted to Dr. R.K.S. Rathore from whom I have learned a great deal and who constantly inspired and encouraged me.

I owe a special debt of gratitude to Dr. P. Munshi, Mrs. Neera Dhariyal, and Mrs. Sandhya Rathore for their unfailing kindness and their help during the hours of need. I also wish to express thanks to Upasana, Divya and Satya for cheerful moments.

I must also mention gratefully the co-operation, suggestions and encouragement rendered by Kaushal.

I am also thankful to my freinds Neeraj, Shubha, Vellaisamy, Sangeeta Munshi, Deomurari and Somesh for their constant support.

Finally, to my Mother-in-law and Parents....

Tanuja Srivastava

CONTENTS

LIST OF TABLES

hence

$$C_{\mathcal{Z}_{A,r,\bar{\phi}}}(\underline{y}) = \frac{1}{2\pi}\int_0^{2\pi} C_{\mathcal{Z}_A}(y_1 + r\cos\phi,\ y_2 + r\sin\phi)\, d\phi$$

$$= \frac{1}{2\pi}\int_0^{2\pi}\int\int\int_{\mathbb{R}^2\mathbb{R}^2} C_{\mathcal{Z}}(\underline{w})\, K_A(\underline{w} + \underline{u}).$$

$$K_A(y_1 - u_1 + r\cos\phi,\ y_2 - u_2 + r\sin\phi).$$

$$d\underline{w}\, d\underline{u}\, d\phi\ .$$

$K(\underline{x}) \in L^1[0, \infty)$ implies the applicability of Fubini's theorem. Thus we have

$$C_{\mathcal{Z}_{A,r,\bar{\phi}}}(\underline{y}) = \int\int_{\mathbb{R}^2\ \mathbb{R}^2} C_{\mathcal{Z}}(\underline{w})\, K_A(\underline{w} + \underline{u})\, A^2.$$

$$K_{Ar,\bar{\phi}}(A(\underline{y} - \underline{u}))\, d\underline{w}\, d\underline{u}$$

and

$$D^{4p}_{r,\bar{\phi}}\, C_{\mathcal{Z}}(\underline{y}) = \frac{\partial^{4p}}{\partial r^{4p}}\int\int_{\mathbb{R}^2\ \mathbb{R}^2} C_{\mathcal{Z}}(\underline{w})\, K_A(\underline{w} + \underline{u})\, A^2.$$

$$K_{Ar,\bar{\phi}}(A(\underline{y} - \underline{u}))\, d\underline{w}\, d\underline{u}$$

$$= \int\int_{\mathbb{R}^2\ \mathbb{R}^2} C_{\mathcal{Z}}(\underline{w})\, K_A(\underline{w} + \underline{u})\, A^2.$$

$$\frac{\partial^{4p}}{\partial r^{4p}}(K_{Ar,\bar{\phi}}(A(\underline{y} - \underline{u})))\, d\underline{w}\, d\underline{u}$$

LIST OF FIGURES

$$= A^{4p} \| C_{\mathcal{Z}} \|_0 M_4, \quad \text{(say).} \qquad (M_4 = M_3(M_3 + L))$$

Hence

$$\| C_{\mathcal{Z}_A} \|_{4p} \leq M_4 A^{4p} \| C_{\mathcal{Z}} \|_0 .$$

LEMMA 4.2.6

Let $\mathcal{Z} \in \mathcal{S}_{4p}$, $K(\underline{x}) \in L^1[0, \infty)$, then

$$\| C_{\mathcal{Z}_A} \|_{4p} \leq M_3 \| C_{\mathcal{Z}} \|_{4p} ,$$

where M_3 is same as in Lemma 4.2.2.

PROOF:—

$$C_{\mathcal{Z}_A}(\underline{y}) = E\left(Z_A(\underline{x}) Z_A(\underline{x} + \underline{y}) \right)$$

$$= E \int_{\mathbb{R}^2} \int_{\mathbb{R}^2} Z(\underline{x} - \underline{u}/A) Z(\underline{x} + \underline{y} - \underline{v}/A) K(\underline{u}) K(\underline{v}) \, d\underline{u} \, d\underline{v}$$

$$= \int_{\mathbb{R}^2} \int_{\mathbb{R}^2} C_{\mathcal{Z}}\left(\underline{y} + (\underline{u} - \underline{v})/A \right) K(\underline{u}) K(\underline{v}) \, d\underline{u} \, d\underline{v} .$$

Hence

$$C_{\mathcal{Z}_A, r, \bar{\phi}}(\underline{y}) = \frac{1}{2\pi} \int_0^{2\pi} C_{\mathcal{Z}_A}(y_1 + r\cos\phi, y_2 + r\sin\phi) \, d\phi$$

$$\leq \frac{1}{2}\left[A^{4p} M_3^2 \| C_{(Z - \mathcal{Z}_B)} \|_0 + M_3 L \| C_{\mathcal{Z}_B} \|_{4p} \right] .$$

.....(4.3.4)

Hence by (4.3.3) and (4.3.4)

$$| D^{4p}_{r,\bar{\phi}} C_{\mathcal{Z}_A}(\underline{y}) |$$

$$\leq | D^{4p}_{r,\bar{\phi}} C_{(\mathcal{Z} - \mathcal{Z}_B)_A}(\underline{y}) | + | D^{4p}_{r,\bar{\phi}} C_{(\mathcal{Z}_B)_A}(\underline{y}) |$$

$$+ | D^{4p}_{r,\bar{\phi}} \frac{1}{2\pi} \int_0^{2\pi} E\,(Z - Z_B)_A\,(\underline{x})\,(Z_B)_{A,r,\phi}\,(\underline{x} + \underline{y})\,d\phi |$$

$$+ | D^{4p}_{r,\bar{\phi}} \frac{1}{2\pi} \int_0^{2\pi} E\,(Z_B)_A\,(\underline{x})\,(Z - Z_B)_{A,r,\phi}\,(\underline{x} + \underline{y})\,d\phi |$$

$$\leq \| D^{4p}_{r,\bar{\phi}} C_{(\mathcal{Z} - \mathcal{Z}_B)_A} \|_0 + \| D^{4p}_{r,\bar{\phi}} C_{(\mathcal{Z}_B)_A} \|_0$$

$$+ M_3^2 A^{4p} \| C_{(\mathcal{Z} - \mathcal{Z}_B)} \|_0 + M_3 L \| C_{\mathcal{Z}_B} \|_{4p} .$$

This implies that,

$$\| D^{4p}_{r,\bar{\phi}} C_{\mathcal{Z}_A} \|_0$$

$$\leq \| D^{4p}_{r,\bar{\phi}} C_{(\mathcal{Z} - \mathcal{Z}_B)_A} \|_0 + \| D^{4p}_{r,\bar{\phi}} C_{(\mathcal{Z}_B)_A} \|_0$$

5.3 ESTIMATION OF REGRESSION CO-EFFICIENTS

Consider forty two distances starting from 0 to $8\sqrt{2}$ pixel length corresponding to the distances between the centres of two pixels in an image. For each of the 70 simulated images in sample 1, the covariance kernel was estimated at the 42 distances by taking appropriate average of the products of the object function values, thus obtaining 70 values for 42x1 vector of covariances.

Using the simulated projection data for 100 views and 64 rays, reconstruction of these 70 images were done by CBP algorithm with the 'Sinc' window given by

$$W(R) = \begin{cases} \dfrac{\sin(\pi R/2R_c)}{(\pi R/2R_c)} & |R| \leq R_c \\ 0\,, & |R| > R_c \end{cases}$$

We used $R_c = 16$, which gives the convolving co-efficients as

$$q(s_k) = \frac{2}{\pi}\,\frac{1}{1-4k^2}, \qquad k = 1,\ldots,64.$$

Finally the ESE was calculated as

$$e = \frac{1}{MP}\sum_i \sum_j \left(\tilde{z}(x_{ij}) - z(x_{ij})\right)^2$$

where $z(x_{ij})$ (respectively $\tilde{z}(x_{ij})$) denotes the simulated

Tables 5.4 - 5.11 give these errors for samples 2-9 respectively, while Tables 5.12- 5.19 give the normalized errors in the same order. These tables show that ESE is reduced when either R_c is increased or when the covariance kernel becomes smoother. The rate of decrease in error with R_c is faster for images having smoother covariance kernels than for those having compardtively less smooth covariance kernels. Fig.5.1 and 5.2 shows the actual simulated images of different samples and Fig.5.3 to Fig.5.8 shows the corresponding reconstruction with R_c equal to 16,32, and 64.

CHAPTER 1

INTRODUCTION, NOTATION AND LITERATURE

1.1 INTRODUCTION AND OUTLINE

Computerized Tomography (CT) is a technique of reconstructing a function (representing the cross-section of an object) from its line or plane integrals called projections. This technique has been successfully applied in the fields of medical imaging, nuclear engineering, radio astronomy, electron microscopy, X-ray crystallography and geophysics etc. Continuing research for developing more efficient algorithms to improve the quality of reconstructed images calls for a theoretical analysis of various errors in the process.

A large number of algorithms for CT reconstructions have been developed, one of them being the Convolution Backprojection (CBP). The CBP algorithm is probably the most widely used of all methods, as it is fast, efficient, reasonably accurate, and easy to implement on computer.

Non-statistical aspects of the analysis of error in CBP have been extensively studied by Natterer (1980,1986) and Munshi(1988). This dissertation continues this study further

TABLE 5.11 (Contd....)

PIC	R_c	ER1	ERS	ERMax	$\tilde{E}$
6	16	0.90792	2.10333	9.50445	2.18561
	32	0.38250	0.26267	5.31303	0.39268
	64	0.22571	0.06583	1.38080	0.07544
7	16	0.91043	2.06865	9.26359	2.16035
	32	0.37887	0.25974	4.90167	0.39173
	64	0.21988	0.06311	1.36921	0.06629
8	16	0.90836	2.09990	9.12071	2.18624
	32	0.38016	0.25937	4.75157	0.40057
	64	0.21837	0.06216	1.34444	0.07165

by developing some statistical error estimates for the CBP method.

In order to make the presentation as self contained as possible a review of the relevent literature is done in this chapter (section 1.4). In section 1.2 we introduce preliminary definitions and notation. The CBP algorithm is explained in section 1.3.

In chapter 2, the problem is formally stated and various assumptions made to develop the theory are given. Various classes of spatial stochastic processes are defined, which play important role in the analysis of expected squared error (ESE).

In chapter 3, a modulus of continuity of the covariance kernel is defined and an estimate of ESE is given in its terms. An asymptotic formula giving the order of the ESE as a function of cut-off frequency is also developed for those spatial processes, for which the covariance kernel is very smooth in the neighbourhood of the origin. In section 3.5 we give an estimate of the ESE for the class of spatial processes which have very smooth covariance kernels.

The main theorem of the thesis is proved in chapter 4, where it is shown that the spatial processes (cross-sections) can be characterized by the order of the expected squared error in reconstruction by CBP when the convolving functions belong to a certain class.

TABLE 5.19 (Contd....)

PIC	R_c	ER1N	ERSN	$\tilde{E}N$
6	16	0.05889	0.09315	0.14176
	32	0.02481	0.03743	0.02547
	64	0.01464	0.01874	0.00489
7	16	0.05921	0.09266	0.14050
	32	0.02464	0.03733	0.02548
	64	0.01430	0.01840	0.00431
8	16	0.06019	0.09521	0.14487
	32	0.02519	0.03805	0.02654
	64	0.01447	0.01863	0.00475

Chapter 5, summarizes the numerical results of reconstructions performed using a discrete implementation of the CBP algorithm. A linear relationship has been established between the error in reconstruction by CBP and the covariance kernel of the process, where the covariance kernel is estimated by sample observations (images). The test cases have been simulated as random images from certain classes of spatial stochastic processes on computer.

Chapter 6, deals with a related problem of obtaining statistically optimal convolving functions in discrete implementation of CBP. A method for derivation of a convolving function is given which optimally takes care of (i) the process giving rise to the object image to be reconstructed, (ii) the data collection geometry, (iii) the cross-sectional discretization scheme, and (iv) the projection data noise, while at the same time it minimizes the ESE in reconstruction.

1.2 DEFINITIONS AND NOTATION

We will denote by $\mathbb{R}^n$, the n-dimensional Euclidean space. We will restrict ourselves here to the case n=2. $\mathbb{R}^+$ denotes the positive half of the real line $\mathbb{R}$, i.e., $\mathbb{R}^+ = \{ x \in \mathbb{R} : x \geq 0 \}$ The set of directions in $\mathbb{R}^n$ is the set of unit vectors in $\mathbb{R}^n$, they form the set $S^{n-1} = \{ \underline{x} \in \mathbb{R}^n : \|\underline{x}\| = 1 \}$, where $\|\underline{x}\|$ is the

If $\mathbf{Q}$ is non-singular, it follows that

$$\mathbf{q}_n = \mathbf{Q}_n^{-1}\mathbf{R}_n \longrightarrow \mathbf{q}_{opt}, \quad \text{w.p.1} \quad \text{as} \quad n \longrightarrow \infty$$

and thus $\mathbf{q}_n$ provides a strongly consistent estimator of $\mathbf{q}_{opt}$. If $\mathbf{Q}$ is not known to be non-singular, any of the following two methods may be used to estimate $\mathbf{q}_{opt}$ from this data:

(I) TRUNCATED S.V.D. APPLICATION PROCEDURE: Let the rank of matrix $\mathbf{Q}$ be r ($\leq$ K). Consider the singular value decomposition (S.V.D.)

$$\mathbf{Q}_n = \mathbf{U}_n \begin{bmatrix} \lambda_1^{(n)} & & & \\ & \lambda_2^{(n)} & & \\ & & & \\ & & & \lambda_K^{(n)} \end{bmatrix} \mathbf{V}_n^*,$$

where $\lambda_1^{(n)} \geq \ldots \geq \lambda_K^{(n)}$ are singular values of $\mathbf{Q}_n$ and $\mathbf{U}_n$, and $\mathbf{V}_n$ are the unitary matrices

Let

$$\tilde{\mathbf{Q}}_n = \mathbf{V}_n \left[\begin{array}{ccc:c} \frac{1}{\lambda_1^{(n)}} & & & 0 \\ & & & \\ & & \frac{1}{\lambda_r^{(n)}} & \\ \hdashline 0 & & & 0 \end{array}\right] \mathbf{U}_n^*$$

Euclidean length of the vector $\underline{x} \in \mathbb{R}^n$.

Let $\mathcal{Z} = \{ Z(\underline{u}) ; \underline{u} \in \mathbb{R}^2 \}$ be a spatial stochastic process. In our case a realization $z(\underline{u})$ of $Z(\underline{u})$, $\underline{u} \in \mathbb{R}^2$, corresponds to an observed image (cross-section). Thus, $\mathcal{Z}$ denotes an ensemble of all images belonging to a class, z is a real valued function on $\mathbb{R}^2$ representing the sought-after density distribution or object function. In section 1.3 and 1.4 we shall use the notation f in place of z to denote the object function. We will restrict z to take nonzero values only inside a unit ball in $\mathbb{R}^n$ (or $\mathbb{R}^2$) centred at origin and the support of z (or f) will be denoted by Ω.

Parallel Beam Geometry [Fig.1.1]: A line in $\mathbb{R}^2$ can be specified by two parameters; its (signed) distance s from the origin and the angle θ it makes with the y axis. We denote by $p(s,\theta)$ that function of two variables whose value for any (s,θ) is defined as the line integral of z along the line (s,θ), i.e.

$$p(s,\theta) = \int_{-T}^{T} z(s\cos\theta - t\sin\theta,\ s\sin\theta + t\cos\theta)\, dt$$

where the limits of integration depend, in general, on s,θ and Ω. For any s and θ, (s,θ) and $(-s,\theta+\pi)$ represent the same line in $\mathbb{R}^2$, so that $p(s,\theta) = p(-s, \theta+\pi)$.

The collection of values of $p(s,\theta)$ for various s and θ

TABLE 6.4: L_2 ERROR IN PETCATSTRIP INTEGRAL(NOISE-FREE) CASE

PIC/FILTER	OPT	RAM	RKS	SHE	CSI
LIN	3.715	4.006	3.909	4.064	4.277
FAC	3.630	4.455	4.325	4.499	4.760
BRA	4.964	5.052	4.946	5.088	5.248
STA	3.446	3.590	3.506	3.626	3.759
COR	14.886	14.955	14.909	15.000	15.046
SAT	4.295	5.401	5.200	5.501	5.828
THO	4.272	4.564	4.451	4.629	4.857
SMO	0.955	1.026	1.026	1.026	1.055
PLA	3.141	3.282	3.229	3.299	3.440
BOY	3.926	3.867	3.750	3.926	4.140
MON	2.761	3.265	3.177	3.330	3.506
WOR	3.554	3.692	3.649	3.713	3.771
CHA	6.110	6.964	6.777	7.044	7.310
FIN	3.105	3.670	3.589	3.710	3.811
CRO	3.824	4.014	3.928	4.048	4.169
JET	4.385	4.535	4.442	4.573	4.741
GEO	2.812	3.203	3.105	3.276	3.472
AVERAGE	4.340	4.679	4.583	4.727	4.894

is known as projection data and this method of data collection is said to be parallel beam geometry. Clearly, in the parallel beam geometry for data collection we require many source-detector positions, which can be either time consuming or costly.

Fan-Beam Geometry [Fig.1.2]: In this case a single rotating source is sufficient for an outer ring of stationary detectors. The projection data for this case will be denoted by $g(\sigma, \beta)$, where σ is the angle between a data ray and the central ray and β is the source direction.

The Fourier transform (FT) of a function f in $\mathbb{R}^2$ will be denoted by $\hat{f}$. Thus,

$$\hat{f}(X,Y) = \int_{-\infty}^{\infty}\int_{-\infty}^{\infty} e^{-i2\pi(Xx+Yy)} f(x,y)\, dx\, dy$$

in Cartesian co-ordinates and

$$\hat{f}(R\cos\theta, R\sin\theta) = \int_{0}^{\pi}\int_{-\infty}^{\infty} f(r,\phi)\, e^{-i2\pi Rr\cos(\theta-\phi)}\, |r|\, dr\, d\phi$$

in polar co-ordinates. The inverse Fourier transform of a function g will be denoted by $\check{g}$. Thus,

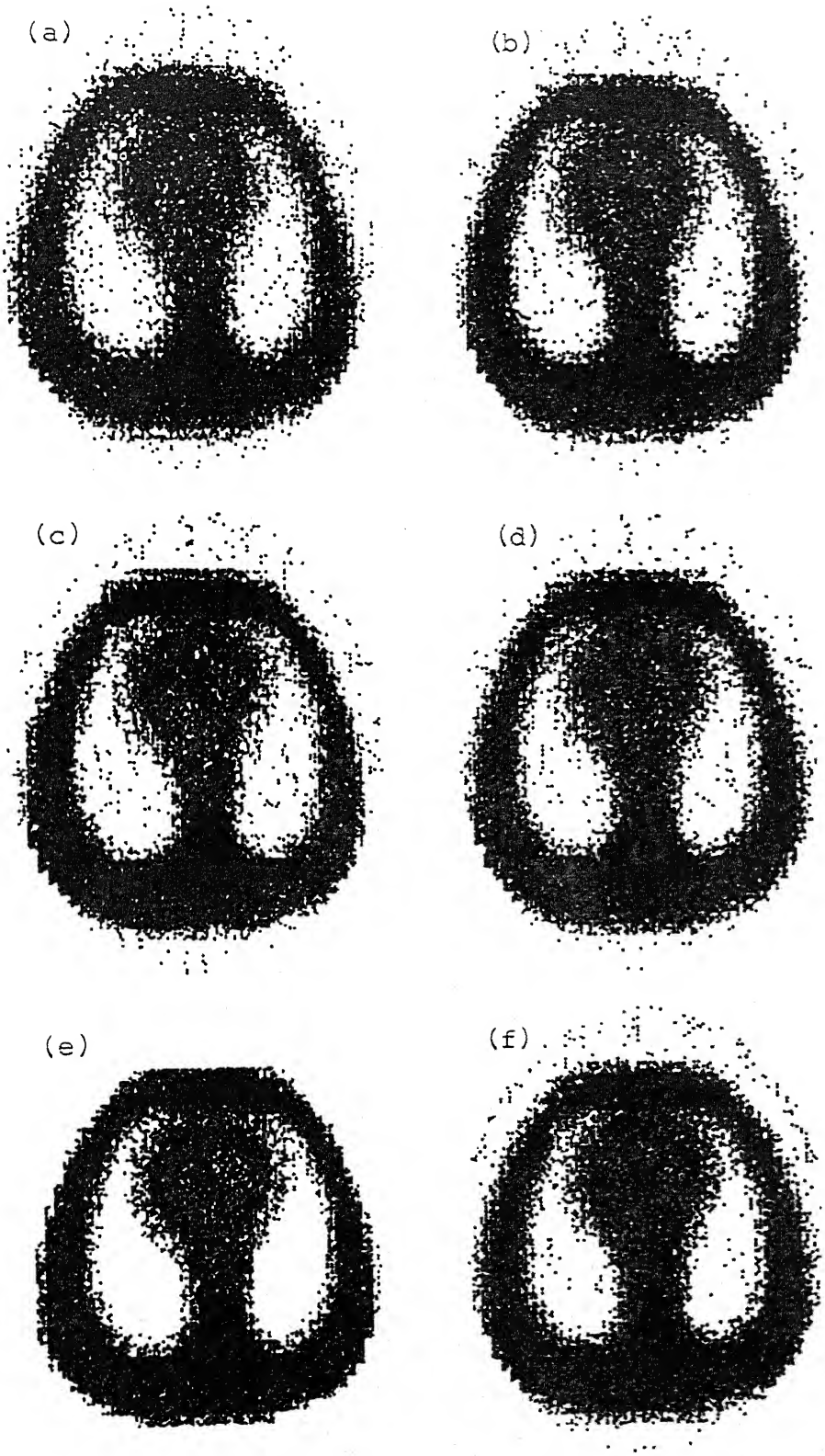

Fig. 6.7 Reconstruction of Thorax in CAT line integral noise-free case (a) CSI filter, (b) RAM filter, (c) RKS filter, (d) Shepp filter, (e) original picture, (f) optimal filter.

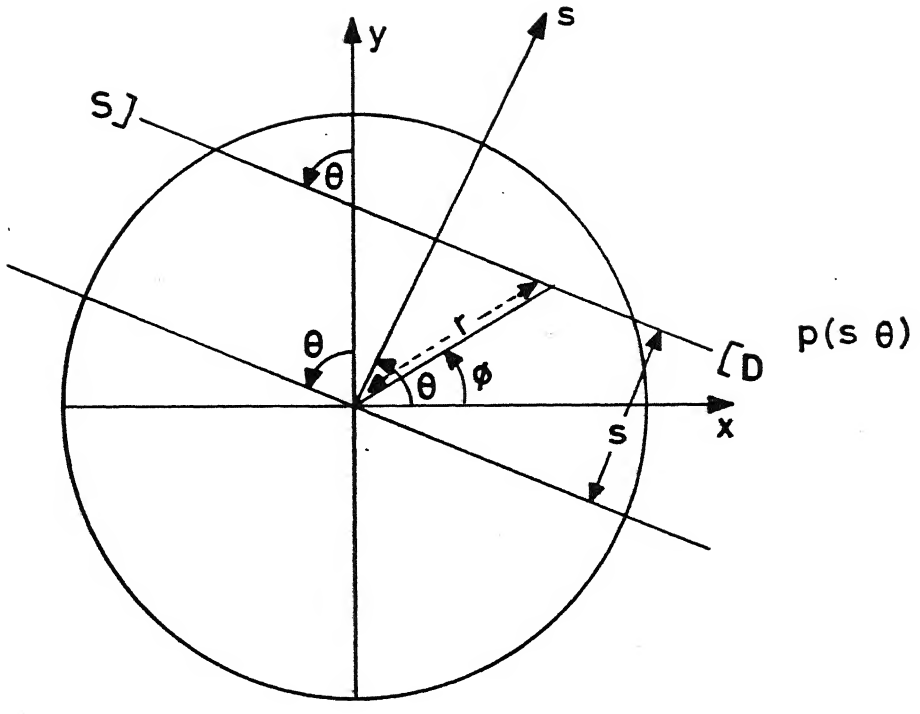

S = Source

D = Detector

Ray ≡ (s,θ)

f = (r,φ)

Fig. 1.1 Parallel beam data collection geometry.

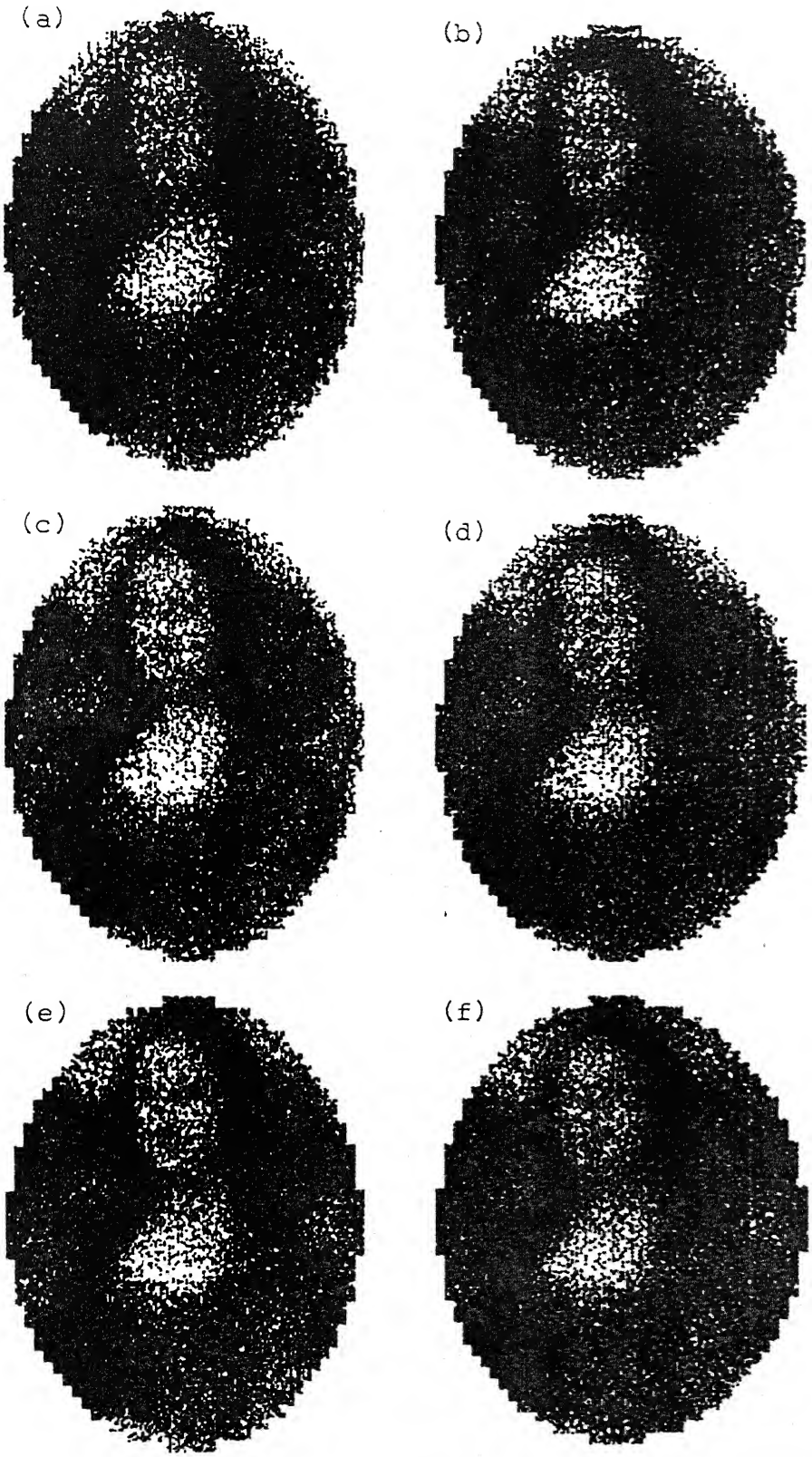

Fig. 6.17 Reconstruction of MonaLisa in CAT strip integral noise-free case (a) CSI filter, (b) RAM filter, (c) RKS filter, (d) Shepp filter, (e) original picture, (f) optimal filter.

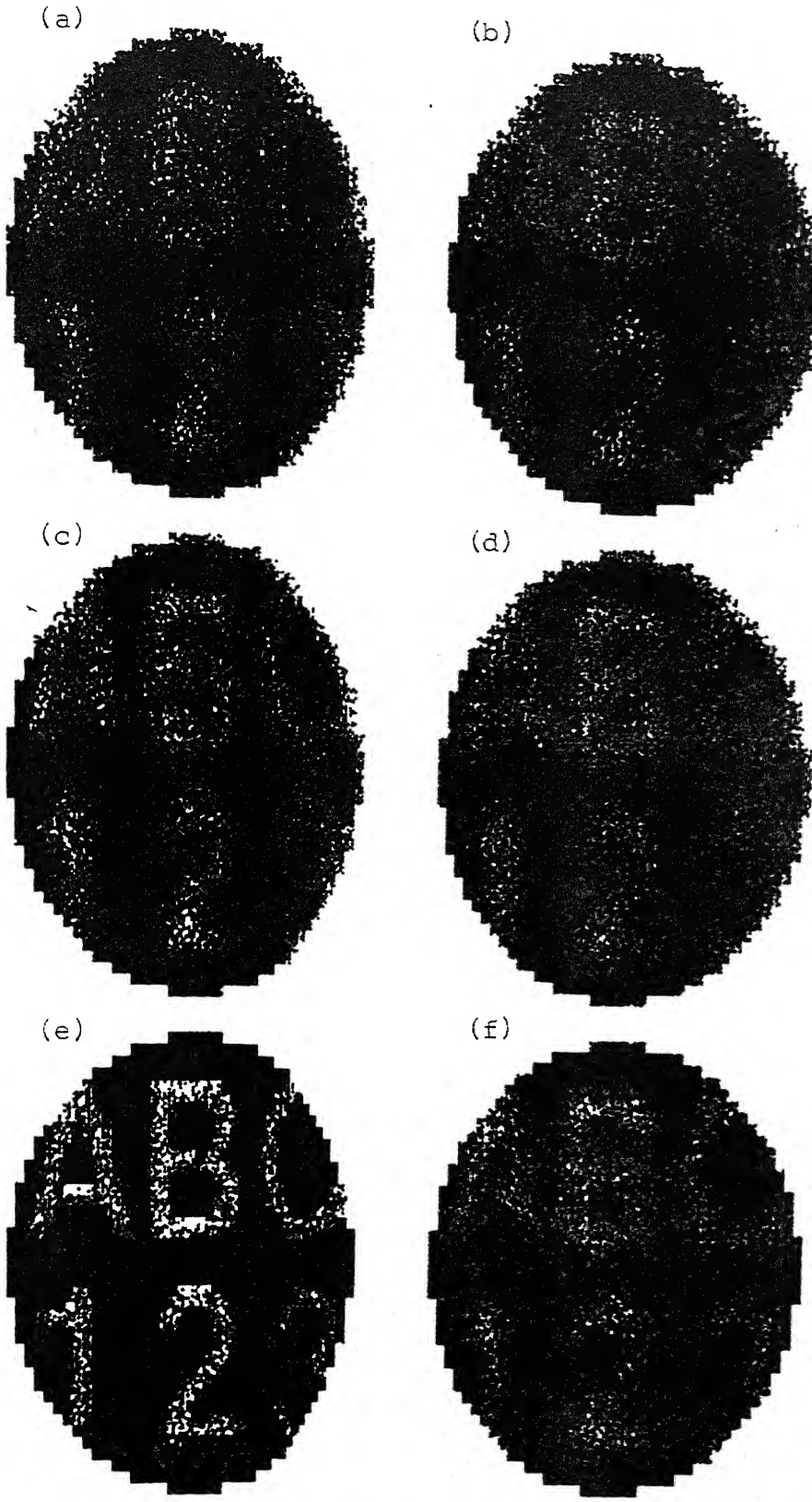

Fig. 6.27 Reconstruction of Characters in PET line integral noise-free case (a) CSI filter, (b) RAM filter, (c) RKS filter, (d) Shepp filter, (e) original picture, (f) optimal filter.

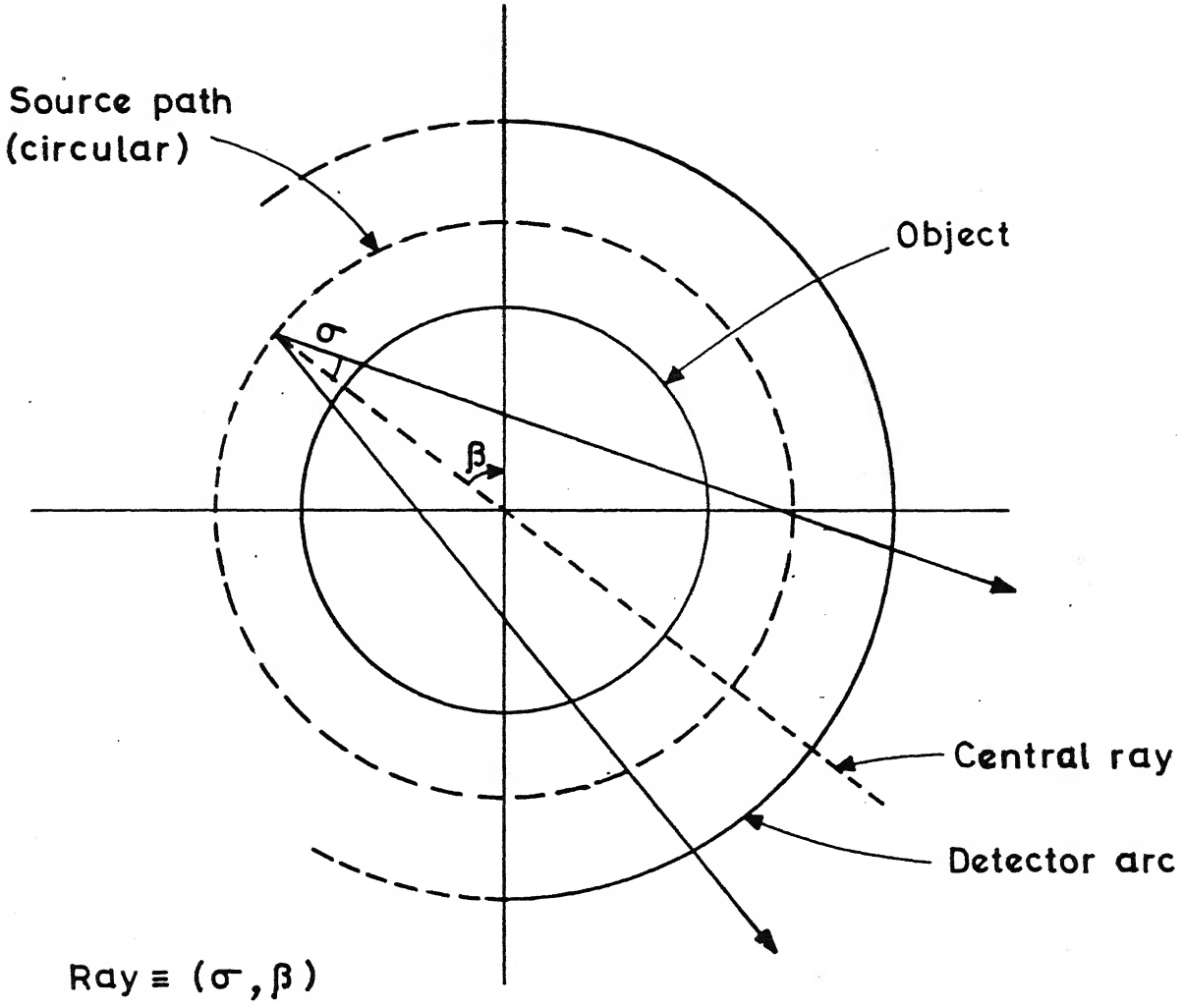

Fig. 1.2 Fan-beam data collection geometry.

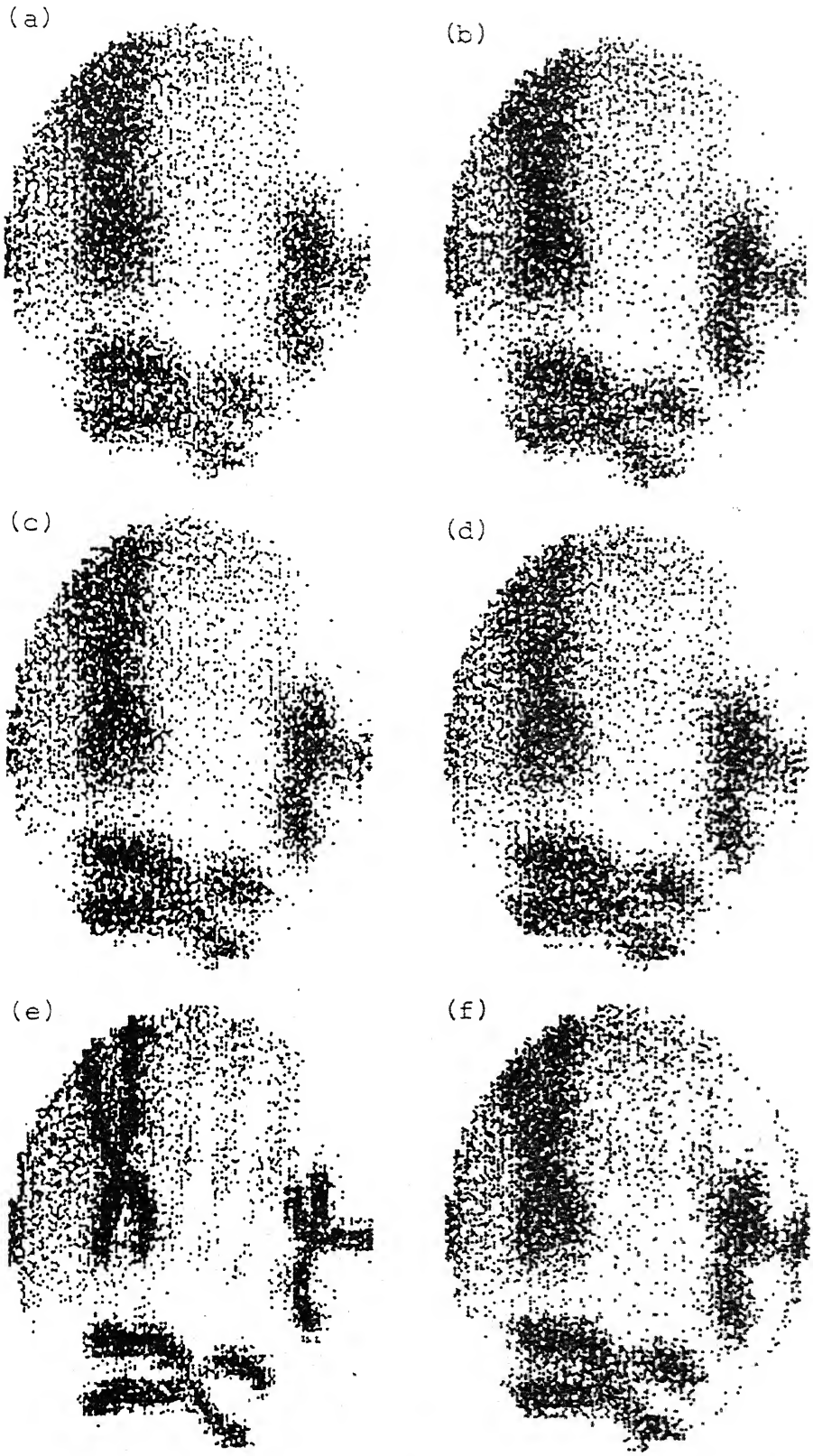

Fig. 6.37 Reconstruction of Chromosomes in PET strip integral noise-free case (a) CSI filter, (b) RAM filter, (c) RKS filter, (d) Shepp filter, (e) original picture, (f) optimal filter.

$$\check{g}(r,\phi) = \int_0^{\pi} \int_{-\infty}^{\infty} g(R\cos\theta, R\sin\theta)\, e^{i2\pi Rr\cos(\theta-\phi)}\, |R|\, dR\, d\theta$$

The notation $P(\underline{x})$ is used for the probability density of an n-dimensional random vector at $\underline{x} \in \mathbb{R}^n$, and $P(x)$ will denote the probability density of a random variable at $x \in \mathbb{R}$. A random vector $\underline{X}$ is said to follow a multivariate normal distribution if,

$$P(\underline{x}) = (1/\ (2\pi)^{n/2}\ |\Sigma|^{1/2}).\ \exp(-\tfrac{1}{2}\ (\underline{x}-\underline{\mu})'\ \Sigma^{-1}(\underline{x}-\underline{\mu}))$$

where $\underline{\mu}$ is called the mean vector and Σ the covariance matrix. A random variable X follows Poisson distribution with parameter λ if,

$$P(\ X = x) = \frac{e^{-\lambda}\ \lambda^{x}}{x\ !}\ , \qquad x = 0, 1, 2, \ldots$$

$P(\underline{x}/\underline{y}\ )$ will denote the conditinal probability density of random vector $\underline{X}$ given $\underline{Y} = \underline{y}$, thus

$$P(\underline{x}/\underline{y}) = P(\underline{x},\ \underline{y})\ /\ P(\underline{y}).$$

1.3 THE CBP ALGORITHM

The CBP algorithm is derived from the well known Projection slice theorem [Bracewell (1956)]. Let $\hat{p}(R, \theta)$

denote 1-dimensional FT of $p(s,\theta)$ with respect to the first variable s, and $\hat{f}(R\cos\theta, R\sin\theta)$ denote the FT of $f(r,\phi)$in two dimensions, i.e.,

$$\hat{p}(R,\theta) = \int_{-\infty}^{\infty} p(s,\theta)\ e^{-i2\pi Rs}\ ds,$$

and

$$\hat{f}\ (R\cos\theta,\ R\sin\theta) = \int_{0}^{\pi}\int_{-\infty}^{\infty} f(r,\ \phi)\ e^{-i2\pi Rr\cos(\theta-\phi)}\ |r|\ dr\ d\phi\ .$$

Then this theorem states that

$$\hat{p}\ (R,\ \theta) = \hat{f}\ (R\cos\theta,\ R\sin\theta) \qquad \ldots.(1.3.1)$$

A two dimensional inverse FT of (1.3.1) leads to the well known tomographic formula,

$$f\ (r,\phi) = \int_{0}^{\pi}\int_{-\infty}^{\infty} \hat{p}\ (R,\theta)\ e^{i2\pi Rr\cos(\theta-\phi)}\ |R|\ dR\ d\theta \qquad \ldots(1.3.2)$$

In practical implementation of equation (1.3.2), the factor $|R|$ in the integral is replaced by $|R|\ W(R)$, where $W(R)$ is a suitably chosen function called a window function. Normally, $W(R)$ is an even function of R, the Fourier frequency and has

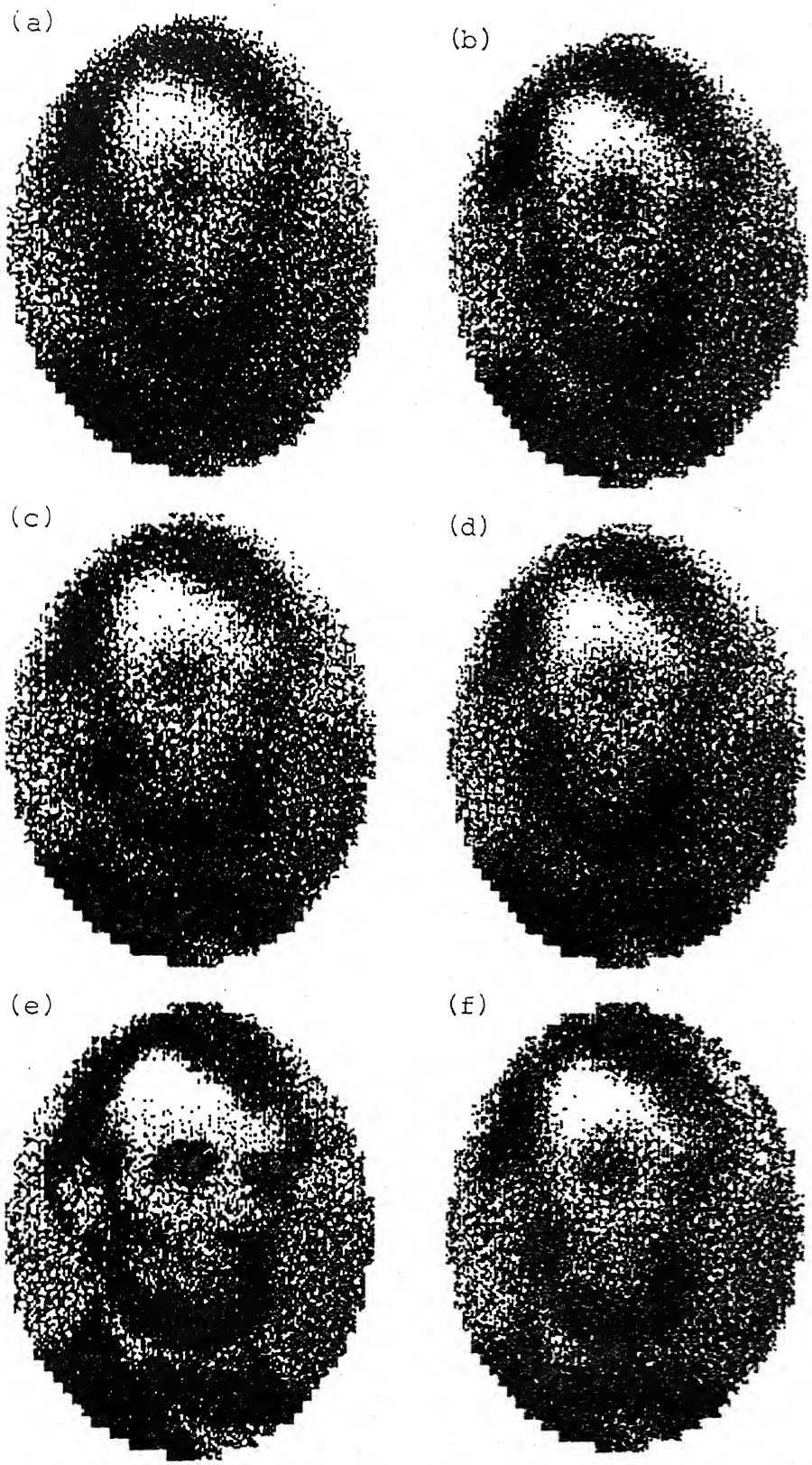

Fig. 6.47 Reconstruction of Lincoln in CAT strip integral noisy case (a) CSI filter, (b) RAM filter, (c) RKS filter, (d) Shepp filter, (e) original picture, (f) optimal filter.

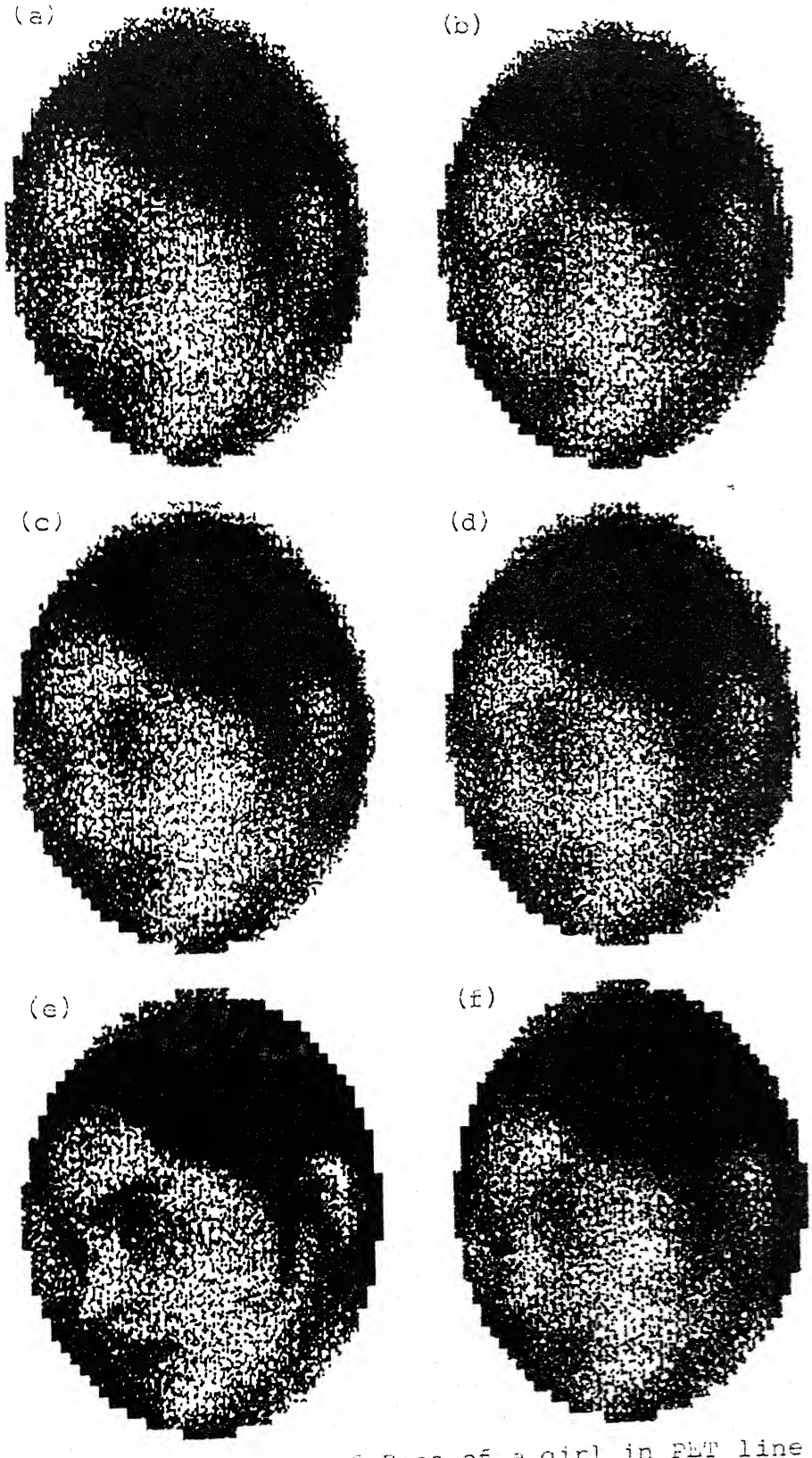

Fig. 6.57 Reconstruction of Face of a girl in PET line integral noisy case (a) CST filter, (b) RAM filter, (c) RNS filter, (d) Shepp filter, (e) original picture, (f) optimal filter.

a compact support $[-R_c, R_c]$. If the frequency content of p is also supported in $[-R_c, R_c]$, i.e., if $\hat{p}(R, \theta)$ vanishes for $|R| > R_c$, then the filtered version with $W(R) = 1$, for $R \in [-R_c, R_c]$, and zero for $|R| > R_c$,

$$\tilde{f}(r, \phi) = \int_0^{\pi} \int_{-\infty}^{\infty} \hat{p}(R, \theta)\, e^{i2\pi Rr\cos(\theta-\phi)}\, |R|\, W(R)\, dR\, d\theta \qquad \ldots(1.3.3)$$

agrees with $f(r, \phi)$ as given in (1.3.2). In the general case introduction of $W(R)$ with a finite cut-off R_c helps in stabilizing the singular nature of the integral in (1.3.2).

An implementation of (1.3.3) in the spatial domain is as follows:

$$\tilde{f}(r, \phi) = \int_0^{\pi} \int_{-\infty}^{\infty} p(s, \theta)\, q(s' - s)\, ds\, d\theta \qquad \ldots.(1.3.4)$$

with $s' = r\cos(\theta-\phi)$, and

$$q(s) = \int_{-\infty}^{\infty} |R|\, W(R)\, e^{i2\pi Rs}\, dR \qquad \ldots..(1.3.5)$$

The inner integral in equation (1.3.4) is a one dimensional convolution while the outer integral corresponds to the backprojection operation. Thus it is named convolution backprojection method. The CBP is also known as filtered

backprojection method indicating filtering of projection data p, by window function W(R). The practical implementation of CBP as given by equation (1.3.3) was initially suggested by Bracewell and Riddle (1967). Ramachandran and Lakshminarayanan (1971) described the method which took care of the discrete nature of projection data. Both Bracewell and Riddle and Ramachandran and Lakshminarayanan used the band limited window

$$W(R) = \begin{cases} 1 & |R| \leq R_c \\ 0 & |R| > R_c \end{cases} \qquad (1.3.6)$$

in their work. Shepp and Logan (1974) suggested the use of 'sinc' window given by

$$W(R) = \begin{cases} \dfrac{\sin (\pi R / 2R_c)}{(\pi R / 2R_c)}, & |R| \leq R_c \\ 0, & |R| > R_c \end{cases}$$

Use of several other window functions has been reported in the literature. We note that these window functions are radially symmetric in the Fourier domain.

In practical situations where projection data is available for only a finite number of rays and views, a recommended value of R_c, based on sampling theorem [see Jerry (1977)] is given by $R_c \geq 1/2\Delta s$, where Δs is the spacing between two consecutive data rays.

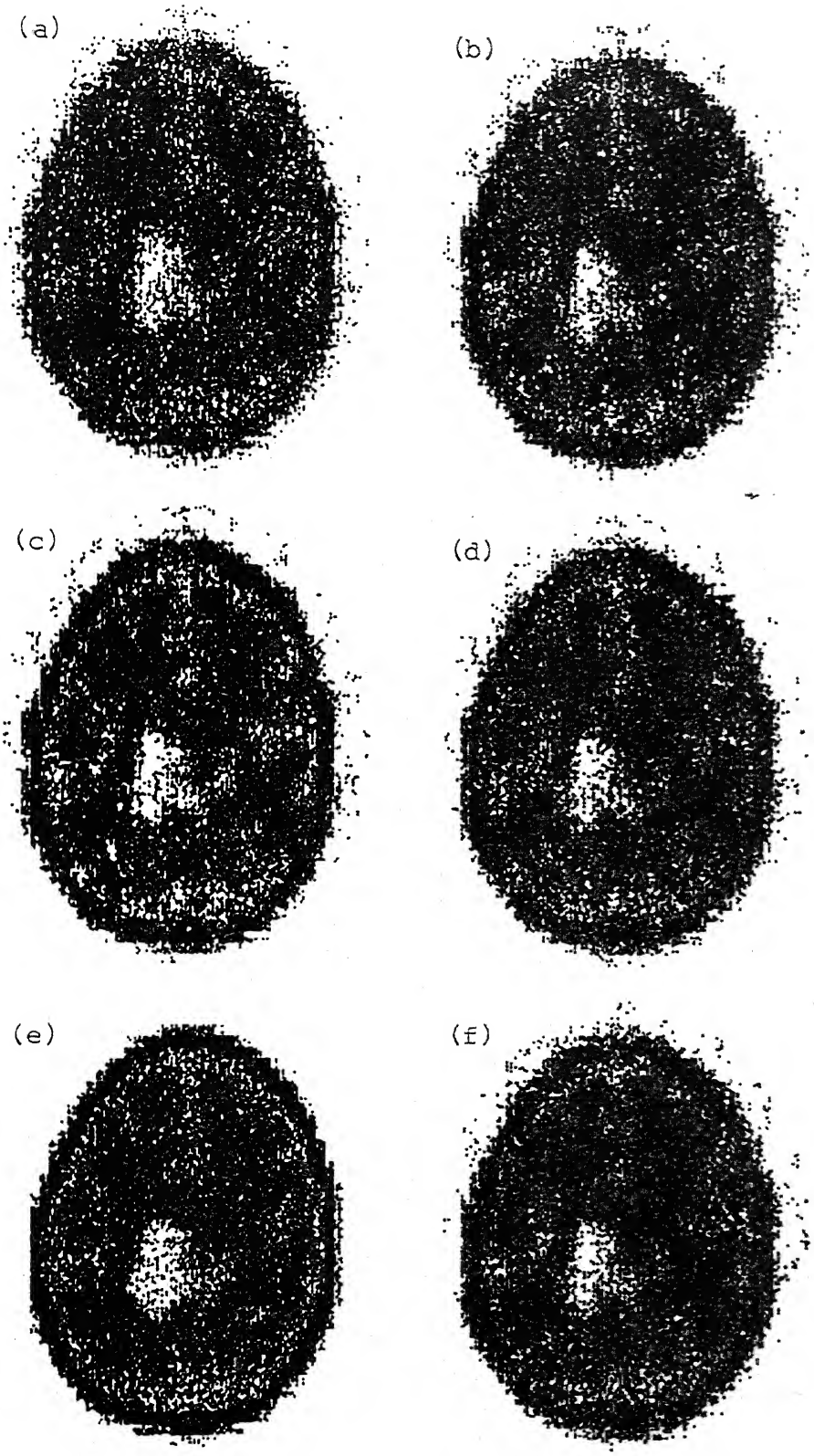

Fig. 6.67 Reconstruction of Brain in PET strip integral noisy case (a) CSI filter, (b) RAM filter, (c) RKS filter, (d) Shepp filter, (e) original picture, (f) optimal filter.

1.4 A REVIEW OF THE LITERATURE

In this section an attempt is made to give a reasonable review of the available literature in reconstruction methods and their error analysis. A reasonably complete bibliography of introductory literature in CT can be found in Deans (1983) and Herman (1980). These books also give an excellent survey on the applications of CT. A state-of-the-art review is contained in March 1983 issue of the Proceedings of the IEEE, which is devoted to CT. A good account of the mathematics of CT is available in Herman and Natterer (1981), Natterer (1986), and Stark (1987).

The first mathematical formulation of the problem of CT is due to Radon (1917). He defined an integral tranform R, which maps a function f on $\mathbb{R}^n$ into the set of integrals over the hyperplanes of $\mathbb{R}^n$. More specifically, if $\underline{\theta} \in S^{n-1}$ and $s \in \mathbb{R}$, then

$$(Rf)(\underline{\theta}, s) = \int_{\underline{x}.\underline{\theta}=s} f(\underline{x})\, dx = \int_{\underline{\theta}^{\perp}} f(s\,\underline{\theta} + \underline{y})\, d\underline{y}$$

where $\underline{\theta}^{\perp} = \{ \underline{x} \in \mathbb{R}^n : \underline{x}.\underline{\theta} = 0 \}$, and $\underline{x}.\underline{\theta}$ denotes the inner product of the vectors $\underline{x}$ and $\underline{\theta}$. This transform is known as the Radon transform. Louis and Natterer (1983) defined the x-ray transform P, which maps a function on $\mathbb{R}^n$ into a set of its

Lautsch, M.(1989): A spline inversion formula for the, Radon transform, *SIAM Journal on Numerical Analysis*, **26**, pp. 456-467.

Lewitt, R.M.(1983): Reconstruction algorithms: Transform methods, *Proceedings of the IEEE*, **71**, pp. 390-405.

Lewitt, R.M. and Muehllehner, G.(1986): Accelerated iterative reconstruction for positron emission tomography based on the EM algorithm for maximum likelihood estimation, *IEEE Transactions on Medical Imaging*, **MI-5**, pp. 16-22.

Louis, A.K. and Natterer, F.(1983): Mathemetical problems of computerized tomography, *Proceedings of the IEEE*. **71**, pp. 379-389.

Löw, K.H. and Natterer, F.(1981): An altrafast algorithm in tomography, Technical Report A81/03, Fachbereich 10 der, Universität des Saarlandes, Germany.

Madych, W.R.(1980): Degree of approximation in computerized tomography in *Approximation Theory III*, Ed. by E.W. Cheney, pp. 615-622.

Medoff, B.P., Brody, W.R., Nassi, M. and Macovaski, A.(1983): Iterative Convolution Backprojection algorithm for image reconstruction from limited data, *Journal of the Optical Society of America*, **73**, pp. 1493-1500.

Medoff, B.P.(1987): Image reconstruction from limited data: Theory and application in computerized tomography in *Image Recovery: Theory and Application*, Ed. by H.Stark, Academic Press pp 321-368.

Minerbo, G.(1979): MENT: A maximum entropy algorithm for reconstructing a source from projection data, *Computer Graphics and Image Processing*, **10**, pp. 48-68.

Munshi, P.(1988): Error estimate for Convolution Backprojection Algorithm in Computerized Tomography, Ph.D. thesis, Indian Institute of Technology, Kanpur, India.

line integrals, i.e., if $\underline{\theta} \in S^{n-1}$ and $\underline{x} \in \mathbb{R}^n$, then

$$(Pf)\ (\underline{\theta},\ \underline{x}) = \int_{-\infty}^{\infty} f(\underline{x} + t\ \underline{\theta})\ dt.$$

For n = 2, with $\underline{x} \in \underline{\theta}^{\perp}$, p and R coincide, i.e.,

$$(Rf)\ (\underline{\theta},\ s) = (Pf)\ (s.\underline{\theta},\ \underline{x}).$$

Another way to label the straight lines in $\mathbb{R}^n$ leads to the divergent beam transformation

$$(Df)\ (\underline{x},\ \underline{\theta}) = \int_{0}^{\infty} f(\underline{x} + t\underline{\theta})\ dt$$

where $\underline{x}$ is thought of as the source of a ray with direction $\underline{\theta}$. In emission tomograpy the transform which decribes the data is known as the attenuated Radon transform

$$(R_{\mu}f)\ (s,\ \underline{\theta}) = \int_{\underline{x}.\underline{\theta}=s} f(\ \underline{x})\ e^{-D\mu(\underline{x},\ \underline{\theta}^{\perp})}\ dx\ .$$

where μ is the attenuation coefficient and f is the activity distribution.

All these transforms describe the generation of projection data using different data collection methods. The data in Positron emission tomography (PET) corresponds to the values of the product

$$e^{-R_{\mu}} Rf$$

and doesnot give rise to new mathematical problems.

Thus the reconstruction problem of CT simply calls for the inversion of Radon transform in $\mathbb{R}^2$. The first inversion formula was given by Radon (1917) himself. It is given by

$$f(x) = \frac{1}{\pi} \int_0^{\infty} dF_{\kappa}(s) \,/\, s$$

where,

$$F_{\kappa}(s) = \frac{1}{2\pi} \int_{\underline{\theta}^{\perp}} p(\underline{\theta},\ \underline{x}.\underline{\theta} + s)\ d\underline{\theta}\ ,$$

and $p(s, \underline{\theta})$ is the projection data.

Bracewell (1956) gave the Projection theorem, which expresses the relationship between an image, its projection data, and its two dimensional Fourier transform in a way that is both mathematically precise and intuitively clear. In mathematical notation it says that

$$\hat{p}\ (R, \theta) = \hat{f}\ (R\cos\theta, R\sin\theta) \qquad (1.4.1).$$

Later, Bracewell and Riddle (1967) obtained the famous tomographic formula

$$\tilde{f}(r, \phi) = \int_0^{\pi} \int_{-\infty}^{\infty} p(s, \theta)\ q(s' - s\ )\ ds\ d\theta$$

by taking a two-dimensional inverse FT. This is known as Convolution Backprojection (CBP) method or filtered backprojection method. A practical implementation of this method was derived by Shepp and Logan (1974).

Herman and Naparstek (1977) derived the reconstruction formula for "fan-beam" geometry (or divergent beam transform). This reconstruction method is given by the following equations:

$$f(r, \phi) = (1/4\pi^2) \int_0^{2\pi} \int_{-\delta}^{\delta} (1/ \sin(\sigma' - \sigma)) \, D_v \, g(\sigma, \beta) \, d\sigma \, d\beta$$

where δ is the object radius,

$$\sigma' = \tan^{-1} \left[\frac{r \cos (\beta - \phi)}{D + r \sin(\beta - \phi)} \right],$$

$$D_v \, g(\sigma, \beta) = \frac{1}{U} \left[\frac{\partial g}{\partial \sigma} - \frac{\partial g}{\partial \beta} \right]$$

and

$$U = \left[(r \cos(\beta - \phi))^2 + (D + r \sin(\beta - \phi))^2 \right]^{1/2},$$

where $g(\sigma, \beta)$ is the projection data collected in fan beam geometry and D is the distance of source from the object centre. It is also shown that the singular integral in

(1.4.2) can be regularized in a number of ways each of which gives an efficient numerical evaluation of the function structure and speed is same as that of "convolution reconstruction technique". The reconstruction formula for divergent beam data as in (1.4.2) is also derived independently by Lakshminarayanan (1975) by a method different from that of Herman and Naparstek.

Instead of inverting the FT in projection theorem exactly the use of numerical inversion with the fast Fourier transform (FFT) is the so-called Fourier method of reconstruction. This is also a transform method. Fourier reconstruction in $\mathbb{R}^2$ has been suggested by Bracewell (1979) in radio astronomy and by Crowther et.al. (1970) in electron microscopy. The method is to use direct Fourier inversion in projection theorem. The problem with this arises in discretization hence in approximation of $\hat{f}$ on a regular grid from the known values of $\hat{f}$ on a polar grid. The critical point here lies in interpolating $\hat{f}$ in s directions. Bracewell (1979) has observed that failure of the standard Fourier reconstruction method results from interpolation. It is also shown that interpolation which is correct in the sense of sampling theorem requires a huge number of operations. Low and Natterer (1981) give some optimality criteria for interpolation points, [see Stark et.al. (1981a)]. Stark et.al. (1981b) replaced the nearest neighbour interpolation

by a more sophisticated interpolation named near exact interpolation method and showed that quality of image is same as that obtained by CBP method, but time taken is less than that by CBP. Natterer (1985) also discusses errors in interpolation.

A different type of inversion formula is produced by series expansion method in terms of special functions. This approach differs fundamentally from transform methods as this is based on discretization of the image domain prior to any mathematical analysis, whereas in transform method first the formula for inversion of Radon transform is obtained and then dicretization is done. These methods are also known as algebraic methods, iterative algorithms, or optimization theory techniques. Censor (1983) has formulated a fundamental model in this approach to image reconstruction problem as follows :—

A Cartesian grid of square picture elements, called pixels, is introduced into the region of interest so that it covers the whole picture that is to be reconstructed. The pixels are numbered in some agreed manner, say from 1 to n. The X-ray attenuation function is assumed to take a constant value x_j throughout the j-th pixel, for j=1,...,n. Source and detector are assumed to be points and rays between them are assumed to be lines. Let a_{ij} denote the length of i-th ray segment that is intersected by the j-th pixel, for i=1,...,m,

j=1,...,n. Thus physical measurement of total attenuation of the i-th ray, denoted by g_i, represents the line integral of the unknown attenuation function. Let $R_i f$ be the line integral of $f(r,\phi)$ along i-th ray. Then g_i is an approximation of $R_i f$. The whole model is described by a system of linear equations,

$$\sum_{j=1}^{n} x_i a_{ij} \cong g_i \qquad i=1,....,m,$$

or

$$\underline{g} \cong A\underline{x}.$$

Algebraic reconstruction technique (ART) was first published as a reconstruction algorithm in a paper by Gordon et.al. (1970) and was later recognised to be identical with Kaczmarz's(1937) algorithm for solving system of linear equations by Guenther et.al. (1974). Realizing the difficulty in handling such a large system of equations Gordon et.al. (1970) suggested an iterative process, starting with an initial approximation $\underline{x}^0 \in \mathbb{R}^n$ to the image vector. In an iterative step, the current iterate $\underline{x}^k$ is corrected to give new iterate $\underline{x}^{k+1}$ by taking into account only a single ray, say the i-th and changing only the image values of the pixels which intersect this ray. The discrepancy between the measurement g_i and pseudo-projection data $\sum_{j=1}^{n} a_{ij} x_j^k$ obtained from current iterate $\underline{x}^k$ is redistributed among the

pixels along the whole of i-th ray in proportion to a_{ij}'s. Thus an iterative procedure is given which in practice stops, but unfortunately not much is known about how "good" the iterates themselves are in comparison to the limit. Also in practice limits are not achieved and one has to make approximations. Hounsfield (1973) has obtained ART independent of Gordon et.al. (1970). Censor et.al. (1983) and Eggerment et.al. (1981) have studied the behaviour of the algorithm for the inconsistent system when relaxation parameters are allowed. Tanabe (1971) found that the ART works well for both singular and non-singular systems and also gave the affine space formed by the solutions if they exist. A complete tutorial of ART algorithm is given in a paper by Gordon (1974).

Based on statistical nature of data and image, certain statistical reconstruction methods are also proposed in literature. Hanson (1987) considers the projection data g as a weighted integral of the object function f with weight functions h_i, which are characterstic functions of lines or strips in the plane. Thus

$$g_i = \int_{-\infty}^{\infty}\int_{-\infty}^{\infty} h_i(x, y)\, f(x, y)\, dx\, dy$$

give rise to the linear system

$$\underline{g} = \underline{H}\ \underline{f}\ .$$

With noise in data the model becomes

$$\underline{g} = \underline{H}\ \underline{f} + \underline{n}\ ,$$

where $\underline{n}$ is the noise vector. Suppose that $\underline{n}$ follows a multivariate normal distribution, with mean zero and the covariance matrix R_n, so that the conditional probability of $\underline{g}$ given $\underline{f}$, $P(\underline{g}\ /\underline{f}\ )$ is multivariate normal with mean $\underline{Hf}$, and covariance matrix R_n, i.e.,

$$P\ (\underline{g}\ /\underline{f}\ ) \propto \exp\ [\ -\frac{1}{2}\ (\underline{g} - \underline{Hf}\ )'\ R_n^{-1}\ (\underline{g} - \underline{Hf}\ )\ ] \qquad ...(1.4.3)$$

If the *a priori* probabilty distribution for the ensemble of images, is assumed to be a multivariate normal distribution with mean value $\underline{f}_0$ and covariance matrix R_f, i.e., if

$$P(\underline{f}) \propto \exp\ \left[\ -\frac{1}{2}\ (\underline{f} - \underline{f}_0)'\ R_f^{-1}\ (\underline{f} - \underline{f}_0)\ \right], \qquad ....(1.4.4)$$

then the best estimate for the object image $\underline{f}$ is that particular image $\underline{f}$ which maximizes the *a posteriori* probability

$$P\ (\underline{f}\ /\underline{g}) = \frac{P\ (\underline{g}\ /\underline{f}).\ P(\ \underline{f}\ )}{P(\ \underline{g}\ )} \qquad .....(1.4.5)$$

Under these assumptions Herman et.al. (1979) have shown that

maximum *a posteriori* (MAP) solution satisfies the MAP equation,

$$R_f^{-1} (\underline{f}_0 - \underline{f}) + \underline{H}' R_n^{-1} (\underline{g} - \underline{H}\underline{f}) = 0 \qquad \ldots(1.4.6)$$

Herman and Lent (1976) have given a computer implemenation of Bayesian (or MAP) approach as an iterative procedure, the iteration scheme was given with initial guess $\underline{f}_0$, i.e.,

$$\left.\begin{aligned} \underline{f}^0 &= \underline{f}_0 \\ \underline{f}^{k+1} &= \underline{f}^k + c^k \underline{r}^k \\ \underline{r}^k &= \underline{f}_0 - \underline{f}^k + R_f H' R_n^{-1} (\underline{g} - \underline{H}\underline{f}^k), \\ c^k &= \underline{r}^k \underline{s}^k / \underline{s}^k \cdot \underline{s}^k, \quad \underline{s}^k = (I + R_f H' R_n^{-1} H) \underline{r}^k, \end{aligned}\right\} \ldots(1.4.7)$$

where the vector $\underline{r}^k$ is the residual of the equation (1.4.6) (multiplied by R_f), the scalar c^k is chosen to minimize the norm of $\underline{r}^{k+1}$, and I is the identity matrix. Similar scheme for Image restoration is proposed by Hunt (1977). Trussel and Hunt (1979) redefined the iterative scheme given by Hunt (1977) to improve the rate of convrgence. Hanson (1987) found that the scheme (1.4.7) does converge but takes at least 10 to 20 iterations. When there is an absence of *a priori* information, as is often the case, then *a priori* probability distribution $P(\underline{f})$ does not play any role in (1.4.5). The MAP approach then reduces to that of maximizing the conditional

probability (1.4.5), or equivalently to that of minimizing the so called chi-square

$$\chi^2 = (\underline{g} - \underline{Hf})^{T} R_n^{-1} (\underline{g} - \underline{Hf}).$$

and then the method is called the minimum chi-square method or the least squares method. The solution of this is also refered to as maximum likelihood solution as this term is the likelihood function for normal distribution. Rockmore and Mackovaski (1977) have used maximum-likelihood (ML) method for reconstruction without the normality assumption. The method is summerized as follows:

Let f(x,y) represent the linear attenuation co-efficient, and the incident process (as a source of photons is incident on object) has rate λ_0 then the rate of detected process is given by

$$\lambda = \lambda_0 \exp \left(- \int\int_{\mathcal{L}} f(x, y)\, dx\, dy \right)$$

where $\mathcal{L}$ is the line by which photons are detected (Collimator is alligned with the line $\mathcal{L}$). It is assumed that the detectors observe a set of random counts, each having a Poisson distribution, corresponding to a series of N projections over time interval of length t. Let these projections be indexed in an arbitrary way. By virtue of the

properties of the Poisson process, they are independent, thus the observables, denoted by $[n_i]_{i=1}^{N}$, obey the joint Poisson probabilty density function,

$$P(n_1 = k_1,\ n_2 = k_2, \ldots) = \prod_{i=1}^{N} P(n_i = k_i)$$

$$= \prod \frac{e^{-\lambda_i t}(\lambda_i t)^{k_i}}{(k_i)!}$$

where the λ_i's are given by

$$\lambda_i = \lambda_0 \exp\left(-\int\int_{\mathscr{L}_i} f(x, y)\, dx\, dy\right)$$

$\mathscr{L}_i$ being the i-th source-detector line. In order to apply ~~the~~ the ML estimation technique the function f (x, y) is expanded on an arbitrary complete set of basis functions $\{\phi_l(x, y)\}$, and for a finite number L, it is given as

$$f(x, y) = \sum_{l=1}^{L} f_l \phi_l(x, y) = \underline{f} \cdot \underline{\phi}(x, y) \quad ..(1.4.8)$$

where,

$\underline{f} = (f_1, f_2, \ldots, f_L)$, and $\underline{\phi}(x, y) = (\phi_1(x, y), \ldots, \phi_L(x, y))$

Then the parameters to be estimated is the vector $\underline{f}$. Using (1.4.8) it is shown that

$$\iint_{\mathcal{L}_i} f(x, y)\, dx\, dy = \sum_{l=1}^{L} f_l \iint_{\mathcal{L}_i} \phi_l(x, y)\, dx\, dy$$

$$\cong \sum f_l \psi_{li} = \underline{f}' \underline{\psi}_i .$$

With these notations the problem is to find the best estimate of $\underline{f}$ (ML sense) given a particular set of realizations $(k_1, k_2, \ldots, k_N)$ corresponding to number of counts for each projection where the number of counts are independent Poisson variates. Thus the ML estimate is that $\tilde{\underline{f}}$ which maximizes the conditional probability density function $P(\underline{n} = \underline{k} / \underline{f})$, i.e, the estimate is the vector $\tilde{\underline{f}}$ solving the equation

$$\frac{\partial}{\partial \underline{f}} P(\underline{n} = \underline{k} \mid \underline{f}) = 0$$

for transmission case the ML equation is

$$\sum_{i=1}^{N} [\, \lambda_0 t\, e^{-\tilde{\underline{f}}' \underline{\psi}_i} \psi_{li} - k_i \psi_{li} \,] = 0 \qquad l = 1, 2, \ldots, L.$$

The solution is given by

$$\tilde{\underline{f}} = (\psi^{-})^{+} \underline{\beta} + \underline{y},$$

where $\underline{\beta} = (-\ln((k_1+z_1)/\lambda_0 t), \ldots, -\ln((k_N+z_N)/\lambda_0 t))$, $\underline{z}$ is any vector in null space of $\underline{\psi}$, and $\underline{y}$ a vector in null space of $\underline{\psi}'$. Rockmore and Macovaski (1976) used ML method for emission tomography using the rates

$$\lambda = \iint_{\mathscr{E}} f\ (x,\ y)\ dx\ dy$$

instead of $\lambda_0 \exp\left(- \iint_{\mathscr{E}} f(x,\ y)\ dx\ dy \right)$

the approach remaining the same. The ML equations now become

$$\sum_{i=1}^{N} [\ - \psi_{li}\ t + k_i\ (\psi_{li}\ /\ \tilde{\underline{f}}'\ \psi_i)\ ]\ = 0, \qquad l = 1,2,\ldots,\ L.$$

and the solution is given by $\tilde{\underline{f}} = (1/t)\ (\ \underline{\psi}\ \underline{\psi}'\ )^{-1}.\underline{\psi}\ \underline{k}$, where, $\underline{\psi} = (\ \underline{\psi}_1, \ldots, \underline{\psi}_N\ )$.

Shepp and Vardi (1982) have used maximum-likelihood estimation in case of Positron emission tomography (PET).They give a general mathematical model for PET where an unknown emission density λ is to be reconstructed from the number of counts, $n^*(d)$ in detector unit d, d = 1,...,D. The unobserved emissions n(b) in b-th pixel are assumed to be independent Poisson variables with unknown means $\lambda(b)$, for b= 1,...,B. Suppose each emission in pixel b is detected in detector unit d with probability p(b, d), d= 1,...,D with p(b, d) a one step transition matrix, assumed to be known. For estimation of $\lambda(b)$ the Expection Maximization (EM) algorithm of Dempster et.al. (1977) is used. The algorithm contains two steps the expection step and the maximization of likelihood step. It

starts with an initial estimate λ^0 and gives a new estimate $\hat{\lambda}^{new}$ from an old estimate $\hat{\lambda}^{old}$, iteratively as follows:

$$\hat{\lambda}^{new}(b) = \hat{\lambda}^{old}(b) \sum_{d=1}^{D} \frac{n^*(b)\, p(b,\, d)}{\sum_{b'=1}^{B} \hat{\lambda}^{old}(b')\, p(b',d)}, \qquad b=1,\ldots,B.$$

It is shown that this iterative procedure converges. Vardi et.al.(1985) have also investigated further estimation methods in PET such as least squares method, method of moments, etc. They have compared EM algorithm with other methods, and observed that it gives better results than least squares method. Lewitt and Muehllehner (1986) give accelerated version of EM algorithm which takes about half number of iterations than that taken by of standard EM algorithm.

Another statistical method of reconstructing an image from its projection data is known as a Maximum Entropy (MENT) algorithm, which also uses *a priori* information about object function. Let $f_1, f_2, \ldots, f_n$ denote pixel values of the image to be reconstructed and $p_i = r_i / \sum r_i$, where r_i is the average rate of emission of photons from i-th pixel. The entropy is defined as

$$H(p_1,\ldots,p_n) = -\sum_{i=1}^{n} p_i \log p_i = f_i \Big/ \sum_{i=1}^{n} f_i \qquad i = 1,\ldots,n$$

The entropy depends only on the distribution of gray levels and not on the total intensity $\sum_i f_i$. The observed data is given by

$$g_j = \sum_{i=1}^{n} A_{ji} f_i + e_j \quad , \qquad j = 1,\ldots,m.$$

where e_j is independent random noise with mean zero and variance σ^2.Let

$$Q (f_1,\ldots,f_n) = \frac{1}{2} \sum_{j=1}^{n} (1/\sigma_j^2) (\sum_{i=1}^{m} A_{ji} f_i - g_j)^2$$

$$= \frac{1}{2} \| Af - g \|_D^2$$

where D =diag [$1/\sigma_1^2,\ldots, 1/\sigma_m^2$] . With these notations the problem of image reconstruction becomes that of maximizing the entropy

$$H (f_1,\ldots,f_n)$$

subject to constraint

$$Q (f_1,\ldots,f_n) = m/2 \text{ and } \sum f_i = t \ (t>0).$$

Zhuang et.al.(1987) give a differential equation approach to solve this problem. The differential equations are as follows:

$$\frac{\partial}{\partial \lambda} \nabla J (\underline{f}; \mu, \lambda) \equiv 0$$

$$\nabla J (\underline{f}; \mu, 0) = 0,$$

where,

$$J(\underline{f};\ \mu,\ \lambda) = H(f_1,\ldots,f_n) + \mu \sum_i f_i - \lambda\, Q(f_1,\ldots,f_n)$$

and

$$\nabla J = -\left[\log f_1^0,\ldots,\log f_n^0\right]' + (\mu-1)\,\underline{h} - \lambda\,\underline{a}'D\,(A\underline{f}^0 - \underline{g})$$

a discretization of these equations is given by

$$\underline{f}^0 = \exp(\mu - 1)\,\underline{h},$$

$$k \geq 0:\ (F^k + \lambda_k A'D A)\,\underline{f}^{k+1}$$

$$= (2\lambda_k - \lambda_{k+1})\,A'D A\,\underline{f}^k + \underline{h} + (\lambda_{k+1} - \lambda_k)\,A'D\,\underline{g}$$

where $\underline{F}^k = \text{diag}\,[1/f_1^k,\ldots,1/f_n^k]$, $\lambda_0 = 0$, and $\lambda_{k+1} > \lambda_k$, and $\underline{h}$ is a nx1 vector containing 1's. Using Gauss-Seidel technique following iterative scheme is obtained

$$k \geq 0:\ (\underline{F}^k + \lambda_k \underline{f}^{k+1}) = (2\lambda_k - \lambda_{k+1})\underline{d}^k + \underline{h} + (\lambda_{k+1} - \lambda_k)\,\underline{p},$$

$$k \geq 1:\ \underline{g}^{k+1} = (2 - \lambda_{k+1}/\lambda_k)\,\underline{d}^k$$

$$+ (1/\lambda_k)\left((f_1^k - f_1^{k+1})/f_1^k,\ \ldots,\ (f_n^k - f_n^{k+1})/f_n^k\right)'$$

$$+ \left((\lambda_{k+1}/\lambda_k) - 1\right)\underline{p}.$$

where

$$\underline{L} = A'D A,$$

$$\underline{p} = A \, {}^{\prime}D \, \underline{g},$$

$$\underline{d}^{k} = \underline{L}\underline{f}^{k}, \qquad k = 0,1,2,\ldots.$$

The initial values $\underline{f}^{0}$, $\underline{d}^{0}$, $\underline{d}^{1}$ are as follows:

$$\underline{f}^{0} = \exp\,(\nu - 1)\,\underline{h},$$

$$\underline{d}^{0} = \underline{L}\underline{f}^{0} = \exp\,(\mu - 1)\,\Big(\sum_{i=1}^{n} L_{1i}, \ldots, \textstyle\sum_{i=1}^{n} L_{ni}\Big)^{\prime},$$

$$\underline{d}^{1} = \underline{L}\underline{f}^{1}.$$

Wernecke and D'Addario (1977) give a solution of this problem in radio astronomy using Fourier synthesis. Minerbo (1979) defined the entropy as

$$H\,(\underline{f}) = -\iint_{D} f\,(x, y)\,\log\,\big(f(x, y)\,A\big)\,dx\,dy$$

where A is the area of D.The constraints are

$$g_{jm} = \int_{s_{jm}}^{s_{jm+1}} \int_{-\infty}^{\infty} f\,(s\cos\theta_j - t\sin\theta_j,\ s\sin\theta_j + t\cos\theta_j)\,dt\,ds$$

$$m = 1,\ldots,M(j),\quad j = 1,\ldots,J$$

where $s_{j1} < \ldots. < s_{jM(j)}$ is a set of abscissas for j-th veiw. The iterative algorithm is given as

$$H_{jm}^{0} = 1,\ m \in \mathcal{M}\ ,\quad (\mathcal{M} \text{ is set of m values for which } g_{jm} \geq 0)$$

$$H_{jm}^{k+1} = \frac{A\, g_{jm}}{\int\int \chi_{jm}(s) \prod_{i \neq j} \sum H_{in}^{k} \chi_{in}(s \cos \theta_{ji} - t \sin \theta_{ji})}$$

$$m \in \mathcal{M}, \quad j = k \bmod (J+1)$$

$$H_{jm}^{k+1} = H_{jm}^{k}, \qquad m \in \mathcal{M}, \quad j \neq k \bmod (J+1)$$

where,

$$H_{jm} = \exp (\lambda_{jm} - 1) / J,$$

$$\chi_{jm} = \begin{cases} 1, & s_{jm} < s < s_{jm+1} \\ 0. & \text{otherwise} \end{cases}$$

Wood and More (1981) give a minimum variance estimator in CT, they assumed the measurement vector $\underline{g} = (\underline{g}_1 | \ \ldots \ | \ \underline{g}_k)$ and projection matrix $H' = [H_1' | \ \ldots \ | \ H_k']$ where $\underline{g}_j$ is the nx1 measurement vector for j-th rotational position thus the usual measurement equation is $\underline{g}_j = H_j \underline{f} + \underline{n}$, the minimum variance estimator for vector $\underline{f}$ is given by

$$\tilde{\underline{f}} = \underline{f}_0 + P_0 H' R_{\underline{g}\underline{g}}^{-1} (\underline{g} - H\underline{f}_0)$$

where f and n are assumed to be random variables, the *a priori* information is given by

$$\underline{f}_0 = E (\underline{f}), \quad P_0 = E ((\underline{f} - \underline{f}_0) (\underline{f} - \underline{f}_0)')$$

and the assumptions about the measurement noise are E (n) =0,

$R_n = E(\underline{n}\,\underline{n}')$, $E(\underline{n}\,\underline{f}') = 0$. $R_{\underline{g}\underline{g}} = (H P_0 H' + R_n)$ can be identified as the measurement covariance matrix. A fast implementation of this method on computer is also given.

The problem of image reconstruction when projection data is available for limited number of angles, is known as "limited data problem". It has been considered by many researchers. Hanson (1987) and Medoff (1987) give a review of this problem in context of statistical and deterministic case respectively. Medoff et.al. (1983) have discussed the iterative convolution backprojection algorithm for limited data situation to reduce artifacts. Invouye (1979) gives a solution to this problem by Fourier reconstruction method using the analyticity of the Fourier transforms. Assuming that data are given at following L points.

$\theta_1 = \theta_\alpha, \theta_2, \ldots\ldots, \theta_L = \theta_\beta$. $(\theta_\alpha < \theta < \theta_\beta)$, the expressions

$$(a) \sum_{i=1}^{L} \left| \sum_{m=1}^{M} [a_m(\omega) \cos 2m\theta_i + b_m(\omega) \sin 2m\theta_i] - \hat{Ref}(\omega, \theta_i) \right|^2$$

$$(b) \sum_{i=1}^{L} \left| \sum_{n=0}^{N} [c_n(\omega) \cos(2n+1)\theta_i + d_n(\omega) \sin(2n+1)\theta_i] - \hat{Imf}(\omega, \theta_i) \right|^2$$

are minimized with respect to constants a_m, b_m, c_n, d_n, where M and N are finite numbers for which Fourier series expansion is taken. The values of a_m, b_m, c_n, d_n, are obtained for

given θ_i's which minimizes (a) and (b) and making use of these constants the missing data is extrapolated. Gilbert (1972) proposed a method of reconstruction known as Simultaneous Iterative Reconstruction Technique (SIRT). Lakshminarayanan and Lent (1979) have shown that this method strongly resembles the Richardson least squares algorithm. They also gave generalized SIRT (GSIRT) algorithm, which converges faster than the SIRT.

The mathematical analysis of the error for CBP method has been done firstly by Natterer (1980,1986). He has given the error for CBP algorithm for object functions belonging to certain Sobolev spaces. One of the main theorems of Natterer (1986) states that for $f \in C_0^{\infty}(\Omega)$; i.e., f being infinitely differentiable with comapct support Ω, the discretization errors in CBP are given by e_1 and e_2, for some φ , $0 < \varphi < 1$, $R_c < \varphi m$, and $R_c \leq 1/2\ \Delta s$,

$$e_1 \leq \frac{1}{2}\ \xi_o^*(f, R_c), \text{ and}$$

$$e_2 \leq \| f \|_{L_{\infty}(\Omega)}\ \eta(\varphi, m) ,$$

where

$$\xi_0^*(f, R_c) = 2\pi \sup_{\theta \in S^{n-1}} \int_{|R| \geq R_c} |R|\ |\hat{f}(R, \theta)|\ dR ,$$

m is an integer such that the quadrature formula for

integration is exact for the function belonging to H_{2m}', the class of even spherical harmonics of degree 2m, and η ($\mathcal{P}$, m) is such that $0 \leq \eta$ ($\mathcal{P}$, R_c) $\leq C$ ($\mathcal{P}$) $e^{-\lambda(\mathcal{P})R_c}$; with $R > R_c$, $C(\mathcal{P})$ and R_c are positive numbers. These errors are introduced by discretization of continuous integral in the inversion formula. If a function is essentialy R_c-band limited, then the term ξ_0^* is negligible and error in CBP is strictly due to discretization of the backprojection integral.

Natterer (1980) has developed reconstruction error bounds for the function f belonging to Sobolev space H^α, α real, with norm given by

$$\|f\|^2_{H^\alpha(\mathbb{R}^2)} = \int_{\mathbb{R}^2} (1 + |R|^2)^\alpha |\hat{f}(R)|^2 \, dR \quad < \infty$$

The reconstruction error r is defined as,

$$r(\alpha, n, \xi) = \sup \left[\|f_1 - f_2\|_{L_2(\Omega)} : \|Rf_i - g\| \leq \xi, \right.$$
$$\left. \|f_i\|_{H_0^\alpha(\Omega)} \leq 1, \; i=1,2 \text{ for some } g \right]$$

The lower bound of r is shown to be given by

$$r(\alpha, n, \xi) \geq c(\alpha, \Omega) \, (n^{-\alpha/2} + \xi^{\alpha/(\alpha+1/2)})$$

where c is a constant and projection data p is known for n lines with a root mean square error ξ, Rf_i is the Radon

transform or true projection data for f.

Natterer in this study of errors has assumed that the cross-section (image) has band limited projection data. But in general object cross-sections have a finite support, hence the projection data is necessarily not band limited. Nevertheless, in the implementation of CBP method, the approximaton obtained is band limited. Munshi (1988) has studied the error in CBP algorithm due to this band limiting aspect. The analysis assumes ~~the~~ perfect (noise-free) data. The total error, e_T, in reconstruction is assumed to consist of three additive parts:

$$e_T = e_R + e_B + e_c,$$

where, e_R is the inherent error due to finite cut-off R_c, e_B, and e_c are discretization errors due to discrete implementation of backprojection and convolution integrals respectively. The error estimates for the inherent error due to finite cut-off R_c are obtained. The estimates are given for f belonging to certain circular Sobolev space Ω_{2m} and a characterization of functions f is given in terms of interpolation space Ω_{2m}^{β}, where m is a positive integer and $0 < \beta < 2m$. It is assumed that the convolving functions satisfy certain regularity conditons.

Bertro et.al.(1980) considered the inversion of Radon transform as ill-posed problem in estimating f from the available data g = Rf + h, where h is the noise in the data.

The error in estimation is defined as

$$\delta(\xi, E; g) = \max_{f} \| f - \tilde{f} \|_F$$

where F and G, solution and data spaces, are considered as the spaces of square integrable functions and f has support on a unit circle with following constraints

$$\text{(i)} \| Rf - g \|_G \leq \xi, \text{ and (ii)} \| Bf \|_F \leq E$$

with $B : F \longrightarrow F$, a constraint on f and E is a prescribed constant. The stability estimate of this error is given as

$$\delta(\xi, E; g) \leq \delta(\xi, E)$$

The estimate is given by

$$\delta(\xi, E) = \sqrt{2}\, \xi \sup_{\nu} [\, |\nu|^{-1} + (\xi / E)^2 |\nu|^2 \,]^{-1/2}$$

Madych(1980) also has defined Sobolev spaces $A^p_\alpha(D)$ as the class of those Schwartz distributions, f, on $\mathbb{R}^2$ which are supported in D with the property that $f_y - f$ is in $L^p(\mathbb{R}^2)$ for all y and f_y denotes the y translate of f, with finite norm

$$\| f \|_{A^p_\alpha} = \sup_{|y|>0} \{ |y|^\alpha \| f_y - f \|_{L^p(\mathbb{R}^2)} \}.$$

Then he gave a reconstruction formula R_n, using n projection data such that for f being in $L^p(D)$

$$R_n\, pf\,(x) = Q_n * f\,(x) \qquad \ldots(1.4.8)$$

where n is the total number of lines for which projection data is given and $Q_n(x) = (1/\pi)\, q(|x|^2)$, with

$q(t) = c(t-\xi_1)^{-2} (P_m(t))^2$ where P_m is the Legendre polynomial of degree m. Then the theorem states that: Suppose f is in $\Lambda_\alpha^p(D)$, $0 < \alpha \leq 1$, $1 \leq p < \infty$. Then given n distinct projection data p and the reconstruction formula (1.4.8),it follows that $\| f - R_n pf \|_{L^p(D)} \leq c\, n^{-\alpha} \| f \|_{\Lambda_\alpha^p}$ where c is a constant independent of f and n.

Lautsch(1989) gave an error analysis for spline inversion of Radon transform in the set-up of Sobolev spaces used by Natterer.

CHAPTER 2

STATIONARY PROCESSES: SOME BASIC RESULTS

2.1 SOME DEFINITIONS AND ASSUMPTIONS

In this thesis we assume that the object function $Z(\underline{u})$ is a random variable for each $\underline{u} \in \mathbb{R}^2$. Thus realization z of an object cross-section is a function on $\mathbb{R}^2$ to $\mathbb{R}$ or $\mathbb{R}^+ = [0, \infty)$ and $\mathcal{Z} = \{Z(\underline{u}): \underline{u} \in \mathbb{R}^2\}$ is a spatial stochastic process representing the ensemble of all cross-sections of interest of which the given cross-section is a sample realization.

DEFINITION 2.1.1 Translation of an image (cross-section) $Z(\underline{u})$ by a constant $\underline{c} = (c_1, c_2) \in \mathbb{R}^2$ is denoted by

$$T_{\underline{c}}\, Z(\underline{u}) = Z(\underline{u} + \underline{c})$$

DEFINITION 2.1.2 Rotation of an image $Z(\underline{u})$ by an angle θ about a point $\underline{x} \in \mathbb{R}^2$ is given by

$$R_{\underline{x},\,\theta} Z(\underline{u}) = Z\begin{bmatrix} (u_1 - x_1)\cos\theta + (u_2 - x_2)\sin\theta \\ (u_1 - x_1)\sin\theta - (u_2 - x_2)\cos\theta \end{bmatrix}$$

DEFINITION 2.1.3 The expected value function of the spatial

stochastic process $\mathcal{Z}$ is given by

$$E\ Z(\underline{u}) = \int_{\mathcal{Z}} Z\ (\underline{u})\ dP\ (Z)$$

and the product moment function is given by

$$K\ (\underline{u},\ \underline{v}) = E\ [\ Z\ (\underline{u}).\ Z(\underline{v})\ ] = \int_{\mathcal{Z}} Z\ (\underline{u})\ Z\ (\underline{v})\ dP\ (Z)$$

where P is a probability measure on the space $\mathcal{Z}$.

DEFINITION 2.1.4

$$C_{\mathcal{Z}}\ (u,\ v\ ) = E[\ Z\ (u)\ -E\ Z(u)\ ][\ Z\ (v)\ -\ E\ Z(v)\ ]$$

is called the covariance kernel of the process $\mathcal{Z}$.

DEFINITION 2.1.5 The process $\mathcal{Z}$ is said to be invariant under translations if

$$Z \in \mathcal{Z} \text{ implies that } T_{\underline{c}}\ Z \in \mathcal{Z}$$

and

$$P\ (\ T_{\underline{c}}\ Z \in B\ ) = P\ (\ Z \in B\ ),$$

$$\forall\ \underline{c} \in \mathbb{R}^2 \text{ and } \forall \text{ Borel set } B \text{ in } \mathbb{R}^2$$

DEFINITION 2.1.6 The process $\mathcal{Z}$ is said to be invariant under rotations if

$$Z \in \mathcal{Z} \text{ implies that } R_{\underline{x},\,\theta} Z \in \mathcal{Z}$$

and

$$P\,(\, R_{\underline{x},\,\theta} Z \in B\,) = P\,(\, Z \in B\,),\ \forall\ \theta,\ \underline{x},\ \text{and } B$$

DEFINITION 2.1.7 A spatial stochastic process $\mathcal{Z}$ is said to be second order wide sense (or weakly) stationary if $C_{\mathcal{Z}}(\underline{u}, \underline{v})$ depends only on the distance between the points $\underline{u}$ and $\underline{v}$

In practice the object function $Z(\underline{u})$ is composed of two parts: $m(\underline{u}) = E\, Z(\underline{u})$, the fixed part and the random part $\mathcal{E}(\underline{u})$, i.e. $Z(\underline{u}) = m(\underline{u}) + \mathcal{E}(\underline{u})$. The error analysis for the fixed part $m(\underline{u})$ in CBP algorithm has been done by Munshi (1988). Here, we consider the random part, $\mathcal{E}(\underline{u}) = Z(\underline{u}) - m(\underline{u})$ only. Thus without loss of generality we assume that $E\, Z(\underline{u}) = 0$, $\forall\ \underline{u} \in \mathbb{R}^2$. Also then, the product moment function is the covariance kernel $C_{\mathcal{Z}}(\underline{u}, \underline{v})$.

THEOREM 2.1.1: Let $\mathcal{Z}$ be a spatial stochastic process invariant under translations and rotations. Then if $E\, Z(\underline{u})$ and $E(\, Z(\underline{u}).\, Z(\underline{v})\,)$ exist, the process $\mathcal{Z}$ is second order wide sense stationary.

PROOF: We have to prove that $C_{\mathcal{Z}}(\underline{u}, \underline{v})$ is a function only of the distance $d = \| \underline{u} - \underline{v} \|$ between the points $\underline{u}$ and $\underline{v}$. Now,

$$C_{\mathcal{Z}}(\underline{u}, \underline{v}) = E\left(Z(\underline{u}).\ Z(\underline{v}) \right)$$

$$= \int_{\mathcal{Z}} Z(\underline{u}).\ Z(\underline{v})\ dP(Z)$$

$$= \int_{\mathcal{Z}} Z(\underline{u}).\ R_{\underline{u},\,\theta} Z(\underline{v})\ dP\ (R_{\underline{u},\,\theta} Z)$$

$$= \int_{\mathcal{Z}} Z(\underline{u}).\ \left[\frac{1}{2\pi} \int_{0}^{2\pi} R_{\underline{u},\,\theta} Z(\underline{v})\ d\theta \right] dP(Z)$$

$$= \int_{\mathcal{Z}} Z(\underline{u}).\ Z_{d,\,\bar{\theta}}\ Z(\underline{v})\ dP(Z)$$

$$= \int_{\mathcal{Z}} Z(\underline{u} + \underline{c}).\ Z_{d,\,\bar{\theta}}\ Z(\underline{v} + \underline{c})\ dP\ (T_{\underline{c}}\ Z)$$

$$= \int_{\mathcal{Z}} Z(\underline{u}').\ Z_{d,\,\bar{\theta}}\ Z(\underline{v}')\ dP(Z)\ ,$$

where $\underline{u}' = \underline{u} + \underline{c}$, $\underline{v}' = \underline{v}' + \underline{c}$. Now $d = \| \underline{u}' - \underline{v}' \|$, i.e,

distance between points $\underline{u}'$ and $\underline{v}'$. Hence $C_{\mathcal{Z}}(\underline{u}, \underline{v})$ is a function of d only.

2.2 THE ERROR IN CBP ALGORITHM

The discrete implementation of the CBP algorithm as given by Lewitt (1983) involves three kinds of errors. Firstly, the object function Z is supposed to be a sample realization of the process $\mathcal{Z}$, and the reconstructed image $\tilde{Z}$ by CBP algorithm is also of statistical nature. Thus a random error $Z - \tilde{Z}$ in reconstruction is introduced. A measure of this statistical error in reconstruction is the expected squared error (ESE) $E(Z - \tilde{Z})^2 = E^2_{\mathcal{Z}}$.

Besides the inherent statistical error there are two types of discretization errors as explained in the following:

Suppose that the image is discretized on MxN pixels, and the projection data $p(s, \theta)$ is available for K rays and L views. Let Δs and $\Delta\theta$ be the ray and the angular spacings respectively. Then

$$\tilde{Z}(m\Delta x_1, n\Delta x_2) \cong \Delta\theta \sum_{l=1}^{L} \tilde{p}(s', \theta_l), \qquad \ldots (2.2.1)$$

where, $s' = m\,\Delta x_1 \cos\theta_l + n\,\Delta x_2 \sin\theta_l$. The values of $p(s', \theta_l)$, the convolved projection data, are required for each of MxN points $(m\Delta x_1, n\Delta x_2)$, $0 < m \leq M$, $0 < n \leq N$. For

large number of rays, a practical approach is to evaluate $\tilde{p}(k\Delta s, \theta_l)$ for $K^- \leq k \leq K^+$ and then use "inexpensive" interpolation to estimate the required MxN values of $\tilde{p}$ from these K calculated values. Thus the convolution in (1.3.4) is approximated by two operations on discrete data, a discrete convolution for $K^- \leq k \leq K^+$

$$\tilde{p}_c(k'\Delta s, \theta_l) = (\Delta s) \sum_{k=K^-}^{K^+} p(k\Delta s, \theta_l)\, q(\Delta s\,(k' - k)) \qquad .....(2.2.1)$$

followed by an interpolation operation

$$\tilde{p}_I(s', \theta_l) = (\Delta s) \sum_{k'} \tilde{p}_c(k'\Delta s, \theta_l)\, I(s' - k'\Delta s) \qquad ...(2.2.3)$$

where I(s) is an interpolating function and the number of terms in sum depends on the width of non-zero part of I(s). For example, the mid-point interpolation takes only two points for summation. In practice popular interpolation schemes are the linear interpolation and nearest neighbour interpolation schemes.

We note that the discrete convolution makes use of equispaced projection data.

So the errors in reconstruction by CBP at a point $\underline{x} \in \mathbb{R}^2$ are given as:—

(i) The expected squared error (ESE) denoted by $E^2_{\mathcal{Z}}$:

$$E^2_{\mathcal{Z}}(x) = E_{\mathcal{Z}}(Z(\underline{x}) - \tilde{Z}(\underline{x}))^2$$

where $\tilde{Z}(\underline{x})$ is same as $\tilde{f}$ in (1.3.4) with Cartesian co-ordinates (x_1, x_2) instead of polar co-ordinates (r, ϕ). The ESE $E^2_{\mathcal{Z}}$ depends only on the finite Fourier frequency cut-off R_c. It can be made zero in the case of R_c-band limited projection data with window function $W(R) = 1$ for $R \in [-R_c, R_c]$ and $W(R) = 0$ for $|R| > R_c$. Our analysis in this thesis is for this error $E^2_{\mathcal{Z}}$.

(ii) The convolution error E_c, which is due to discrete implementation of the convolution integral in which interpolation also takes place. However, this error can be made arbitrarily small by taking a large number of rays.

(iii) The Backprojection error E_B, which is due to discretization of the backprojection integral. This error can also be made arbitrarily small by taking large number of views and rays.

So the total error in the reconstruction at point $\underline{x} \in \mathbb{R}^2$, using CBP algorithm is a combination of these three errors $E^2_{\mathcal{Z}}$, E_c and E_B of which $E^2_{\mathcal{Z}}$ is inherent in the process while E_c and E_B can be kept under control.

2.3 WINDOW FUNCTIONS

The window functions considered are of the form

$$W_A(R) = W(R / A)$$

where W is a fixed function and A is the same as R_c.

Let

$$K(\underline{x}) = \int_{-\infty}^{\infty}\int_{-\infty}^{\infty} W(R)\, e^{i2\pi (\underline{x}'\underline{X})}\, d\underline{X}$$

Then,

$$W(R) = \int_{-\infty}^{\infty}\int_{-\infty}^{\infty} K(\underline{x})\, e^{-i2\pi (\underline{x}'\underline{X})}\, d\underline{x}\ , \qquad \ldots.(2.3.1)$$

where $R = \| \underline{X} \|$.

For polar co-ordinate (r, ϕ) of $\underline{x}$,

$$K(r\cos\phi,\ r\sin\phi) = \int_{0}^{\pi}\int_{-\infty}^{\infty} W(R)\, e^{i2\pi Rr\cos(\theta - \phi)}\, |R|\, dR\, d\theta \qquad (2.3.2)$$

Using (2.3.2) in (1.3.4) we get

$$K(r\cos\phi,\ r\sin\phi) = \int_{0}^{\pi} q(r\cos(\theta - \phi))\, d\theta \qquad \ldots(2.3.3)$$

As we know that W(R) is a radially symmetric function and that the FT of a radially symmetric function is also radially symmetric, the function $K(r\cos\phi,\ r\sin\phi)$ is radially symmetric. Therefore, without loss of generality, we may take $\phi = 0$. Thus (2.3.3) reduces to,

$$K(r) = \int_0^{\pi} q(r \cos\theta)\, d\theta$$

$$= (W)^{\vee}(r)$$

i.e., K is inverse FT of W.

Writing $K_A(r) = (W_A)^{\vee}(R)$, we have,

$$K_A(r) = A^2 K(Ar)$$

Hence we have,

$$\tilde{Z}(\underline{x}) = (\hat{p}\, W)^{\vee}(\underline{x})$$

$$= (\hat{Z}\, \hat{K})^{\vee}(\underline{x})$$

$$= (Z * K)(\underline{x})$$

and with K replaced by K_A,

$$Z_A(\underline{x}) = (Z * K_A)(\underline{x}) \qquad \ldots(2.3.4)$$

Thus, $\mathcal{Z}_A = \{ Z_A(\underline{x}) : \underline{x} \in \mathbb{R}^2 \}$, the ensemble of all reconstructed images using CBP algorithm is also a spatial stochastic process.

2.4 VARIOUS SPACES

For a real valued function g on $\mathbb{R}^2$, we define,

$$g_{r,\phi}(\underline{x}) = g(x_1 + r\cos\phi,\ x_2 + r\sin\phi),$$

where $r \in [0, \infty)$, $\phi \in [0, \pi]$ and $\underline{x} \in \mathbb{R}^2$.

Let

$$g_{r,\bar{\phi}}(\underline{x}) = \frac{1}{2\pi}\int_0^{2\pi} g_{r,\phi}(\underline{x})\, d\phi,$$

provided $g_{r,\phi}(\underline{x})$ is integrable with respect to ϕ.

DEFINITION 2.4.1 The k-th radial derivative of function $g_{r,\bar{\phi}}(\underline{x})$ is given by

$$D^k_{r,\bar{\phi}}\, g(\underline{x}) = \frac{\partial^k}{\partial r^k} g_{r,\bar{\phi}}(\underline{x}), \qquad \forall\ r \geq 0,\ \underline{x} \in \mathbb{R}^2, \text{ and } k = 0,1,2,\ldots$$

Whenever interchange of the order of integration and differentiation is permissible,

$$D^k_{r,\bar{\phi}}\, g(\underline{x}) = \frac{1}{2\pi}\int_0^{2\pi} \frac{\partial^k}{\partial r^k}\, g_{r,\phi}(\underline{x})\, d\phi.$$

Let p be a positive integer. In order to further develop the theory we define the following spaces:—

DEFINITION 2.4.2 The Space Ω_{4p} is the class of all bounded and continuous real valued functions g on $\mathbb{R}^2$, for which $g_{r,\bar{\phi}}(\underline{x})$ is 4p times continuously differentiable function of $r \in [0, \infty)$, and $D^k_{r,\bar{\phi}}\, g(\underline{x})$ are bounded and continuous

functions of $(r, \underline{x})$ in $\mathbb{R}^+ \times \mathbb{R}^2$ for $k=1,2,\ldots,4p$.

DEFINITION 2.4.3 The Space $\mathcal{Z}_0$ is the class of all second order wide sense stationary spatial stochastic processes such that $C_{\mathcal{Z}}(\underline{x})$ is a bounded and continuous function on $\mathbb{R}^2$, with the norm

$$\| C_{\mathcal{Z}} \|_0 = \| C_{\mathcal{Z}} \|_c = \sup_{\underline{x} \in \mathbb{R}^2} | C_{\mathcal{Z}}(\underline{x}) |$$

Note that $\| C_{\mathcal{Z}} \|_0 = \text{var } Z(\underline{x}) = C_{\mathcal{Z}}(\underline{0})$, a quantity independent of $\underline{x}$.

DEFINITION 2.4.4 The Space $\mathcal{Z}_{4p}$ is the class of all second order wide sense stationary spatial stochastic processes, such that $C_{\mathcal{Z}}(\underline{x})$ belongs to the class Ω_{4p}. The norm in $\mathcal{Z}_{4p}$ is defined as

$$\| C_{\mathcal{Z}} \|_{4p} = \| C_{\mathcal{Z}} \|_c + \| D^{4p}_{r, \underline{\phi}} C_{\mathcal{Z}} \|_c$$

DEFINITION 2.4.5 The Space $\mathbb{K}_{2p}$ is the class of all radially symmetric functions $K(r)$, satisfying:

$$\text{(i)} \qquad \int_0^\infty | r^j K(r) | \, dr = \int_0^\infty r^j | K(r) | \, dr < \infty$$

$$\forall \; j = 1,2,\ldots,4p+1.$$

(ii) $2\pi \int_0^\infty r\, K(r)\, dr = 1$

(iii) $\int_0^\infty r^{2j+1} K(r)\, dr = 0 \qquad \forall\ j = 1,\ldots,(p-1).$

(iv) $\int_0^\infty r^{2p+1} K(r)\, dr = A_{2p} \neq 0.$

and $K(\underline{x}) = K(\|\underline{x}\|) \in \Omega_{4p}$.

DEFINITION 2.4.6 The Peetre's functional $K_p(t^{4p}, \mathcal{Z})$ is defined as follows:

$$K_p(t^{4p}, \mathcal{Z}) = \inf\left\{ \| C_{\mathcal{Z}_0} \|_0 + t^{4p} \| C_{\mathcal{Z}_{4p}} \|_{4p} : \mathcal{Z} = \mathcal{Z}_0 + \mathcal{Z}_{4p} \right\}$$

where $\mathcal{Z}_0 \in \mathcal{S}_0$, $\mathcal{Z}_{4p} \in \mathcal{S}_{4p}$, $t \in \mathbb{R}$.

DEFINITION 2.4.7 For $0 \leq \beta \leq 4p$, the Space $\mathcal{S}_{4p}^{\beta}$ is a space intermediate between spaces $\mathcal{S}_0$ and $\mathcal{S}_{4p}$, which we call an "interpolation space". It is the class of all such second order wide sense stationary spatial stochastic processes $\mathcal{Z}$

belonging to $\mathcal{E}_0$, which can be decomposed in two second order wide sense stationary spatial stochastic processes, such that one of them (say, $\mathcal{Z}_0$) belongs to $\mathcal{E}_0$ and the other (say, $\mathcal{Z}_{4p}$) belongs to $\mathcal{E}_{4p}$ and such that $t^{-\beta} K_P (t^{4p}, \mathcal{Z})$ is bounded.

REMARK : Note that $\mathcal{E}_{4p}^{\beta}$ is not empty unless $\mathcal{E}_0$ is empty, because any spatial stochastic process $\mathcal{Z}$ in $\mathcal{E}_0$ can be trivially decomposed as $\mathcal{Z} = \mathcal{Z} + 0$, where 0 is the zero-valued spatial stochastic process which obviously belongs to $\mathcal{E}_{4p}$.

2.5 SOME PRELIMINARY RESULTS

LEMMA 2.5.1 If $\mathcal{Z}$ is second order wide sense stationary spatial stochastic process, then $\mathcal{Z}_A$ is also second order wide sense stationary spatial process.

PROOF:— Using definition of $\mathcal{Z}_A$ as in (2.3.4)

$$E (Z_A (\underline{x}) . Z_A (\underline{y}))$$

$$= E \int_{\mathbb{R}^2}\int_{\mathbb{R}^2} Z (\underline{u}) Z (\underline{v}) K_A (\underline{x} - \underline{u}) K_A (\underline{y} - \underline{v}) d\underline{u} d\underline{v}$$

$$= E \int_{\mathbb{R}^2}\int_{\mathbb{R}^2} Z (\underline{u}) Z (\underline{u} + \underline{w}) K_A (\underline{x} - \underline{u}) K_A (\underline{y} - \underline{u} - \underline{w}) d\underline{u} d\underline{w}$$

$$= \int_{\mathbb{R}^2}\int_{\mathbb{R}^2} E\, Z(\underline{u})\, Z(\underline{u}+\underline{w})\, K_A(\underline{x}-\underline{u})\, K_A(\underline{y}-\underline{u}-\underline{w})\, d\underline{u}\, d\underline{w}$$

$$= \int_{\mathbb{R}^2}\int_{\mathbb{R}^2} C_{\mathcal{Z}}(\|\underline{w}\|)\, K_A(\underline{x}-\underline{u})\, K_A(\underline{y}-\underline{u}-\underline{w})\, d\underline{u}\, d\underline{w}$$

$$= \int_{\mathbb{R}^2}\int_{\mathbb{R}^2} C_{\mathcal{Z}}(\|\underline{w}\|)\, K_A(\underline{x}-\underline{y}-\underline{v})\, K_A(-\underline{v}-\underline{w})\, d\underline{v}\, d\underline{w}$$

$$= \int_{\mathbb{R}^2} h(\underline{v})\, K_A(\underline{x}-\underline{y}-\underline{v})\, d\underline{v}$$

$$= h_A(\underline{x}-\underline{y}), \text{ (say)}$$

where

$$h(\underline{v}) = \int_{\mathbb{R}^2} C_{\mathcal{Z}}(\|\underline{w}\|)\, K_A(\underline{v}+\underline{w})\, d\underline{w}.$$

For stationarity it is necessary to show that

$$h_A(\underline{x}-\underline{y}) = h_A(\|\underline{x}-\underline{y}\|).$$

First, we will show $h(\underline{v}) = h(\|\underline{v}\|)$

Let $\underline{v} = (v \cos \theta, v \sin \theta)$, $v = \| \underline{v} \|$, $\theta = \tan^{-1}(v_2 / v_1)$,

and $\underline{w} = (w \cos \phi, w \sin \phi)$, $w = \| \underline{w} \|$, $\phi = \tan^{-1}(w_2 / w_1)$.
Using these notations, $h (\underline{v})$ can be written as

$$h (\underline{v}) = \int_0^{2\pi} \int_0^{\infty} C_{\mathcal{Z}} (w) \cdot K_A(w\cos \phi + v \cos \theta, w\sin \phi + v \sin \theta)w \, dw \, d\phi$$

$$= \int_0^{2\pi} \int_0^{\infty} C_{\mathcal{Z}} (w) \cdot K_A(v + w\cos (\phi - \theta), v + w\sin (\phi - \theta))w \, dw \, d\phi$$

$$= h (v) = h (\| \underline{v} \|).$$

Similarly,

$$h_A (\underline{x} - \underline{y}) = \int_{\mathbb{R}^2} h (\| \underline{v} \|) K_A (\underline{x} - \underline{y} - \underline{v}) \, d\underline{v}$$

$$= h_A (\| \underline{x} - \underline{y} \|).$$

Hence $E (Z_A (\underline{x}) . Z_A (\underline{y}))$ depends only on the distance between $\underline{x}$ and $\underline{y}$, i.e., $\mathcal{Z}_A$ is second order wide sense stationary spatial stochastic process.

DEFINITION 2.5.1 The difference process $\mathcal{Z} - \mathcal{Z}_A$ is defined as

$$\mathcal{Z} - \mathcal{Z}_A = \{ Z(\underline{x}) - Z_A(\underline{x}) : \underline{x} \in \mathbb{R}^2 \},$$

for $Z \in \mathcal{Z}$, and $Z_A \in \mathcal{Z}_A$.

LEMMA 2.5.2 If $\mathcal{Z}$ is second order wide sense stationary spatial stochastic process, then $\mathcal{Z} - \mathcal{Z}_A$ is also second order wide sense stationary spatial stochastic process.

PROOF:- $E(Z(\underline{x}) \; Z_A(\underline{x} + \underline{u}))$

$$= E \int_{\mathbb{R}^2} Z(\underline{x}) Z(\underline{x} + \underline{u} - \underline{v}) K_A(\underline{v}) \, d\underline{v}$$

$$= \int_{\mathbb{R}^2} E(Z(\underline{x}) Z(\underline{x} + \underline{u} - \underline{v})) K_A(\underline{v}) \, d\underline{v}$$

$$= \int_{\mathbb{R}^2} C_{\mathcal{Z}}(\| \underline{u} - \underline{v} \|) K_A(\underline{v}) \, d\underline{v}$$

Let $\underline{u} = (r \cos\theta, r \sin\theta)$, and $\underline{v} = (v \cos\phi, v \sin\phi)$.

Then

$$E\left(Z(\underline{x}) \right) . Z_A(\underline{x} + \underline{u}) \Big)$$

$$= \int_{0}^{2\pi} \int_{0}^{\infty} C_{\mathcal{Z}}(r - v\cos(\phi - \theta), r - v\sin(\phi - \theta)) . K_A(v)\, v\, dv\, d\phi$$

$$= g_1(\| \underline{u} \|), \text{ (say), a function of r only.}$$

Similarly,

$$E\left(Z_A(\underline{x}) Z(\underline{x} + \underline{u}) \right) = g_2(\| \underline{u} \|), \text{ (say).}$$

By Lemma 2.5.1, $\mathcal{Z}_A$ is second order wide sense stationary spatial stochastic process. Hence

$$E\left((Z - Z_A)(\underline{x}) (Z - Z_A)(\underline{x} + \underline{u}) \right)$$

$$= E\left(Z(\underline{x}) Z(\underline{x} + \underline{u}) \right) + E\left(Z_A(\underline{x}) Z_A(\underline{x} + \underline{u}) \right)$$

$$- E\left(Z(\underline{x}) Z_A(\underline{x} + \underline{u}) \right) - E\left(Z_A(\underline{x}) Z(\underline{x} + \underline{u}) \right)$$

$$= C_{\mathcal{Z}}(\| \underline{u} \|) + C_{\mathcal{Z}_A}(\| \underline{u} \|) - g_1(\| \underline{u} \|)$$

$$- g_2(\| \underline{u} \|) \qquad \forall\ \underline{x} \in \mathbb{R}^2,\ \underline{u} \in \mathbb{R}^2,$$

which is a function of $\| \underline{u} \|$ only.

Hence $\mathcal{Z} - \mathcal{Z}_A$ is second order wide sense stationary spatial

stochastic process.

REMARK: Since $\mathcal{Z} - \mathcal{Z}_A$ is a second order wide sense stationary spatial stochastic process, the ESE

$$E^2_{\mathcal{Z}} = E\,(Z - Z_A)^2\,(\underline{x}) = E\left[(Z - Z_A)(\underline{x})\,(Z - Z_A)\,(\underline{x})\right]$$

is independent of point $\underline{x} \in \mathbb{R}^2$. As it depends on R_c or A, it will be denoted by $E^2_A(\mathcal{Z})$ now onwards.

CHAPTER 3

DIRECT THEOREMS

3.1 INTRODUCTION

In chapter 2 three types of errors in reconstruction of an object image by CBP algorithm were defined. In this thesis our main emphasis will be on the theoretical estimates of the ESE, $E_A^2 (\mathcal{Z})$.

In this chapter we will discuss some direct estimates of the ESE for the object stochastic processes belonging to the classes defined in section 2.4. It is assumed that window functions used in the reconstruction by CBP, belong to the class $\mathbb{K}_{2p}$.

The results established here use the derivatives of the covariance kernel of the object stochastic process and a modulus of continuity, which is appropriate for the analysis of ESE in CBP, i.e.,

$$\omega_c (C_{\mathcal{Z}}^{[k]} ; \delta) = \sup_{\substack{0<|h|<\delta \\ \underline{x} \in \mathbb{R}^2}} | D_{h_1}^k, \bar{\phi} \, C_{\mathcal{Z}} (\underline{x}) - D_{h_2}^k, \bar{\phi} \, C_{\mathcal{Z}} (\underline{x}) | \qquad .....(3.1.1)$$

where $h = h_1 - h_2$, and $h_1, h_2 \in \mathbb{R}^+$.

3.2 LEMMAS

Some lemmas are given here which will be needed for proving the direct theorems.

LEMMA 3.2.1

$$\lim_{\delta \to 0} \omega_c \left(C_{\mathbb{R}}^{[k]} ; \delta \right) = 0 \text{ if and only if}$$

$$\lim_{|h| \to 0} D_{h_1}^k \bar{\phi} \, C_{\mathbb{R}}(\underline{x}) = D_{h_2}^k \bar{\phi} \, C_{\mathbb{R}}(\underline{x}) \quad \text{for every } x \in \mathbb{R}^2.$$

This result is evident from the definition of $\omega_c \left(C_{\mathbb{R}}^{[k]} ; \delta \right)$. Similarly another easy consequence of definition is

LEMMA 3.2.2 $\delta_1 \leq \delta_2$ implies that

$$\omega_c \left(C_{\mathbb{R}}^{[k]} ; \delta_1 \right) \leq \omega_c \left(C_{\mathbb{R}}^{[k]} ; \delta_2 \right)$$

for $k = 0,1,2,\ldots$.

LEMMA 3.2.3 For any λ and $\delta \geq 0$, we have

$$\omega_c \left(C_{\mathbb{R}}^{[k]} ; \lambda\delta \right) \leq (1 + \lambda) \, \omega_c \left(C_{\mathbb{R}}^{[k]} ; \delta \right)$$

PROOF:-

Without loss of generality it suffices to prove the Lemma for the case $h_1 > h_2$, $h_1, h_2 \in \mathbb{R}^+$. We have from lemma 3.2.2

$$\omega_c \left(C_{\mathcal{Z}}^{[k]} ; \lambda\delta \right) \leq \omega_c \left(C_{\mathcal{Z}}^{[k]} ; (1 + [\lambda])\,\delta \right)$$

Now, we have, with $h = h_1 - h_2$

$$\omega_c \left(C_{\mathcal{Z}}^{[k]} ; (1 + [\lambda])\,\delta \right)$$

$$= \sup_{\substack{0 < h < (1+[\lambda])\,\delta \\ \underline{x} \in \mathbb{R}^2}} \left| D^k_{h_1, \bar{\phi}} C_{\mathcal{Z}}(\underline{x}) - D^k_{h_2, \bar{\phi}} C_{\mathcal{Z}}(\underline{x}) \right|$$

$$= \sup_{\substack{0 < h < (1+[\lambda])\,\delta \\ \underline{x} \in \mathbb{R}^2}} \left| D^k_{h_2+h, \bar{\phi}} C_{\mathcal{Z}}(\underline{x}) - D^k_{h_2, \bar{\phi}} C_{\mathcal{Z}}(\underline{x}) \right|$$

$$= \max_{1 \leq j \leq 1+[\lambda]} \left\{ \sup_{\substack{(j-1)\,\delta < h < j\,\delta \\ \underline{x} \in \mathbb{R}^2}} \left| D^k_{h_2+h, \bar{\phi}} C_{\mathcal{Z}}(\underline{x}) - D^k_{h_2, \bar{\phi}} C_{\mathcal{Z}}(\underline{x}) \right| \right\}$$

$$= \max_{1 \leq j \leq 1+[\lambda]} \left\{ \sup_{\substack{0 < h < \delta \\ \underline{x} \in \mathbb{R}^2}} \left| D^k_{h_2+jh, \bar{\phi}} C_{\mathcal{Z}}(\underline{x}) - D^k_{h_2+(j-1)h, \bar{\phi}} C_{\mathcal{Z}}(\underline{x}) \right| \right\}$$

$$\leq \sum_{j=1}^{1+[\lambda]} \left\{ \sup_{\substack{0 < h < \delta \\ \underline{x} \in \mathbb{R}^2}} \left| D^k_{h_2+jh, \bar{\phi}} C_{\mathcal{Z}}(\underline{x}) - D^k_{h_2+(j-1)h, \bar{\phi}} C_{\mathcal{Z}}(\underline{x}) \right| \right\}$$

$$= (1 + [\lambda])\, \omega_c \left(C_{\mathcal{Z}}^{[k]} ; \delta \right)$$

$$\leq (1 + \lambda)\, \omega_c \left(C_{\mathcal{Z}}^{[k]} ; \delta \right).$$

LEMMA 3.2.4 The integral-type remainder in Taylor's expansion is given by

$$C_{\mathcal{Z},\, r,\, \bar{\phi}}\,(\underline{x}) - \sum_{j=0}^{k} \frac{r^j}{j!}\, D^j_{0,\, \bar{\phi}}\, C_{\mathcal{Z}}\,(\underline{x})$$

$$= \frac{1}{(k-1)!} \int_0^r \left\{ D^k_{s,\, \bar{\phi}}\, C_{\mathcal{Z}}\,(\underline{x}) - D^k_{0,\, \bar{\phi}}\, C_{\mathcal{Z}}\,(\underline{x}) \right\} (r-s)^{k-1}\, ds.$$

3.3 THE ω_c- ESTIMATE

For a second order wide sense spatial stationary process $\mathcal{Z}$, the following theorem relates the ESE $E_A^2(\mathcal{Z})$ to the smoothness of the covariance kernel $C_{\mathcal{Z}}$. This thoerem gives an estimate of ESE for the cross-sections belonging to those processes which have derivatives of covariance kernel with ω_c property i.e. $\omega_c(C_{\mathcal{Z}}^{[k]}; \delta) \longrightarrow 0$ as $\delta \longrightarrow 0$.

THEOREM:

Let the CBP window $K \in \mathbb{K}_{2p}$. Then for $k = 0,1,\ldots,(4p-1)$

$$E_A^2(\mathcal{Z}) \leq \frac{B_k}{A^k}\, \omega_c\left(C_{\mathcal{Z}}^{[k]}; \frac{1}{A}\right)$$

where B_k is a positive constant independent of $\mathcal{Z}$ and A;

provided

$$\omega_c \left(C_{\mathscr{Z}}^{[k]} ; \delta \right) \longrightarrow 0 \quad (\delta \longrightarrow 0)$$

PROOF:

$$E_A^2 (\mathscr{Z}) = E (Z_A - Z)^2 (\underline{x})$$

$$= E \int_0^{2\pi} \int_0^{2\pi} \int_0^{\infty} \int_0^{\infty} (Z(x_1 - \frac{r}{A} \cos \theta, x_2 - \frac{r}{A} \sin \theta) - Z(x_1, x_2)).$$

$$(Z(x_1 - \frac{s}{A} \cos \phi, x_2 - \frac{s}{A} \sin \phi) - Z(x_1, x_2)).$$

$$r\, K(r)\, s\, K(s)\, dr\, ds\, d\theta\, d\phi$$

$$= \int_0^{2\pi} \int_0^{2\pi} \int_0^{\infty} \int_0^{\infty} E (Z (x_1 - \frac{r}{A} \cos \theta, x_2 - \frac{r}{A} \sin \theta).$$

$$Z (x_1 - \frac{s}{A} \cos \phi, x_2 - \frac{s}{A} \sin \phi)$$

$$- Z (x_1 - \frac{r}{A} \cos \theta, x_2 - \frac{r}{A} \sin \theta). Z (x_1, x_2)$$

$$- Z (x_1 - \frac{s}{A} \cos \phi, x_2 - \frac{s}{A} \cos \phi). Z (x_1, x_2)$$

$$+ Z (x_1, x_2)\, Z (x_1, x_2)).$$

$$r\, K(r)\, s\, K(s)\, dr\, ds\, d\theta\, d\phi$$

$$= \int_0^{2\pi} \int_0^{2\pi} \int_0^{\infty} \int_0^{\infty} \left[C_{\mathscr{Z}} ((r^2 + s^2 - 2rs \cos (\theta - \phi))^{1/2} / A \right.$$

$$- C_{\mathcal{Z}}(r/A) - C_{\mathcal{Z}}(s/A) + C_{\mathcal{Z}}(0) \Big]$$

$$r\, K(r)\, s\, K(s)\, dr\, ds\, d\theta\, d\phi$$

$$= 2\pi \int_0^{2\pi}\int_0^{\infty}\int_0^{\infty} \Big[C_{\mathcal{Z}}((r^2 + s^2 - 2rs\cos\theta)^{1/2} / A)$$

$$- C_{\mathcal{Z}}(r/A) - C_{\mathcal{Z}}(s/A) + C_{\mathcal{Z}}(0) \Big]$$

$$r\, K(r)\, s\, K(s)\, dr\, ds\, d\theta$$

Using Taylor's expansion given in Lemma 3.2.4, for

$C_{\mathcal{Z}}(\cdot/A) = C_{\mathcal{Z}, \cdot/A}(\underline{0})$,

$$E_A^2(\mathcal{Z}) = 2\pi \int_0^{2\pi}\int_0^{\infty}\int_0^{\infty} \Big[\sum (1/A^j j!) \Big[(r^2 + s^2 - 2rs\cos\theta)^{j/2}$$

$$- r^j - s^j \Big] D^j_{0,\bar{\phi}}\, C_{\mathcal{Z}}(\underline{0}) \Big].$$

$$r\, K(r)\, s\, K(s)\, dr\, ds\, d\theta$$

$$+ \frac{2\pi}{(k-1)!} \int_0^{2\pi}\int_0^{\infty}\int_0^{\infty}\Big[\int_0^{\rho/A} (D^k_{t,\bar{\phi}}\, C_{\mathcal{Z}}(\underline{0}) - D^k_{0,\bar{\phi}}\, C_{\mathcal{Z}}(\underline{0}))$$

$$(\tfrac{\rho}{A} - t)^{k-1}\, dt$$

$$+ \int_0^{r/A} \left(D^k_{t,\,\bar{\phi}}\, C_{\mathcal{Z}}(\underline{0}) - D^k_{0,\,\bar{\phi}}\, C_{\mathcal{Z}}(\underline{0}) \right) \left(\frac{r}{A} - t \right)^{k-1} dt$$

$$+ \int_0^{s/A} \left(D^k_{t,\,\bar{\phi}}\, C_{\mathcal{Z}}(\underline{0}) - D^k_{0,\,\bar{\phi}}\, C_{\mathcal{Z}}(\underline{0}) \right) \left(\frac{s}{A} - t \right)^{k-1} dt \Bigg) .$$

$$r\, K(r)\, s\, K(s)\, dr\, ds\, d\theta ,$$

where $\rho^2 = r^2 + s^2 - 2rs \cos\theta$.

Since $C_{\mathcal{Z}}(\underline{x}) = C_{\mathcal{Z}}(\| \underline{x} \|)$ is an even function of $\| \underline{x} \|$, $D^k_{0,\,\bar{\phi}}\, C_{\mathcal{Z}}(\underline{x})$ will be zero for k odd, and since $K \in \mathbb{K}_{2p}$

$$E^2_A(\mathcal{Z}) = | E^2_A(\mathcal{Z}) |$$

$$= \left| \frac{2\pi}{(k-1)!} \int_0^{2\pi} \int_0^{\infty} \int_0^{\infty} \left(\int_0^{\rho/A} \left(D^k_{t,\,\bar{\phi}}\, C_{\mathcal{Z}}(\underline{0}) - D^k_{0,\,\bar{\phi}}\, C_{\mathcal{Z}}(\underline{0}) \right) \right.\right.$$

$$\left(\frac{\rho}{A} - t \right)^{k-1} dt$$

$$+ \int_0^{r/A} \left(D^k_{t,\,\bar{\phi}}\, C_{\mathcal{Z}}(\underline{0}) - D^k_{0,\,\bar{\phi}}\, C_{\mathcal{Z}}(\underline{0}) \right) \left(\frac{r}{A} - t \right)^{k-1} dt$$

$$+ \int_0^{s/A} \left(D^k_{t,\bar{\phi}}\, C_{\mathcal{Z}}(\underline{0}) - D^k_{0,\bar{\phi}}\, C_{\mathcal{Z}}(\underline{0}) \right) \left(\frac{s}{A} - t \right)^{k-1} dt \Big] .$$

$$r\, K(r)\, s\, K(s)\, dr\, ds\, d\theta \Big|$$

$$\leq \frac{2\pi}{(k-1)!} \int_0^{2\pi} \int_0^{\infty} \int_0^{\infty} \Big(\int_0^{\rho/A} \Big| D^k_{t,\bar{\phi}}\, C_{\mathcal{Z}}(\underline{0}) - D^k_{0,\bar{\phi}}\, C_{\mathcal{Z}}(\underline{0}) \Big| .$$

$$\Big| \frac{\rho}{A} - t \Big|^{k-1} dt$$

$$+ \int_0^{r/A} \Big| D^k_{t,\bar{\phi}}\, C_{\mathcal{Z}}(\underline{0}) - D^k_{0,\bar{\phi}}\, C_{\mathcal{Z}}(\underline{0}) \Big| \Big| \frac{r}{A} - t \Big|^{k-1} dt$$

$$+ \int_0^{s/A} \Big| D^k_{t,\bar{\phi}}\, C_{\mathcal{Z}}(\underline{0}) - D^k_{0,\bar{\phi}}\, C_{\mathcal{Z}}(\underline{0}) \Big| \Big| \frac{s}{A} - t \Big|^{k-1} dt \Big] .$$

$$r\, K(r)\, K(s)\, dr\, ds\, d\theta \qquad \ldots(3.3.1)$$

Now, the integrand in (3.3.1) is

$$\leq \omega_c \left(C^{[k]}_{\mathcal{Z}} ; \frac{\rho}{A} \right) \int_0^{\rho/A} \left(\frac{\rho}{A} - t \right)^{k+1} dt + \omega_c \left(C^{[k]}_{\mathcal{Z}} ; \frac{r}{A} \right)$$

$$\int_0^{r/A} \left(\frac{r}{A} - t\right)^{k-1} dt + \omega_c\left(C_{\mathcal{X}}^{[k]}; \frac{s}{A}\right) \int_0^{s/A} \left(\frac{s}{A} - t\right)^{k-1} dt$$

$$= \frac{1}{k}\left[\omega_c\left(C_{\mathcal{X}}^{[k]}; \frac{\rho}{A}\right)\left(\frac{\rho}{A}\right)^k + \omega_c\left(C_{\mathcal{X}}^{[k]}; \frac{r}{A}\right)\left(\frac{r}{A}\right)^k + \omega_c\left(C_{\mathcal{X}}^{[k]}; \frac{s}{A}\right)\left(\frac{s}{A}\right)^k\right]$$

$$\leq \frac{1}{kA^k}\left[(1+\rho)\rho^k + (1+r)r^k + (1+s)s^k\right] \cdot \omega_c\left(C_{\mathcal{X}}^{[k]}; \frac{1}{A}\right), \qquad \text{(by Lemma 3.2.3)}$$

Hence,

$$E_A^2(\mathcal{X}) \leq \frac{2\pi}{k!\,A^k}\,\omega_c\left(C_{\mathcal{X}}^{[k]}; \frac{1}{A}\right).$$

$$\left[\int_0^{2\pi}\int_0^{\infty}\int_0^{\infty} \left((1+\rho)\rho^k + (1+r)r^k + (1+s)s^k\right) r\,|K(r)|\,s\,|K(s)|\,dr\,ds\,d\theta\right]$$

$$\leq \frac{2\pi}{k!\,A^k}\,\omega_c\left(C_{\mathcal{X}}^{[k]}; \frac{1}{A}\right).$$

$$\left[\int_0^{2\pi}\int_0^{\infty}\int_0^{\infty} \left(r^2+s^2-2rs\cos\theta\right)^{k/2}\right.$$

$$+(r^2+s^2-2rs\cos\theta)^{(k+1)/2}\Big).$$

$$r\,|\,K(r)\,|\,s\,|\,K(s)\,|\,dr\,ds\,d\theta$$

$$+\,2\pi\int_0^\infty\int_0^\infty (\,r^{k+1}+r^k\,)\,r\,|\,K(r)\,|\,s\,|\,K(s)\,|\,dr\,ds$$

$$+\,2\pi\int_0^\infty\int_0^\infty (s^{k+1}+s^k)\,r\,|\,K(r)\,|\,s\,|\,K(s)\,|\,dr\,ds\Big\}$$

$$=\frac{B_k}{A^k}\,\omega_c\,(\,C_{\mathcal{X}}^{[k]}\,;\,\frac{1}{A}\,),$$

where

$$B_k=2\,\frac{(4\pi)^2}{k!}\int_0^\infty\int_0^\infty (\,s^{k+1}+s^k\,)\,r\,|\,K(r)\,|\,s\,|\,K(s)\,|\,dr\,ds$$

$$+\,\frac{(4\pi)}{k!}\int_0^{2\pi}\int_0^\infty\int_0^\infty\Big(\,(r^2+s^2-2rs\cos\theta)^{k/2}$$

$$+(r^2+s^2-2rs\cos\theta)^{(k+1)/2}\Big).$$

$$r\,|\,K(r)\,|\,s\,|\,K(s)\,|\,dr\,ds\,d\theta$$

Note that since $K\in\mathbb{K}_{2p}$, $B_k<\infty$.

Thus the existence of higher order derivatives of covariance

kernel with ω_c property implies less ESE, because of A^k occuring in the denominator.

3.4 ASYMPTOTIC FORMULA

The following theorem in this section gives an estimate of ESE for those spatial stationary object processes $\mathcal{Z}$ possessing a covariance kernel which is very smooth in the neighbourhood of origin.

THEOREM 3.4.1

Let $K \in \mathbb{K}_{2p}$, $\mathcal{Z} \in \mathcal{S}_0$ and suppose that $D^{4p}_{r,\bar{\phi}}\, C_{\mathcal{Z}}(\underline{x})$ exists at $\underline{x} = \underline{0}$, for $r \in [0, \infty)$. Then following asymptotic formula for ESE holds:

$$E^2_A(\mathcal{Z}) = \left[\frac{(2\pi)^2}{(4p)!}\right] \binom{2p}{p}^2 A^2_{2p}\, D^{4p}_{0,\bar{\phi}}\, C_{\mathcal{Z}}(\underline{0})\, A^{-4p} + o(A^{-4p}) \quad \text{as } (A \longrightarrow \infty).$$

PROOF: —

Since $D^{4p}_{r,\bar{\phi}}\, C_{\mathcal{Z}}(\underline{0})$ exists for $r \in [0, \infty)$. The Taylor expansion of covariance kernel $C_{\mathcal{Z},r,\bar{\phi}}(\underline{0})$ about $r = 0$ can be written as follows:

$$C_{\mathcal{Z},r,\bar{\phi}}(\underline{0}) = C_{\mathcal{Z}}(\underline{0}) + \sum_{j=1}^{4p} \frac{r^j}{j!} D^j_{0,\bar{\phi}}\, C_{\mathcal{Z}}(\underline{0}) + r^{4p}\, h_{\mathcal{Z}}(r), \qquad \ldots.(3.4.1)$$

where

$$h_{\mathcal{Z}}(r) = \left(C_{\mathcal{Z},r,\bar{\phi}}(\underline{0}) - \sum_{j=0}^{4p} \frac{r^j}{j!} D_{0,\bar{\phi}}^{j} C_{\mathcal{Z}}(\underline{0}) \right) / r^{4p}. \qquad \ldots\ldots(3.4.2).$$

We note that,

$$\lim_{r \to 0} h_{\mathcal{Z}}(r) = 0 \qquad \ldots\ldots(3.4.3)$$

and

$$\lim_{r \to \infty} h_{\mathcal{Z}}(r) \text{ exists.} \qquad \ldots\ldots(3.4.4).$$

Since $C_{\mathcal{Z},r,\bar{\phi}}(.)$ is a continuous function of r, $h_{\mathcal{Z}}(r)$ is also continuous. Hence by continuity of $h_{\mathcal{Z}}(r)$, (3.4.3) and (3.4.4), the function $h_{\mathcal{Z}}(r)$ is bounded. Let M be the bound of $h_{\mathcal{Z}}(r)$, i.e.,

$$| h_{\mathcal{Z}}(r) | < M, \text{ for } r \in [0, \infty). \qquad \ldots(3.4.5)$$

Now,

$$E_A^2(\mathcal{Z}) = E\left(Z_A - Z \right)^2 (\underline{x})$$

$$= E \int_0^{2\pi} \int_0^{2\pi} \int_0^{\infty} \int_0^{\infty} \left(Z(x_1 - \frac{r}{A}\cos\theta,\ x_2 - \frac{r}{A}\sin\theta) - Z(x_1, x_2) \right) :$$

$$\left(Z(x_1 - \frac{s}{A}\cos\phi,\ x_2 - \frac{s}{A}\sin\phi) - Z(x_1, x_2) \right)$$

$$r\,K(r)\,s\,K(s)\,dr\,ds\,d\theta\,d\phi$$

where

$$h_{\mathcal{Z}}(r) = \left(C_{\mathcal{Z},r,\bar{\phi}}(\underline{0}) - \sum_{j=0}^{4p} \frac{r^j}{j!} D^j_{\underline{0},\bar{\phi}} C_{\mathcal{Z}}(\underline{0}) \right) / r^{4p}. \qquad \ldots\ldots(3.4.2).$$

We note that,

$$\lim_{r \to 0} h_{\mathcal{Z}}(r) = 0 \qquad \ldots\ldots(3.4.3)$$

and

$$\lim_{r \to \infty} h_{\mathcal{Z}}(r) \text{ exists.} \qquad \ldots\ldots(3.4.4).$$

Since $C_{\mathcal{Z},r,\bar{\phi}}(.)$ is a continuous function of r, $h_{\mathcal{Z}}(r)$ is also continuous. Hence by continuity of $h_{\mathcal{Z}}(r)$, (3.4.3) and (3.4.4), the function $h_{\mathcal{Z}}(r)$ is bounded. Let M be the bound of $h_{\mathcal{Z}}(r)$, i.e.,

$$| h_{\mathcal{Z}}(r) | < M, \text{ for } r \in [0, \infty). \qquad \ldots(3.4.5)$$

Now,

$$E^2_A(\mathcal{Z}) = E\left(Z_A - Z \right)^2 (\underline{x})$$

$$= E \int_0^{2\pi} \int_0^{2\pi} \int_0^{\infty} \int_0^{\infty} \left(Z(x_1 - \frac{r}{A}\cos\theta,\ x_2 - \frac{r}{A}\sin\theta) - Z(x_1, x_2) \right) \cdot$$

$$\left(Z(x_1 - \frac{s}{A}\cos\phi,\ x_2 - \frac{s}{A}\sin\phi) - Z(x_1, x_2) \right)$$

$$r\, K(r)\, s\, K(s)\, dr\, ds\, d\theta\, d\phi$$

$$= \int_0^{2\pi}\int_0^{2\pi}\int_0^{\infty}\int_0^{\infty} E\Big(Z\Big(x_1 - \frac{r}{A}\cos\theta,\ x_2 - \frac{r}{A}\sin\theta \Big)\cdot$$

$$Z\Big(x_1 - \frac{s}{A}\cos\phi,\ x_2 - \frac{s}{A}\sin\phi \Big)$$

$$- Z\Big(x_1 - \frac{r}{A}\cos\theta,\ x_2 - \frac{r}{A}\sin\theta \Big) Z(x_1, x_2)$$

$$- Z\Big(x_1 - \frac{s}{A}\cos\phi,\ x_2 - \frac{s}{A}\cos\phi \Big) Z(x_1, x_2)$$

$$+ Z(x_1, x_2)\, Z(x_1, x_2) \Big),$$

$$r\, K(r)\, s\, K(s)\, dr\, ds\, d\theta\, d\phi$$

$$= \int_0^{\infty}\int_0^{\infty}\int_0^{2\pi}\int_0^{2\pi} \Big[C_{\mathcal{Z}}\Big((r^2 + s^2 - 2rs\cos(\theta - \phi))^{1/2} / A \Big)$$

$$- C_{\mathcal{Z}}(r/A) - C_{\mathcal{Z}}(s/A) + C_{\mathcal{Z}}(0) \Big].$$

$$r\, K(r)\, s\, K(s)\, dr\, ds\, d\theta\, d\phi$$

Since $\mathcal{Z} \in \mathcal{E}_0$ and $K \in \mathbb{K}_{2p}$, an application of Fubini's theorm gives,

$$E_A^2(\mathcal{Z}) = \int_0^{\infty}\int_0^{\infty}\int_0^{2\pi}\int_0^{2\pi} \Big[C_{\mathcal{Z}}\big((r^2 + s^2 - 2rs\cos(\theta - \phi))^{1/2}/ A \Big)$$

$$- C_{\mathcal{Z}}(r/A) - C_{\mathcal{Z}}(s/A) + C_{\mathcal{Z}}(0) \Big].$$

$$r\, K(r)\, s\, K(s)\, dr\, ds\, d\theta\, d\phi$$

$$= 2\pi \int_0^\infty \int_0^\infty \int_0^{2\pi} \Big[C_{\mathcal{Z}} \left((r^2 + s^2 - 2rs \cos\theta)^{1/2} / A \right) - C_{\mathcal{Z}} \left(r/A \right) - C_{\mathcal{Z}} \left(s/A \right) + C_{\mathcal{Z}} \left(0 \right) \Big].$$

$$r\, K(r)\, s\, K(s)\, dr\, ds\, d\theta$$

$$= 2\pi \int_0^\infty \int_0^\infty \int_0^{2\pi} \Big(C_{\mathcal{Z},t/A,\bar{\phi}} (\underline{0}) - C_{\mathcal{Z},r/A,\bar{\phi}} (\underline{0}) - C_{\mathcal{Z},s/A,\bar{\phi}} (\underline{0}) + C_{\mathcal{Z}} (\underline{0}) \Big).$$

$$r\, K(r)\, s\, K(s)\, d\theta\, dr\, ds\ ,$$

where $t^2 = r^2 + s^2 - 2rs \cos\theta$.

Therefore, Taylor's expansion of $C_{\mathcal{Z},r,\bar{\phi}} (\underline{0})$ about $r = 0$ gives

$$E_A^2 (\mathcal{Z}) = 2\pi \int_0^\infty \int_0^\infty \int_0^{2\pi} \Big[\sum_{j=1}^{4p} \frac{1}{j! A^j} \left((r^2 + s^2 - 2rs \cos\theta)^{1/2} - r^j - s^j \right). D^j_{\underline{0},\bar{\phi}}\, C_{\mathcal{Z}} (\underline{0}) + (t/A)^{4p}\, h_{\mathcal{Z}} \left(\frac{t}{A} \right) - (r/A)^{4p}\, h_{\mathcal{Z}} \left(\frac{r}{A} \right) - (s/A)^{4p}\, h_{\mathcal{Z}} \left(\frac{s}{A} \right) \Big].$$

$$r\, K(r)\, s\, K(s)\, d\theta\, dr\, ds$$

Since as $A \longrightarrow \infty$, r/A, s/A, $t/A \longrightarrow 0$, using 3.4.3 and (3.4.5) we get that

(i) $\left|\left(\frac{r}{A}\right)^{4p+1} h_{\mathscr{Z}}(r)\, K(r)\right|$ is bounded by $M\,(r/A)^{4p+1}\,|K(r)|$ an integrable function.

(ii) Since $h_{\mathscr{Z}}\left(\frac{r}{A}\right) \longrightarrow 0$ as $A \longrightarrow \infty$,

$$(r/A)^{4p+1}\, h_{\mathscr{Z}}\left(\frac{r}{A}\right) K(r) \longrightarrow 0 \text{ as } A \longrightarrow \infty$$

(i) and (ii) imply the applicability of Lebesgue dominated convergence theorem. Hence,

$$\int_0^\infty (r/A)^{4p+1}\, h_{\mathscr{Z}}\left(\frac{r}{A}\right) K(r)\, dr \longrightarrow 0 \quad \text{as } A \longrightarrow \infty .$$

Thus,

$$\int_0^\infty\int_0^\infty\int_0^\infty \Big[(t/A)^{4p}\, h_{\mathscr{Z}}\left(\frac{t}{A}\right) - (r/A)^{4p}\, h_{\mathscr{Z}}\left(\frac{r}{A}\right) - (s/A)^{4p}\, h_{\mathscr{Z}}\left(\frac{s}{A}\right) \Big].$$

$$r\,K(r)\,s\,K(s)\,d\theta\,dr\,ds \longrightarrow 0 \qquad \text{as} \quad A \longrightarrow \infty$$

Hence,

$$E_A^2(\mathscr{Z}) = 2\pi \int_0^\infty\int_0^\infty\int_0^{2\pi} \Big(\sum_{j=1}^{4p} \frac{1}{j!A^j} \left((r^2+s^2-2rs\cos\theta)^{1/2} - r^j - s^j\right).$$

$$D^j_{0,\bar{\phi}}\, C_{\mathscr{Z}}(\underline{0}) \Big)\, r\,K(r)\,s\,K(s)\,d\theta\,dr\,ds$$

$$+ o(A^{-4p}) \qquad (A \longrightarrow \infty)$$

Recall that $C_{\mathcal{Z},r,\bar{\phi}}(\underline{x})$ is an even function of r, therefore $D^{j}_{0,\bar{\phi}}\, C_{\mathcal{Z}}(\underline{0}) = 0$ for j odd, and since $K \in \mathbb{K}_{2p}$ we have

$$2\pi \int_0^\infty \int_0^\infty \int_0^{2\pi} \Big(\sum_{j=1}^{4p} \frac{1}{j! A^j} \big((r^2+s^2-2rs\cos\theta)^{j/2} - r^j - s^j \big) \cdot D^{j}_{0,\bar{\phi}}\, C_{\mathcal{Z}}(\underline{0}) \Big) \, r\,K(r)\, s\,K(s)\, d\theta\, dr\, ds$$

$$= 2\pi \int_0^\infty \int_0^\infty \int_0^{2\pi} \Big(\sum_{j=1}^{2p} \frac{1}{A^{2j}(2j)!} \big(r^{2j} + s^{2j} + (-2rs\cos\theta)^j + \sum_{i=1}^{j-1} \binom{j}{i} \big[r^{2i}s^{2j-2i} + (r^2+s^2)^i (-2rs\cos\theta)^{j-i} \big] \big) \cdot D^{2j}_{0,\bar{\phi}}\, C_{\mathcal{Z}}(\underline{0}) \Big) \, r\,K(r)\, s\,K(s)\, d\theta\, dr\, ds$$

$$= 2\pi \int_0^\infty \int_0^\infty \int_0^{2\pi} \Big(D^{4p}_{0,\bar{\phi}}\, C_{\mathcal{Z}}(\underline{0}) / A^{4p}(4p)! \Big) \Big[\binom{2p}{p} (rs)^{2p} + (2rs\cos\theta)^{2p} + \sum_{i=1}^{p-1} \binom{2p}{i} \binom{2i}{i} (2\cos\theta)^{2p-2i} (rs)^{2p} \Big] \cdot r\,K(r)\, s\,K(s)\, d\theta\, dr\, ds$$

$$= 2\pi \Big(D^{4p}_{0,\bar{\phi}}\, C_{\mathcal{Z}}(\underline{0})/A^{4p}(4p)! \Big) \int_0^\infty \int_0^\infty (rs)^{2p+1} K(r)\, K(s)\, dr\, ds .$$

$$\int_0^{2\pi} \sum_{i=0}^{p} \binom{2p}{2i} \binom{2i}{i} (2\cos\theta)^{2p-2i} \, d\theta$$

$$= \left[D_{0,\bar{\phi}}^{4p} C_{\mathcal{Z}}(\underline{0}) / A^{4p} \right] \left[(2\pi)^2 / (4p)! \right].$$

$$\left[\sum_{i=0}^{p} \binom{2p}{2i} \binom{2i}{i} \binom{2p-2i}{p-i} \right] \left[\int_0^{\infty} r^{2p+1} k(r) \, dr \right]^2$$

$$= \left[M_1 A_{2p}^2 / A^{4p} \right] D_{0,\bar{\phi}}^{4p} C_{\mathcal{Z}}(\underline{0}),$$

where

$$M_1 = \left[(2\pi)^2 / (4p)! \right] \left[\binom{2p}{p} \right]^2 \text{ and } A_{2p} = \int_0^{\infty} r^{2p+1} K(r) \, dr$$

Hence,

$$E_A^2(\mathcal{Z}) = O(A^{-4p}) \qquad \text{as } A \longrightarrow \infty .$$

3.5 THE $\| C_{\mathcal{Z}} \|_{4p}$ ESTIMATE

THEOREM 3.5.1

If $\mathcal{Z} \in \mathcal{E}_{4p}$ and $K \in \mathbb{K}_{2p}$, then

$$E_A^2(\mathcal{Z}) \leq (M_2 / A^{4p}) \| C_{\mathcal{Z}} \|_{4p} ,$$

where

$$M_2 = \Big(\int_0^\infty \int_0^\infty \int_0^{2\pi} (r^2 + s^2 - 2rs\cos\theta)^{2p}\, rs\, |K(r)|\, |K(s)|\, d\theta\, dr\, ds$$

$$+ 4\pi \int_0^\infty \int_0^\infty r^{4p+1}\, s\, |K(r)|\, |K(s)|\, dr\, ds \Big)$$

PROOF:—

For any $\underline{x} \in \mathbb{R}^2$,

$$E_A^2(\mathcal{Z}) = E\,(Z_A - Z)^2\,(\underline{x})$$

$$= E \int_0^{2\pi} \int_0^{2\pi} \int_0^\infty \int_0^\infty \Big(Z(x_1 - \tfrac{r}{A}\cos\theta,\ x_2 - \tfrac{r}{A}\sin\theta) - Z(x_1, x_2) \Big) \cdot$$

$$\Big(Z(x_1 - \tfrac{s}{A}\cos\phi,\ x_2 - \tfrac{s}{A}\sin\phi) - Z(x_1, x_2) \Big) \cdot$$

$$r\, K(r)\, s\, K(s)\, dr\, ds\, d\theta\, d\phi$$

$$= \int_0^{2\pi} \int_0^{2\pi} \int_0^\infty \int_0^\infty E\Big(Z\big(x_1 - \tfrac{r}{A}\cos\theta,\ x_2 - \tfrac{r}{A}\sin\theta\big) \cdot$$

$$Z\big(x_1 - \tfrac{s}{A}\cos\phi,\ x_2 - \tfrac{s}{A}\sin\phi\big)$$

$$- Z\big(x_1 - \tfrac{r}{A}\cos\theta,\ x_2 - \tfrac{r}{A}\sin\theta\big)\, Z(x_1, x_2)$$

$$- Z\left(x_1 - \frac{s}{A}\cos\phi,\ x_2 - \frac{s}{A}\sin\phi\right) Z(x_1, x_2)$$

$$+ Z(x_1, x_2)\, Z(x_1, x_2)\Big).$$

$$r\, K(r)\, s\, K(s)\, dr\, ds\, d\theta\, d\phi$$

$$= \int_0^{2\pi}\int_0^{2\pi}\int_0^{\infty}\int_0^{\infty} \Big[C_{\mathcal{Z}}\left((r^2 + s^2 - 2rs\cos(\theta - \phi))^{1/2} / A\right)$$

$$- C_{\mathcal{Z}}(r/A) - C_{\mathcal{Z}}(s/A) + C_{\mathcal{Z}}(0)\Big].$$

$$r\, K(r)\, s\, K(s)\, dr\, ds\, d\theta\, d\phi$$

$$= 2\pi \int_0^{2\pi}\int_0^{\infty}\int_0^{\infty} \Big[C_{\mathcal{Z}}\left((r^2 + s^2 - 2rs\cos\theta)^{1/2} / A\right)$$

$$- C_{\mathcal{Z}}(r/A) - C_{\mathcal{Z}}(s/A) + C_{\mathcal{Z}}(0)\Big].$$

$$r\, K(r)\, s\, K(s)\, dr\, ds\, d\theta$$

Since $\mathcal{Z} \in \mathcal{E}_{4p}$ implies that $C_{\mathcal{Z}} \in \Omega_{4p}$, Taylor's expansion with $t^2 = r^2 + s^2 - 2rs\cos\theta$ gives, for some $\alpha_i \in (0, 1)$, $i = 1, 2, 3$

$$E_A^2(\mathcal{Z}) = 2\pi \int_0^{2\pi}\int_0^{\infty}\int_0^{\infty} \Big[\sum_{j=1}^{4p-1} \frac{1}{j!A^j}\left((r^2 + s^2 - 2rs\cos\theta)^{1/2} - r^j - s^j\right).$$

$$D_{0,\bar{\phi}}^{j} C_{\mathcal{Z}}(\underline{0}) + \left(1/A^{4p}(4p)!\right)\left(t^{4p}\right).$$

$$D_{\alpha_1 t/A,\bar{\phi}}^{4p} C_{\mathcal{Z}}(\underline{0}) - r^{4p} D_{\alpha_2 r/A,\bar{\phi}}^{4p} C_{\mathcal{Z}}(\underline{0})$$

$$- s^{4p} D^{4p}_{\alpha_3 s/A,\bar{\phi}} C_{\mathscr{Z}}(\underline{0})\Big].$$

$$r\,K(r)\,s\,K(s)\,d\theta\,dr\,ds$$

$$= \Big(\frac{2\pi}{A^{4p}(4p)!}\Big) \int_0^\infty\int_0^\infty\int_0^{2\pi} \Big\{ (r^2+s^2-2rs\cos\theta)^{2p} \cdot$$

$$D^{4p}_{\alpha_1 t/A,\bar{\phi}} C_{\mathscr{Z}}(\underline{0}) - r^{4p} D^{4p}_{\alpha_2 r/A,\bar{\phi}} C_{\mathscr{Z}}(\underline{0})$$

$$- s^{4p} D^{4p}_{\alpha_3 s/A,\bar{\phi}} C_{\mathscr{Z}}(\underline{0})\Big].$$

$$r\,K(r)\,s\,K(s)\,d\theta\,dr\,ds$$

because $D^j_{\underline{0},\bar{\phi}} C_{\mathscr{Z}}(\underline{0}) = 0$ for j odd and $K \in \mathbb{K}_{2p}$. Hence

$$E^2_A(\mathscr{Z}) = |E^2_A(\mathscr{Z})|$$

$$\le \Big(\frac{2\pi}{A^{4p}(4p)!}\Big) \Big\{ \int_0^\infty\int_0^\infty\int_0^{2\pi} |(r^2+s^2-2rs\cos\theta)^{2p}|\,rs\cdot$$

$$|D^{4p}_{\alpha_1 t/A,\bar{\phi}} C_{\mathscr{Z}}(\underline{0})|\,|K(r)|\,|K(s)|\,d\theta\,dr\,ds$$

$$+ 2\pi \int_0^\infty\int_0^\infty r^{4p+1}\,|D^{4p}_{\alpha_2 r/A,\bar{\phi}} C_{\mathscr{Z}}(\underline{0})|\cdot$$

$$|K(r)|\,s\,|K(s)|\,dr\,ds$$

$$+ 2\pi \int_0^\infty\int_0^\infty s^{4p+1}\,|D^{4p}_{\alpha_3 s/A,\bar{\phi}} C_{\mathscr{Z}}(\underline{0})|\cdot$$

$$| K(s) | r | K(r) | ds\, dr \Big]$$

$$\leq \left(\frac{2\pi}{A^{4p}(4p)!}\right) \| D^{4p}_{r,\bar{\phi}} C_{\mathcal{X}} \|_0 \left[\int_0^{\infty}\int_0^{\infty}\int_0^{2\pi} (r^2+s^2-2rs\cos\theta)^{2p} \cdot rs \,|\, K(r) \,|\, |\, K(s) \,|\, d\theta\, dr\, ds \right.$$

$$\left. + 4\pi \int_0^{\infty}\int_0^{\infty} r^{4p+1}\, s \,|\, K(r) \,|\, |\, K(s) \,|\, dr\, ds \right]$$

$$= \left(M_2 / A^{4p} \right) \| D^{4p}_{r,\bar{\phi}} C_{\mathcal{X}} \|_0 .$$

Since $K \in \mathbb{K}_{2p}$, we have $M_2 < \infty$ and thus

$$E^2_A (\mathcal{X}) \leq \left(M_2 / A^{4p} \right) \| D^{4p}_{r,\bar{\phi}} C_{\mathcal{X}} \|_0$$

$$\leq \left(M_2 / A^{4p} \right) \| C_{\mathcal{X}} \|_{4p}$$

Note that, this theorem gives an estimate of ESE for those stochastic processes $\mathcal{X}$, which belong to the class $\mathcal{E}_{4p}$.

CHAPTER 4

INVERSE THEOREM

4.1 INTRODUCTION

In chapter 3 we have seen some estimates of the ESE $E_A^2(\mathcal{Z})$ for CBP, whenever the object process $\mathcal{Z}$ is known to have certain theoretical properties. For example, either the process belongs to some class of stochastic processes as defined in chapter 2, or it has some other properties such as smoothness of its covariance function and the conditions related to the modulus of continuity.

In this chapter we solve the inverse problem, i.e., if the order of ESE is known then to which class does the object process $\mathcal{Z}$ belong? The result in this chapter states that the ESE is of order $O(A^{-\beta})$ if and only if $\mathcal{Z} \in \mathcal{C}_{4p}^{\beta}$, the interpolation class, provided the CBP window $K \in \mathbb{K}_{2p}$. This theorem guarntees the error order to be $A^{-\beta}$ if the object process can be represented as a member of the interpolation class $\mathcal{C}_{4p}^{\beta}$. Note that as β increases the covariance function of the object process becomes smoother.

4.2 LEMMAS

The following Lemmas are required in the proof of the main theorem.

LEMMA 4.2.1

Let $\mathcal{Z} \in \mathcal{E}_0$, $K \in \Omega_{4p} \cap L^1 [\, 0, \infty \,)$ and $D^{4p}_{r, \bar{\phi}} K(\underline{x}) \in L^1 [\, 0, \infty \,)$ and be bounded. Then $\mathcal{Z}_A \in \mathcal{E}_{4p}$.

PROOF:-

For proving that $\mathcal{Z}_A \in \mathcal{E}_{4p}$, we need only to show that $C_{\mathcal{Z}_A} \in \Omega_{4p}$, because Lemma 2.5.1 states that $\mathcal{Z}_A$ is second order wide sense stationary process.

$$C_{\mathcal{Z}_A}(\underline{y}) = E\left(Z_A(\underline{x}) . Z_A(\underline{x} + \underline{y}) \right)$$

$$= E \int_{\mathbb{R}^2} \int_{\mathbb{R}^2} Z(\underline{u})\, Z(\underline{v})\, K_A(\underline{x} - \underline{u})\, K_A(\underline{x} + \underline{y} - \underline{v})\, d\underline{u}\, d\underline{v}$$

$$= \int_{\mathbb{R}^2} \int_{\mathbb{R}^2} E\left(Z(\underline{w} + \underline{v})\, Z(\underline{v}) \right) K_A(\underline{x} - \underline{w} - \underline{v}) .$$

$$K_A(\underline{x} + \underline{y} - \underline{v})\, d\underline{w}\, d\underline{v}$$

$$= \int_{\mathbb{R}^2}\int_{\mathbb{R}^2} C_{\mathcal{Z}}(\underline{w})\, K_A(\underline{x} - \underline{w} - \underline{v})\, K_A(\underline{x} + \underline{y} - \underline{v})\, d\underline{w}\, d\underline{v}$$

$$= \int_{\mathbb{R}^2}\int_{\mathbb{R}^2} C_{\mathcal{Z}}(\underline{w})\, K_A(-\underline{w} - \underline{u})\, K_A(\underline{y} - \underline{u})\, d\underline{w}\, d\underline{u}$$

$$= \int_{\mathbb{R}^2} h_{\mathcal{Z}}(\underline{u})\, K_A(\underline{y} - \underline{u})\, d\underline{u}$$

$$= h_{\mathcal{Z}_A}(\underline{y}), \qquad \ldots.(4.2.1)$$

where

$$h_{\mathcal{Z}}(\underline{u}) = \int_{\mathbb{R}^2} C_{\mathcal{Z}}(\underline{w})\, K_A(\underline{w} + \underline{u})\, d\underline{w}$$

Now,

$$|\, h_{\mathcal{Z}}(\underline{u})| = \left| \int_{\mathbb{R}^2} C_{\mathcal{Z}}(\underline{w})\, K_A(\underline{w} + \underline{u})\, d\underline{w} \right|$$

$$= \left| \int_{\mathbb{R}^2} C_{\mathcal{Z}}(\underline{w}/A - \underline{u})\, K(\underline{w})\, d\underline{w} \right|$$

$$\leq \int_{\mathbb{R}^2} | C_{\mathscr{Z}} (\underline{w}/A - \underline{u}) | |K(\underline{w})| \, d\underline{w}$$

$$\leq \| C_{\mathscr{Z}} \|_0 \int_{\mathbb{R}^2} | K(\underline{w}) | \, d\underline{w} = \| C_{\mathscr{Z}} \|_0 M_1, \text{ (say)},$$

Hence $h_{\mathscr{Z}}(\underline{u})$ is bounded in $\mathbb{R}^2$.

Let $\underline{u}, \underline{v} \in \mathbb{R}^2$,

$$| h_{\mathscr{Z}}(\underline{u}) - h_{\mathscr{Z}}(\underline{v}) |$$

$$= \left| \int_{\mathbb{R}^2} \left(C_{\mathscr{Z}} (\underline{u} - \underline{w}/A) - C_{\mathscr{Z}} (\underline{v} - \underline{w}/A) \right) K(\underline{w}) \, d\underline{w} \right|$$

$$\leq \int_{\mathbb{R}^2} | C_{\mathscr{Z}} (\underline{u} - \underline{w}/A) - C_{\mathscr{Z}} (\underline{v} - \underline{w}/A) | \, | K(\underline{w}) | \, d\underline{w}$$

Since integrand is bounded by $2 \| C_{\mathscr{Z}} \|_0 | K(\underline{w}) |$, an integrable function. Applying bounded convergence theorem,

$$\lim_{\underline{u} \to \underline{v}} | h_{\mathscr{Z}}(\underline{u}) - h_{\mathscr{Z}}(\underline{v}) |$$

$$\leq \int_{\mathbb{R}^2} \lim_{\underline{u} \to \underline{v}} | C_{\mathscr{Z}} (\underline{u} - \underline{w}/A) - C_{\mathscr{Z}} (\underline{v} - \underline{w}/A) | \cdot |K(\underline{w})| \, d\underline{w} = 0.$$

Since $\mathcal{Z} \in \mathcal{E}_0$, $C_{\mathcal{Z}}$ is continuous in $\mathbb{R}^2$. This implies that $h_{\mathcal{Z}}$ is a continuous and bounded function in $\mathbb{R}^2$.

From (4.2.1)

$$C_{\mathcal{Z}_A}(\underline{y}) = \int_{\mathbb{R}^2} h_{\mathcal{Z}}(\underline{u})\, K_A(\underline{y} - \underline{u})\, d\underline{u}$$

$$= \int_{\mathbb{R}^2} h_{\mathcal{Z}}(\underline{y} - \underline{u}/A)\, K(\underline{u})\, d\underline{u}$$

Hence, on similar lines, $C_{\mathcal{Z}_A}$ is bounded by $M_1^2 \| C_{\mathcal{Z}} \|_0$ and continuous in $\mathbb{R}^2$.

Since $h_{\mathcal{Z}}$ is bounded and continuous in $\mathbb{R}^2$ and $K(\underline{x}) \in \Omega_{4p}$, and $D^{4p}_{r,\bar{\phi}}\, K(\underline{x}) \in L^1[0, \infty)$, $D^{k}_{r,\bar{\phi}}\, C_{\mathcal{Z}_A}(\underline{y})$ exists and is bounded and continuous function of $(r, \underline{y}) \in \mathbb{R}^+ \times \mathbb{R}^2$, and is given by

$$D^{k}_{r,\bar{\phi}}\, C_{\mathcal{Z}_A}(\underline{y}) = \int_{\mathbb{R}^2} h_{\mathcal{Z}}(\underline{u})\, A^2\, \frac{\partial^k}{\partial r^k} \left(K_{Ar,\bar{\phi}}(A(\underline{y} - \underline{u})) \right) d\underline{u}$$

Since $K(\underline{x}) = K(\|\underline{x}\|) \in L^1[0, \infty)$ and $D^{4p}_{r,\bar{\phi}}\, K(\underline{x}) \in L^1[0, \infty)$ the integrability of $D^{k}_{r,\bar{\phi}}\, K(\underline{x})$ follows from interpolation inequalities [see Goldberg(1966)].

Hence, $C_{\mathcal{Z}_A} \in \Omega_{4p}$ implying that $\mathcal{Z}_A \in \mathcal{E}_{4p}$.

LEMMA 4.2.2

Let $\mathcal{Z} \in \mathcal{Z}_0$, $K(\underline{x}) \in L^1[0, \infty)$, then there exists a constant $M_3 < \infty$ such that

$$E_A^2(\mathcal{Z}) \leq (2 M_3)^2 \| C_{\mathcal{Z}} \|_0$$

PROOF:—

$$E_A^2(\mathcal{Z}) = E(Z_A - Z)^2(\underline{x})$$

$$= E \int_{\mathbb{R}^2} \int_{\mathbb{R}^2} (Z(\underline{x} - \underline{u}/A) - Z(\underline{x}))(Z(\underline{x} - \underline{v}/A) - Z(\underline{x})) K(\underline{u}) K(\underline{v}) \, d\underline{u} \, d\underline{v}$$

$$= \int_{\mathbb{R}^2} \int_{\mathbb{R}^2} (C_{\mathcal{Z}}((\underline{u} - \underline{v})/A) - C_{\mathcal{Z}}(\underline{u}/A) - C_{\mathcal{Z}}(\underline{v}/A) + C_{\mathcal{Z}}(0)) K(\underline{u}) K(\underline{v}) \, d\underline{u} \, d\underline{v}$$

Hence,

$$E_A^2(\mathcal{Z}) = |E_A^2(\mathcal{Z})|$$

$$\leq \int_{\mathbb{R}^2} \int_{\mathbb{R}^2} \Big(|C_{\mathcal{Z}}((\underline{u} - \underline{v})/A)| + |C_{\mathcal{Z}}(\underline{u}/A)| + |C_{\mathcal{Z}}(\underline{v}/A)| + |C_{\mathcal{Z}}(\underline{0})| \Big) K(\underline{u}) K(\underline{v}) \, d\underline{u} \, d\underline{v}$$

$$\leq 4 \| C_{\mathscr{Z}} \|_0 \left(\int_{\mathbb{R}^2} | K(\underline{u}) | \, d\underline{u} \right)^2$$

$$= (2 M_3)^2 \| C_{\mathscr{Z}} \|_0 ,$$

where $M_3 = \int_{\mathbb{R}^2} | K(\underline{u}) | \, d\underline{u}$.

LEMMA 4.2.3

Let $\mathscr{Z}$ and $\mathscr{Y} \in \mathscr{E}_0$ be such that the process $\mathscr{Z} + \mathscr{Y} \in \mathscr{E}_0$. Then

$$\| C_{\mathscr{Z}+\mathscr{Y}} \|_0 \leq 2 (\| C_{\mathscr{Z}} \|_0 + \| C_{\mathscr{Y}} \|_0).$$

LEMMA 4.2.4

Let $\mathscr{Z} \in \mathscr{E}_0$, $K \in L^1 [0, \infty)$, then there exists a constant $M_3 < \infty$ such that

$$\| C_{\mathscr{Z}_A} \|_0 \leq M_3^2 \| C_{\mathscr{Z}} \|_0 ,$$

where M_3 is same as in Lemma 4.2.2.

LEMMA 4.2.5

Let $\mathscr{Z} \in \mathscr{E}_0$, $K(\underline{x}) \in L^1[0, \infty)$, and $D^{4p}_{r,\bar{\phi}} K(\underline{x}) \in L^1[0, \infty)$. Then there exists a constant $M_4 < \infty$ independent of A and $\mathscr{Z}$

such that

$$\| C_{\mathcal{Z}_A} \|_{4p} \leq A^{4p} M_4 \| C_{\mathcal{Z}} \|_0 .$$

PROOF:-

$$C_{\mathcal{Z}_A}(\underline{y}) = E\left(Z_A(\underline{x}) Z_A(\underline{x}+\underline{y}) \right)$$

$$= E \int_{\mathbb{R}^2}\int_{\mathbb{R}^2} Z(\underline{u}) Z(\underline{v}) K_A(\underline{x}-\underline{u}) K_A(\underline{x}+\underline{y}-\underline{v})\, d\underline{u}\, d\underline{v}$$

$$= \int_{\mathbb{R}^2}\int_{\mathbb{R}^2} E\left(Z(\underline{w}+\underline{u}) Z(\underline{v}) \right) K_A(\underline{x}-\underline{w}-\underline{v}) \cdot K_A(\underline{x}+\underline{y}-\underline{v})\, d\underline{w}\, d\underline{v}$$

$$= \int_{\mathbb{R}^2}\int_{\mathbb{R}^2} C_{\mathcal{Z}}(\underline{w}) K_A(\underline{x}-\underline{w}-\underline{v}) K_A(\underline{x}+\underline{y}-\underline{v})\, d\underline{w}\, d\underline{v}$$

$$= \int_{\mathbb{R}^2}\int_{\mathbb{R}^2} C_{\mathcal{Z}}(\underline{w}) K_A(-\underline{w}-\underline{u}) K_A(\underline{y}-\underline{u})\, d\underline{w}\, d\underline{u}$$

$$= \int_{\mathbb{R}^2}\int_{\mathbb{R}^2} C_{\mathcal{Z}}(\underline{w}) K_A(\underline{w}+\underline{u}) K_A(\underline{y}-\underline{u})\, d\underline{w}\, d\underline{u} \ .$$

$$= A^{4p} \int\int_{\mathbb{R}^2\,\mathbb{R}^2} C_{\mathscr{Z}}(\underline{w})\, K_A(\underline{w}+\underline{u})\, A^2 \cdot \frac{\partial^{4p}}{\partial(Ar)^{4p}} \left(K_{Ar,\bar{\phi}}(A(\underline{y}-\underline{u})) \right) d\underline{w}\, d\underline{u}$$

$$= A^{4p} \int\int_{\mathbb{R}^2\,\mathbb{R}^2} C_{\mathscr{Z}}(\underline{w})\, K_A(\underline{w}+\underline{u})\, D^{4p}_{r,\bar{\phi}} K_A(\underline{y}-\underline{u})\, d\underline{w}\, d\underline{u}$$

Hence,

$$\left| D^{4p}_{r,\bar{\phi}} C_{\mathscr{Z}_A}(\underline{y}) \right| \le A^{4p} \int\int_{\mathbb{R}^2\,\mathbb{R}^2} \left| C_{\mathscr{Z}}(\underline{w}) \right| \left| K_A(\underline{w}+\underline{u}) \right| \cdot \left| D^{4p}_{r,\bar{\phi}} K_A(\underline{y}-\underline{u}) \right| d\underline{w}\, d\underline{u}$$

$$= A^{4p} \| C_{\mathscr{Z}} \|_0 M_3 L, \text{ (say)}$$

this implies that

$$\| D^{4p}_{r,\bar{\phi}} C_{\mathscr{Z}_A} \|_0 \le A^{4p} \| C_{\mathscr{Z}} \|_0 M_3 L,$$

where $L < \infty$ and $M_3 < \infty$.

Using Lemma 4.2.4

$$\| C_{\mathscr{Z}_A} \|_{4p} = \| C_{\mathscr{Z}_A} \|_0 + \| D^{4p}_{r,\bar{\phi}} C_{\mathscr{Z}_A} \|_0$$

$$\le M_3^2 \| C_{\mathscr{Z}} \|_0 + L M_3 A^{4p} \| C_{\mathscr{Z}} \|_0$$

$$\le M_3 A^{4p} \| C_{\mathscr{Z}} \|_0 (M_3 + L) \qquad \text{because } A > 1.$$

Using Lemma 4.2.4

$$\| C_{\mathcal{Z}_A} \|_{4p} = \| C_{\mathcal{Z}_A} \|_0 + \| D^{4p}_{r,\bar{\phi}} C_{\mathcal{Z}_A} \|_0$$

$$\leq M_3^2 \| C_{\mathcal{Z}} \|_0 + M_3^2 \| D^{4p}_{r,\bar{\phi}} C_{\mathcal{Z}} \|_0$$

$$= M_3^2 \| C_{\mathcal{Z}} \|_{4p} .$$

4.3 MAIN THEOREM

THEOREM:

Let $\mathcal{Z} \in \mathcal{E}_0$ and suppose that $K \in \mathbb{K}_{2p}$. Then

$$E_A^2 (\mathcal{Z}) = 0 (A^{-\beta}) \qquad \text{as } A \longrightarrow \infty$$

if and only if $\mathcal{Z} \in \mathcal{E}^{\beta}_{4p}$ for $0 < \beta < 4p$.

PROOF:—

First, let $E_A^2 (\mathcal{Z}) = 0 (A^{-\beta})$ as $A \longrightarrow \infty$. Then we have to show that $\mathcal{Z} \in \mathcal{E}^{\beta}_{4p}$, i.e., $\mathcal{Z}$ can be decomposed as

$\mathcal{Z} = \mathcal{Z}_0 + \mathcal{Z}_{4p}$ such that $\mathcal{Z}_0 \in \mathcal{E}_0$, $\mathcal{Z}_{4p} \in \mathcal{E}_{4p}$

and $K_p (t^{4p} , \mathcal{Z}) = 0 (t^{\beta})$ as $t \longrightarrow 0$

Let us define another Peetre's functional as:

$$K_p^* (t^{4p}, \mathcal{Z}) = \inf_A (\| C_{\mathcal{Z}} - \mathcal{Z}_A \|_0 + t^{4p} \| C_{\mathcal{Z}_A} \|_{4p}).$$

Thus

$$K_p (t^{4p}, \mathcal{Z}) \leq K_p^* (t^{4p}, \mathcal{Z})$$

Now,

$$\mathcal{Z}_A (\underline{x}) = (\mathcal{Z} - \mathcal{Z}_B)_A(\underline{x}) + (\mathcal{Z}_B)_A (\underline{x})$$

and hence,

$$C_{\mathcal{Z}_A} (\underline{y}) = C_{(\mathcal{Z} - \mathcal{Z}_B)_A}(\underline{y}) + C_{(\mathcal{Z}_B)_A}(\underline{y})$$

$$+ E (Z - Z_B)_A(\underline{x}) (Z_B)_A (\underline{x} + \underline{y})$$

$$+ E (Z_B)_A(\underline{x}) (Z - Z_B)_A (\underline{x} + \underline{y})$$

and

$$C_{\mathcal{Z}_{A,r,\bar{\phi}}}(\underline{y}) = C_{(\mathcal{Z} - \mathcal{Z}_B)_{A,r,\bar{\phi}}}(\underline{y}) + C_{(\mathcal{Z}_B)_{A,r,\bar{\phi}}}(\underline{y})$$

$$+ \frac{1}{2\pi} \int_0^{2\pi} E (Z - Z_B)_A (\underline{x}) (Z_B)_{A,r,\phi} (\underline{x} + \underline{y}) \, d\phi$$

$$+ \frac{1}{2\pi} \int_0^{2\pi} E (Z_B)_A (\underline{x}) (Z - Z_B)_{A,r,\phi} (\underline{x} + \underline{y}) \, d\phi .$$

Let $\mu (\underline{x})$ be a measure on $\mathbb{R}^2$ such that $\mu (\mathbb{R}^2) = 1$, and $Y (\underline{x}) = Z (-\underline{x})$. Then,

$$\frac{1}{2\pi} \int_0^{2\pi} E (Z - Z_B)_A (\underline{x}) (Z_B)_{A,r,\phi} (\underline{x} + \underline{y}) \, d\phi$$

$$= \frac{1}{2\pi} \int_0^{2\pi} \int_{\mathbb{R}^2} E\,(Z - Z_B)_A\,(\underline{x})\,(Z_B)_{A,r,\phi}\,(\underline{x} + \underline{y})\,d\mu\,(\underline{x})\,d\phi$$

$$= E \int_{\mathbb{R}^2} (Z - Z_B)_A\,(\underline{x})\,\frac{1}{2\pi} \int_0^{2\pi} (Z_B)_{A,r,\phi}(\underline{x} + \underline{y})\,d\phi\,d\mu\,(\underline{x})$$

$$= E \int_{\mathbb{R}^2} (Z - Z_B)_A\,(\underline{x})\,(Z_B)_{A,r,\bar{\phi}}\,(\underline{x} + \underline{y})\,d\mu\,(\underline{x})$$

$$= E\,(Z - Z_B)_A \overset{*}{\mu} (Y_B)_{A,r,\bar{\phi}}\,(-\underline{y}),$$

where $\overset{*}{\mu}$ denotes convolution with respect to measure μ.

Also,

$$\frac{1}{2\pi} \int_0^{2\pi} E\,(Z_B)_A\,(\underline{x})\,(Z - Z_B)_{A,r,\phi}\,(\underline{x} + \underline{y})\,d\phi$$

$$= \frac{1}{2\pi} \int_0^{2\pi} \int_{\mathbb{R}^2} E\,(Z_B)_A\,(\underline{x})\,(Z - Z_B)_{A,r,\phi}\,(\underline{x} + \underline{y})\,d\mu\,(\underline{x})\,d\phi$$

$$= E \int_{\mathbb{R}^2} (Z_B)_A (\underline{x}) \frac{1}{2\pi} \int_0^{2\pi} (Z - Z_B)_{A,r,\phi}(\underline{x} + \underline{y})\, d\phi\, d\mu\, (\underline{x})$$

$$= E \int_{\mathbb{R}^2} (Z_B)_A (\underline{x})\, (Z - Z_B)_{A,r,\bar{\phi}} (\underline{x} + \underline{y})\, d\mu\, (\underline{x})$$

$$= E\, (Z_B)_A \overset{*}{\mu} (Y - Y_B)_{A,r,\bar{\phi}} (-\underline{y})$$

$$= E\, (Y - Y_B)_A \overset{*}{\mu} (Z_B)_{A,r,\bar{\phi}} (-\underline{y}).$$

Hence using the fact that $K \in \mathbb{K}_{2p}$,

$$\left| D^{4p}_{r,\bar{\phi}} \frac{1}{2\pi} \int_0^{2\pi} E\, (Z - Z_B)_A (\underline{x})\, (Z_B)_{A,r,\phi} (\underline{x} + \underline{y})\, d\phi \right|$$

$$= \left| \frac{\partial^{4p}}{\partial r^{4p}} E\, (Z - Z_B)_A \overset{*}{\mu} (Y_B)_{A,r,\bar{\phi}} (-\underline{y}) \right|.$$

$$= \left| E \frac{\partial^{4p}}{\partial r^{4p}} (Z - Z_B)_A \overset{*}{\mu} (Y_B)_{A,r,\bar{\phi}} (-\underline{y}) \right|$$

$$= \left| E\ (Z - Z_B)_A \overset{*}{\mu} \frac{\partial^{4p}}{\partial r^{4p}} (Y_B)_{A,r,\bar{\phi}}(-\underline{y}) \right|$$

$$= \left| E \int_{\mathbb{R}^2} (Z - Z_B)_A (\underline{x})\ D^{4p}_{r,\bar{\phi}} (Z_B)_A (\underline{x} + \underline{y})\ d\mu (\underline{x}) \right|$$

$$= \left| \int_{\mathbb{R}^2} E \left[(Z - Z_B)_A (\underline{x})\ D^{4p}_{r,\bar{\phi}} (Z_B)_A (\underline{x} + \underline{y}) \right] d\mu (\underline{x}) \right|$$

$$\leq \left| \int_{\mathbb{R}^2} \left(E\ (Z - Z_B)^2_A (\underline{x}) \right)^{1/2} \cdot \right.$$

$$\left. \left(E\ (D^{4p}_{r,\bar{\phi}} (Z_B)_A (\underline{x} + \underline{y}))^2 \right)^{1/2} d\mu (\underline{x}) \right|$$

$$\leq \int_{\mathbb{R}^2} \left(\left| C_{(\mathcal{Z} - \mathcal{Z}_B)_A}(\underline{0}) \right| \right)^{1/2} \cdot$$

$$\left(\left| E\ (D^{4p}_{r,\bar{\phi}} (Z_B)_A (\underline{x} + \underline{y}))^2 \right| \right)^{1/2} d\mu (\underline{x})$$

....(4.3.1)

and

$$E \left(D^{4p}_{r,\bar{\phi}} (Z_B)_A (\underline{x} + \underline{y}) \right)^2$$

$$= E \left(\int_{\mathbb{R}^2} Z_B(\underline{u}) \frac{\partial^{4p}}{\partial r^{4p}} K_{A,r,\bar{\phi}}(\underline{x} + \underline{y} - \underline{u})\, d\underline{u} \right).$$

$$\left(\int_{\mathbb{R}^2} \frac{\partial^{4p}}{\partial r^{4p}} Z_{B,r,\bar{\phi}}(\underline{x} + \underline{y} - \underline{v})\, K_A(\underline{v})\, d\underline{v} \right)$$

$$= E \int_{\mathbb{R}^2}\int_{\mathbb{R}^2} Z_B(\underline{u}) \frac{\partial^{4p}}{\partial r^{4p}} Z_{B,r,\bar{\phi}}(\underline{x} + \underline{y} - \underline{v})\, K_A(\underline{v}).$$

$$\frac{\partial^{4p}}{\partial r^{4p}} K_{A,r,\bar{\phi}}(\underline{x} + \underline{y} - \underline{u})\, d\underline{u}\, d\underline{v}$$

$$= \int_{\mathbb{R}^2}\int_{\mathbb{R}^2} \frac{\partial^{4p}}{\partial r^{4p}} E\left(Z_B(\underline{u})\, Z_{B,r,\bar{\phi}}(\underline{x} + \underline{y} - \underline{v})\, K_A(\underline{v}) \right).$$

$$A^2 \frac{\partial^{4p}}{\partial r^{4p}} K_{Ar,\bar{\phi}}\left(A(\underline{x} + \underline{y} - \underline{u}) \right) d\underline{u}\, d\underline{v}$$

$$= \int_{\mathbb{R}^2}\int_{\mathbb{R}^2} \frac{\partial^{4p}}{\partial r^{4p}} C_{\mathcal{Z}_B,r,\bar{\phi}}(\underline{x} + \underline{y} - \underline{u} - \underline{v})\, K_A(\underline{v}).$$

$$A^{4p} D^{4p}_{r,\bar{\phi}} K_{A,r,\bar{\phi}}(\underline{x} + \underline{y} - \underline{u})\, d\underline{u}\, d\underline{v}$$

$$= A^{4p} \int_{\mathbb{R}^2}\int_{\mathbb{R}^2} D^{4p}_{r,\bar{\phi}} C_{\mathcal{Z}_B}(\underline{x} + \underline{y} - \underline{u} - \underline{v})\, K_A(\underline{v}).$$

$$D^{4p}_{r,\bar{\phi}} K_{A,r,\bar{\phi}}(\underline{x} + \underline{y} - \underline{u})\, d\underline{u}\, d\underline{v}$$

Hence,

$$| E (D^{4p}_{r,\bar{\phi}} (Z_B)_A (\underline{x} + \underline{y}))^2 |$$

$$\leq A^{4p} \int_{\mathbb{R}^2} \int_{\mathbb{R}^2} | D^{4p}_{r,\bar{\phi}} C_{\mathcal{Z}_B} (\underline{x} + \underline{y} - \underline{u} - \underline{v}) | \, | K_A (\underline{v}) | \cdot$$

$$| D^{4p}_{r,\bar{\phi}} K_{A,r,\bar{\phi}} (\underline{x} + \underline{y} - \underline{u}) | \, d\underline{u} \, d\underline{v}$$

$$\leq A^{4p} \| D^{4p}_{r,\bar{\phi}} C_{\mathcal{Z}_B} \|_0 \int_{\mathbb{R}^2} \int_{\mathbb{R}^2} | K_A (\underline{v}) | \cdot$$

$$| D^{4p}_{r,\bar{\phi}} K_{A,r,\bar{\phi}} (\underline{x} + \underline{y} - \underline{u}) | \, d\underline{u} \, d\underline{v}$$

$$\leq A^{4p} \| C_{\mathcal{Z}_B} \|_{4p} \int_{\mathbb{R}^2} | K_A (\underline{v}) | \, d\underline{v} \cdot$$

$$\int_{\mathbb{R}^2} | D^{4p}_{r,\bar{\phi}} K_{A,r,\bar{\phi}} (\underline{x} + \underline{y} - \underline{u}) | \, d\underline{u} \, d\underline{v}$$

$$= M_3 \, L \, A^{4p} \| C_{\mathcal{Z}_B} \|_{4p} \cdot \qquad \ldots.(4.3.2)$$

Now using Lemma 4.2.2 and (4.3.2) in (4.3.1), we have

$$\left| D^{4p}_{r,\,\bar{\phi}} \frac{1}{2\pi} \int_0^{2\pi} E\,(Z - Z_B)_A\,(\underline{x})\,(Z_B)_{A,r,\,\phi}\,(\underline{x} + \underline{y})\,d\phi \right|$$

$$\leq \int_{\mathbb{R}^2} \left(\| C_{(\mathcal{Z} - \mathcal{Z}_B)_A} \|_0 \right)^{1/2} \cdot \left(A^{4p}\, M_3\, L \| C_{\mathcal{Z}_B} \|_{4p} \right)^{1/2} d\mu\,(\underline{x})$$

$$\leq \int_{\mathbb{R}^2} \left(A^{4p}\, M_3^2 \| C_{(\mathcal{Z} - \mathcal{Z}_B)} \|_0 \right)^{1/2} \cdot \left(M_3\, L \| C_{\mathcal{Z}_B} \|_{4p} \right)^{1/2} d\mu\,(\underline{x})$$

$$= \left(A^{4p}\, M_3^2 \| C_{(Z - \mathcal{Z}_B)} \|_{4p} \right)^{1/2} \left(M_3\, L \| C_{\mathcal{Z}_B} \|_{4p} \right)^{1/2}$$

$$\leq \frac{1}{2} \left[A^{4p}\, M_3^2 \| C_{(Z - \mathcal{Z}_B)} \|_0 + M_3\, L \| C_{\mathcal{Z}_B} \|_{4p} \right] . \qquad \text{.....(4.3.3)}$$

Similarly,

$$\left| D^{4p}_{r,\,\bar{\phi}} \frac{1}{2\pi} \int_0^{2\pi} E\,(Z_B)_A\,(\underline{x})\,(Z - Z_B)_{A,r,\,\phi}\,(\underline{x} + \underline{y})\,d\phi \right|$$

$$= (2 M_4 + M_3^2) A^{4p} \| C_{\mathcal{Z}-\mathcal{Z}_B} \|_0 + (L M_3 + M_3^2) \| C_{\mathcal{Z}_B} \|_{4p} ,$$

$$\leq M_5 (A^{4p} \| C_{\mathcal{Z}-\mathcal{Z}_B} \|_0 + \| C_{\mathcal{Z}_B} \|_{4p})$$

where $M_5 = 2 M_4 + M_3^2 + L M_3$.

Let $\mathcal{Z} = (\mathcal{Z} - \mathcal{Z}_A) + \mathcal{Z}_A$.

Since as $\mathcal{Z} \in \mathcal{E}_0$, $\mathcal{Z} - \mathcal{Z}_A \in \mathcal{E}_0$, and $\mathcal{Z}_A \in \mathcal{E}_{4p}$.

$$K_p^* (t^{4p}, \mathcal{Z}) \leq \| C_{\mathcal{Z} - \mathcal{Z}_A} \|_0 + t^{4p} \| C_{\mathcal{Z}_A} \|_{4p}$$

and since,

$$C_{\mathcal{Z} - \mathcal{Z}_A}(\underline{y}) = E (Z - Z_A) (\underline{x}) (Z - Z_A) (\underline{x} + \underline{y})$$

$$\leq (E (Z - Z_A)^2 (\underline{x}))^{1/2} (E (Z - Z_A)^2 (\underline{x} + \underline{y}))^{1/2}$$

$$= E (Z - Z_A)^2 (\underline{x})$$

$$= E_A^2 (\mathcal{Z}) ,$$

and $E Z^2(\underline{x})$ is independent of $\underline{x}$

$$\| C_{\mathcal{Z} - \mathcal{Z}_A} \|_0 + t^{4p} \| C_{\mathcal{Z}_A} \|_{4p}$$

$$\leq E_A^2 (\mathcal{Z}) + t^{4p} (M_5 (A^{4p} \| C_{\mathcal{Z} - \mathcal{Z}_B} \|_0 + \| C_{\mathcal{Z}_B} \|_{4p}))$$

Finally using Berens-Lorentz Lemma, we have

$$K_p^* (t^{4p}, \mathcal{Z}) = \inf_A (\| C_{\mathcal{Z} - \mathcal{Z}_A} \|_0 + t^{4p} \| C_{\mathcal{Z}_A} \|_{4p})$$

$$= (O (A^{-\beta}) + (tA)^{4p} K_p^* ((\tfrac{1}{A})^{4p}, \mathcal{X}))$$

$$= O (t^{\beta}) \qquad \text{as } t \longrightarrow 0.$$

Hence $\mathcal{X} \in \mathcal{C}_{4p}^{\beta}$.

Conversely, let $\mathcal{X} \in \mathcal{C}_{4p}^{\beta}$. This implies that,

$\mathcal{X} = \mathcal{X}_0 + \mathcal{X}_{4p}$, such that $\mathcal{X}_0 \in \mathcal{C}_0$, $\mathcal{X}_{4p} \in \mathcal{C}_{4p}$, and

$$\| C_{\mathcal{X}_0} \|_0 \leq M_6 \, t^{\beta}$$

and ...(4.3.5)

$$\| C_{\mathcal{X}_{4p}} \|_{4p} \leq M_7 \, t^{\beta-4p}$$

Hence,

$$E_A^2 (\mathcal{X}) = E (Z_A - Z)^2 (\underline{x})$$

$$= E (Z_{0_A} - Z_0 + Z_{4p_A} - Z_{4p})^2 (\underline{x})$$

$$\leq 2 E (Z_{0_A} - Z_0)^2 (\underline{x}) + E (Z_{4p_A} - Z_{4p})^2 (\underline{x})$$

Now, using Theorem of section 3.5 and Lemma 4.2.2, it follows that

$$E_A^2 (\mathcal{X}) \leq 2 ((2 M_3)^2 \| C_{\mathcal{X}_0} \|_0 + (M_2 / A^{4p}) \| C_{\mathcal{X}_{4p}} \|_{4p})$$

With t = (1/A) in (4.3.5), we get

$$E_A^2 (\mathcal{Z}) \leq 2 ((2 M_3)^2 M_6 (1/A)^{\beta} + M_2 M_7 (1/A)^{\beta - 4p + 4p})$$

$$\leq M_8 A^{-\beta} .$$

where, $M_8 = 2 (2 M_3^2 + M_2 M_7) < \infty$. Therefore,

$$E_A^2 (\mathcal{Z}) = 0 (A^{-\beta}) \qquad \text{as } A \longrightarrow \infty .$$

CHAPTER 5

SIMULATION RESULTS

5.1 INTRODUCTION

In chapters 3 and 4, we have discussed some theoretical estimates of ESE in continuous convolution backprojection method. But in practice the discrete version of CBP algorithm is applied on digitized images. In this chapter we consider this practical case of discrete implementation of CBP algorithm and give some estimates of ESE which incorporate the errors due to discretization and interpolation in addition to the inherent error. Thus, we shall estimate the error in reconstruction given by

$$e = \frac{1}{MP} \sum_{i} \sum_{j} \left(\tilde{Z}(x_{ij}) - Z(x_{ij}) \right)^2$$

where, MP is the total number of pixels used in the summation and $Z(x_{ij})$ (respectively $\tilde{Z}(x_{ij})$) denotes the value of function (respectively reconstructed function) at i,j-th pixel.

We recall from Sec. 2.5 that for a second order wide sense stationary spatial stochastic process $\mathcal{Z}$, with covariance kernel $C_{\mathcal{Z}}$, the ESE is given by

$$E_A^2 (\mathcal{Z}) = E (\tilde{Z} - Z)^2$$

$$= \int\int_{\mathbb{R}^2\mathbb{R}^2} \Big[C_{\mathcal{Z}} (\| \underline{u} - \underline{v} \|) - C_{\mathcal{Z}} (\| \underline{u} \|) - C_{\mathcal{Z}} (\| \underline{v} \|) + C_{\mathcal{Z}} (0) \Big] K (\| \underline{u} \|) K (\| \underline{v} \|) \, d\underline{u} \, d\underline{v}$$

....(5.1.1)

Let I be any set of indices and suppose that the values of covariance kernel $C_{\mathcal{Z}}$ are known at points d_i, $i \in I$. Then from (5.1.1) it follows that $E_A^2 (\mathcal{Z})$ can be approximated by

$$E_A^2 (\mathcal{Z}) \cong \sum_{i \in I} \alpha_i \, C_{\mathcal{Z}} (d_i) , \qquad ...(5.1.2)$$

where the co-efficients α_i depend upon the CBP window used. Since by (2.3.3)

$$\tilde{Z} (\underline{x}) = Z * K (\underline{x}),$$

we have,

$$C_{\tilde{\mathcal{Z}}} (\underline{u}) = E (\tilde{Z} (\underline{x}) \tilde{Z} (\underline{x} + \underline{u}))$$

$$= E \int\int_{\mathbb{R}^2\mathbb{R}^2} Z (\underline{v}) Z (\underline{w}) \; K (\underline{x} - \underline{v}) K (\underline{x} + \underline{u} - \underline{w}) \, d\underline{v} \, d\underline{w}$$

$$= E \int\int_{\mathbb{R}^2\mathbb{R}^2} Z(\underline{w} + \underline{y}) Z(\underline{w}) K(\underline{x} - \underline{w} - \underline{y}) K(\underline{x} + \underline{u} - \underline{w}) \, d\underline{y} \, d\underline{w}$$

$$= \int\int_{\mathbb{R}^2\mathbb{R}^2} C_{\mathcal{Z}}(\underline{y})\, K(\underline{x} - \underline{w} - \underline{y})\, K(\underline{x} + \underline{u} - \underline{w})\, d\underline{y}\, d\underline{w}$$

$$= \int\int_{\mathbb{R}^2\mathbb{R}^2} C_{\mathcal{Z}}(\underline{y})\, K(-\underline{v} - \underline{y})\, K(\underline{u} - \underline{v})\, d\underline{v}\, d\underline{y}$$

$$= \int_{\mathbb{R}^2} C_{\mathcal{Z}} * K(-\underline{u})\, K(\underline{u} - \underline{v})\, d\underline{v}$$

$$= C_{\mathcal{Z}} * K * K_{-}(-\underline{u}) ,$$

where $K_{-}(\underline{u}) = K(-\underline{u})$. This implies that $C_{\tilde{\mathcal{Z}}}$ is a linear function of $C_{\mathcal{Z}}$ and hence we have a further approximation of ESE given by

$$E_A^2(\mathcal{Z}) \cong \sum_{i \in I} C_{\tilde{\mathcal{Z}}}(d_i)\, \beta_i \qquad \ldots(5.1.3)$$

where the co-efficients β_i again depend upon the CBP window.

If the values of the covariance kernel $C_{\mathcal{Z}}(d_i)$ are known for $i \in I$, (5.1.2) suggests regressing these on the values of $E_A^2(\mathcal{Z})$ for a sample of object functions and obtaining the estimates of α_i's. Using these estimated values of α_i and the relation (5.1.2) we can predict the reconstruction error for the future object functions for which the values $C_{\mathcal{Z}}(d_i)$ are known for $i \in I$. Even, if these values of covariance kernel are not known, they can be estimated and the estimated values

can be used to determine β_i's in (5.1.3). Finally (5.1.3) can then be used to predict the reconstruction error for future object functions.

The implemetation of the above techniques of predicting the reconstruction errors in CBP algorithm is illustrated by carrying out a detailed simulation study. This simulation study also shows the validity of the ω_c- estimate of ESE.

5.2 SIMULATION OF RANDOM IMAGES

For generating a typical 64x64 stationary image the following method was employed :

a) A 72x72 array of independent pseudo random numbers were generated from a uniform distribution on the interval [0,31]. These numbers when rounded to the nearest integers are called the codes (CD) and represent the pixel intensities in 32 gray levels.

b) For each of the inner 64x64 pixels, a circle with the radius of four unit pixel length centred on the pixel is taken and the weighted average of pixel intensities inside the circle is obtained and substituted as the value of object function in that pixel. This gives rise to a 64x64 stationary image with a covariance kernel depending on the weight function.

In our study, we used the following eight weight

functions :

(i) $\exp(-r)$, (ii) $\exp(-r^2)$, (iii) $\exp(-r^3)$, (iv) $\exp(-r^4)$, (v) $(1 + 10\,r)^{-1}$, (vi) $(1 + 10\,r^2)^{-1}$, (vii) $(1 + 10\,r^3)^{-1}$, and (viii) $(1+ 10\,r^4)^{-1}$.

Weight function (i) was used for generating 70 independent sample object images, and eight sample images were generated by making use of each of the other seven weight functions. Henceforth we shall refer to these sets of images as samples. Thus sample 1 consists of 70 images corresponding to weight function (i), and samples 2-8 corresponding to weight functions (ii)- (viii) respectively consist of eight images each. The projection data for these images were then calculated on computer as follows : For each line (θ_l, s_k), $l = 1,\ldots,L$, and $k = 1,\ldots,K$, the projection data is given as integral

$$p(s_k, \theta_l) = \int_{-T}^{T} z\,(x \cos\theta_l + t \sin\theta_l,\ x \sin\theta_l - t \cos\theta_l)\,dt$$

where limits (-T, T) depend upon s_k, and θ_l. This integral is calculated using trapezoidal rule with step size (Δs) for different values of L and K.

method [see Ramakrishna et.al.(1985) for details] is as follows. We give the description for the system (5.3.1) only. With obvious notational modifications the method applies to (5.3.2) also.

Let α_0 be an initial approximation to the solution which may either be computed by some other method or guessed. Then this iterative method, assuming $\underline{A}$ to be of order mxn, follows the steps outlined below :—

(i) Start with initial vector $\underline{\alpha}^0$.

(ii) Compute the residual $\underline{r}_0^0 = \underline{e} - \underline{A}\,\underline{\alpha}^0$.

(iii) Project the residual computed in (ii) on the j-th column, a_j, of the matrix $\underline{A}$ and compute its component along the j-th column of $\underline{A}$, i.e.,

$$\underline{r}_j^k = \underline{r}_{j-1}^k - \left((\underline{r}_{j-1}^k, \underline{a}_j) / (\underline{a}_j, \underline{a}_j) \right) \underline{a}_j$$

alter the j-th entry in the (k+1)-th approximate solution vector by adding the scalar component of the residual computed in (ii) to it, i.e.,

$$\alpha_j^{k+1} = \alpha_j^k + \left((\underline{r}_{j-1}^k, \underline{a}_j) / (\underline{a}_j, \underline{a}_j) \right)$$

(iv) Repeat step (iii) for all j=1,...,n .

(v) Continue this process till a satisfactory solution is obtained.

Using 200 iterations of this method we estimated $\underline{\alpha}$ (and $\underline{\beta}$). With this estimated $\underline{\alpha}$ substituted in equation (5.3.1) the ESE in the reconstruction of the last 20 images of sample 1 were predicted and compared with calculated errors. We found a maximum of 19% error in the prediction, while average error in prediction was 6% Table 5.1 summerizes these results.

Similarly, with estimated $\underline{\beta}$ substituted in (5.3.2). the predicted ESE in reconstruction of the last 20 images of sample 1 were obtained and compared with actual calculated error. The maximum error in prediction was found to be about 28% and average error was 6.2% Table 5.2 summerizes these findings.

TABLE 5.1

ERROR	PREDICTED ERROR	RELATIVE ERROR
2.08566300	2.09481700	0.00438894
1.97690200	1.91714200	0.03022904
2.04099200	2.10144500	0.02961927
2.08814500	2.12216800	0.01629332
2.16983300	2.07948200	0.04163955
2.01479800	2.21776700	0.10073940
2.41976900	2.12497600	0.12182710
2.17472000	2.08310500	0.04212713
2.09823000	2.13405600	0.01707449
1.96724400	2.35344900	0.19631780
2.10090700	2.05008400	0.02419119
2.10284600	2.05359300	0.02342184
2.01468100	2.16347300	0.07385401
2.06116200	2.34271400	0.13659870
2.03491500	2.36155800	0.16051950
2.00582500	2.24792500	0.12069830
2.03574300	1.99760200	0.01873579
2.08930900	2.09993100	0.00508410
2.18426200	2.16573700	0.00848129
2.07897900	2.17771100	0.04749073

MAXIMUM = .1963, MINIMUM = .0050, AVERAGE = .0609

TABLE 5.2

ERROR	PREDICTED ERROR	RELATIVE ERROR
2.08566300	2.23639500	0.07227033
1.97690200	1.98593900	0.00457148
2.04099200	2.15445300	0.05559099
2.08814500	2.09500600	0.00328545
2.16983300	2.10870000	0.02817424
2.01479800	2.15251300	0.06835194
2.41976900	1.72377900	0.28762670
2.17472000	2.01027300	0.07561736
2.09823000	1.98472000	0.05409770
1.96724400	2.27539400	0.15664050
2.10090700	2.14389300	0.02046053
2.10284600	2.03565000	0.03195485
2.01468100	2.04952900	0.01729678
2.06116200	2.13318000	0.03494067
2.03491500	2.15644000	0.05971985
2.00582500	2.28223400	0.13780310
2.03574300	1.95415300	0.04007882
2.08930900	2.18738000	0.04693926
2.18426200	2.09159400	0.04242534
2.07897900	2.11380400	0.01675082

MAXIMUM = .2817, MINIMUM = .0045, AVERAGE = .0627

5.4 AN EMPIRICAL VALIDATION OF ω_c-ESTIMATE

In section 3.3 we derived an ω_c-estimate of ESE which depends on R_c, namely

$$E_A^2 (\mathcal{Z}) \leq \frac{B_k}{A^k} \omega_c (C_{\mathcal{Z}}^{[k]} ; \frac{1}{A})$$

The expression implies that order of error in reconstruction decreases and hence the accuracy in reconstruction increases with the increase in the smoothness of the covariance kernel, provided $K \in \mathbb{K}_{2p}$.

Now, as the following derivation shows, we note that the use of 'sinc' window implies p = 1.

From equation (2.3.1) with polar co-ordinates, we have,

$$W(R) = \int_0^{2\pi} \int_0^{\infty} K(r)\, e^{-2i\pi Rr \cos \phi}\, r\, dr\, d\phi$$

Differentiating it k-times and putting R = 0, we get

$W^k(0) = 0$, for k odd, and

$$W^k(0) = (2\pi)^k (-1)^{k/2} \int_0^{\infty} r^{k+1} K(r)\, dr \left(\int_0^{2\pi} \cos^k \phi\, d\phi \right),$$

for even k.

Thus, $W^{(1)}(0) = 0$ and,

$$W^{(2)}(0) = -4\pi^3 \int r^3 K(r)\, dr \neq 0$$

for `Sinc' window, it follows that the corresponding $K \in \mathbb{K}_2$, and hence p = 1.

For an empirical validation of ω_c- estimate we first selected at random eight images from sample 1. For discussion in this section we refer to this set of 8 images selected from sample 1 as sample 9. The reconstruction was done by CBP algorithm for all eight images in each one of samples 2 to 9, using 'Sinc' window with R_c equal to 16 and 32. For samples 5 and 9 for each one of the total 16 images, the reconstruction was done for R_c = 64 also. The number of rays N_y are chosen as per sampling criterion and the number of views N_g according to the following equation [see Natterer (1986)],

$$N_g = \left(\frac{N_y - 1}{2}\right)\pi$$

to reduce the discretization error in backprojection integral. The values of N_y, total number of rays and N_g, total number of views for different values of R_c are given in Table 5.3.

TABLE 5.3 : RECONSTRUCTION PARAMETERS

Ray-spacing, ∇s	R_c	Number of views	number of Rays
2/64	16	100	64
2/128	32	200	128
2/256	64	400	256

Note:

(a) Sampling R_c = (1/2 ∇s)

(b) Optimal number of views = ((number of rays-1)/2) π

The errors reported are as follows:

$$ER1 = \frac{1}{MP} \sum_i \sum_j \left| \tilde{z}\,(x_{ij}) - z\,(x_{ij}) \right|$$

$$ERS = \frac{1}{MP} \sum_i \sum_j \left(\tilde{z}\,(x_{ij}) - z\,(x_{ij}) \right)^2$$

$$ERMax = \max_{i,j} \left| \tilde{z}\,(x_{ij}) - z\,(x_{ij}) \right|$$

$$\tilde{E} = \frac{1}{MP} \sum_i \sum_j \left| \tilde{z}^{CD}\,(x_{ij}) - z^{CD}\,(x_{ij}) \right|$$

where superscript CD represents the coded values of function in 32 gray levels.

The error ER1 represents the usual l_1 error, ERS represents the ESE, ERMax is the maximum error in a single pixel reconstruction, and $\tilde{E}$ represents an index of the visual quality of the reconstructed image. For all error computations the region was taken to be a circle of unit radius. The normalised error corresponding to ER1, ERS, and $\tilde{E}$ are given by,

$$ER1N = \left((ER1)\ MP \right) / \left(\sum_i \sum_j z\,(x_{ij}) \right)$$

$$ERSN = \left((ERS)\ MP \right) / \left(\sum_i \sum_j z\,(x_{ij}) \right)^2$$

$$\tilde{E}N = \left((\tilde{E})\ MP \right) / \left(\sum_i \sum_j z^{CD}\,(x_{ij}) \right)$$

TABLE 5.5 : SUMMARY OF ERRORS IN RECONSTRUCTION OF RANDOM IMAGES FROM SAMPLE 3

PIC	R_c	ER1	ERS	ERMax	$\tilde{E}$
1	16	1.60480	4.58385	14.44093	4.64804
	32	0.54412	0.46115	6.87797	0.67109
2	16	1.57853	4.50921	12.76333	4.60985
	32	0.54594	0.46128	6.05161	0.68876
3	16	1.54895	4.26382	12.45509	4.32481
	32	0.52774	0.42986	6.55274	0.64331
4	16	1.57631	4.40098	12.85159	4.55492
	32	0.53904	0.43228	5.88706	0.64078
5	16	1.56878	4.37426	10.82437	4.45170
	32	0.53799	0.43413	5.68387	0.64394
6	16	1.58666	4.47178	13.26219	4.53946
	32	0.54184	0.44864	6.43127	0.65309
7	16	1.57031	4.35021	11.83567	4.45234
	32	0.53137	0.42996	6.17244	0.64173
8	16	1.54074	4.28595	12.16716	4.36837
	32	0.51318	0.39728	6.02370	0.58965

TABLE 5.6 : SUMMARY OF ERRORS IN RECONSTRUCTION OF RANDOM IMAGES FROM SAMPLE 4

PIC	R_c	ER1	ERS	ERMax	$\tilde{E}$
1	16	1.74229	5.25921	14.40790	5.36963
	32	0.57479	0.50102	6.79373	0.70739
2	16	1.71181	5.20067	13.59357	5.30492
	32	0.57437	0.50287	6.17243	0.74211
3	16	1.68099	4.91581	12.68245	5.02557
	32	0.55939	0.46859	6.94053	0.68497
4	16	1.71971	5.10323	12.94719	5.15404
	32	0.57247	0.47359	6.00125	0.69287
5	16	1.70936	5.02695	11.61611	5.10669
	32	0.56798	0.47564	6.04265	0.69602
6	16	1.72677	5.15912	14.12736	5.23674
	32	0.57384	0.49471	6.85965	0.73990
7	16	1.71373	5.06646	11.96473	5.15530
	32	0.56787	0.47624	6.15964	0.70770
8	16	1.67886	4.94280	12.85695	5.04324
	32	0.54414	0.43551	5.98677	0.64994

TABLE 5.7 : SUMMARY OF ERRORS IN RECONSTRUCTION OF RANDOM IMAGES FROM SAMPLE 5

PIC	R_c	ER1	ERS	ERMax	$\tilde{E}$
1	16	1.69169	4.81965	11.11550	4.92456
	32	0.53339	0.43641	5.63172	0.66162
	64	0.31896	0.12656	1.48591	0.21717
2	16	1.70300	4.95327	12.51725	5.06092
	32	0.54207	0.44455	5.66347	0.67361
	64	0.32468	0.13217	1.73761	0.22348
3	16	1.73848	4.92837	11.37895	4.99053
	32	0.54476	0.43898	6.52774	0.64583
	64	0.32535	0.13312	1.88581	0.21622
4	16	1.71720	4.88942	11.56064	4.98864
	32	0.53903	0.42903	5.52768	0.62689
	64	0.32080	0.12840	1.65534	0.21559
5	16	1.71076	4.91810	10.47233	5.04924
	32	0.53676	0.43074	5.71330	0.64047
	64	0.31552	0.12637	1.61744	0.20960

TABLE 5.7 (Contd....)

PIC	R_c	ER1	ERS	ERMax	$\tilde{E}$
	16	1.69525	4.81116	10.96620	4.88573
6	32	0.53148	0.42293	5.60305	0.63068
	64	0.32138	0.12679	1.72970	0.21465
	16	1.71673	4.90204	11.31615	4.98611
7	32	0.53072	0.43050	6.01982	0.64678
	64	0.31942	0.12699	1.67328	0.20581
	16	1.70099	4.76821	10.21865	4.86995
8	32	0.52951	0.40561	5.59421	0.61900
	64	0.31110	0.12039	1.48726	0.19381

TABLE 5.8 : SUMMARY OF ERRORS IN RECONSTRUCTION OF RANDOM IMAGES FROM SAMPLE 6

PIC	R_c	ER1	ERS	ERMax	$\tilde{E}$
1	16	2.29068	8.13229	13.33023	8.15972
	32	0.67101	0.64205	6.67258	0.90720
2	16	2.28511	8.24757	14.09712	8.35006
	32	0.68502	0.65850	6.17501	0.94097
3	16	2.33983	8.34802	13.72709	8.40278
	32	0.68784	0.65192	7.67429	0.92077
4	16	2.32022	8.30365	13.95919	8.37500
	32	0.68889	0.64639	6.21361	0.90246
5	16	2.29941	8.28919	12.49980	8.44634
	32	0.68162	0.64259	6.70382	0.92393
6	16	2.28556	8.16798	12.63069	8.29640
	32	0.67729	0.63584	6.51307	0.91477
7	16	2.29812	8.26638	14.21908	8.28725
	32	0.67548	0.64520	6.64463	0.93813
8	16	2.28029	8.01864	12.16393	8.13920
	32	0.66887	0.60333	6.33409	0.87689

TABLE 5.9 : SUMMARY OF ERRORS IN RECONSTRUCTION OF RANDOM IMAGES FROM SAMPLE 7

PIC	R_c	ER1	ERS	ERMax	$\tilde{E}$
1	16	2.72255	11.18504	14.51111	11.28946
	32	0.77759	0.82865	7.36782	1.15877
2	16	2.70707	11.29198	15.64118	11.38352
	32	0.79302	0.85694	6.86103	1.20044
3	16	2.77559	11.50256	14.66276	11.58807
	32	0.79561	0.84559	8.58786	1.19413
4	16	2.75426	11.43549	15.51450	11.56755
	32	0.80029	0.84789	6.70077	1.18624
5	16	2.73954	11.45025	13.39005	11.49811
	32	0.78983	0.83917	7.20628	1.15783
6	16	2.72089	11.30927	14.42341	11.42929
	32	0.78656	0.83274	7.40941	1.15657
7	16	2.73190	11.38676	15.40907	11.48927
	32	0.78788	0.84354	7.51570	1.16477
8	16	2.69854	11.02025	12.76122	11.10006
	32	0.77123	0.78056	7.05621	1.08744

TABLE 5.10 : SUMMARY OF ERRORS IN RECONSTRUCTION OF RANDOM IMAGES FROM SAMPLE 8

PIC	R_c	ER1	ERS	ERMax	$\tilde{E}$
1	16	2.97979	13.26143	15.35691	13.31660
	32	0.84243	0.95812	7.71013	1.33112
2	16	2.95555	13.32545	16.28948	13.38794
	32	0.85628	0.98611	7.27841	1.35038
3	16	3.03090	13.63298	15.30843	13.76894
	32	0.86083	0.97917	9.01085	1.37374
4	16	3.01287	13.58625	16.63249	13.66635
	32	0.86702	0.98326	7.11649	1.36774
5	16	2.99357	13.54150	14.17572	13.56503
	32	0.85329	0.96535	7.67799	1.32891
6	16	2.97468	13.43073	15.36428	13.42550
	32	0.85440	0.96795	7.87311	1.32860
7	16	2.98069	13.46921	16.27425	13.51894
	32	0.85426	0.97622	7.69080	1.32544
8	16	2.95074	13.04525	13.64192	13.10922
	32	0.83340	0.90135	7.19785	1.23674

TABLE 5.11 : SUMMARY OF ERRORS IN RECONSTRUCTION OF RANDOM IMAGES FROM SAMPLE 9

PIC	R_c	ER1	ERS	ERMax	$\tilde{E}$
1	16	0.91947	2.17561	9.61702	2.24116
	32	0.38984	0.27742	4.84390	0.43529
	64	0.22451	0.06636	1.47740	0.07670
2	16	0.91210	2.18695	9.80218	2.29072
	32	0.39307	0.28037	4.83003	0.43561
	64	0.22779	0.06808	1.48973	0.07860
3	16	0.90719	2.12095	10.47944	2.18119
	32	0.39102	0.27301	5.48529	0.41667
	64	0.22703	0.06761	1.35773	0.07860
4	16	0.91799	2.14057	9.38185	2.22001
	32	0.38794	0.26748	5.02848	0.40972
	64	0.22472	0.06597	1.38346	0.07355
5	16	0.91086	2.13622	8.63433	2.23264
	32	0.38858	0.26859	4.78136	0.41383
	64	0.22516	0.06598	1.30920	0.07607

TABLE 5.13 : SUMMARY OF NORMALIZED ERRORS IN RECONSTRUCTION OF RANDOM IMAGES FROM SAMPLE 3

PIC	R_c	ER1N	ERSN	$\tilde{E}N$
1	16	0.10476	0.13507	0.30342
	32	0.03552	0.04871	0.04381
2	16	0.10198	0.13258	0.29782
	32	0.03527	0.04822	0.04450
3	16	0.09850	0.12736	0.27502
	32	0.03356	0.04598	0.04091
4	16	0.10235	0.13192	0.29575
	32	0.03500	0.04701	0.04161
5	16	0.10136	0.13072	0.28763
	32	0.03476	0.04683	0.04161
6	16	0.10287	0.13227	0.29431
	32	0.03513	0.04764	0.04234
7	16	0.10222	0.13131	0.28983
	32	0.03459	0.04694	0.04177
8	16	0.10220	0.13288	0.28976
	32	0.03404	0.04600	0.03911

TABLE 5.14 : SUMMARY OF NORMALIZED ERRORS IN RECONSTRUCTION OF RANDOM IMAGES FROM SAMPLE 4

PIC	R_c	ER1N	ERSN	$\tilde{E}N$
1	16	0.11370	0.14405	0.35042
	32	0.03751	0.05056	0.04616
2	16	0.11057	0.14180	0.34266
	32	0.03710	0.05014	0.04793
3	16	0.10689	0.13624	0.31956
	32	0.03557	0.04783	0.04356
4	16	0.11172	0.14158	0.33483.
	32	0.03719	0.04904	0.04501
5	16	0.11045	0.13958	0.32997
	32	0.03670	0.04882	0.04497
6	16	0.11200	0.14153	0.33966
	32	0.03722	0.04983	0.04799
7	16	0.11157	0.14111	0.33563
	32	0.03697	0.04919	0.04607
8	16	0.11135	0.14207	0.33449
	32	0.03609	0.04795	0.04311

TABLE 5.15 : SUMMARY OF NORMALIZED ERRORS IN RECONSTRUCTION OF RANDOM IMAGES FROM SAMPLE 5

PIC	R_c	ER1N	ERSN	$\tilde{E}N$
1	16	0.11053	0.14059	0.32176
	32	0.03485	0.04810	0.04323
	64	0.02084	0.02590	0.01419
2	16	0.10999	0.14089	0.32686
	32	0.03501	0.04799	0.04351
	64	0.02097	0.02617	0.01443
3	16	0.11061	0.13863	0.31752
	32	0.03466	0.04705	0.04109
	64	0.02070	0.02591	0.01376
4	16	0.11150	0.14084	0.32392
	32	0.03500	0.04744	0.04070
	64	0.02083	0.02595	0.01400
5	16	0.11050	0.14042	0.32614
	32	0.03467	0.04725	0.04137
	64	0.02038	0.02559	0.01354

TABLE 5.15 (Contd....)

PIC	R_c	ER1N	ERSN	$\tilde{E}N$
6	16	0.10998	0.13944	0.31696
	32	0.03448	0.04701	0.04092
	64	0.02085	0.02574	0.01393
7	16	0.11163	0.14107	0.32422
	32	0.03451	0.04754	0.04206
	64	0.02077	0.02582	0.01338
8	16	0.11269	0.14188	0.32263
	32	0.03508	0.04705	0.04101
	64	0.02061	0.02563	0.01284

TABLE 5.16 : SUMMARY OF NORMALIZED ERRORS IN RECONSTRUCTION OF RANDOM IMAGES FROM SAMPLE 6

PIC	R_c	ER1N	ERSN	$\tilde{E}N$
1	16	0.14966	0.17917	0.53311
	32	0.04384	0.05724	0.05927
2	16	0.14761	0.17842	0.53938
	32	0.04425	0.05733	0.06078
3	16	0.14879	0.17709	0.53433
	32	0.04374	0.05627	0.05855
4	16	0.15072	0.18022	0.54403
	32	0.04475	0.05717	0.05862
5	16	0.14860	0.17897	0.54585
	32	0.04405	0.05666	0.05971
6	16	0.14821	0.17804	0.53799
	32	0.04392	0.05648	0.05932
7	16	0.14956	0.17989	0.53933
	32	0.04396	0.05715	0.06105
8	16	0.15123	0.18072	0.53980
	32	0.04436	0.05637	0.05816

TABLE 5.17 : SUMMARY OF NORMALIZED ERRORS IN RECONSTRUCTION OF RANDOM IMAGES FROM SAMPLE 7

PIC	R_c	ER1N	ERSN	$\tilde{E}N$
1	16	0.17762	0.20630	0.73653
	32	0.05073	0.06385	0.07560
2	16	0.17471	0.20510	0.73467
	32	0.05118	0.06425	0.07747
3	16	0.17649	0.20454	0.73684
	32	0.05059	0.06306	0.07593
4	16	0.17886	0.20790	0.75119
	32	0.05197	0.06437	0.07703
5	16	0.17686	0.20662	0.74230
	32	0.05099	0.06360	0.07475
6	16	0.17649	0.20589	0.74136
	32	0.05102	0.06353	0.07502
7	16	0.17767	0.20741	0.74721
	32	0.05124	0.06419	0.07575
8	16	0.17901	0.20829	0.73633
	32	0.05116	0.06303	0.07214

TABLE 5.18 : SUMMARY OF NORMALIZED ERRORS IN RECONSTRUCTION OF RANDOM IMAGES FROM SAMPLE 8

PIC	R_c	ER1N	ERSN	$\tilde{E}N$
1	16	0.19433	0.22208	0.86846
	32	0.05494	0.06788	0.08681
2	16	0.19077	0.22039	0.86414
	32	0.05527	0.06817	0.08716
3	16	0.19291	0.22050	0.87636
	32	0.05479	0.06719	0.08744
4	16	0.19571	0.22414	0.88774
	32	0.05632	0.06856	0.08885
5	16	0.19348	0.22244	0.87673
	32	0.05515	0.06753	0.08589
6	16	0.19281	0.22168	0.87020
	32	0.05538	0.06767	0.08612
7	16	0.19393	0.22316	0.87957
	32	0.05558	0.06831	0.08624
8	16	0.19583	0.22414	0.87001
	32	0.05531	0.06699	0.08208

TABLE 5.19 : SUMMARY OF NORMALIZED ERRORS IN RECONSTRUCTION OF RANDOM IMAGES FROM SAMPLE 9

PIC	R_c	ER1N	ERSN	$\tilde{E}N$
1	16	0.06012	0.09553	0.14654
	32	0.02549	0.03879	0.02846
	64	0.01468	0.01897	0.00502
2	16	0.05894	0.09464	0.14803
	32	0.02540	0.03853	0.02815
	64	0.01472	0.01899	0.00508
3	16	0.05770	0.09187	0.13873
	32	0.02487	0.03748	0.02650
	64	0.01444	0.01865	0.00500
4	16	0.05956	0.09414	0.14404
	32	0.02517	0.03784	0.02658
	64	0.01458	0.01879	0.00477
5	16	0.05886	0.09358	0.14427
	32	0.02511	0.03773	0.02674
	64	0.01455	0.01870	0.00492

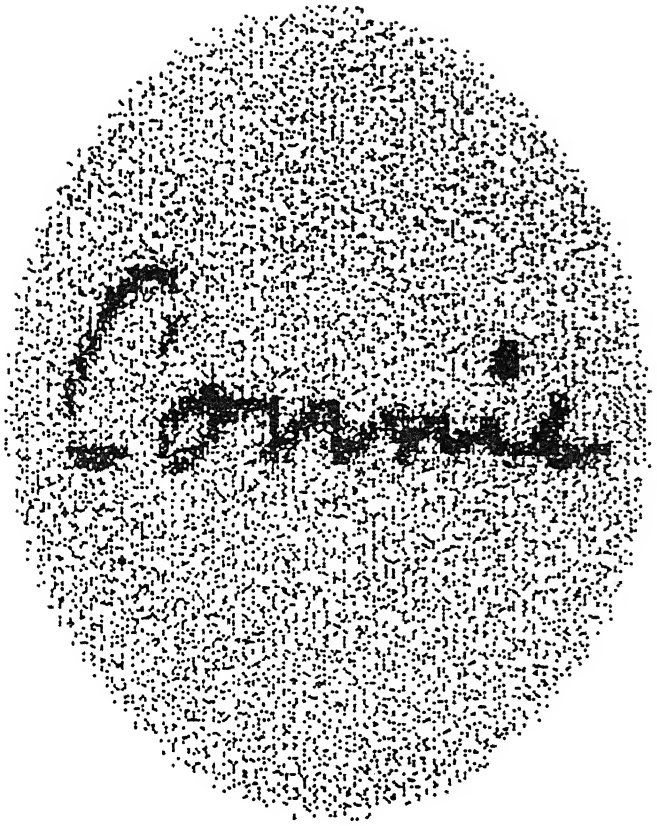

Fig. 5.3 Reconstruction of Fig. 5.1 for $R_c = 16$.

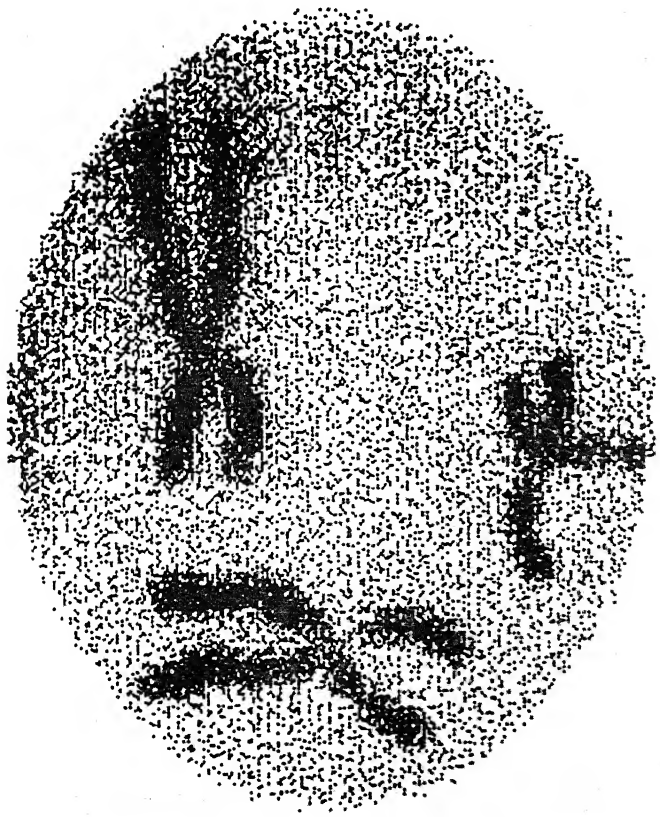

Fig. 5.4 Reconstruction of Fig. 5.2 for $R_c = 16$.

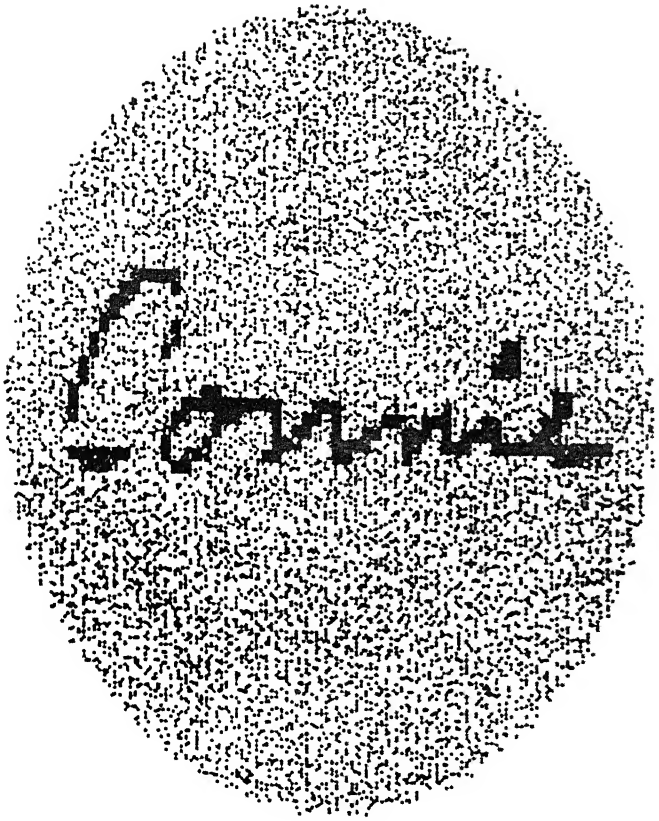

Fig. 5.5 Reconstruction of Fig. 5.1 for $R_c = 32$.

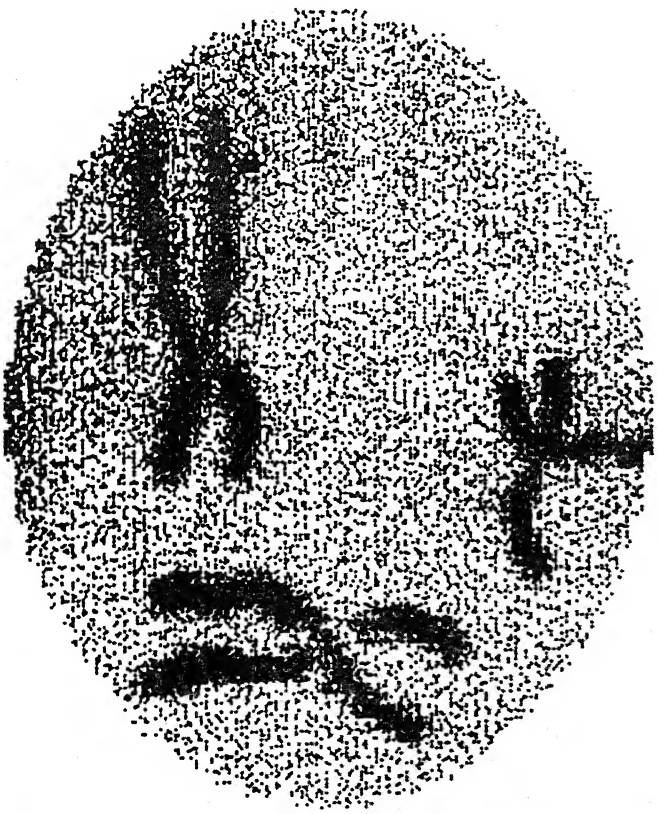

Fig. 5.6 Reconstruction of Fig. 5.2 for $R_c = 32$.

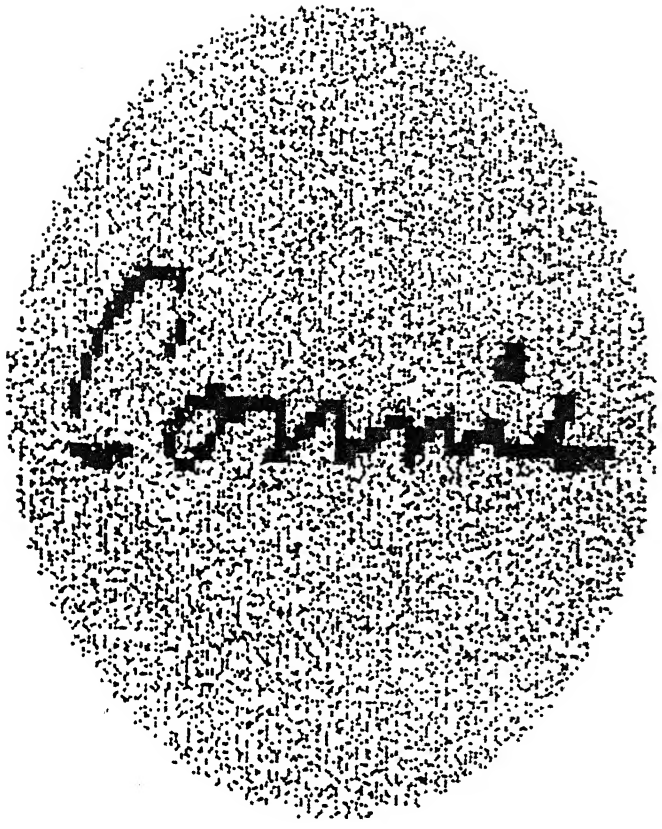

Fig. 5.7 Reconstruction of Fig. 5.1 for $R_c = 64$.

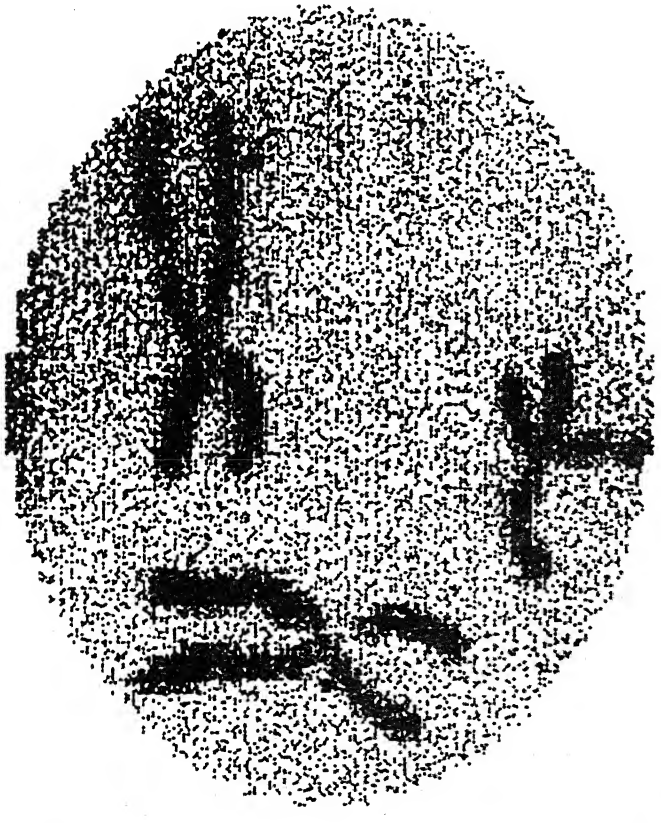

Fig. 5.8 Reconstruction of Fig. 5.2 for $R_c = 64$.

CHAPTER 6

THE OPTIMAL FILTER

6.1 INTRODUCTION

In chapters 1 and 2 we have discussed the CBP method and it's discrete implementation. This method idealizes the projection data as line integrals, but in actual practice the projection data are integrals over strips of finite width. In the case of Positron Emission Tomography (PET), the data collection procedure is entirely different. However, the PET problem gets reduced to the CT problem, using transmission tomography, after a suitable attenuation compensation has been made [see, e.g., Vardi, Shepp and Kaufman (1985)] .

Thus, as shown in section 2.2, in implementing CBP algorithm, approximations are introduced both while taking care of data collection procedure, as well as while performing discrete backprojection operation. In the CBP method one would wish for a convolving function (also called filter in this chapter) q which does the data-noise reduction and compensates for the discretized model, as well as the interpolations made. The question, however, is whether a

single convolving function could be chosen to do all these tricks simultenously.

The present practice seems to be that of experimenting with various analytical convolving functions [see Ramachandran and Lakshminarayanan (1971) and Shepp and Logan (1974)] on a set of standard phantoms and finally using the one which works best for the type of cross-section under study.

In this chapter we propose a method of derivation of a convolving function which optimally takes care of (i) the stochastic process $\mathcal{Z}$ giving rise to object image z(x,y), (ii) the data collection geometry, (iii) the cross-sectional discretization scheme, and (iv) the data noise, while at the same time minimizing a given expected weighted sum of squared error in pixel reconstruction.

6.2 THEORETICAL FORMULATION

We assume that the discretization of object, whose intensity or cross-sectional distribution at point (x,y) is given by z(x,y), is done on an NxN grid of pixels. We also assume that object distribution is limited to a unit circle with origin as centre.

Let

$$z = (z(x_i, y_j), \quad i,j=1,.....,N)$$

denote the N^2-vector (written in matrix form) of discretized object distribution. Let the KxL matrix $P = (p (s_k, \theta_l))$ denote the matrix of projection data where K and L are the total numbers of rays and views, respectively, for which data is available and $p(s_k, \theta_l)$ is the projection along k-th ray and l-th view .

For the reconstruction $\tilde{z} (x_{1i}, x_{2j})$ of $z (x_{1i}, x_{2j})$ by CBP method, equations (2.2.1 - 2.2.3) can be rewritten as follows:

$$\tilde{z} (x_{1i}, x_{2j}) = (\Delta s) \sum_{l=1}^{L} \tilde{p} (x_{1i} \cos \theta_l + x_{2j} \sin \theta_l, \theta_l)$$

$$= (\Delta\theta) \sum_{l=1}^{L} (\Delta s') \sum_{k'} (\Delta s) \sum_{k=1}^{K} p_m(s_k, \theta_l)\, q (s_{k'} - s_k).$$

$$I (x_{1i} \cos \theta_l + x_{2j} \sin \theta_l - s_{k'}) \qquad \ldots(6.2.1)$$

$$= (\Delta\theta)(\Delta s)(\Delta s') \sum_{l=1}^{L} \sum_{k'} \sum_{k=1}^{K} p_m(s_k, \theta_l)\, q (s_{k'} - s_k).$$

$$I (x_{1i} \cos \theta_l + x_{2j} \sin \theta_l - s_{k'})$$

$$= (\Delta\theta)(\Delta s)(\Delta s') \sum_{l=1}^{L} \sum_{k'} \sum_{k=1}^{K} p_m(s_{k'} - s_k, \theta_l)\, q (s_k).$$

$$I (x_{1i} \cos \theta_l + x_{2j} \sin \theta_l - s_{k'})$$

$$= (\Delta\theta)(\Delta s) \sum_{l=1}^{L} \sum_{k=1}^{K} (\Delta s') \sum_{k'} p_m(s_{k'} - s_k, \theta_l).$$

$$I\,(x_{1i}\cos\theta_l + x_{2j}\sin\theta_l - s_{k'}).q\,(s_k)$$

$$= (\Delta\theta)(\Delta s) \sum_{k=1}^{K} \sum_{l=1}^{L} \tilde{p}_m(x_{1i}\cos\theta_l + x_{2j}\sin\theta_l - s_k, \theta_l)\; q\,(s_k). \qquad \ldots(6.2.2)$$

where p_M denote the modified projection data.

Thus in matrix form (6.2.2) can be written as

$$\tilde{\mathbf{z}} = \mathbf{X}\,\mathbf{q} \qquad \ldots\ldots(6.2.3)$$

where $\tilde{\mathbf{z}}$ is N^2-vector of reconstructed object distribution, $\mathbf{X}$ is an N^2x K matrix and the K-vector $\mathbf{q}$ is the convolving function (filter). As the k-th element $q(s_k)$ of $\mathbf{q}$ is taken to be independent of the particular view and depends on the magnitude of s_k alone, it will be denoted by q_k and will be called k-th filter coefficient.

The error in (i,j)-th pixel reconstruction is $z(x_i, y_j) - \tilde{z}(x_i, y_j)$ and the weighted total expected reconstruction error is

$$\mathfrak{E} = E_{\tilde{\mathbf{z}}}\,[(\mathbf{z} - \tilde{\mathbf{z}})'T\,(\mathbf{z} - \tilde{\mathbf{z}})] \qquad \ldots\ldots(6.2.4)$$

where T is a positive semi-definite matrix representing the relative weights given to the pixels. In minimizing the

expected error $\mathcal{E}$ we get the normal equations

$$Qq = R \qquad \ldots.(6.2.5)$$

where $Q = E_{\mathcal{Z}}(X^T X)$ and $R = E_{\mathcal{Z}}(X^T z)$ with X-matrix as in equation (6.2.3). As is well known (6.2.5) is a consistent system, and any solution of the system (6.2.5) gives an optimal filter. In cases when Q is deficient the q of interest is the Moore-Penrose solution of (6.2.5). Note that Q is positive semi-definite and would be positive definite in most cases of practical interest.

When the parameters of the process $\mathcal{Z}$ are unknown we propose the following method to estimate the optimal filter from the ensemble.

6.3 ESTIMATION OF OPTIMAL FILTER

Let $z_1,\ldots,z_n$ be a random sample (consisting of phantoms, in practice) from $\mathcal{Z}$ and let $X_1,\ldots,X_n$ be the corresponding X-matrices determined from projection data on the machine. From the law of large numbers, since z_i(and X_i), i= 1,...,n are independently and identically distributed, it follows that

$$Q_n = \frac{1}{n}\sum_{i=1}^{n} X_i^T X_i \quad \text{and} \quad R_n = \frac{1}{n}\sum_{i=1}^{n} X_i^T z_i \qquad \ldots.(6.3.1)$$

are strongly consistent estimators of Q and R, respectively.

$$q_n = Q_n^+ R_n \longrightarrow Q^+ R = q_{opt} \qquad \text{w.p.1}$$

As $R_n \longrightarrow R$ w.p.1, and Q^+ is unique it follows that the convergence w.p.1 is along the whole sequence rather than just along a subsequence. In such a situation where a choice of r is not readily estimable, one may use a sufficiently small $\in$ and truncate those $\lambda_i^{(n)}$'s which are smaller than $\in$ and estimate them as 0.

(II) APPROXIMATE EXPECTATION MINIMIZATION (AEM): Let $\tilde{z}_1, \ldots, \tilde{z}_n$ be reconstructions of $z_1, \ldots, z_n$. In AEM we estimate q_{opt} by minimizing the error

$$e_n = \frac{1}{n} \sum [(z_i - \tilde{z}_i)' T (z_i - \tilde{z}_i)] \qquad \ldots (6.3.3)$$

Since by law of large numbers, $e_n \longrightarrow \mathcal{E}$ w.p.1, for suffieciently large n a q_n which minimizes e_n, will approximately minimize the errror $\mathcal{E}$ in (6.2.5).

6.4 NUMERICAL IMPLEMENTATION AND COMPARISONS

For the purpose of numerical implemetation of the optimal filter, the sample taken is of 17 40x40 digitized pictures from Gonzalez(1977), Munshi(1988)and Rastogi (1988). Projection data for these object distributions (pictures) were obtained using:

(a) Transmission (CAT) method and line integrals,

(b) Transmission (CAT) method and strip integrals,

(c) Emission (PET) method and line integrals,

and

(d) Emission (PET) method and strip integrals,

thus giving rise to four modes of data collection. The data acquisition was carried out for 40 views and 40 rays in the case of CAT and with 40 detectors in PET case. As shown in Figure 6.1, calculations of strip integrals in PET case involve strips of width $\cos(\theta-\phi)$ $-\cos(\theta+\phi)$. where, 2θ is the angle the two detectors defining the strip make at the centre and 2ϕ is the angle the two adjoining detectors make at the centre. It is assumed that the detectors are fixed at equal distances around the object on a circle in the same plane. All calculations for obtaining the optimal filter were carried out with matrix T as identity and Gaussian elimination method was used for solving the resulting system of linear equations. The comparisons have been done with standard filters. [Ramachandran and Lakshminarayanan (1971), Shepp and Logan (1974), and CSI filter of Rathore et.al. (1988), RKS filter of Rathore(1987)] with respect to the error criterion

$$EL_2 = \left[\sum (\tilde{z}_{ij} - z_{ij})^2 / MP \right]^{1/2}$$

where, z_{ij} and $\tilde{z}_{ij}$ are the actual object function and the

reconstructed object function values in (i,j)-th pixel and MP is the total number of pixels used in the summation.

Results (values of EL_2) in the noise free case are given in Tables 6.1-6.4. These results for test case pictures are shown in Figures 6.2-6.10, for CAT line integral, i.e., case (a), Figures 6.11-6.19 for case (b), Figures 6.20-6.28 for case (c) and Figures 6.29-6.37 for case (d).

In order to simulate a noisy case, independent and identically distributed pseudo random variables having a uniform distribution over the interval(-7.5, 7.5) were generated, projection data for noise alone were obtained and the resulting noise was then added to the noise-free projection data, and from this noisy data reconstructions were made. The EL_2-errors in this case are given in Tables 6.5-6.8. The corresponding results for test case pictures are sown in Figures 6.38-6.46 for case (a), Figures 6.47-6.55 for case (b), Figures 6.56-6.64 for case (c) and Figures 6.65-6.73 for case (d).

6.5 CONCLUSIONS

From the tables of EL_2 it is clear that the proposed filter compares very favorably with any of the other filters used. For certain pictures, in fact, the reduction in error is upto 20 percent, in noise-free case and upto 30 percent, in

noisy case.

The following features of the proposed filter are worth noting:

(1) Since the class of pictures on which it was tested is quite heterogeneous, the derivation gives a filter that is quite robust, as the results show.

(2) A comparative study of noisy and noise-free cases shows that as compared with the standard filters, the optimal filter in noisy environment is indeed effective in noise reduction. Thus in the noisy case, without prefiltering the projection data, the performance of CBP with this optimal filter is expected to be better than that of other methods like ART.

(3) Provisions for further improvement of the filter are also present. As new cross-sectional distributions (phantoms) become available, their information can also be incorporated in deriving the improved filter.

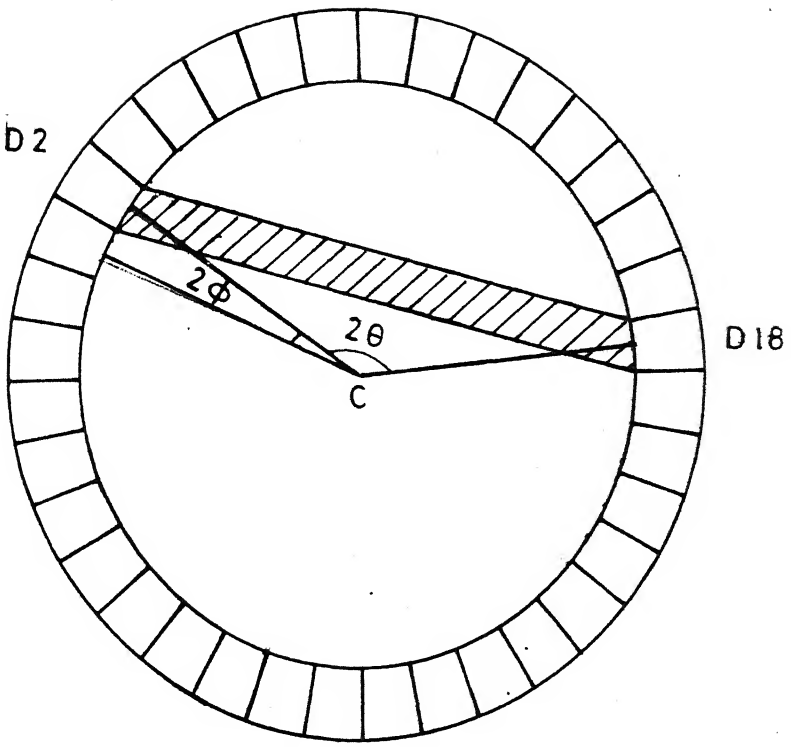

FIG.6.1 Showing width of strip in PET strip.
(D2, D18) is detector strip.
C is the centre.

TABLE 6.1 : L_2 ERROR IN CAT LINE INTEGRAL (NOISE-FREE) CASE

PIC/FILTER	OPT	RAM	RKS	SHE	CSI
LIN	3.406	3.696	3.870	3.657	3.754
FAC	3.304	4.499	4.695	4.412	4.521
BRA	4.661	4.732	4.964	4.661	4.697
STA	3.146	3.182	3.326	3.146	3.206
COR	13.672	14.016	14.634	13.809	13.878
SAT	3.818	5.325	5.551	5.250	5.401
THO	4.077	4.174	4.402	4.093	4.142
SMO	0.941	1.041	1.083	1.026	1.026
PLA	2.913	3.141	3.299	3.071	3.089
BOY	3.574	3.437	3.613	3.398	3.496
MON	2.344	3.177	3.330	3.133	3.221
WOR	3.135	3.161	3.315	3.119	3.151
CHA	5.229	6.270	6.537	6.190	6.350
FIN	2.823	3.751	3.872	3.710	3.791
CRO	3.445	3.531	3.704	3.488	3.531
JET	4.067	4.235	4.423	4.179	4.217
GEO	2.372	3.276	3.374	3.227	3.349
AVERAGE	3.937	4.391	4.588	4.328	4.401

TABLE 6.2: L_2 ERROR IN CATSTRIP INTEGRAL (NOISE FREE) CASE

PIC/FILTER	OPT	RAM	RKS	SHE	CSI
LIN	3.464	3.793	3.619	3.657	3.735
FAC	3.347	4.586	4.390	4.455	4.521
BRA	4.714	4.910	4.643	4.697	4.697
STA	3.170	3.254	3.122	3.146	3.194
COR	13.649	14.313	13.695	13.809	13.787
SAT	3.868	5.426	5.225	5.250	5.401
THO	4.126	4.321	4.061	4.126	4.142
SMO	0.941	1.069	1.012	1.026	1.026
PLA	2.966	3.247	3.054	3.106	3.089
BOY	3.633	3.535	3.359	3.398	3.476
MON	2.410	3.243	3.111	3.133	3.221
WOR	3.135	3.246	3.087	3.113	3.135
CHA	5.256	6.377	6.137	6.190	6.323
FIN	2.843	3.771	3.690	3.690	3.791
CRO	3.463	3.643	3.463	3.497	3.514
JET	4.104	4.348	4.160	4.198	4.217
GEO	2.494	3.301	3.203	3.227	3.349
AVERAGE	3.975	4.493	4.296	4.336	4.389

TABLE 6.3: L_2 ERROR IN PET LINE INTEGRAL (NOISE-FREE) CASE

PIC/FILTER	OPT	RAM	RKS	SHE	CSI
LIN	3.735	4.044	4.141	4.122	4.315
FAC	3.673	4.912	4.868	4.890	5.021
BRA	4.839	4.910	5.052	5.017	5.213
STA	3.542	3.626	3.698	3.674	3.807
COR	15.000	15.023	15.092	15.046	15.115
SAT	4.346	5.853	5.878	5.878	6.104
THO	4.272	4.434	4.597	4.548	4.840
SMO	0.969	1.112	1.055	1.069	1.069
PLA	3.212	3.440	3.422	3.422	3.510
BOY	4.043	3.808	3.945	3.906	4.160
MON	2.761	3.528	3.528	3.506	3.637
WOR	3.570	3.628	3.697	3.676	3.761
CHA	6.217	7.150	7.257	7.230	7.471
FIN	3.226	4.194	4.094	4.114	4.114
CRO	3.850	3.962	4.057	4.031	4.177
JET	4.591	4.798	4.798	4.798	4.910
GEO	2.958	3.569	3.545	3.545	3.667
AVERAGE	4.400	4.823	4.866	4.851	4.994

TABLE 6.6: L_2 ERROR IN PET LINE INTEGRAL (NOISY) CASE

PIC/FILTER	OPT	RAM	RKS	SHE	CSI
LIN	4.044	4.277	4.238	4.296	4.470
FAC	4.108	5.216	5.260	5.194	5.303
BRA	5.106	5.159	5.106	5.195	5.337
STA	3.963	3.939	3.939	3.939	4.011
COR	15.023	15.092	15.046	15.115	15.161
SAT	4.622	6.054	6.054	6.054	6.280
THO	4.580	4.727	4.629	4.759	4.987
SMO	1.768	1.668	1.739	1.639	1.597
PLA	3.475	3.633	3.668	3.615	3.703
BOY	4.160	4.023	3.926	4.062	4.258
MON	3.133	3.834	3.856	3.834	3.944
WOR	3.867	3.877	3.856	3.893	3.930
CHA	6.323	7.230	7.150	7.257	7.471
FIN	3.489	4.295	4.376	4.255	4.295
CRO	4.160	4.195	4.169	4.203	4.281
JET	4.798	4.929	4.948	4.910	5.004
GEO	3.276	3.692	3.765	3.667	3.741
AVERAGE	4.700	5.049	5.043	5.052	5.163

TABLE 6.7: L_2 ERROR IN CAT STRIP INTEGRAL (NOISY) CASE

PIC/FILTER	OPT	RAM	RKS	SHE	CSI
LIN	4.006	4.509	4.954	4.296	4.219
FAC	4.108	5.368	5.781	5.151	5.129
BRA	5.213	5.390	5.889	5.177	5.052
STA	3.951	4.215	4.695	3.987	3.831
COR	13.878	14.176	14.840	13.970	13.993
SAT	4.421	6.003	6.405	5.828	5.853
THO	4.743	5.019	5.490	4.792	4.678
SMO	2.495	3.022	3.621	2.666	2.310
PLA	3.808	4.194	4.721	3.931	3.756
BOY	4.375	4.551	5.078	4.277	4.140
MON	3.396	4.229	4.733	3.966	3.834
WOR	3.782	4.074	4.620	3.808	3.628
CHA	5.576	6.697	7.177	6.510	6.563
FIN	3.569	4.578	5.001	4.376	4.295
CRO	4.177	4.479	4.996	4.238	4.074
JET	4.648	4.985	5.454	4.760	4.629
GEO	3.325	4.254	4.719	4.010	3.936
AVERAGE	4.675	5.279	5.775	5.044	4.936

TABLE 6.8: L_2 ERROR IN PET STRIP INTEGRAL (NOISY) CASE

PIC/FILTER	OPT	RAM	RKS	SHE	CSI
LIN	4.277	4.199	4.102	4.238	4.412
FAC	4.021	4.521	4.390	4.564	4.825
BRA	5.390	5.177	5.106	5.230	5.373
STA	3.843	3.735	3.686	3.759	3.855
COR	15.023	14.977	14.932	15.023	15.069
SAT	4.773	5.627	5.426	5.727	6.079
THO	4.580	4.678	4.564	4.710	4.954
SMO	1.967	1.639	1.697	1.625	1.597
PLA	3.475	3.387	3.352	3.387	3.510
BOY	4.316	4.043	3.926	4.082	4.297
MON	3.374	3.550	3.484	3.571	3.747
WOR	4.020	3.925	3.914	3.936	3.957
CHA	6.670	7.097	6.937	7.177	7.444
FIN	3.448	3.791	3.731	3.831	3.952
CRO	4.264	4.169	4.117	4.195	4.298
JET	4.798	4.704	4.610	4.741	4.891
GEO	3.447	3.569	3.472	3.618	3.790
AVERAGE	4.805	4.870	4.791	4.907	5.062

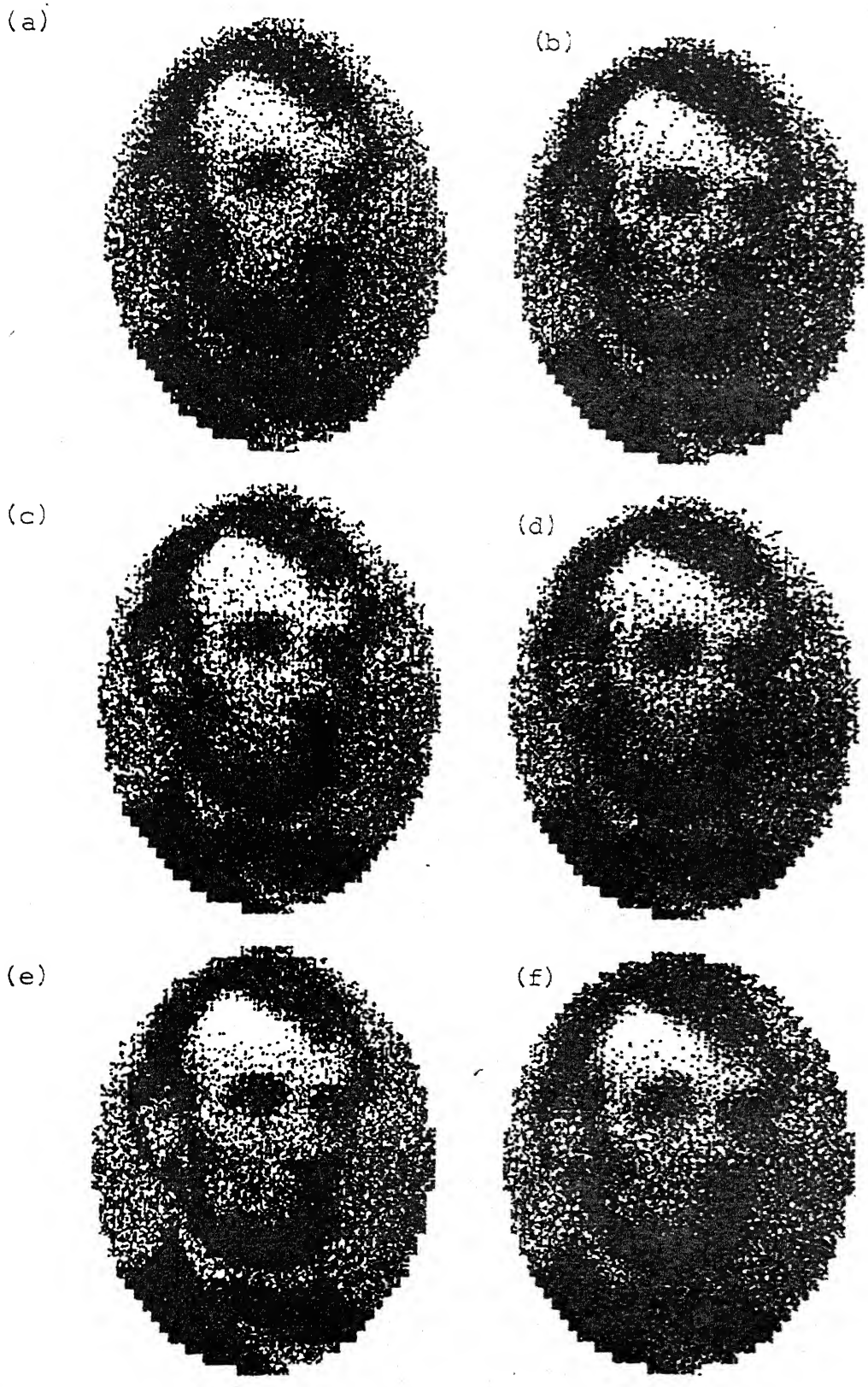

Fig. 6.2 Reconstruction of Lincoln in CAT line integral noise-free case (a) CSI filter, (b) RAM filter, (c) RKS filter, (d) SHEPP filter, (e) original picture, (f) optimal filter.

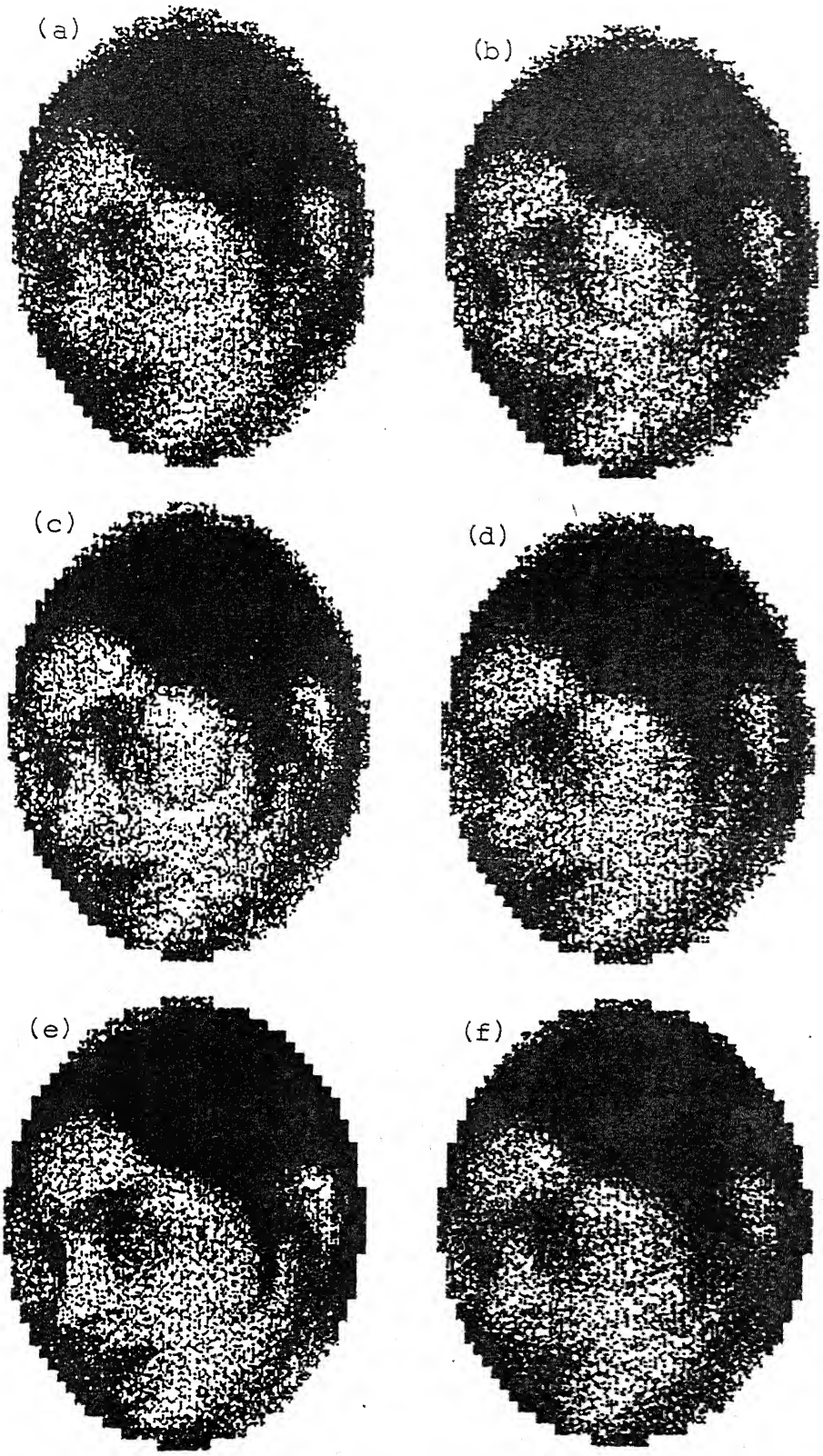

Fig. 6.3 Face of a girl in CAT line integral noise-free case (a) CSI filter, (b) RAM filter, (c) RKS filter, (d) Shepp filter, (e) original picture, (f) optimal filter.

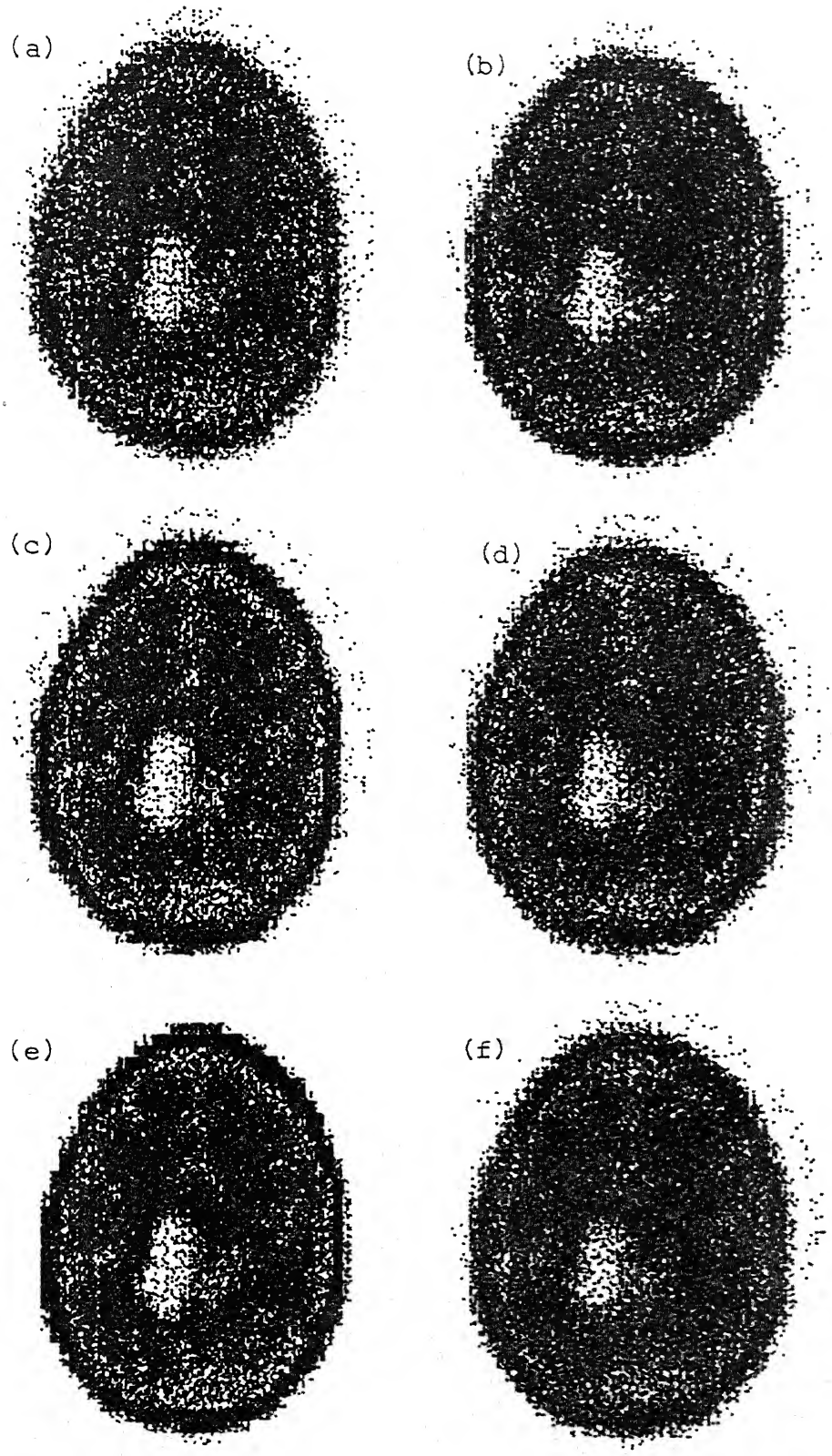

Fig. 6.4 Reconstruction of brain in CAT line integral noise-free case (a) CSI filter, (b) RAM filter, (c) RKS filter, (d) Shepp filter, (e) original picture, (f) optimal filter.

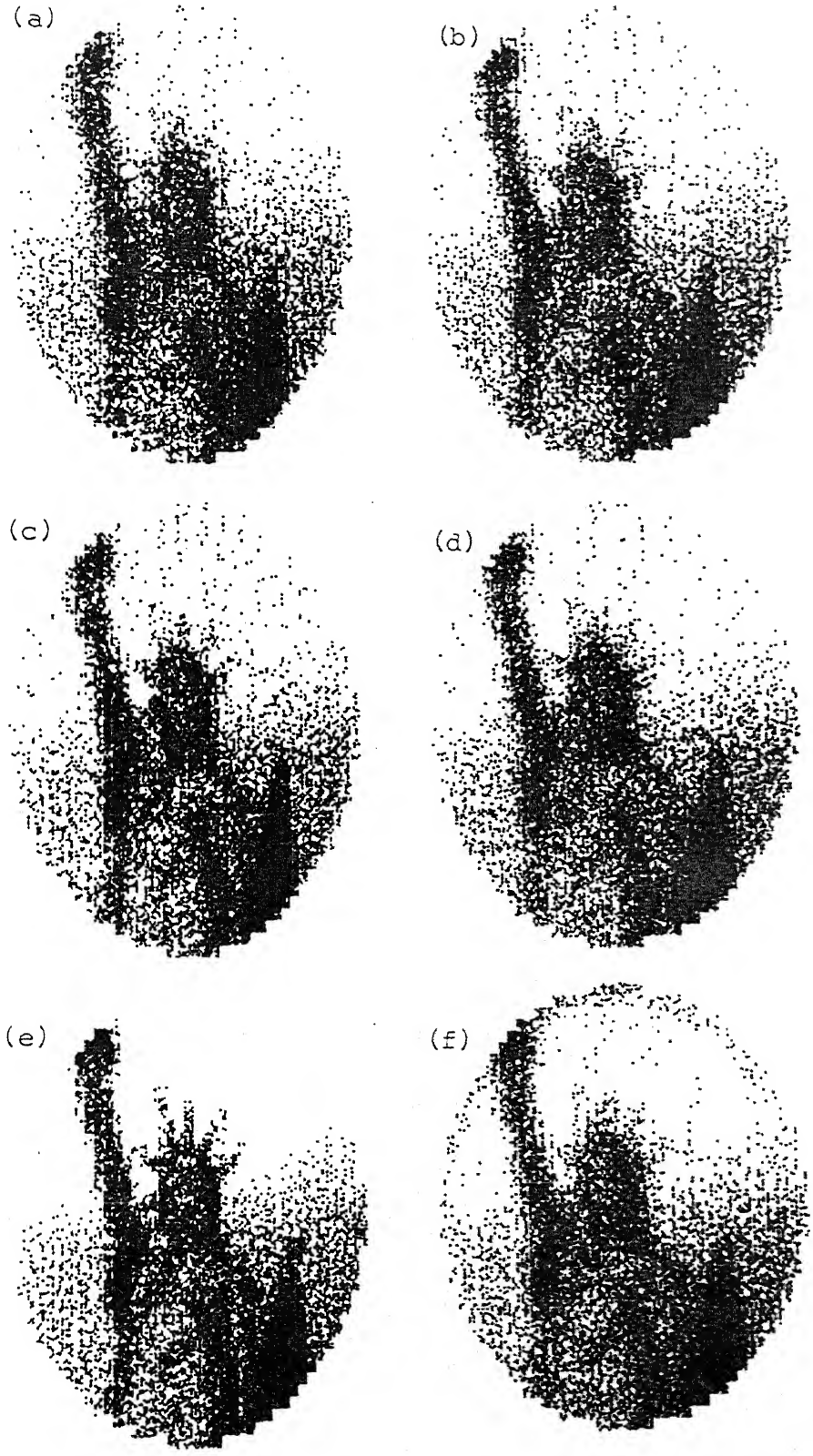

Fig. 6.5 Reconstruction of statue of liberty in CAT line integra noise-free case (a) CSI filter, (b) RAM filter, (c) RKS filter, (d) Shepp filter, (e) original picture (f) opti filter.

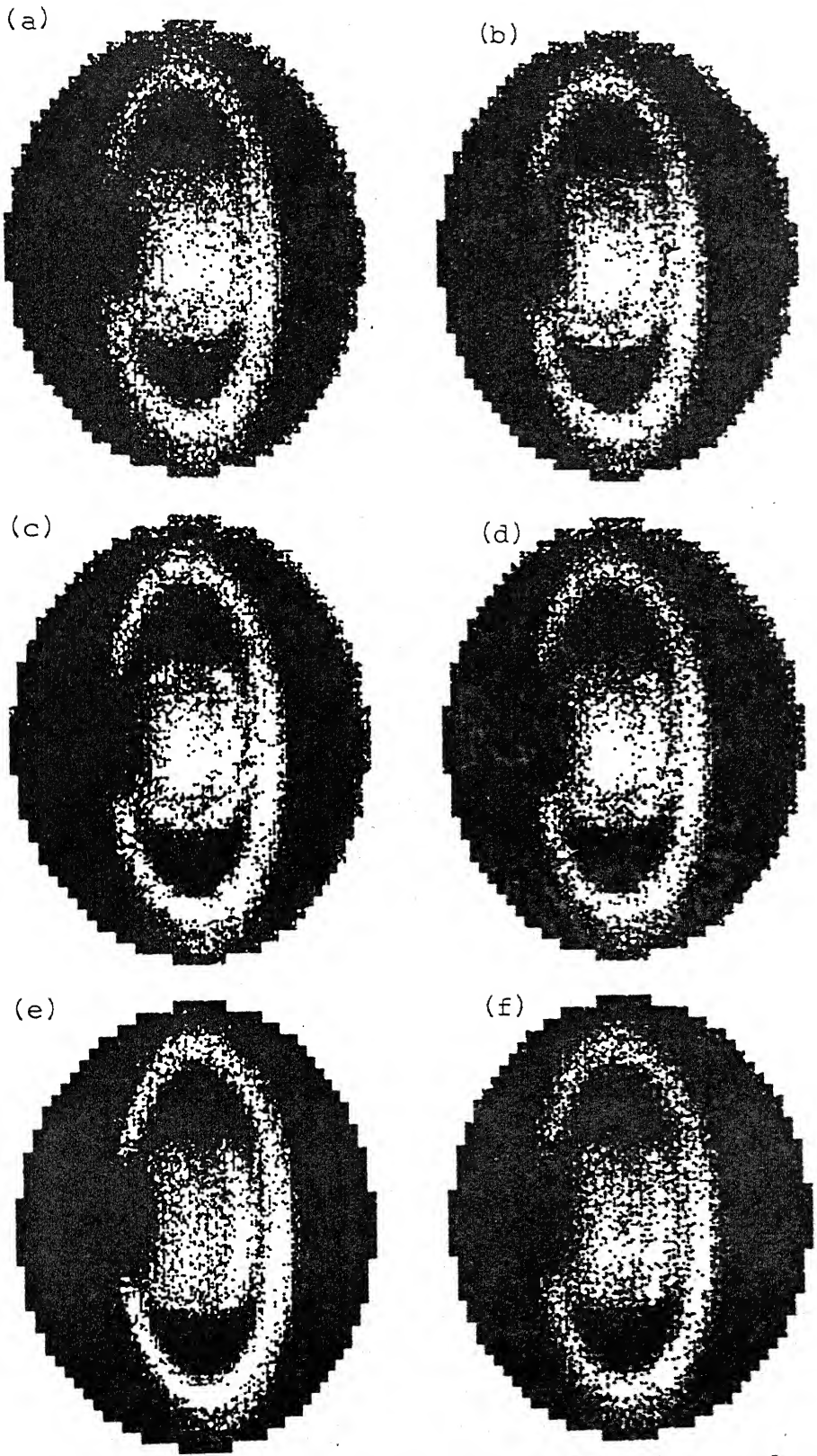

Fig. 6.6 Reconstruction of Saturn in CAT line integral noise-free case (a) CSI filter, (b) RAM filter, (c) RKS filter, (d) Shepp filter, (e) original picture, (f) optimal filte

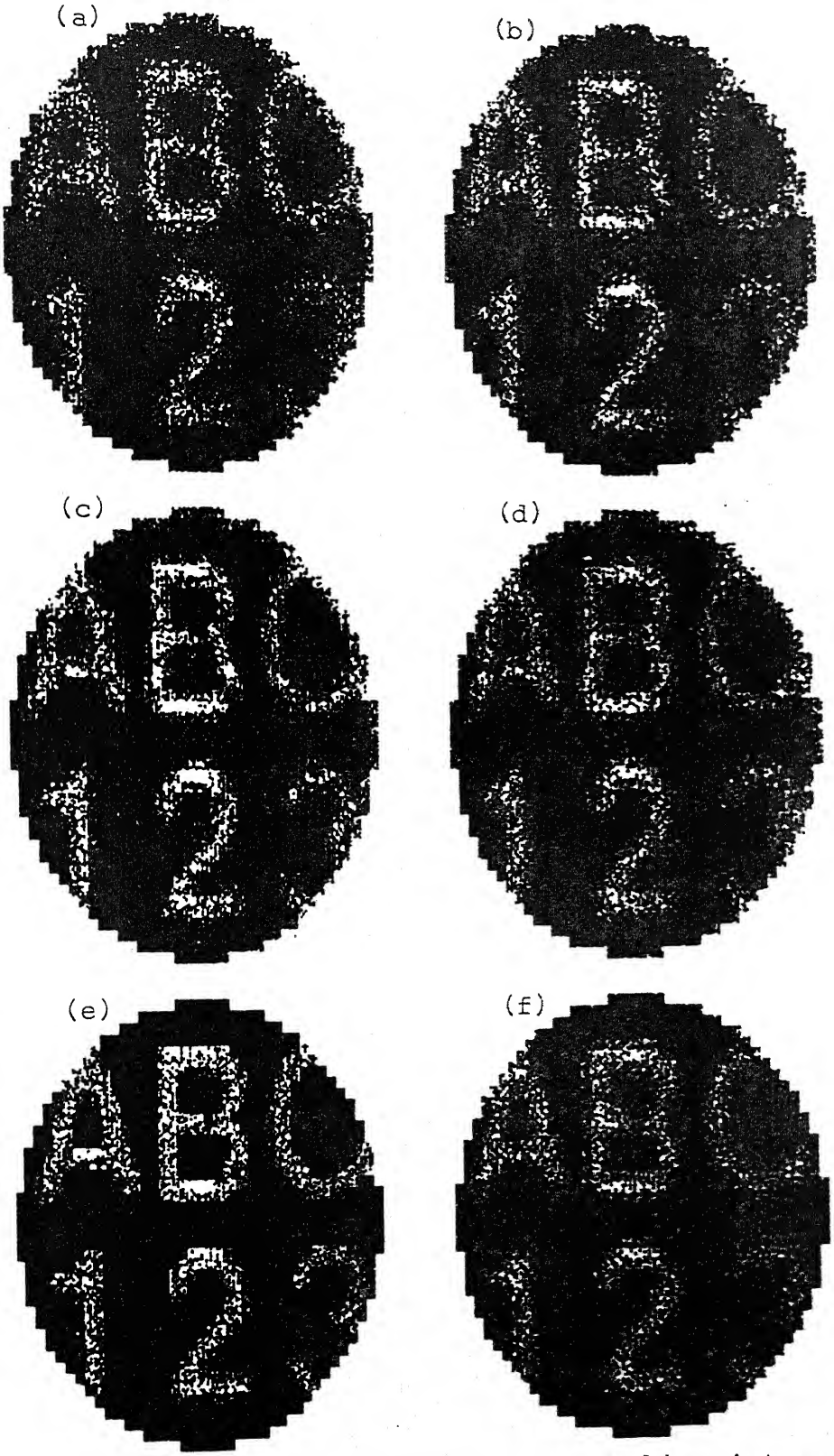

Fig. 6.9 Reconstruction of Characters in CAT line integral noise free case (a) CSI filter, (b) RAM filter, (c) RKS filte (d) Shepp filter, (e) original picture, (f) optimal fi

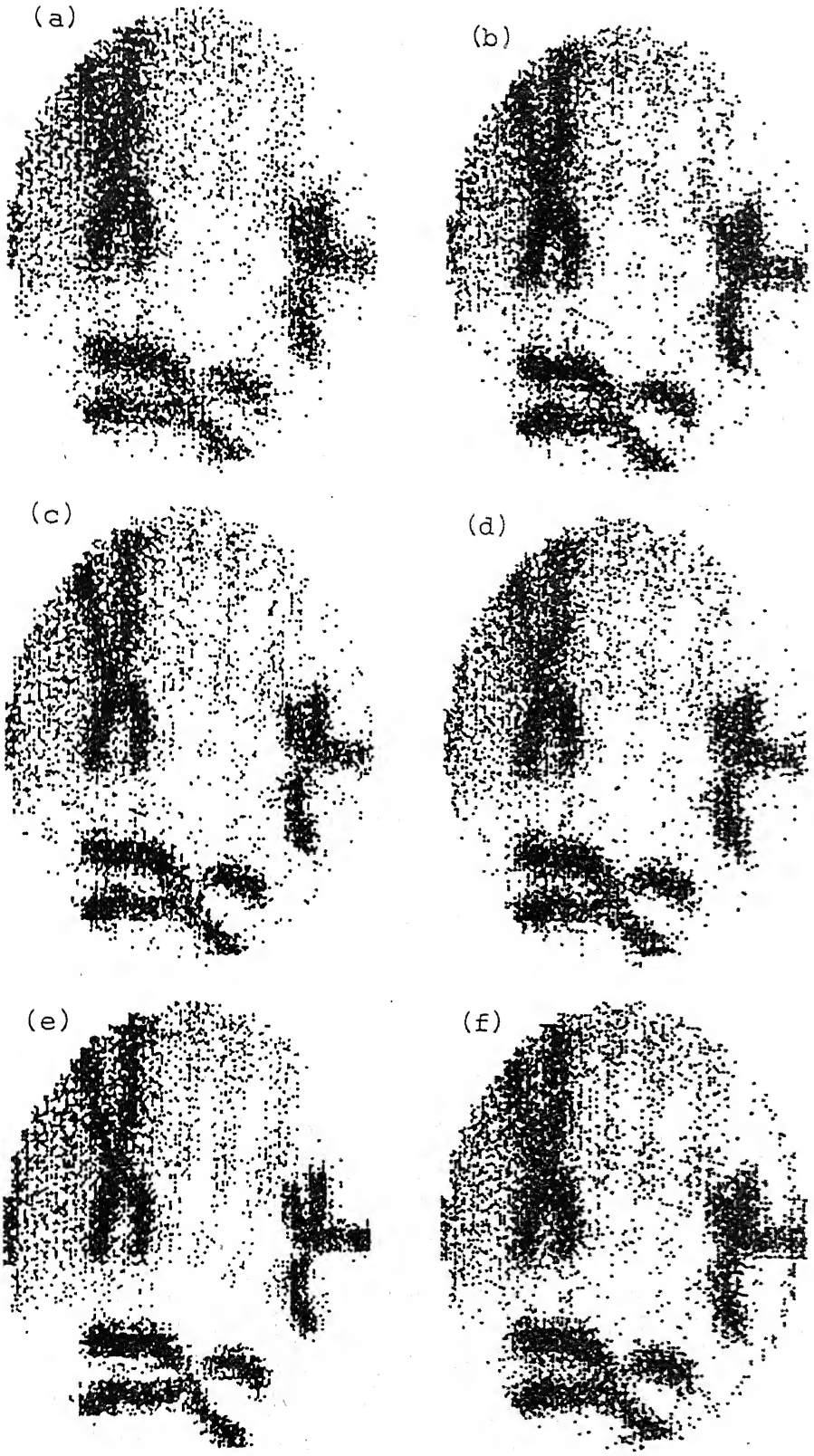

Fig. 6.10 Reconstruction of Chromosomes in CAT line integral noise-free case (a) CSI filter, (b) RAM filter, (c) RKS filter, (d) Shepp filter, (e) original picture, (f) optimal filter.

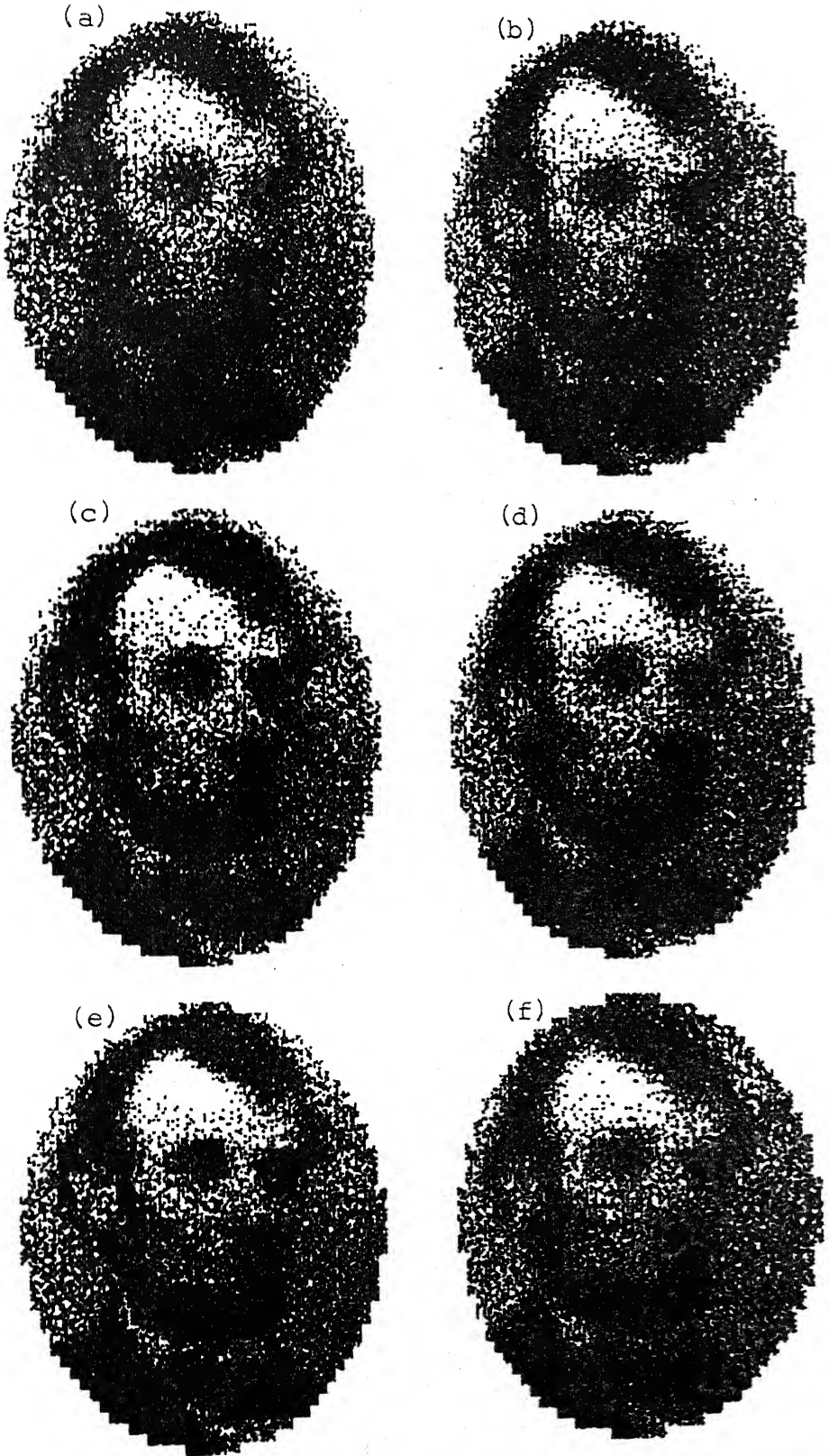

Fig. 6.11 Reconstruction of Lincoln in CAT strip integral noise-free case (a) CSI filter, (b) RAM filter, (c) RKS filter, (d) Shepp filter, (e) original picture, (f) optimal filter

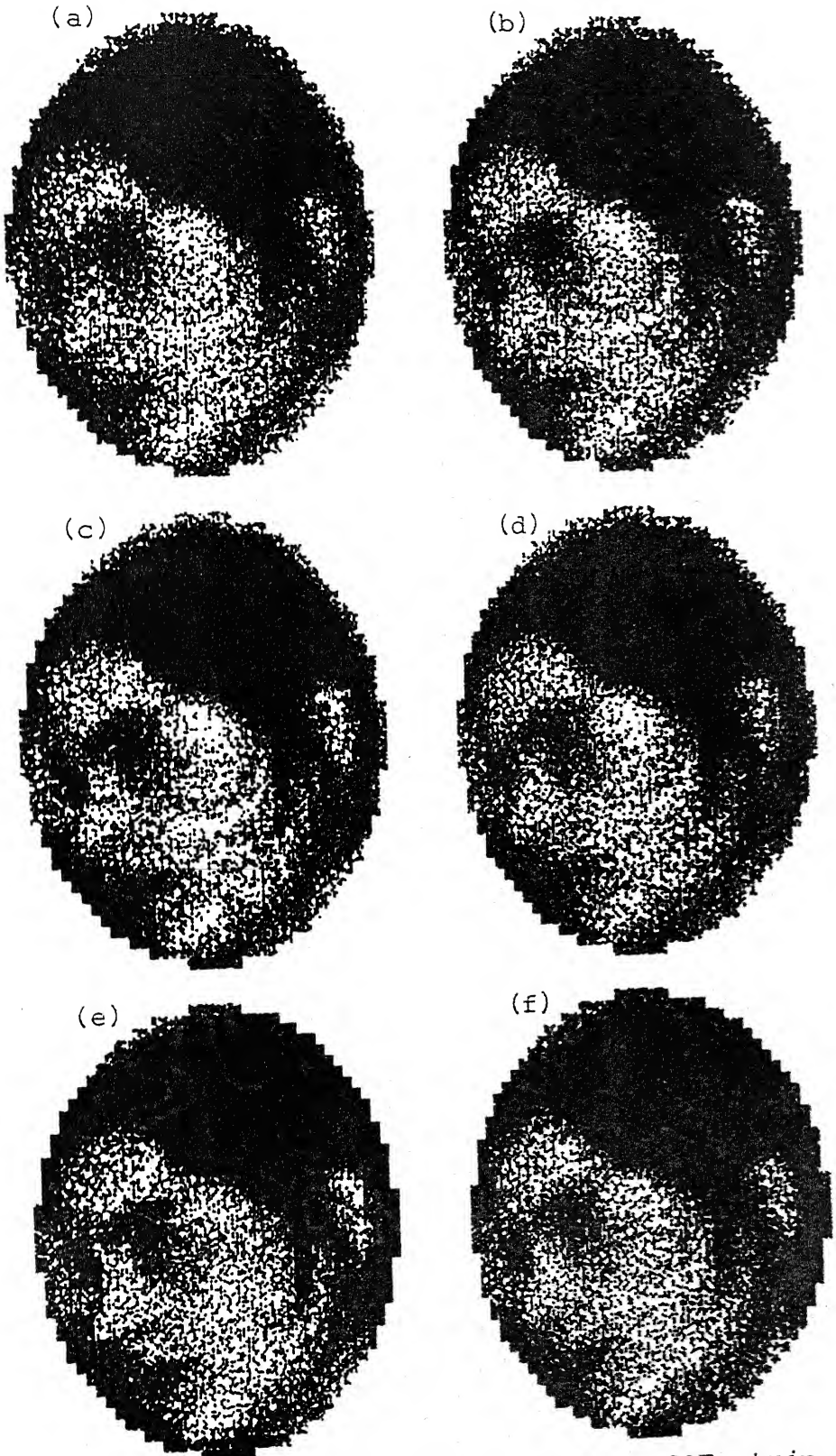

Fig. 6.12 Reconstruction of Face of a girl in CAT strip integral noise-free case (a) CSI filter, (b) RAM filter, (c) RKS filter, (d) Shepp filter, (e) original picture (f) optimal filter.

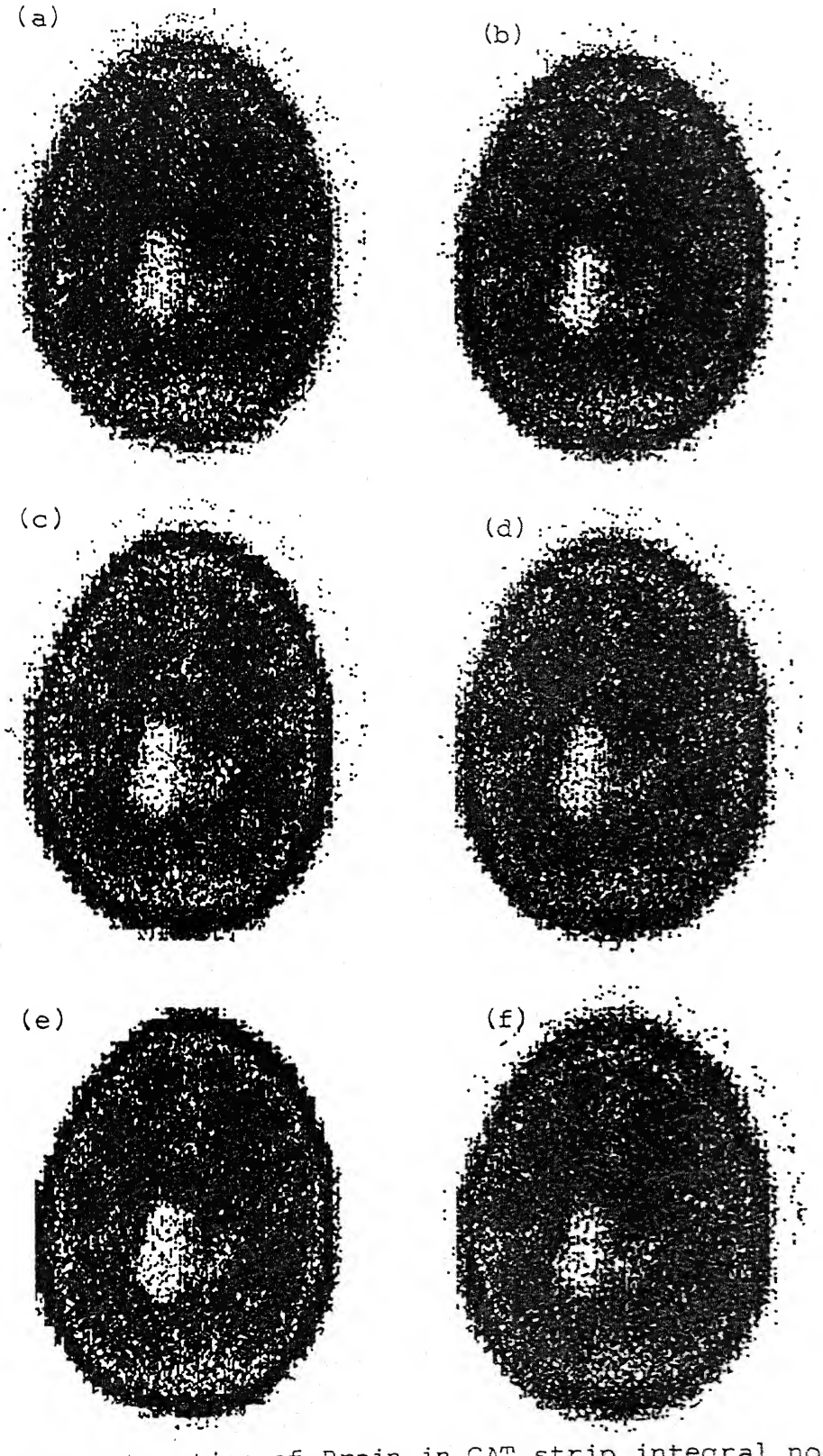

Fig. 6.13 Reconstruction of Brain in CAT strip integral noise-free case (a) CSI filter, (b) RAM filter, (c) RKS filter, (d) Shepp filter, (e) original picture, (f) optimal filter.

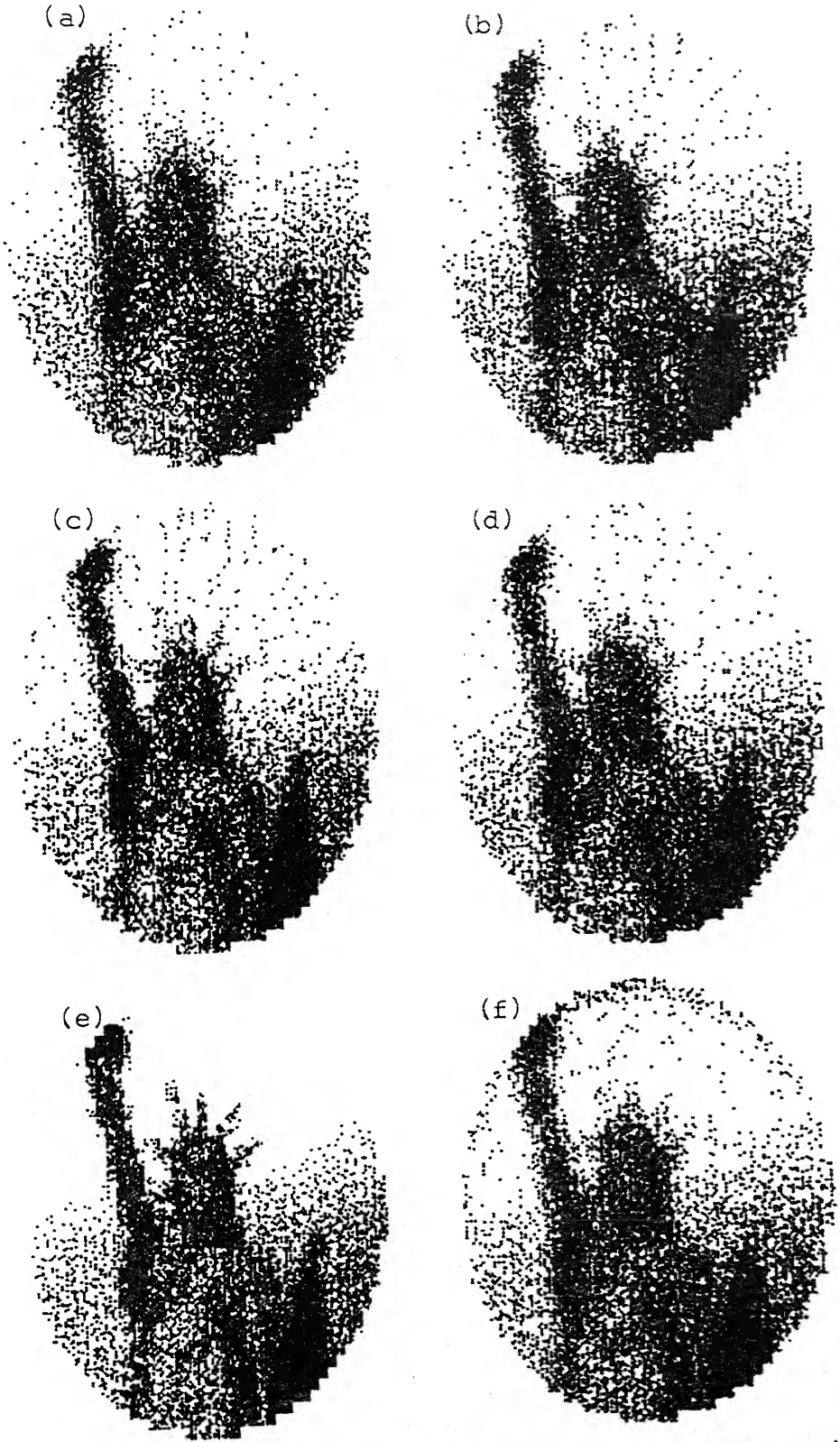

Fig. 6.14 Reconstruction of Statue of Liberty in CAT strip integral noise-free case (a) CSI filter, (b) RAM filter, (c) RKS filter, (d) Shepp filter, (e) original picture, (f) optimal filter.

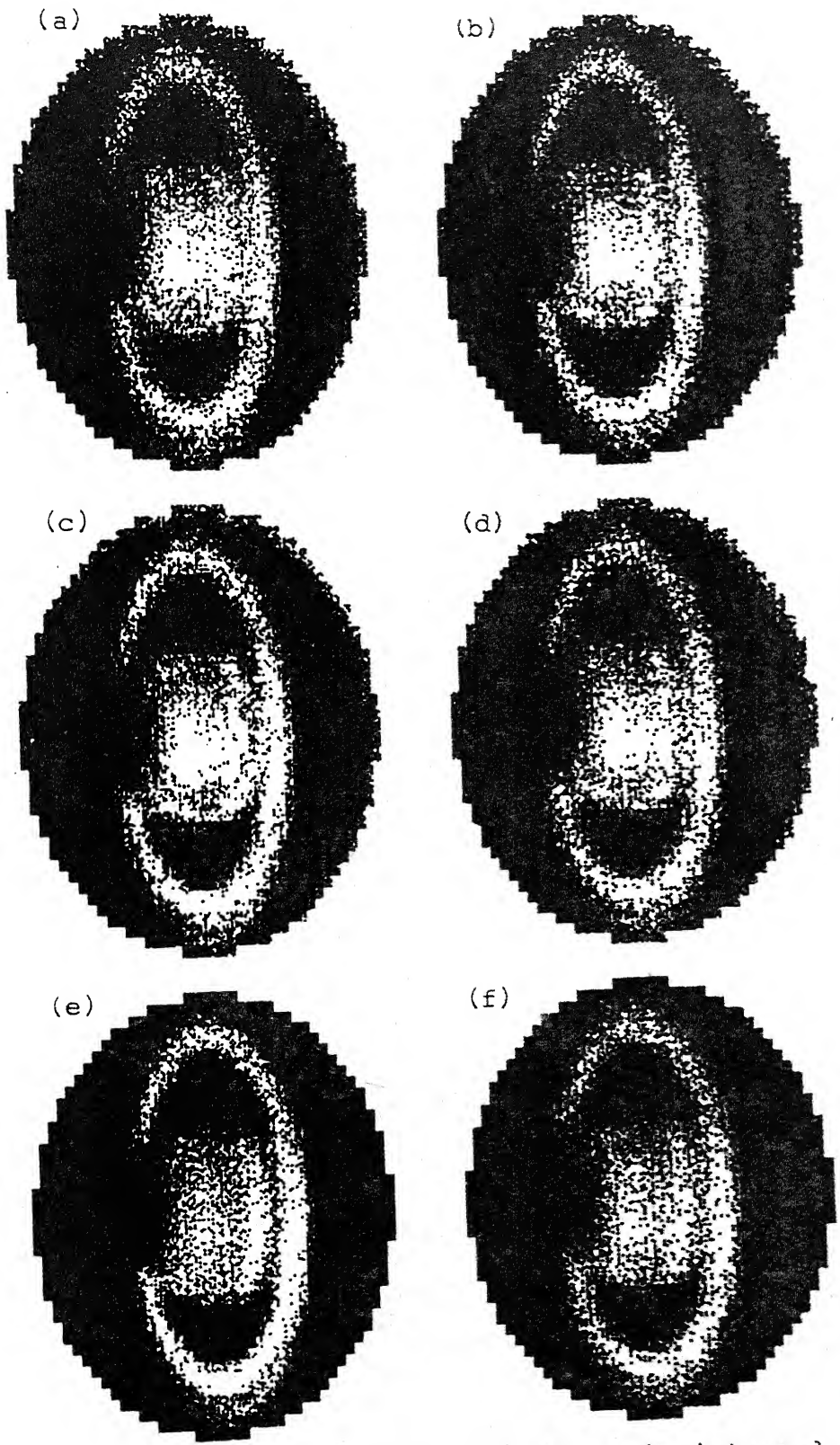

Fig. 6.15 Reconstruction of Saturn in CAT strip integral noise-free case (a) CSI filter, (b) RAM filter, (c) RKS filter, (d) Shepp filter, (e) original picture, (f) optimal filter.

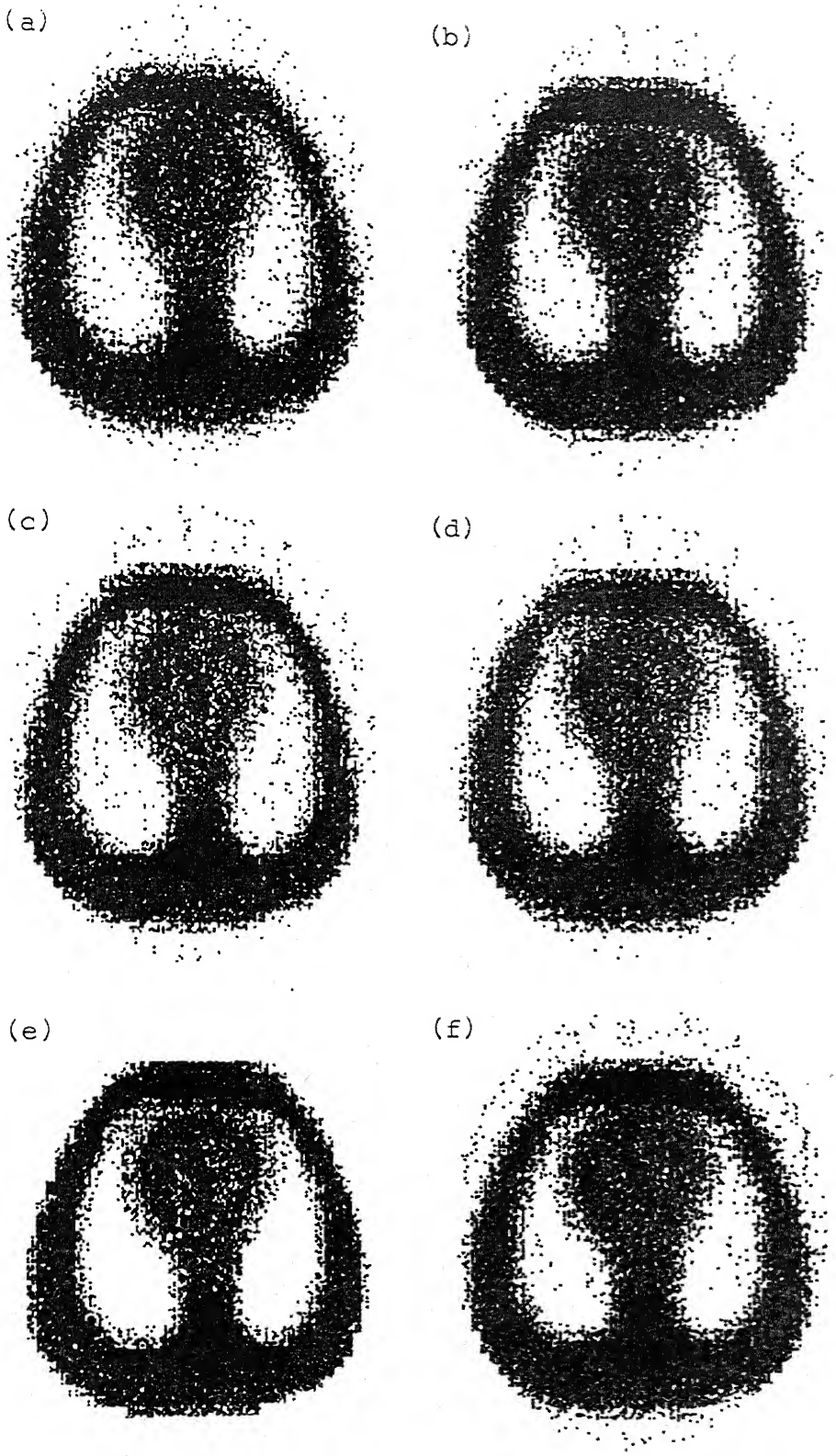

Fig. 6.16 Reconstruction of Thorax in CAT strip integral noise-free case (a) CSI filter, (b) RAM filter, (c) RKS filter, (d) Shepp filter, (e) original picture, (f) optimal filter.

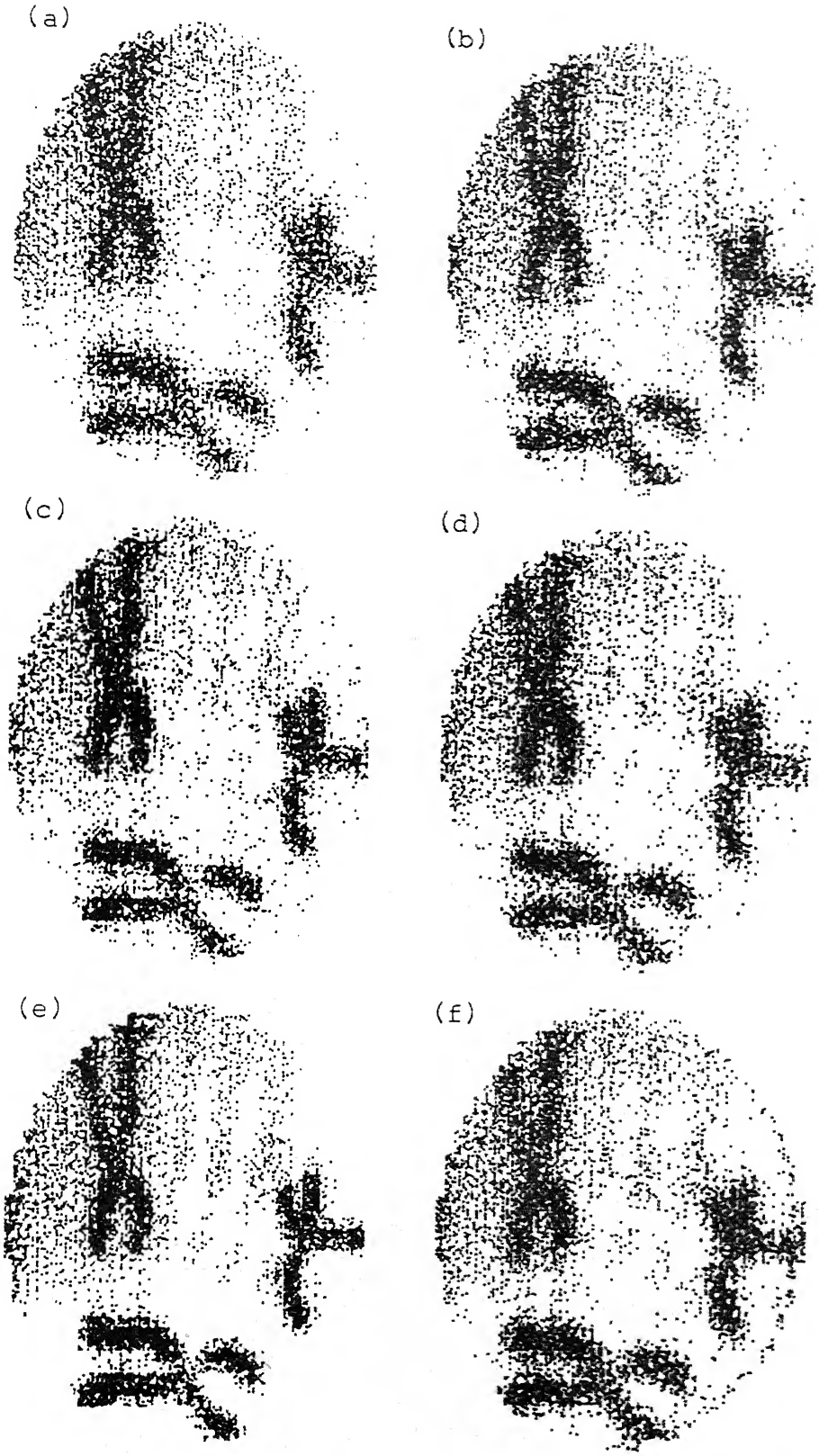

Fig. 6.19 Reconstruction of Chromosomes in CAT strip integral noise-free case (a) CSI filter, (b) RAM filter, (c) RKS filter, (d) Shepp filter, (e) original picture, (f) optimal filter.

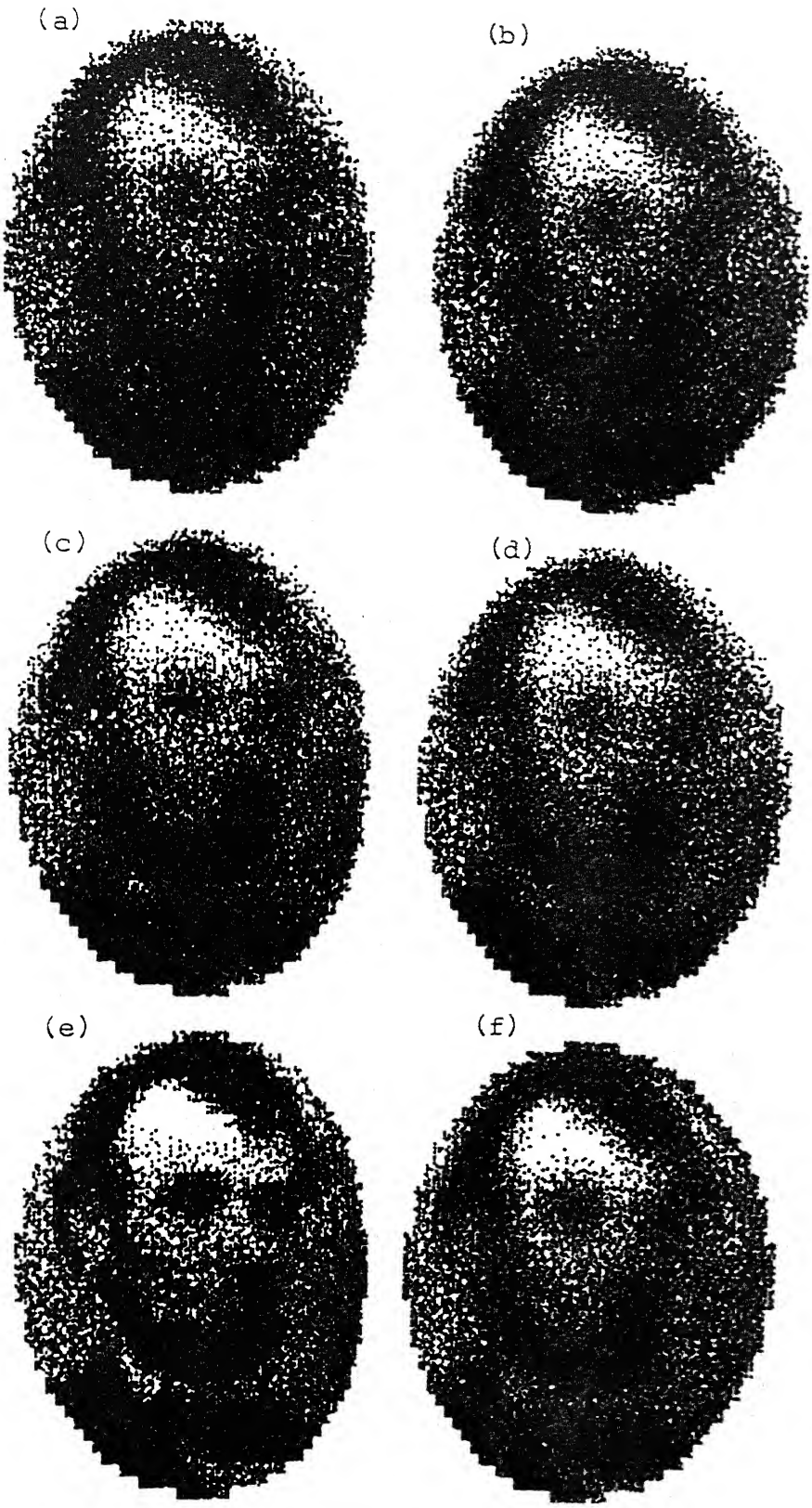

Fig. 6.20 Reconstruction of Lincoln in PET line integral noise-free case (a) CSI filter, (b) RAM filter, (c) RKS filter, (d) Shepp filter, (e) original picture, (d) optimal filter.

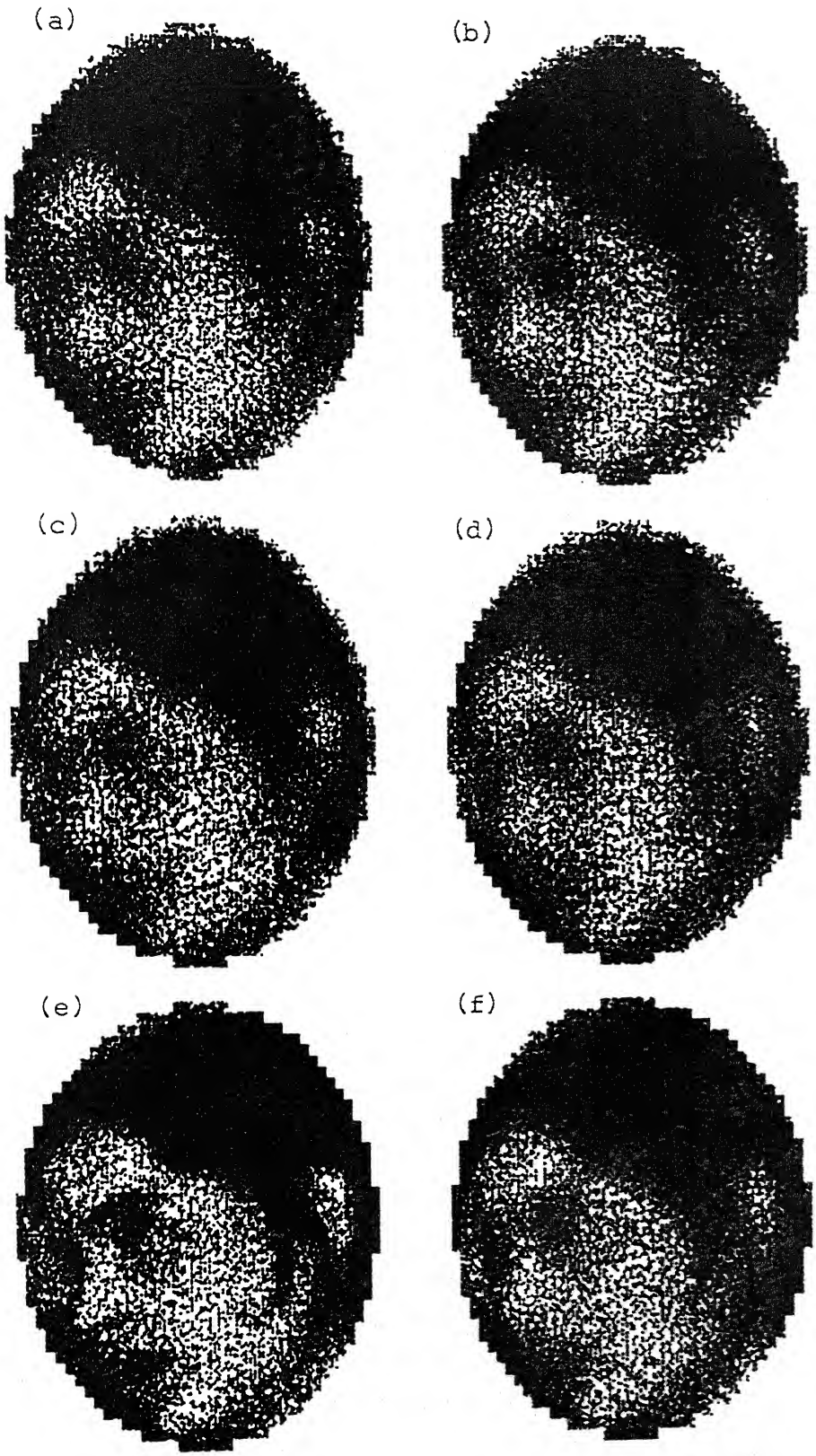

Fig. 6.21 Reconstruction of Face of a girl in PET line integral noise-free case (a) CSI filter, (b) RAM filter, (c) RKS filter, (d) Shepp filter, (e) original picture, (f) optimal filter.

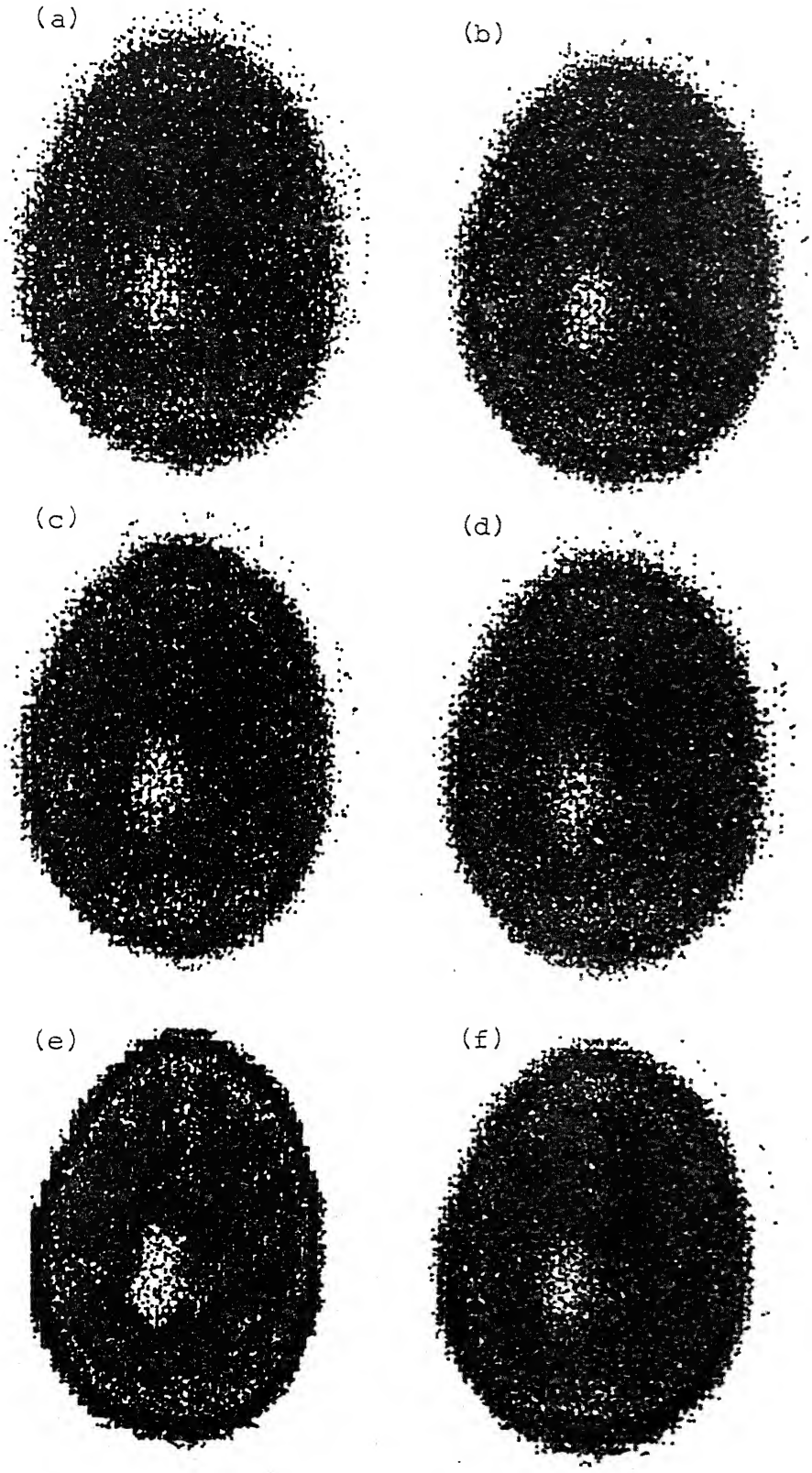

Fig. 6.22 Reconstruction of Brain in PET line integral noise-free case (a) CSI filter, (b) RAM filter, (c) RKS filter, (d) Shepp filter, (e) original picture, (f) optimal filter.

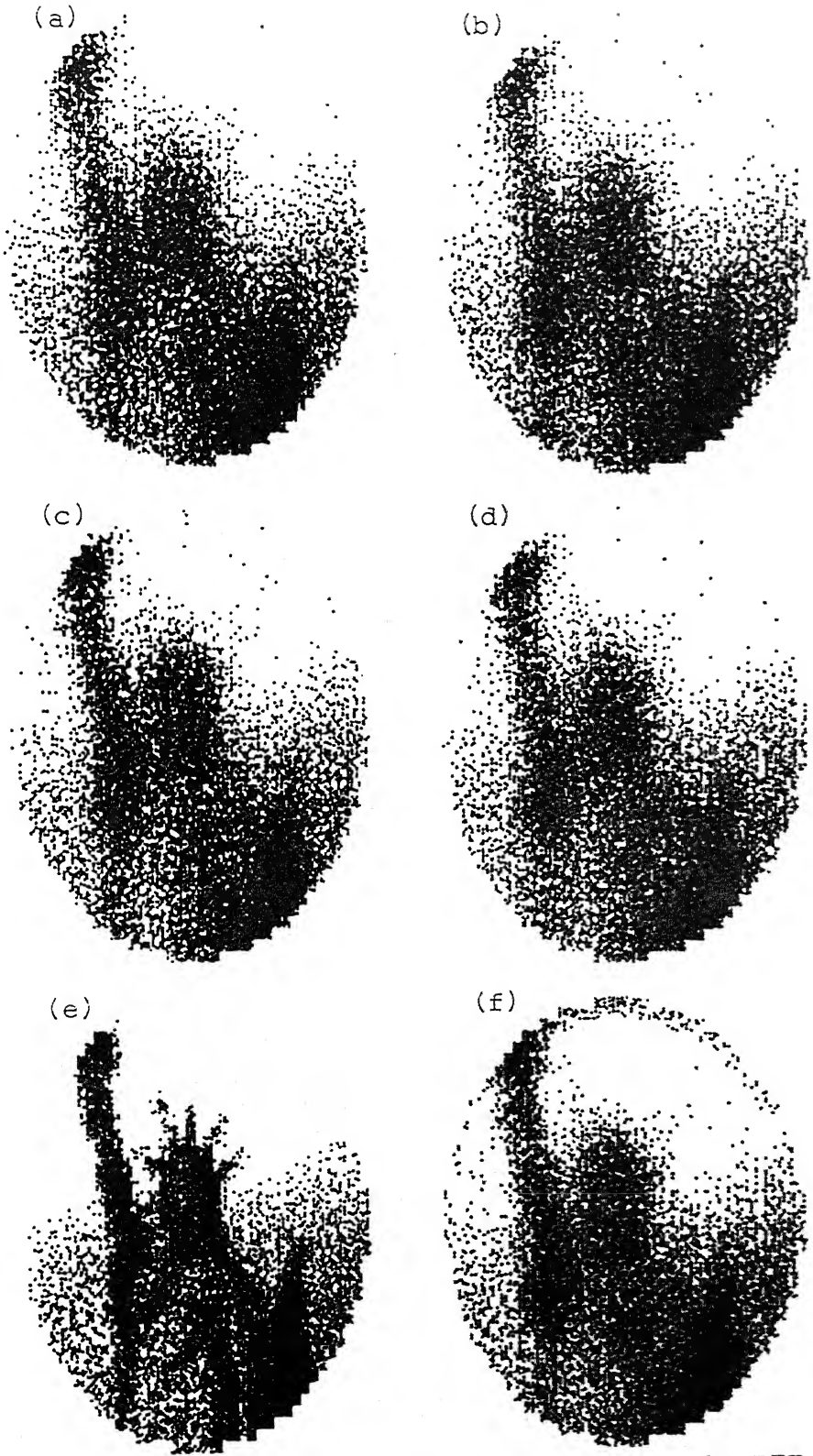

Fig. 6.23 Reconstruction of Statue of Liberty in PET line integral noise-free case (a) CSI filter, (b) RAM filter, (c) RKS filter, (e) Shepp filter, (e) original picture, (f) optimal filter.

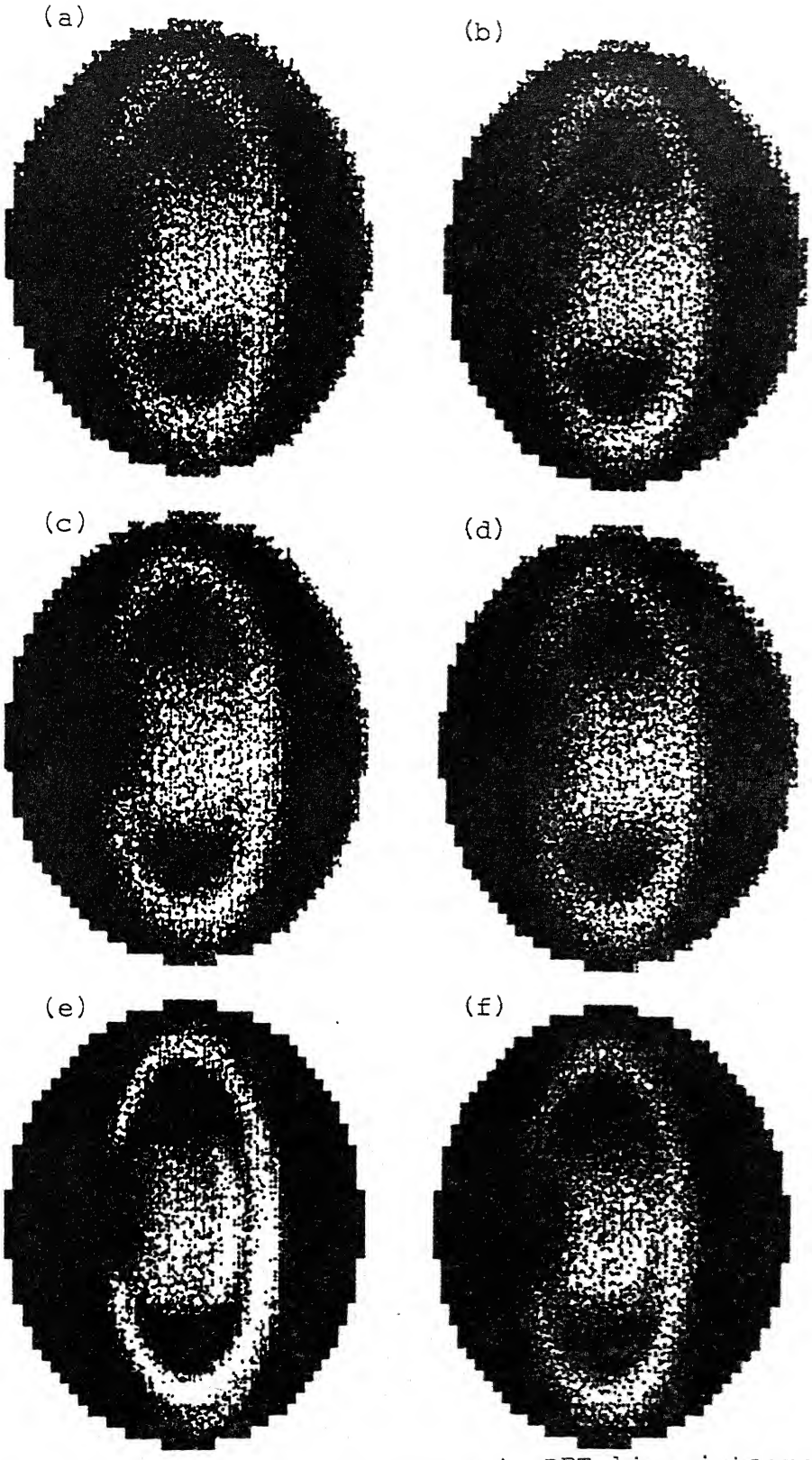

Fig. 6.24 Reconstruction of Saturn in PET line integral noise-free case (a) CSI filter, (b) RAM filter, (c) RKS filter, (d) Shepp filter, (e) original picture, (f) optimal filter.

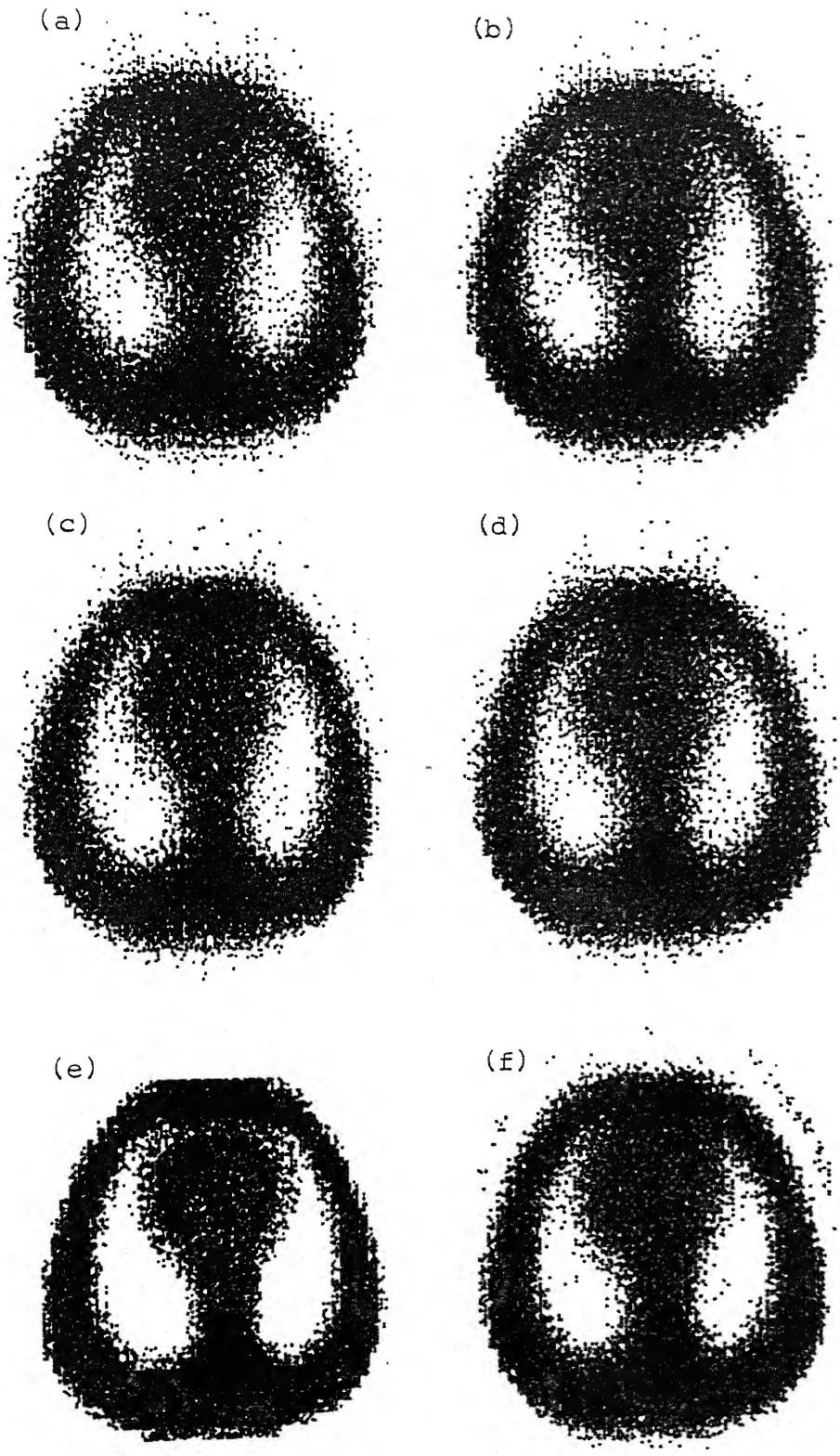

Fig. 6.25 Reconstruction of Thorax in PET line integral noise-free case (a) CSI filter, (b) RAM filter, (c) RKS filter, (d) Shepp filter, (e) original picture, (f) optimal filter.

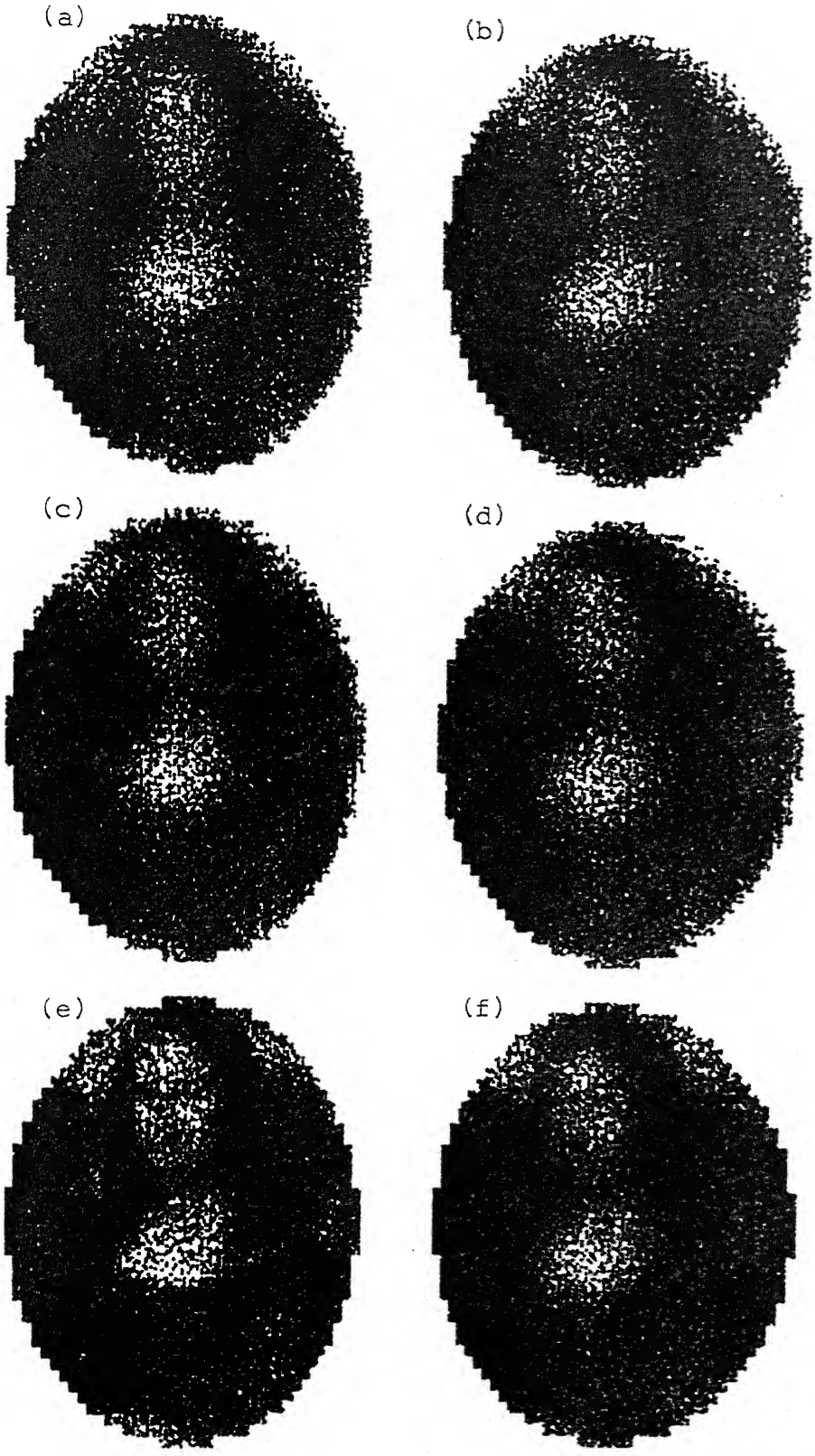

Fig. 6.26 Reconstruction of MonaLisa in PET line integral noise-free case (a) CSI filter, (b) RAM filter, (c) RKS filter, (d) Shepp filter, (e) original picture, (f) optimal filter.

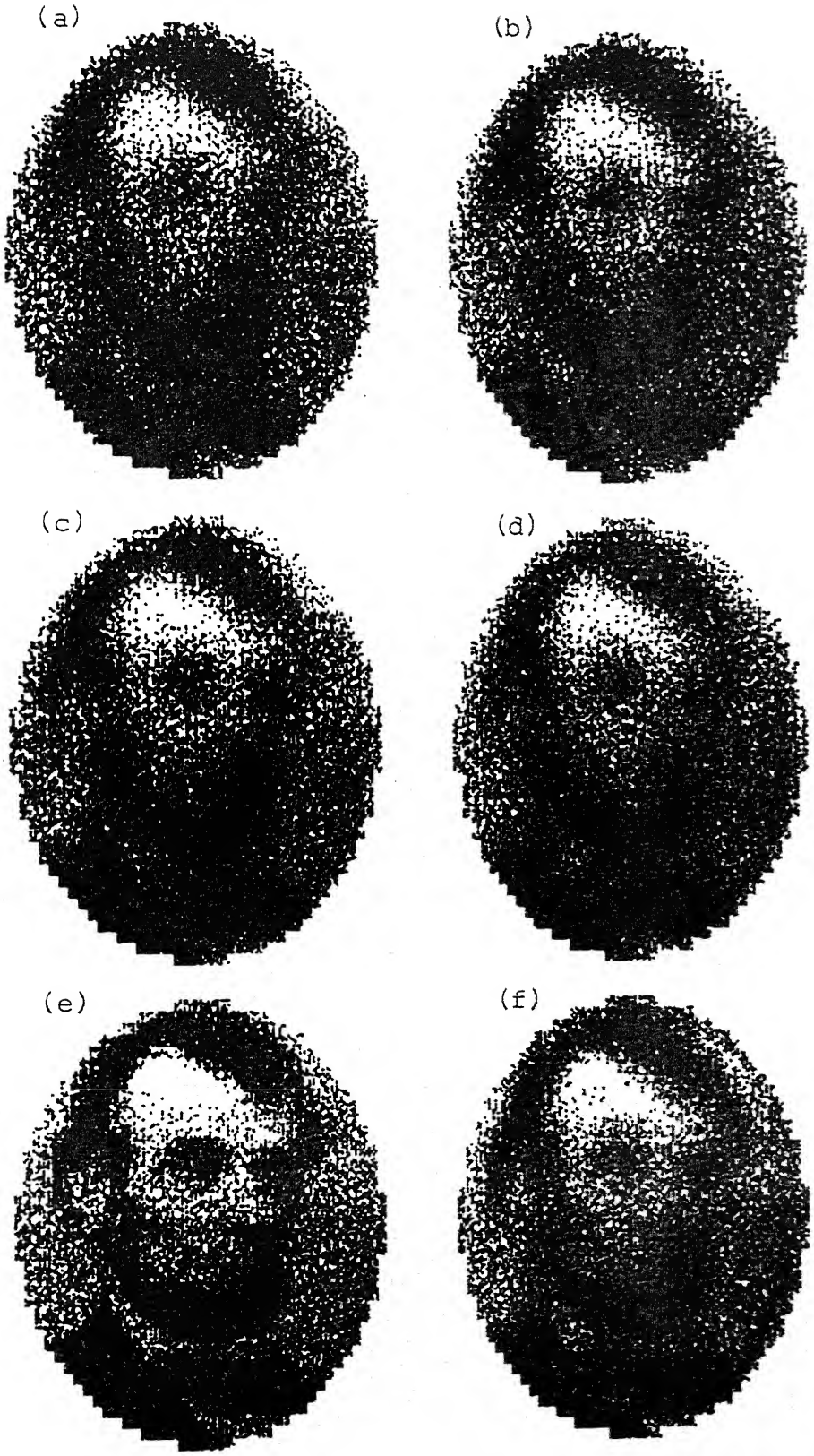

Fig. 6.29 Reconstruction of Lincoln in PET strip integral noise-free case (a) CSI filter, (b) RAM filter, (c) RKS filter, (d) Shepp filter, (e) original picture, (f) optimal filter.

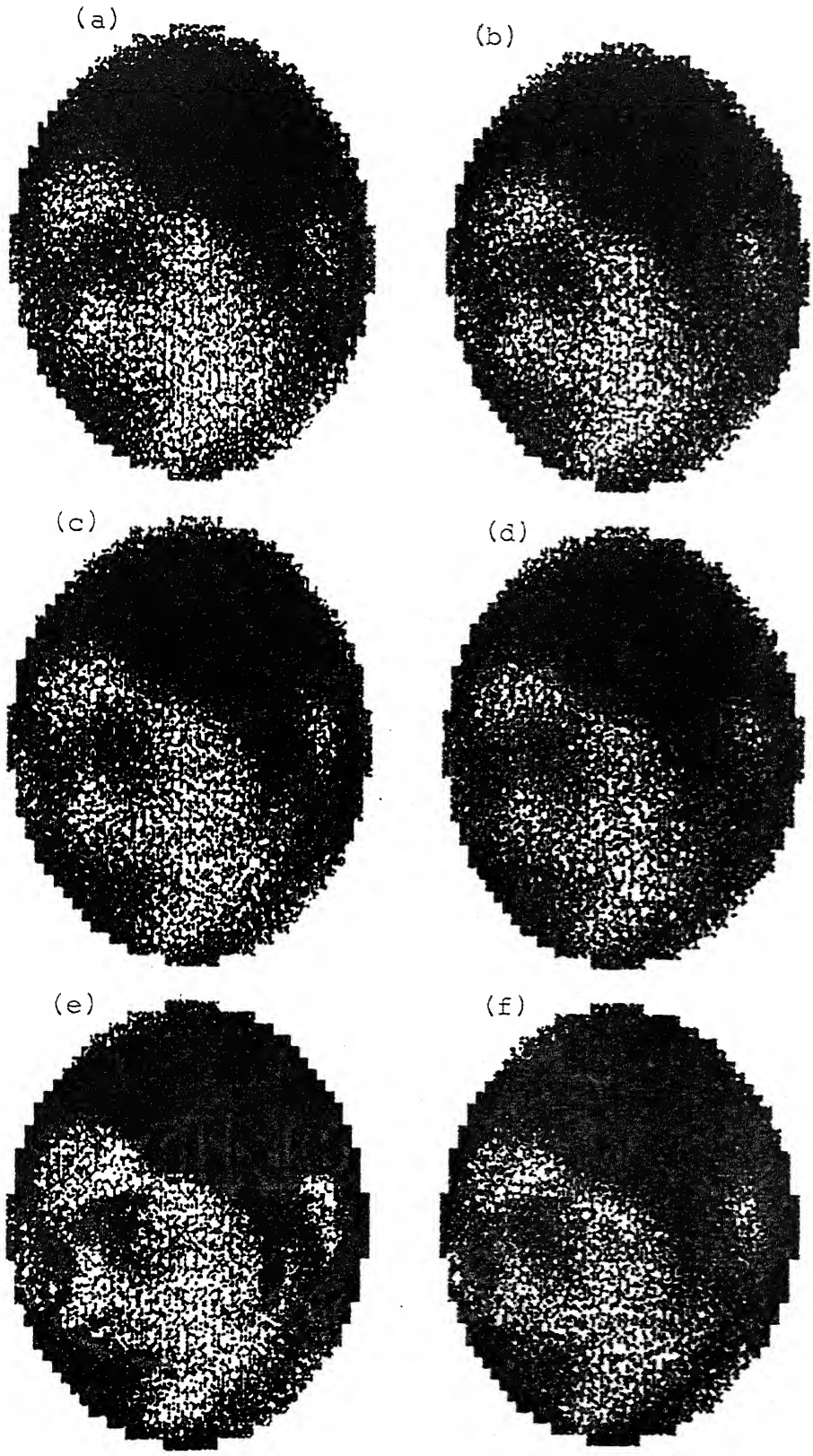

Fig. 6.30 Reconstruction of Face of a girl in PET strip integral noise-free case (a) CSI filter, (b) RAM filter, (c) RKS filter, (d) Shepp filter, (e) original picture, (f) optimal filter.

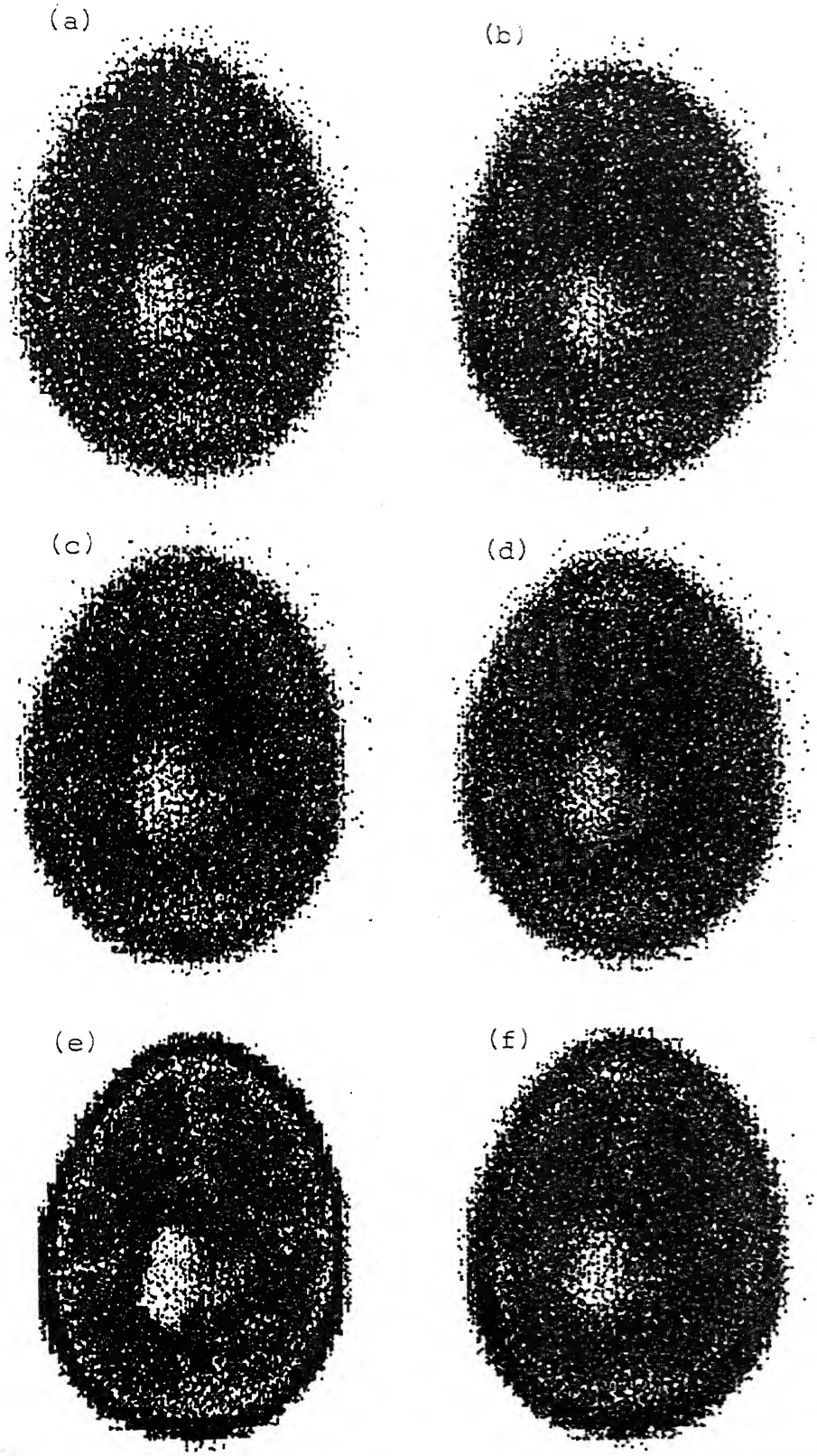

Fig. 6.31 Reconstruction of Brain in PET strip integral noise-free case (a) CSI filter, (b) RAM filter, (c) RKS filter, (d) Shepp filter, (e) original picture, (f) optimal filter.

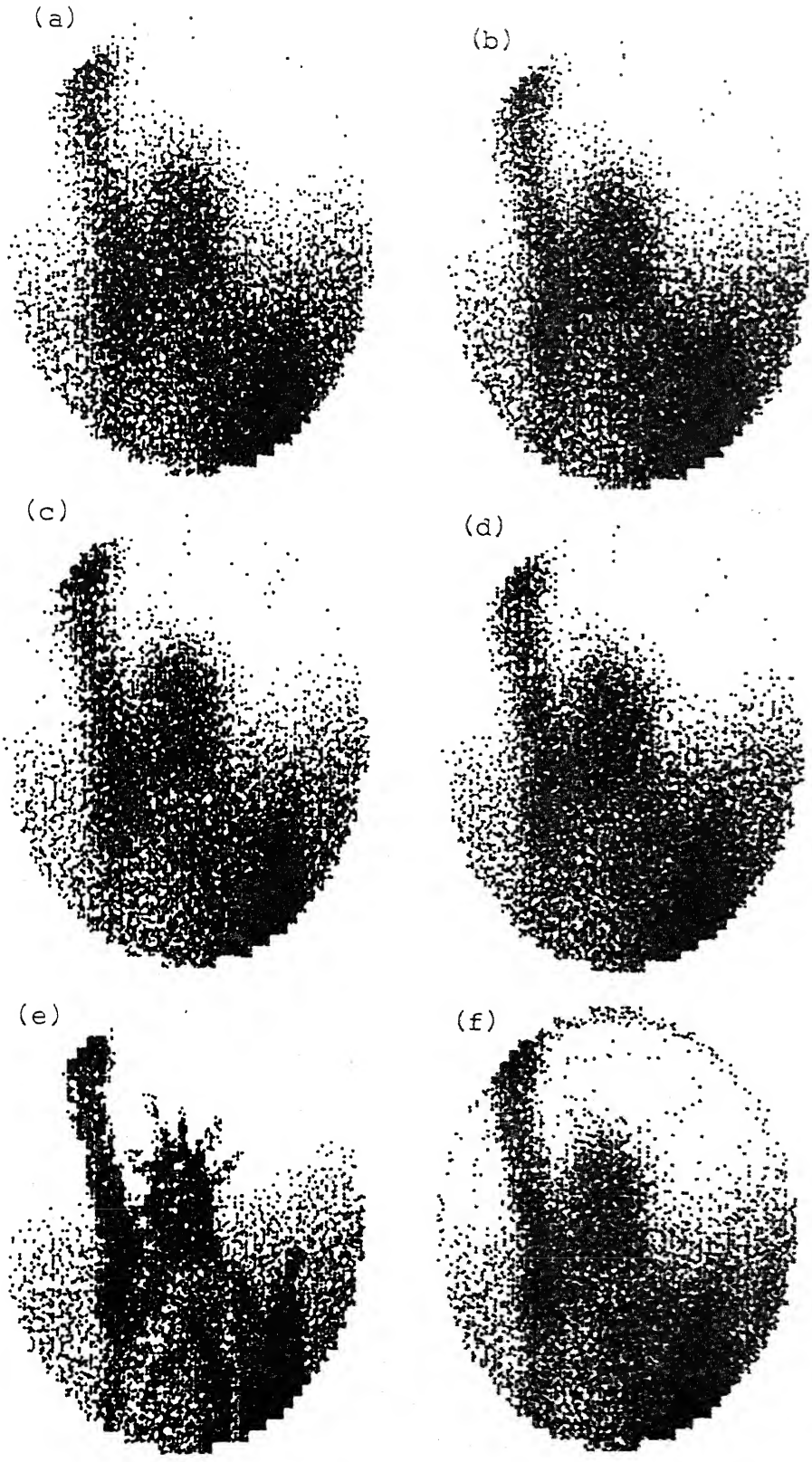

Fig. 6.32 Reconstruction of Statue of Liberty in PET strip integral noise-free case (a) CSI filter, (b) RAM filter, (c) RKS filter, (d) Shepp filter, (e) original picture, (f) optimal filter.

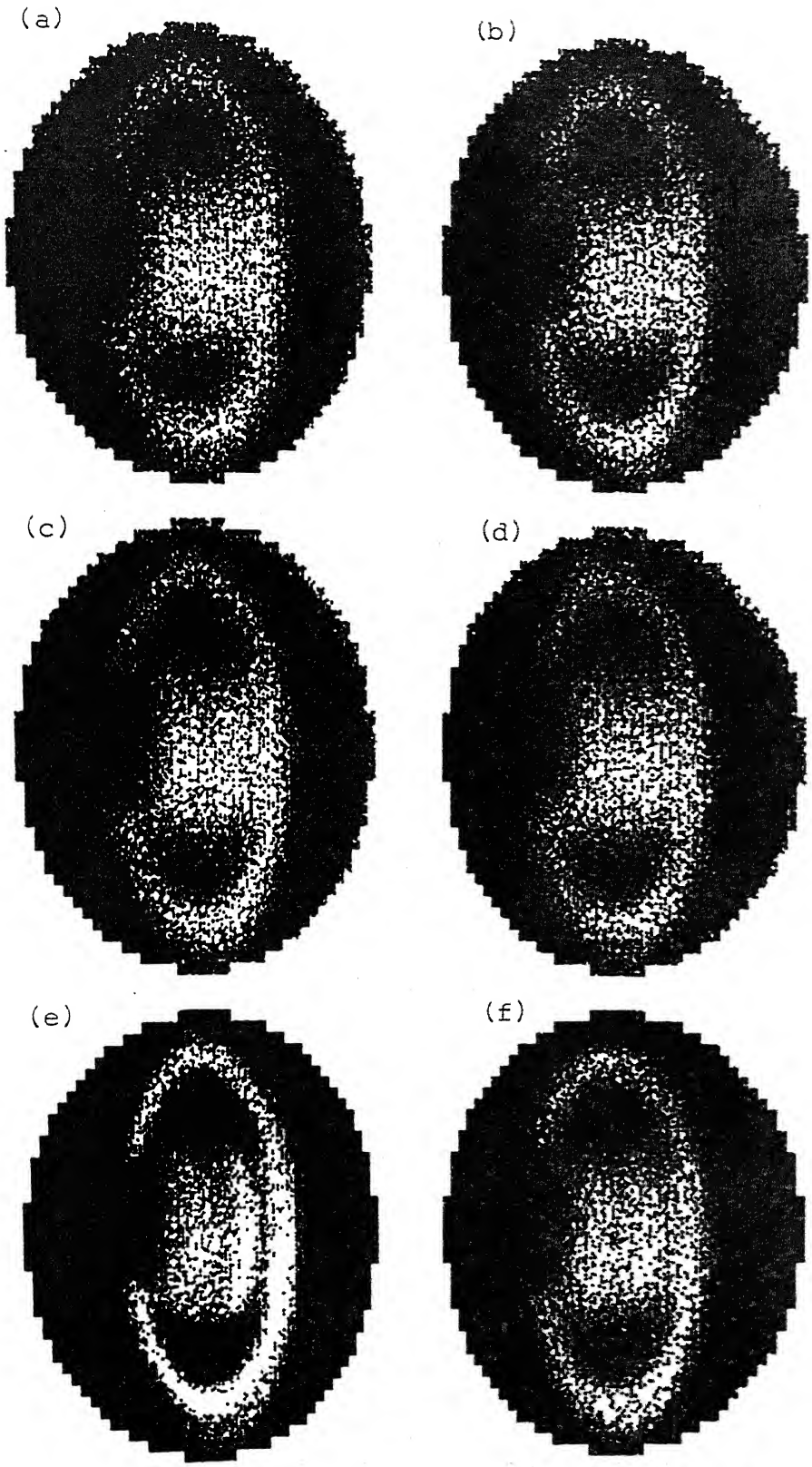

Fig. 6.33 Reconstruction of Saturn in PET strip integral noise-free case (a) CSI filter, (b) RAM filter, (c) RKS filter, (d) Shepp filter, (e) original picture, (f) optimal filter.

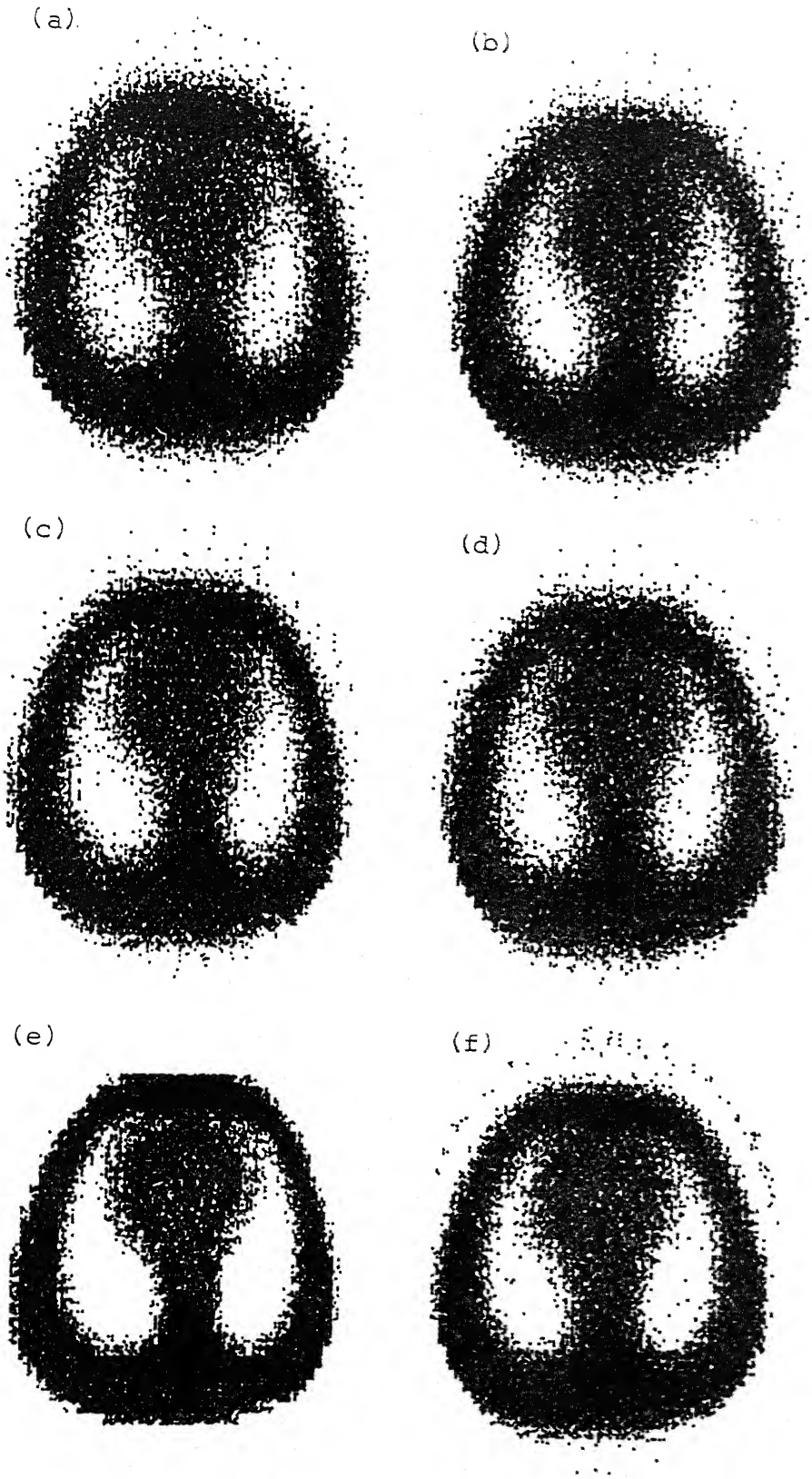

Fig. 6.34 Reconstruction of Thorax in PET strip integral noise-free case (a) CSI filter, (b) RAM filter, (c) RKS filter, (d) Shepp filter, (e) original picture, (f) optimal filter.

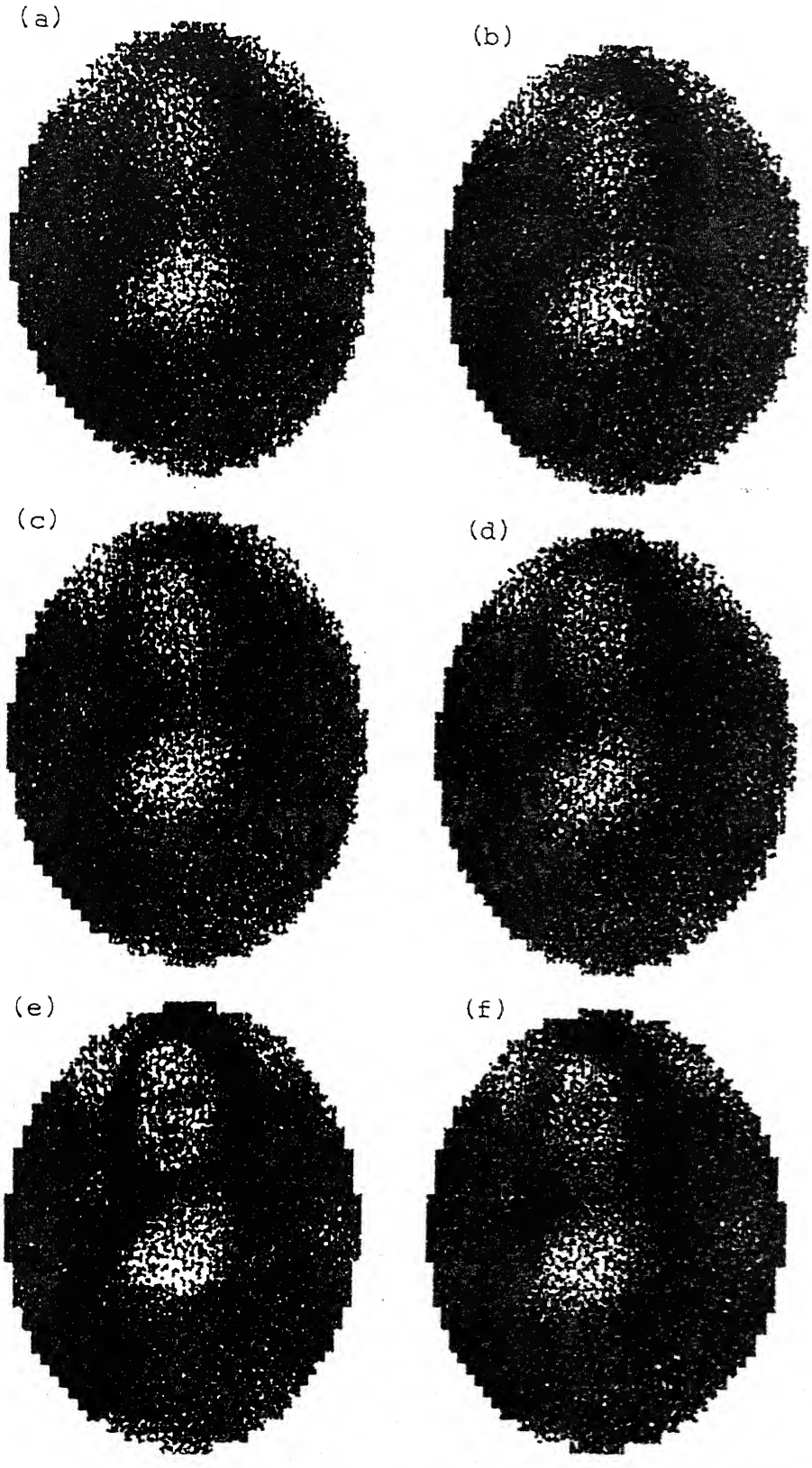

Fig. 6.35 Reconstruction of MonaLisa in PET strip integral noise-free case (a) CSI filter, (b) RAM filter, (c) RKS filter, (d) Shepp filter, (e) original picture, (f) optimal filter.

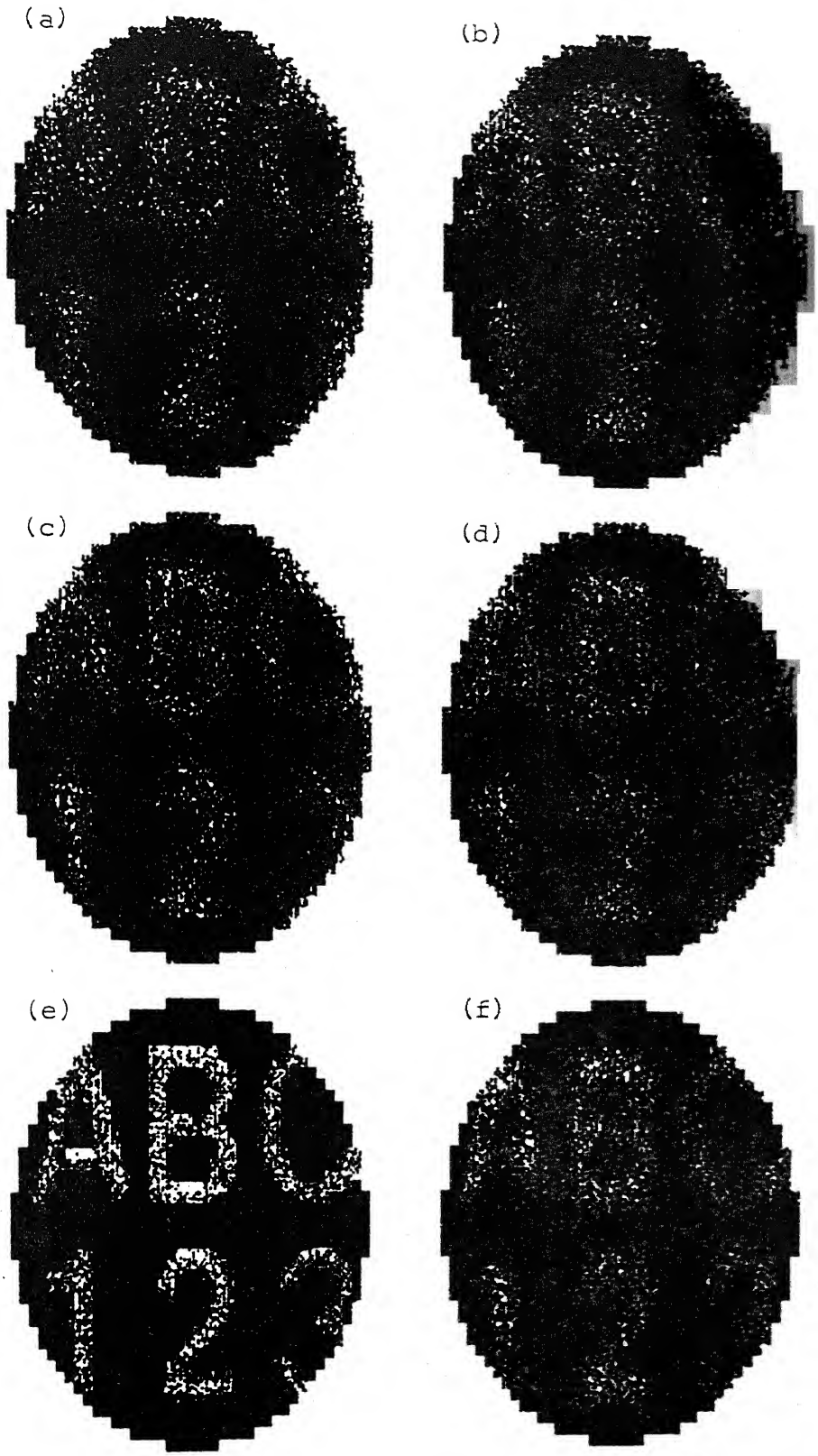

Fig. 6.36 Reconstruction of Characters in PET strip integral noise-free case (a) CSI filter, (b) RAM filter, (c) RKS filter, (d) Shepp filter, (e) original picture, (f) optimal filter.

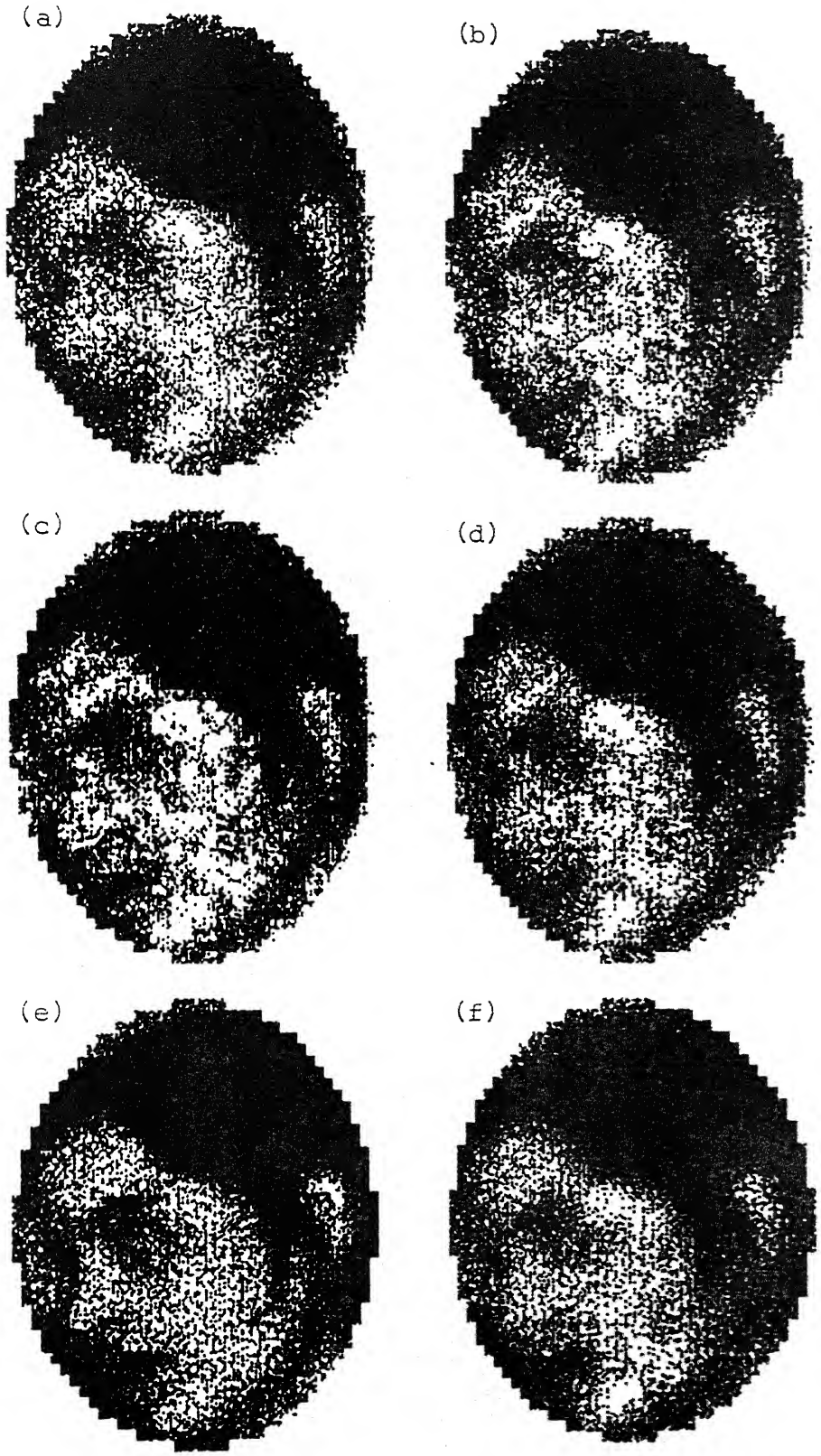

Fig. 6.39 Reconstruction of Face of a girl in CAT line noisy case (a) CSI filter, (b) RAM filter, (c) RKS filter, (d) Shepp filter, (e) original picture, (f) optimal filter.

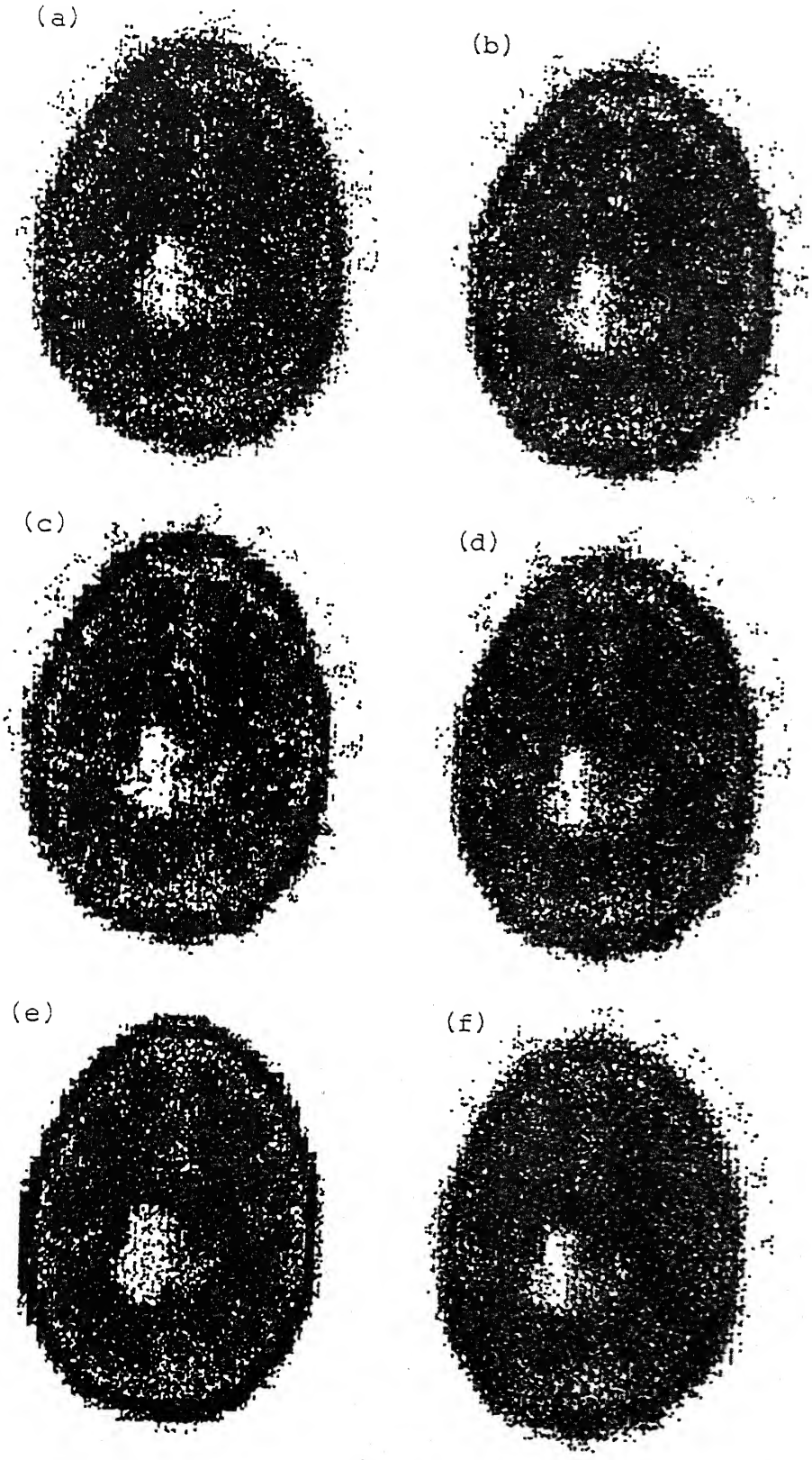

Fig. 6.40 Reconstruction of Brain in CAT line integral noisy case (a) CSI filter, (b) RAL filter, (c) RKS filter, (d) Shepp filter, (e) original picture, (f) optimal filter.

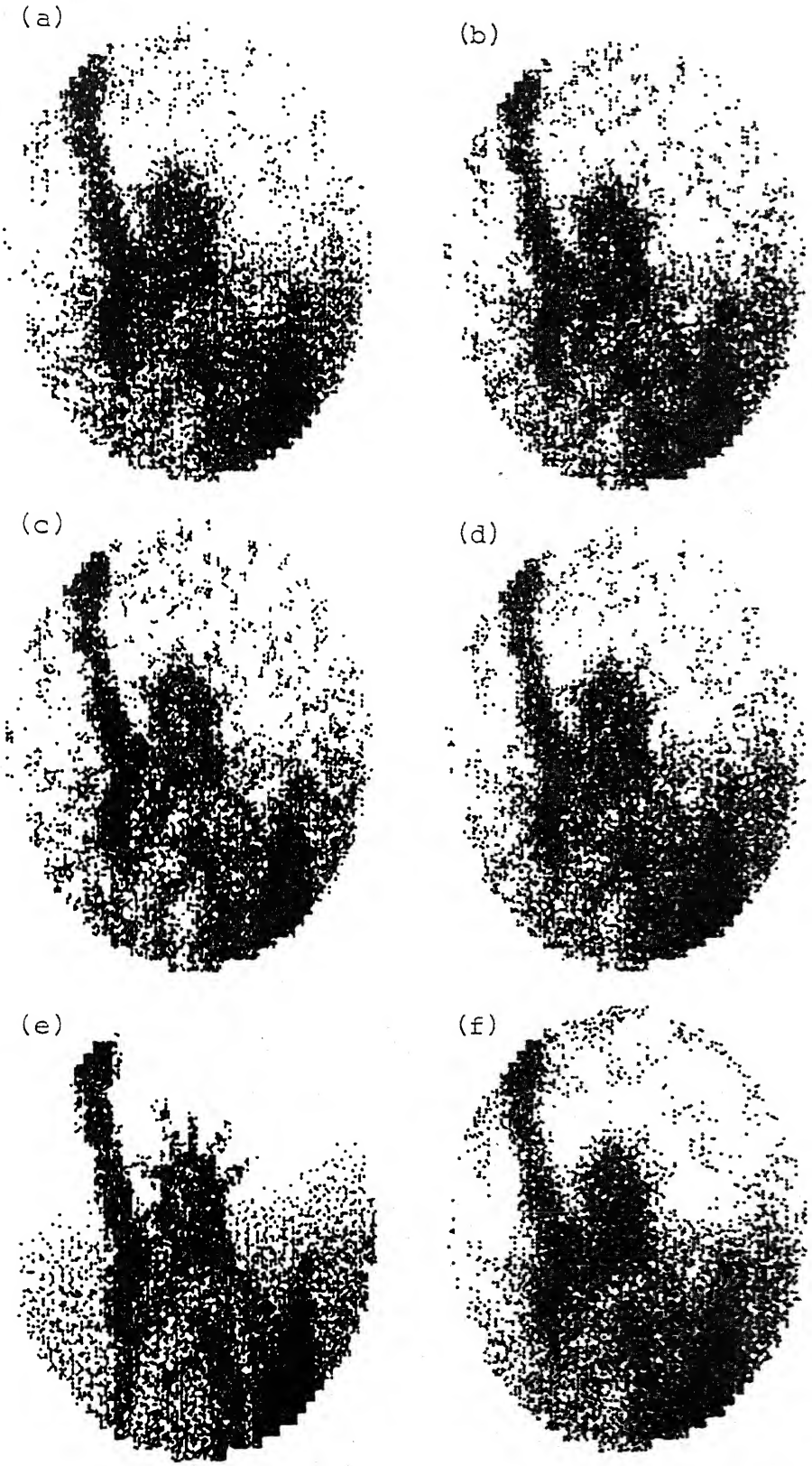

Fig. 6.41 Reconstruction of Statue of Liberty in CAT line integral noisy case (a) CSI filter, (b) RAM filter, (c) RKS filter, (d) Shepp filter, (e) original picture, (f) optimal filter.

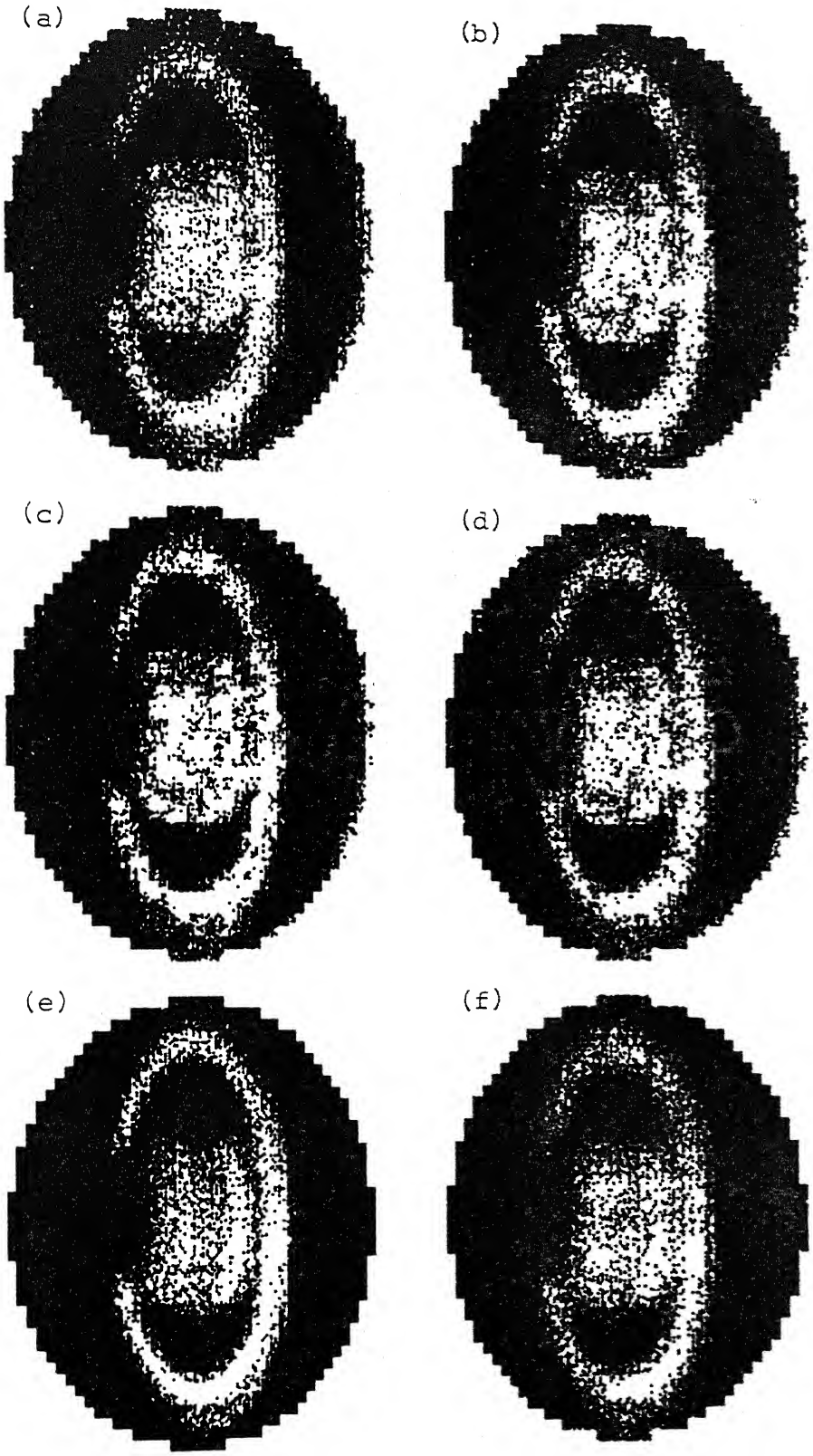

Fig. 6.42 Reconstruction of Saturn in CAT line integral noisy case (a) CSI filter, (b) RAM filter, (c) RKS filter, (d) Shepp filter, (e) original picture, (f) optimal filter.

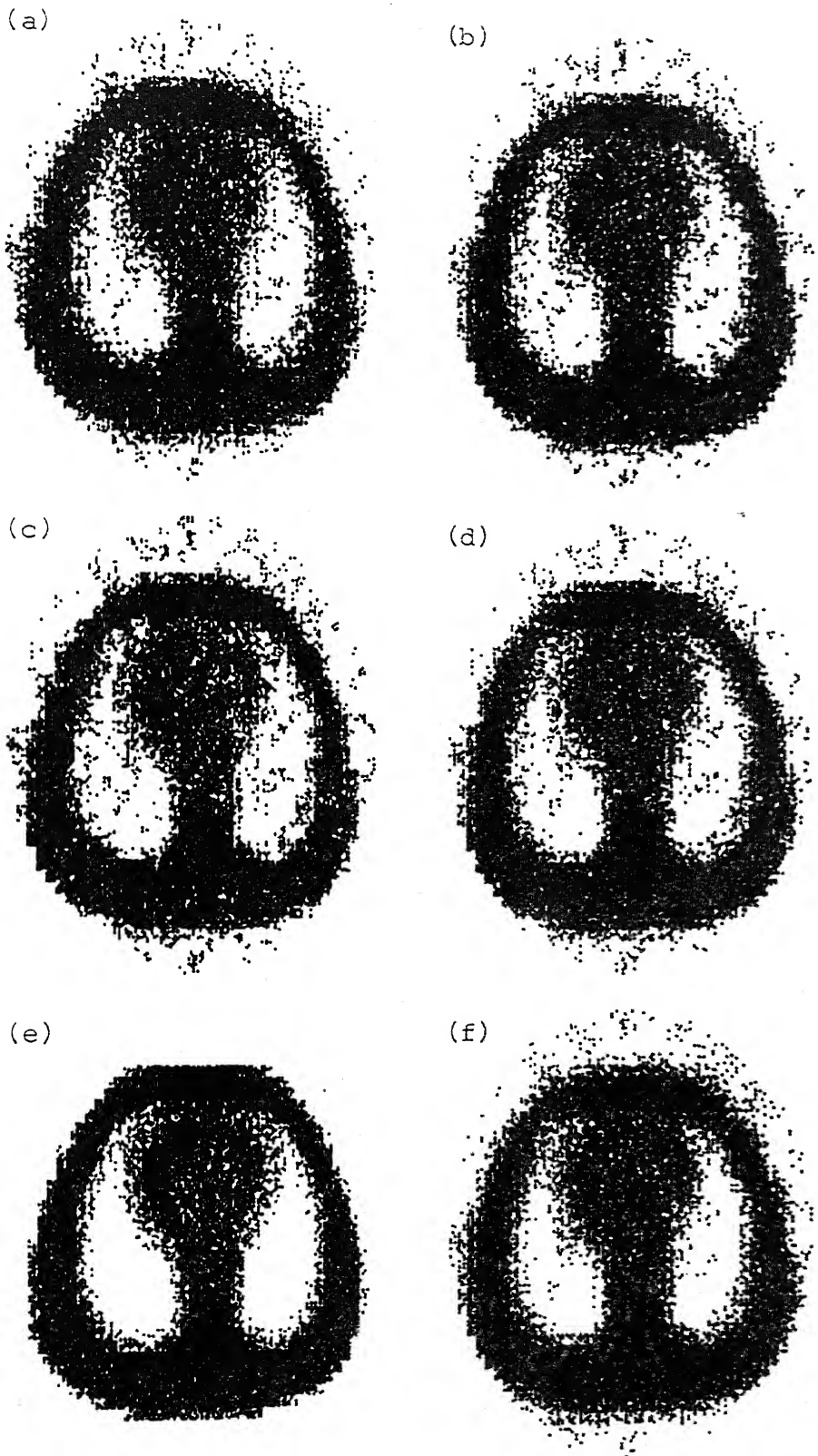

Fig. 6.43 Reconstruction of Thorax in CAT line integral noisy case (a) CSI filter, (b) RAM filter, (c) RKS filter, (d) Shepp filter, (e) original picture, (f) optimal filter.

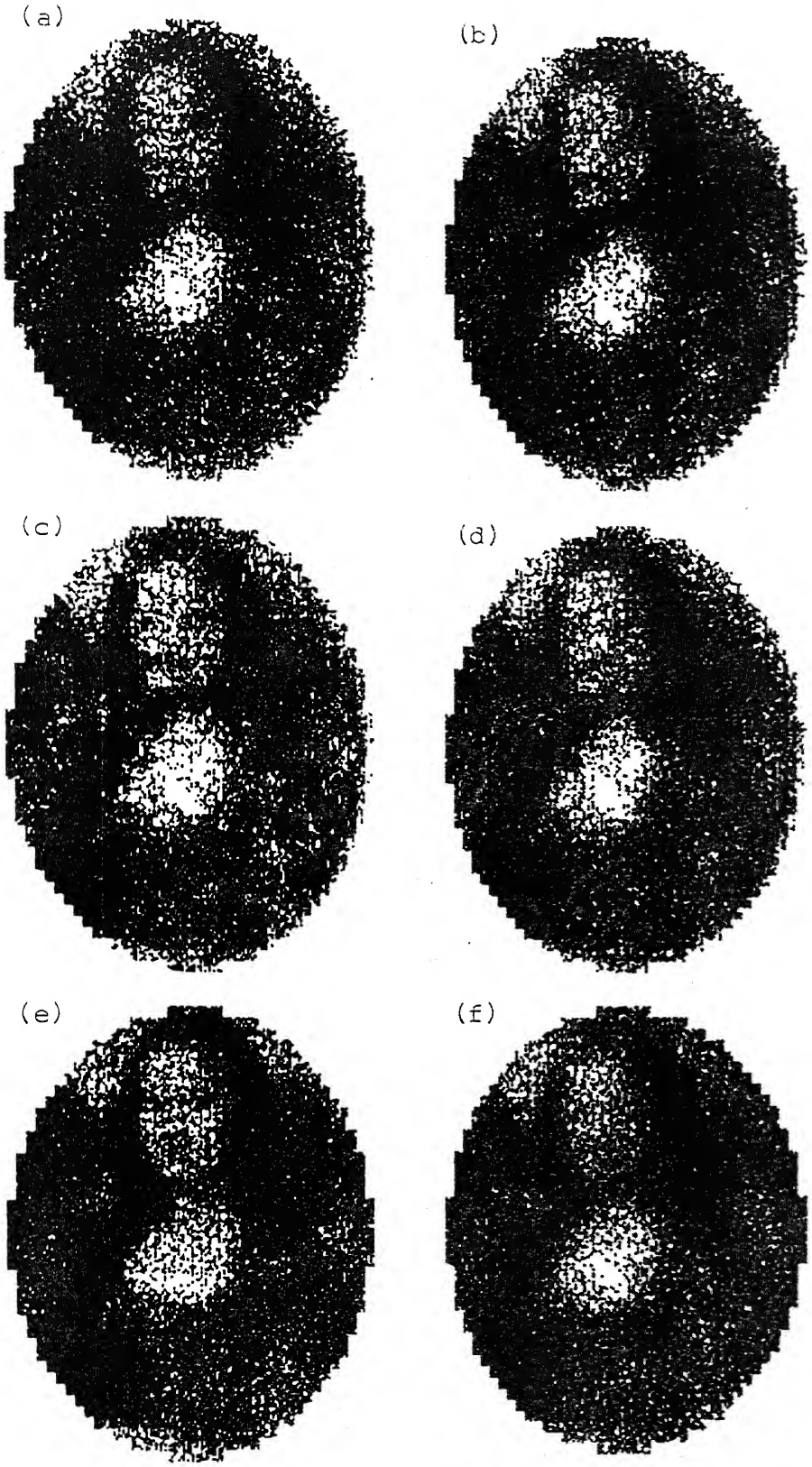

Fig. 6.44 Reconstruction of MonaLisa in CAT line integral noisy case (a) CSI filter, (b) RAM filter, (c) RRS filter, (d) Shepp filter, (e) original picture, (f) optimal filter.

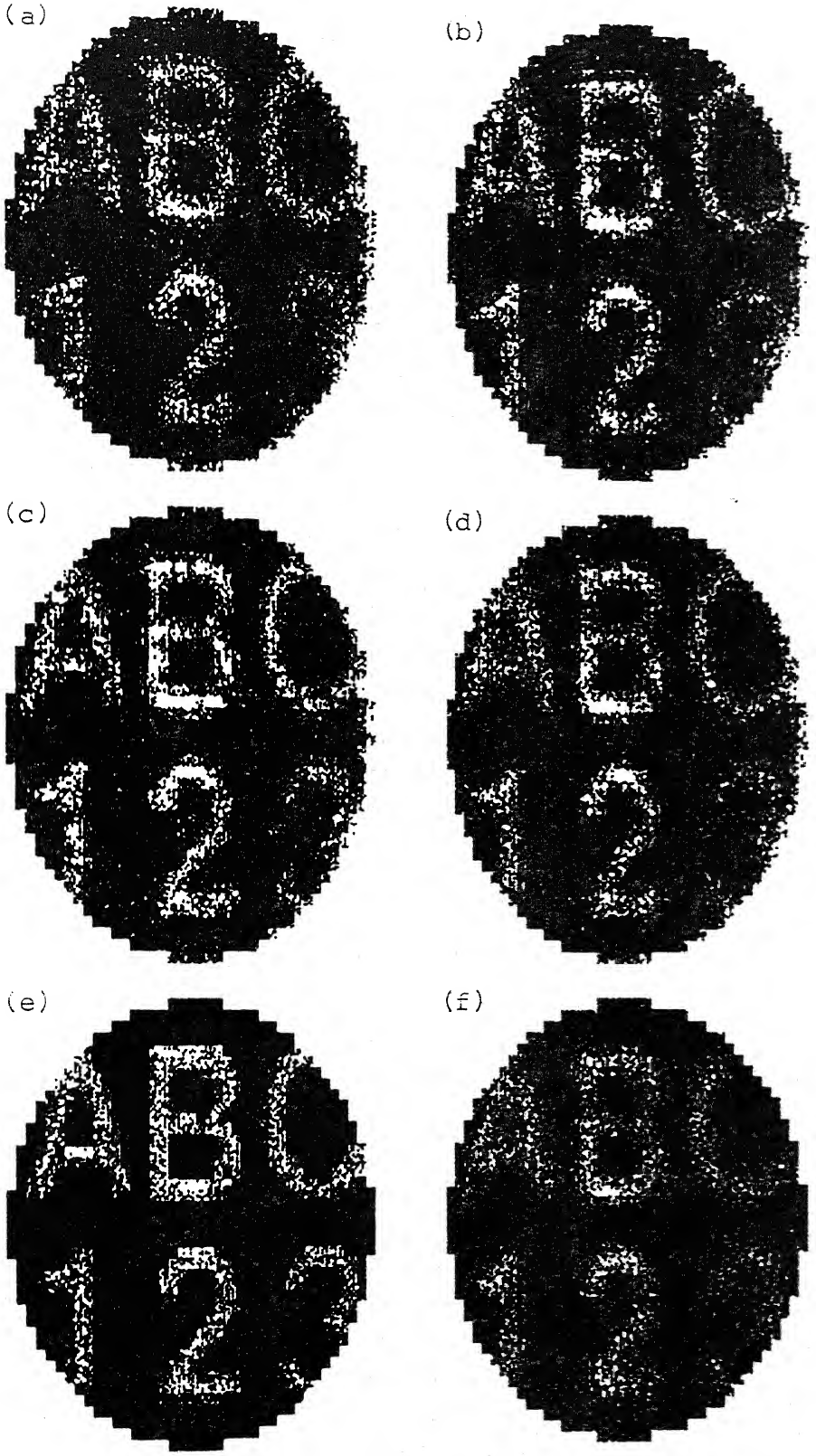

Fig. 6.45 Reconstruction of Characters in CAT line integral noisy case (a) CSI filter, (b) RAM filter, (c) RHS filter, (d) Shepp filter, (e) original picture, (f) optimal filter.

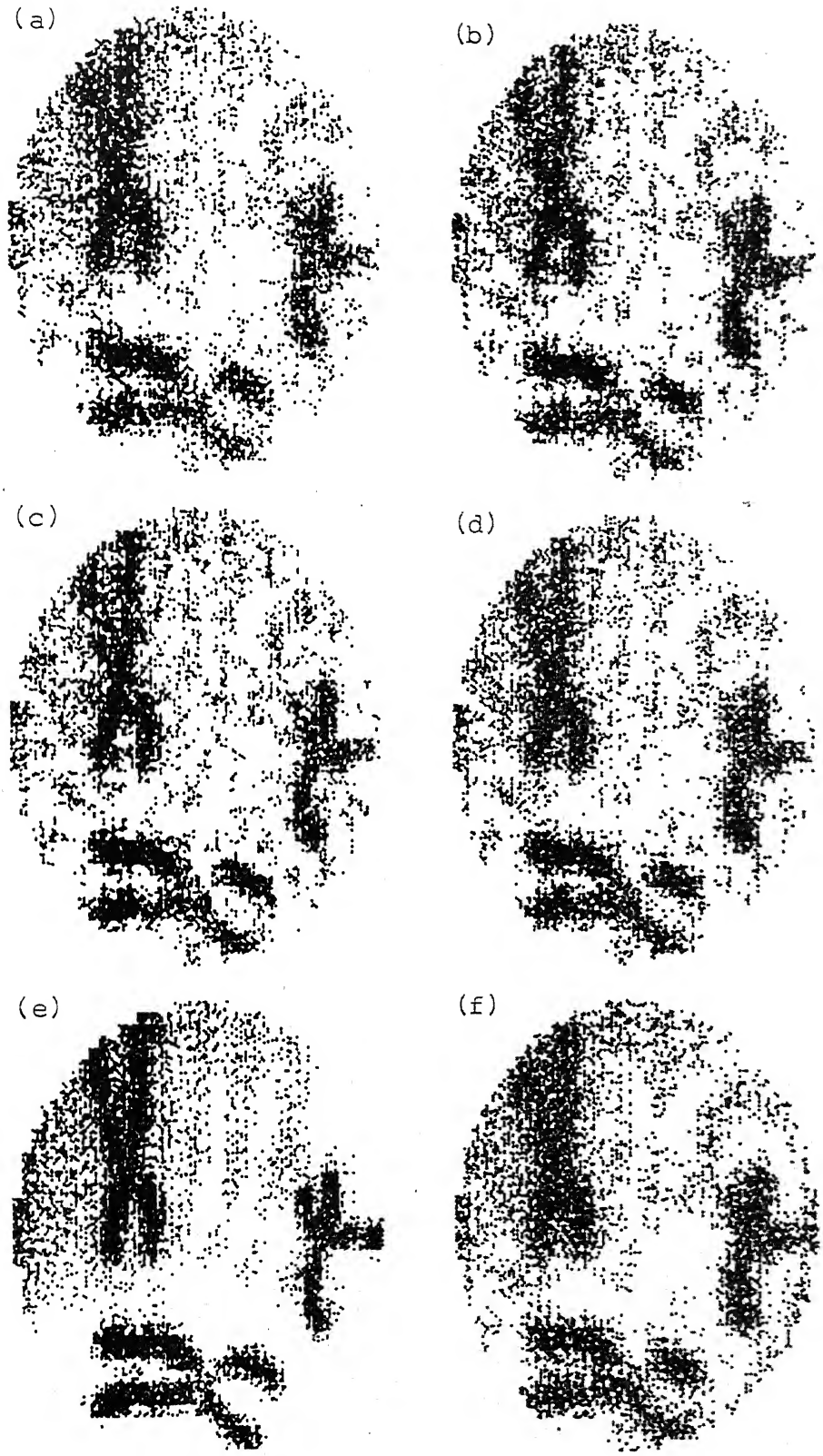

Fig. 6.46 Reconstruction of Chromosomes in CAT line integral noisy case (a) CSI filter, (b) RAM filter, (c) RKS filter, (d) Shepp filter, (e) original picture, (f) optimal filter.

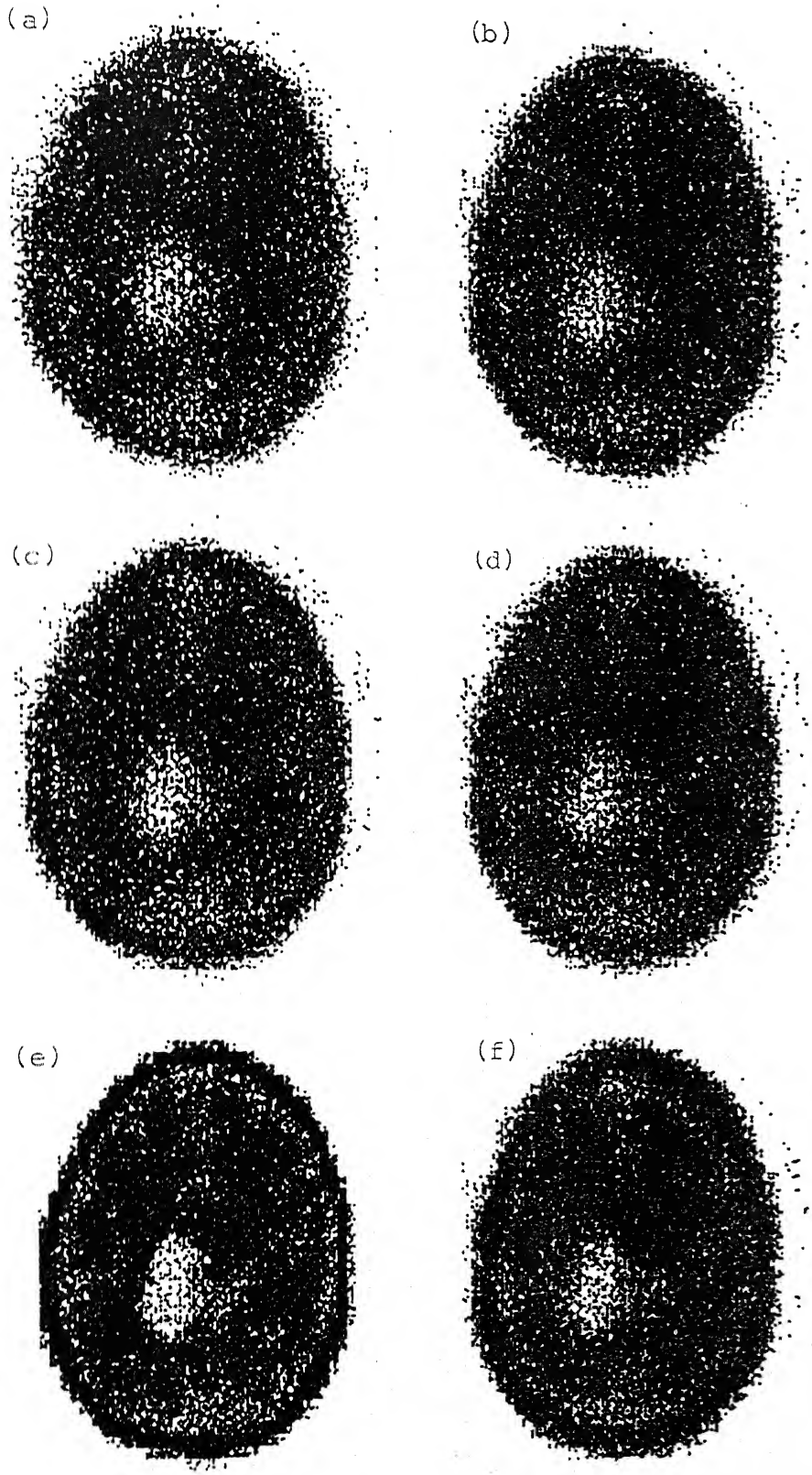

Fig. 6.49 Reconstruction of Brain in CAT strip integral noisy case (a) CSI filter, (b) RAM filter, (c) RKS filter, (d) Shepp filter, (e) original picture, (f) optimal filter.

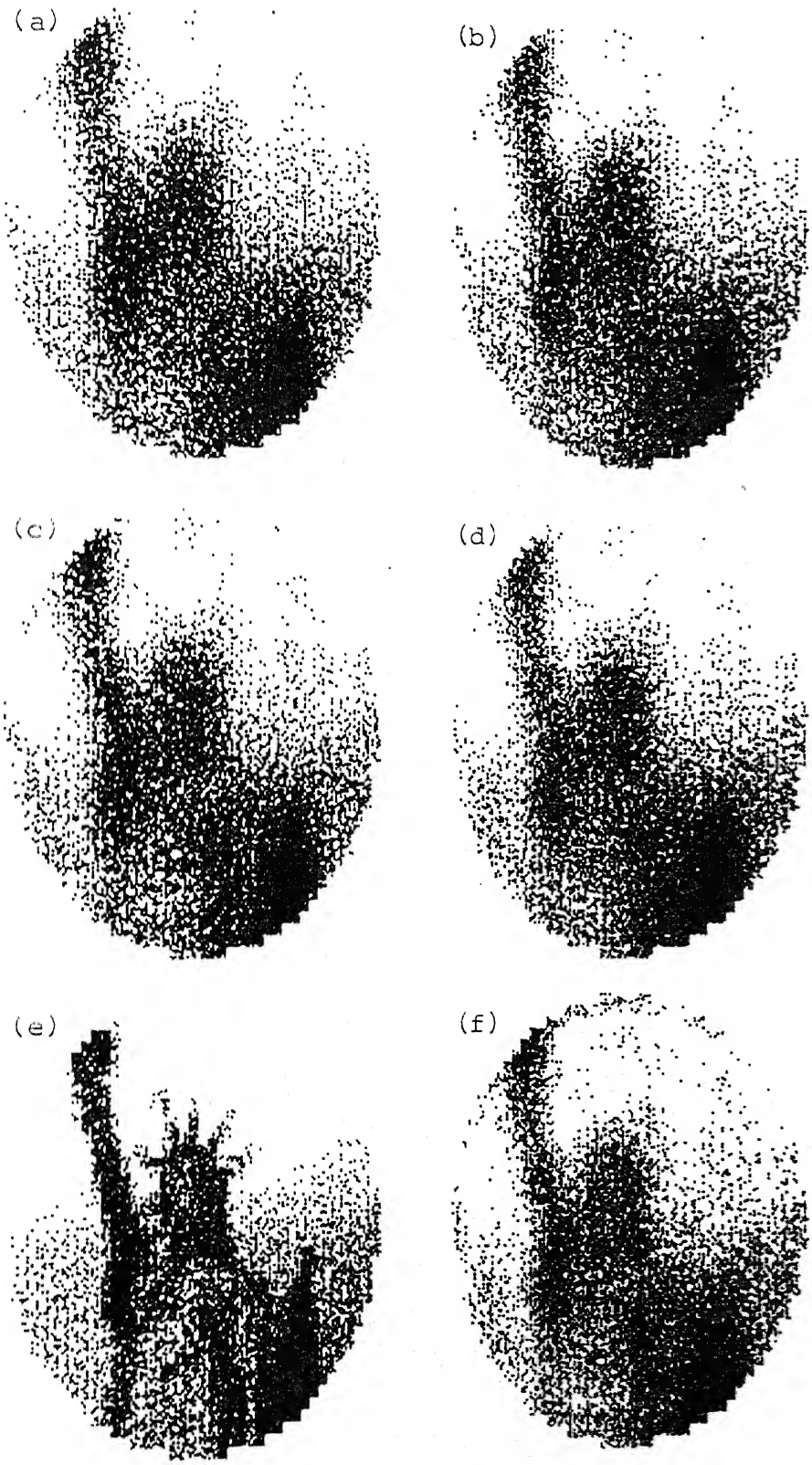

Fig. 6.50 Reconstruction of Statue of Liberty in CAT strip integral noisy case (a) CSI filter, (b) RAM filter, (c) RKS filter, (d) Shepp filter, (e) original filter, (f) optimal filter.

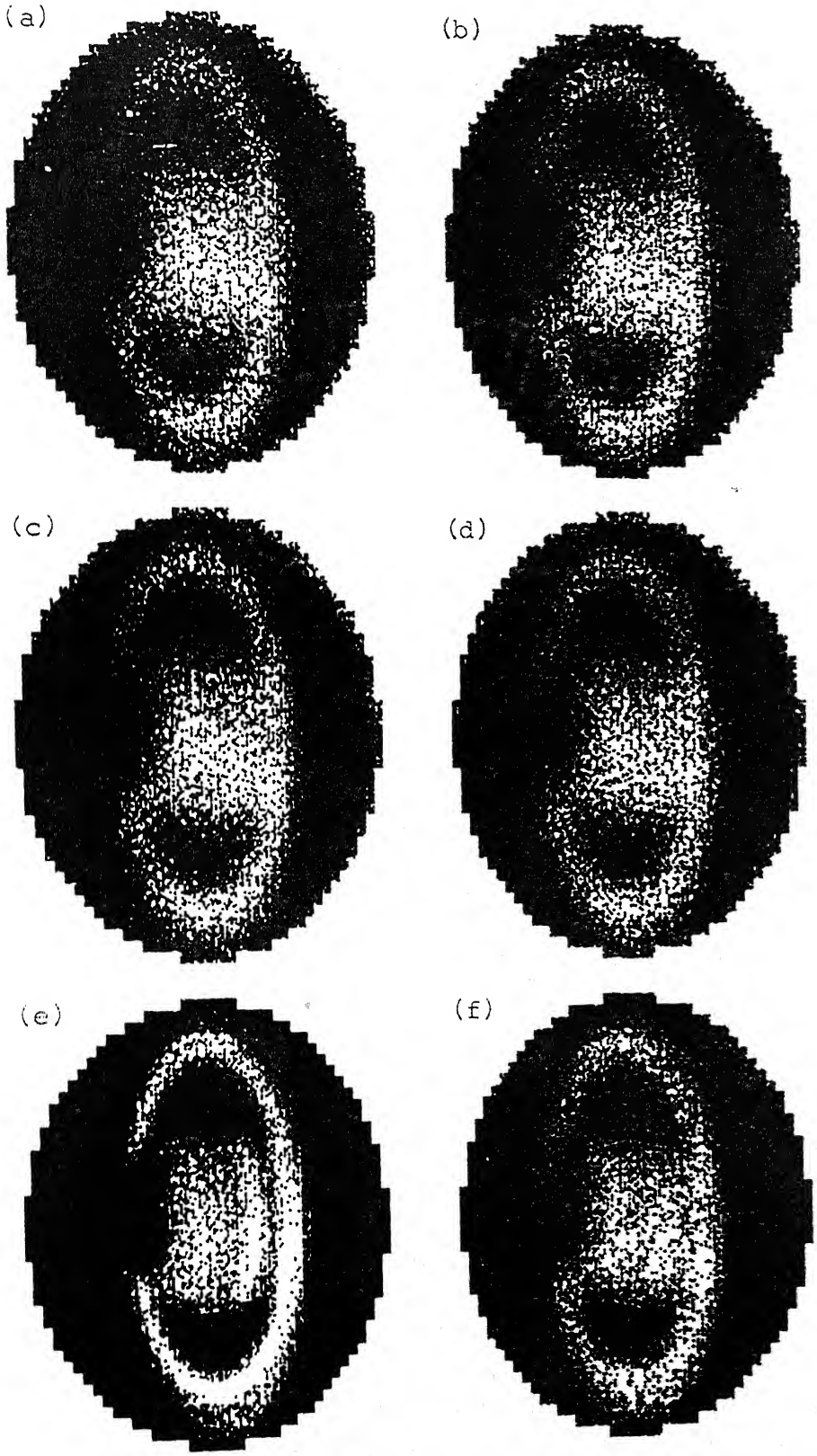

Fig. 6.51 Reconstruction of Saturn in CAT strip integral noisy case (a) CSI filter, (b) RAM filter, (c) RKS filter, (d) Shepp filter, (e) original picture, (f) optimal

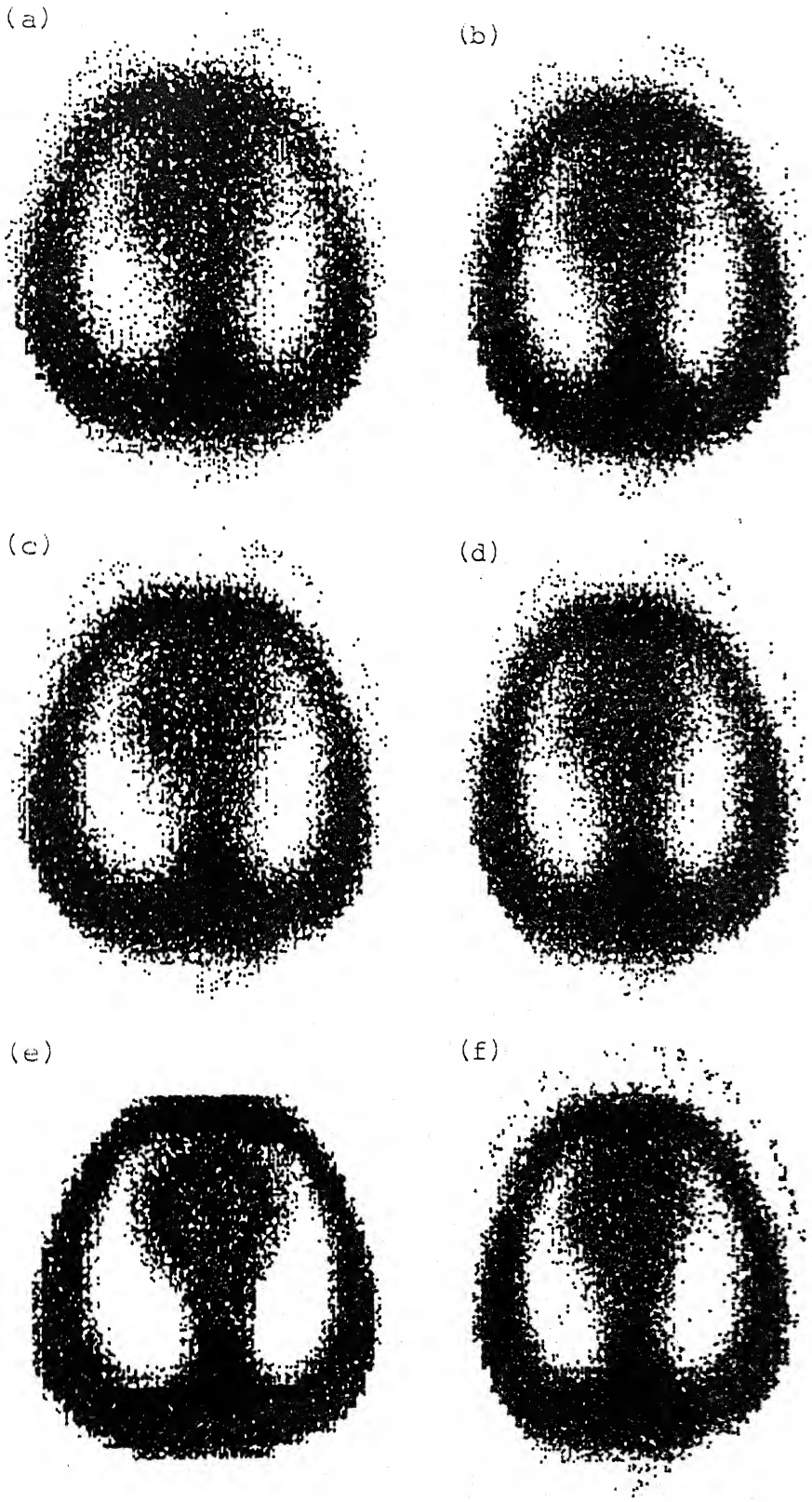

Fig. 6.52 Reconstruction of Thorax in CAT strip integral noisy case (a) CSI filter, (b) RAM filter, (c) RKS filter, (d) Shepp filter, (e) original picture, (f) optimal

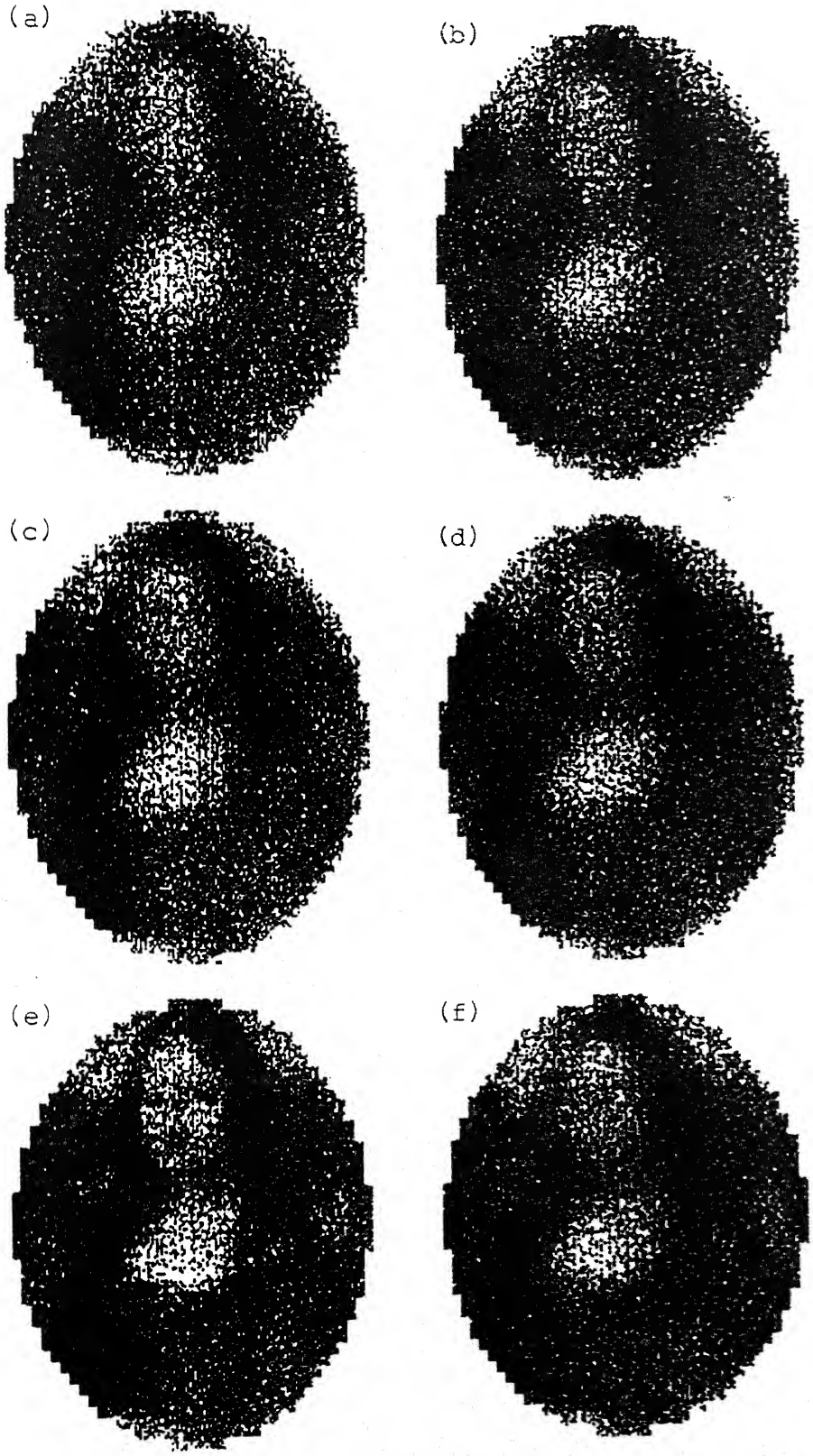

Fig. 6.53 Reconstruction of MonaLisa in CAT strip integral noisy case (a) CSI filter, (b) RAM filter, (c) RKS filter, (d) Shepp filter, (e) original picture, (f) optimal filter.

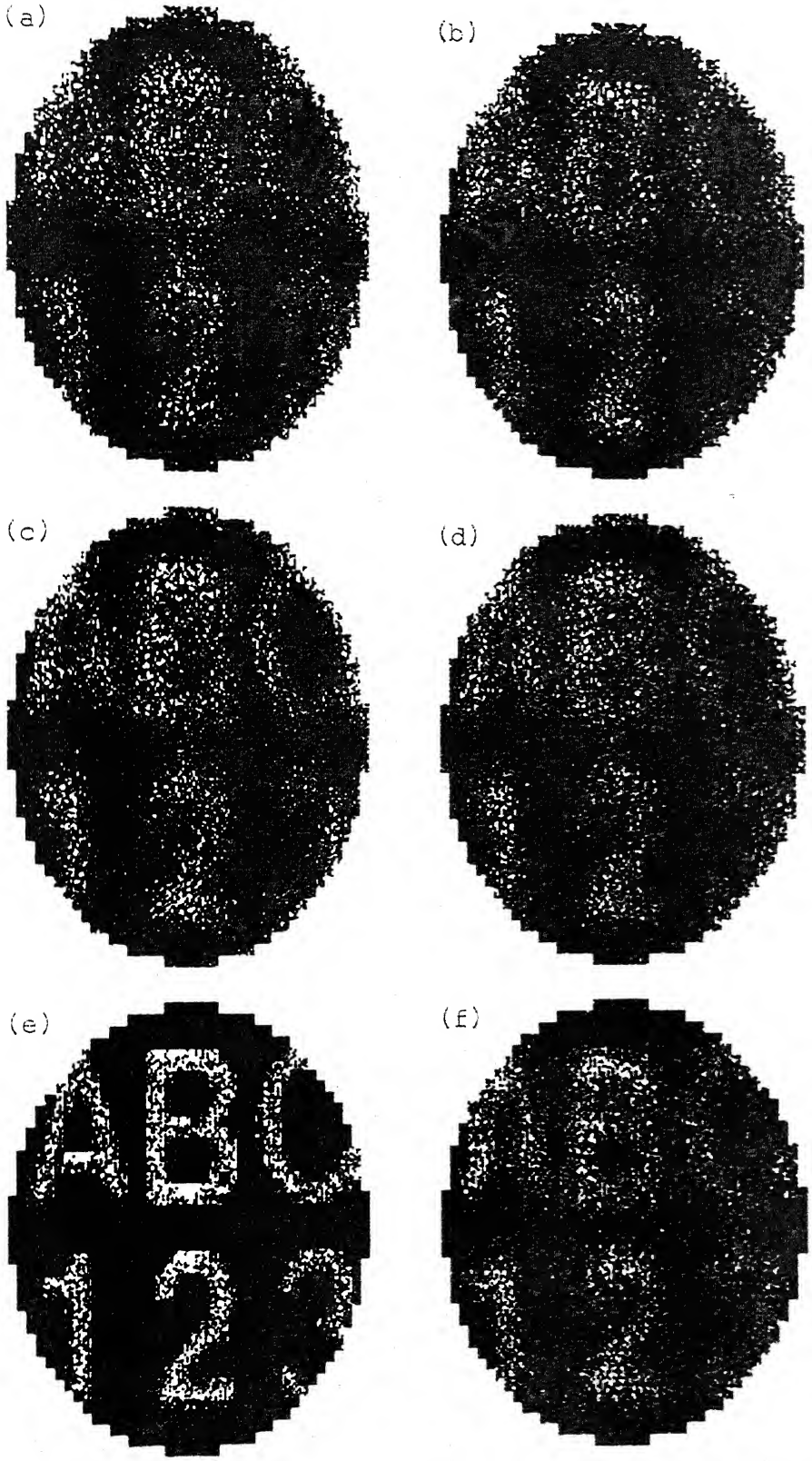

Fig. 6.54 Reconstruction of Characters in CAT strip integral noisy case (a) CSI filter, (b) RAM filter, (c) RKS filter, (d) Shepp filter, (e) original picture, (f) optimal filter.

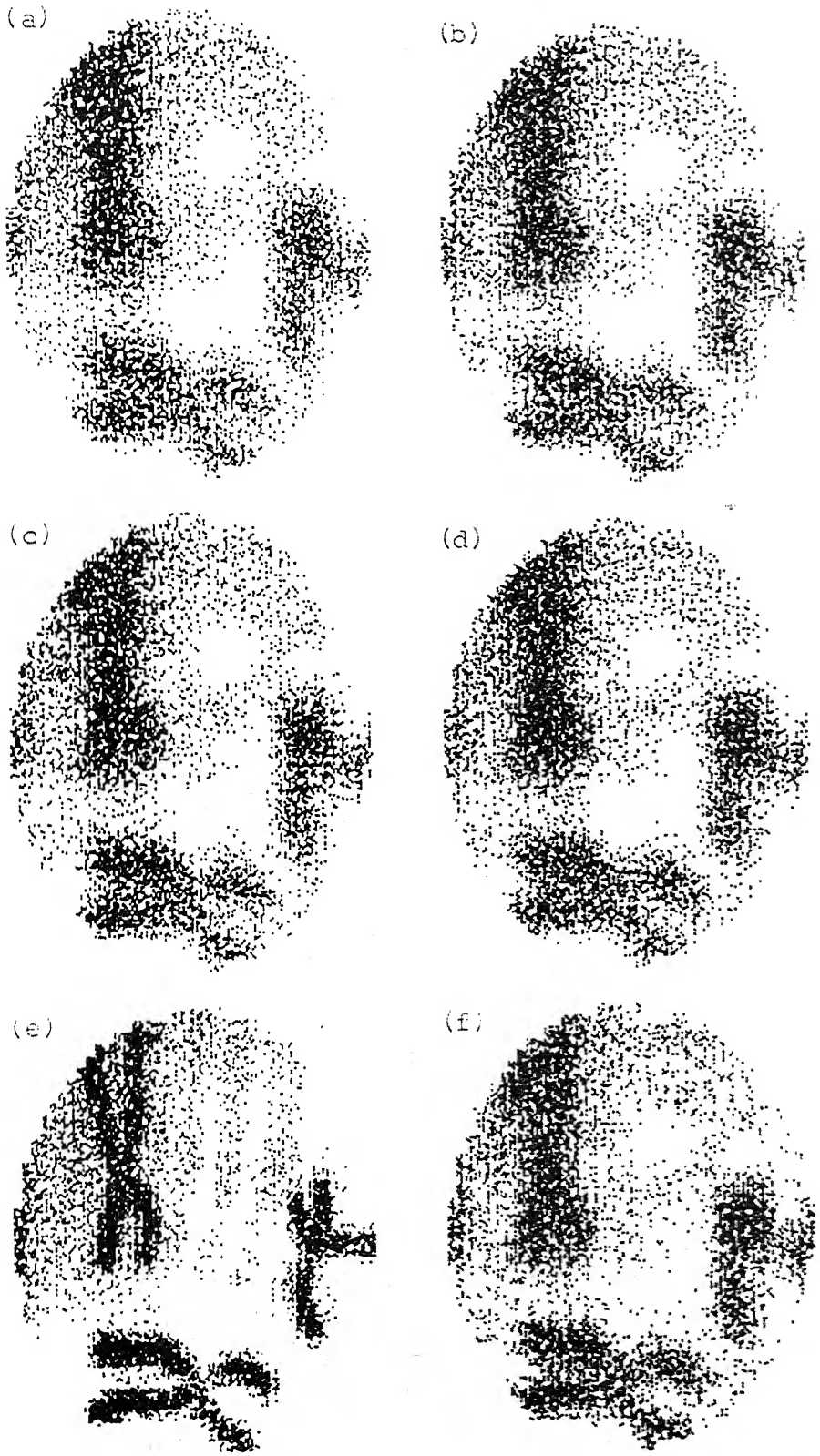

Fig. 6.55 Reconstruction of Chromosomes in CAT strip integral noisy case (a) CSI filter, (b) RAM filter, (c) RKS filter, (d) Shepp filter, (e) original picture, (f) optimal filter.

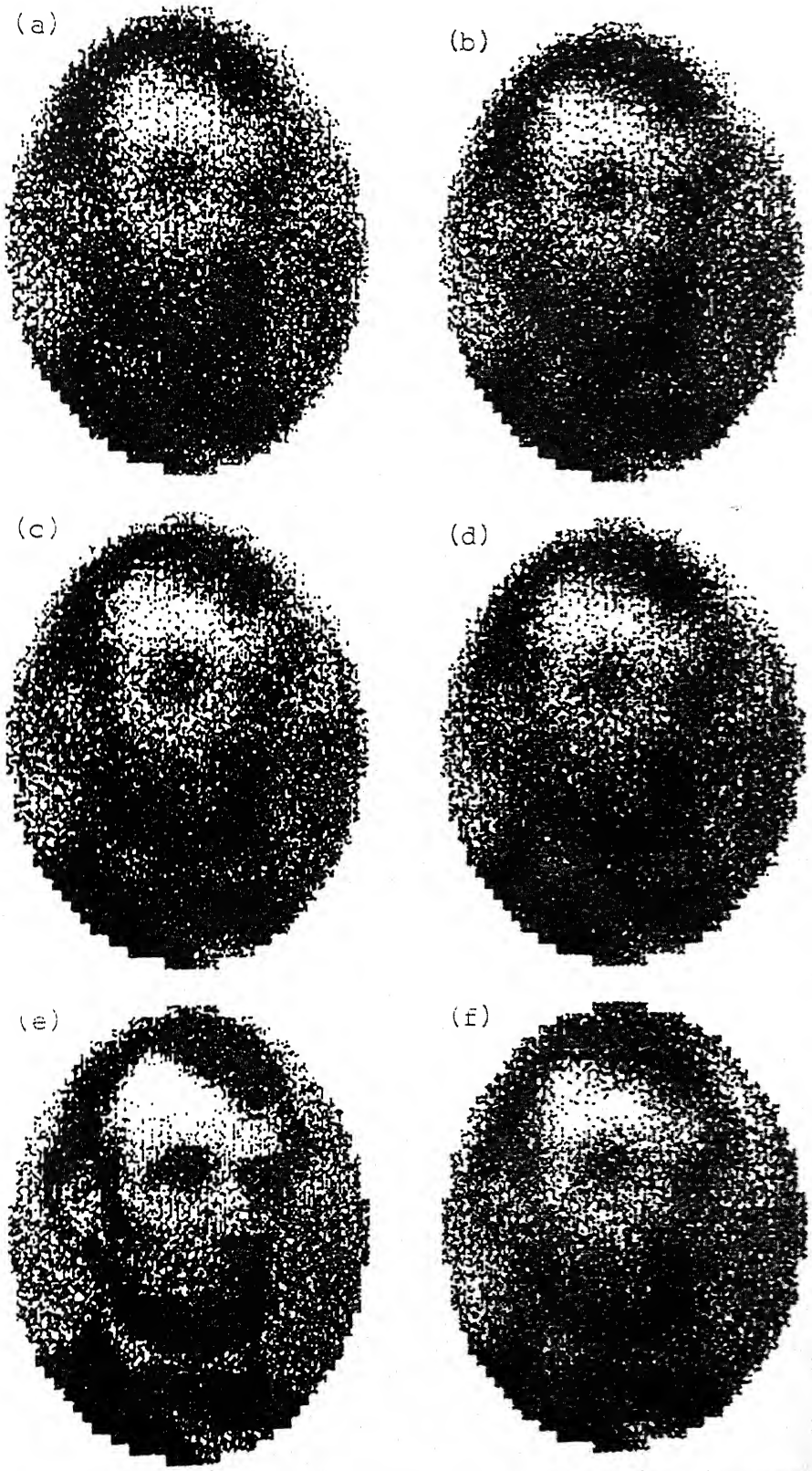

Fig. 6.56 Reconstruction of Lincoln in PET line integral noisy case (a) CSI filter, (b) RAL filter, (c) RKS filter, (d) Shepp filter, (e) original picture, (f) optimal filter.

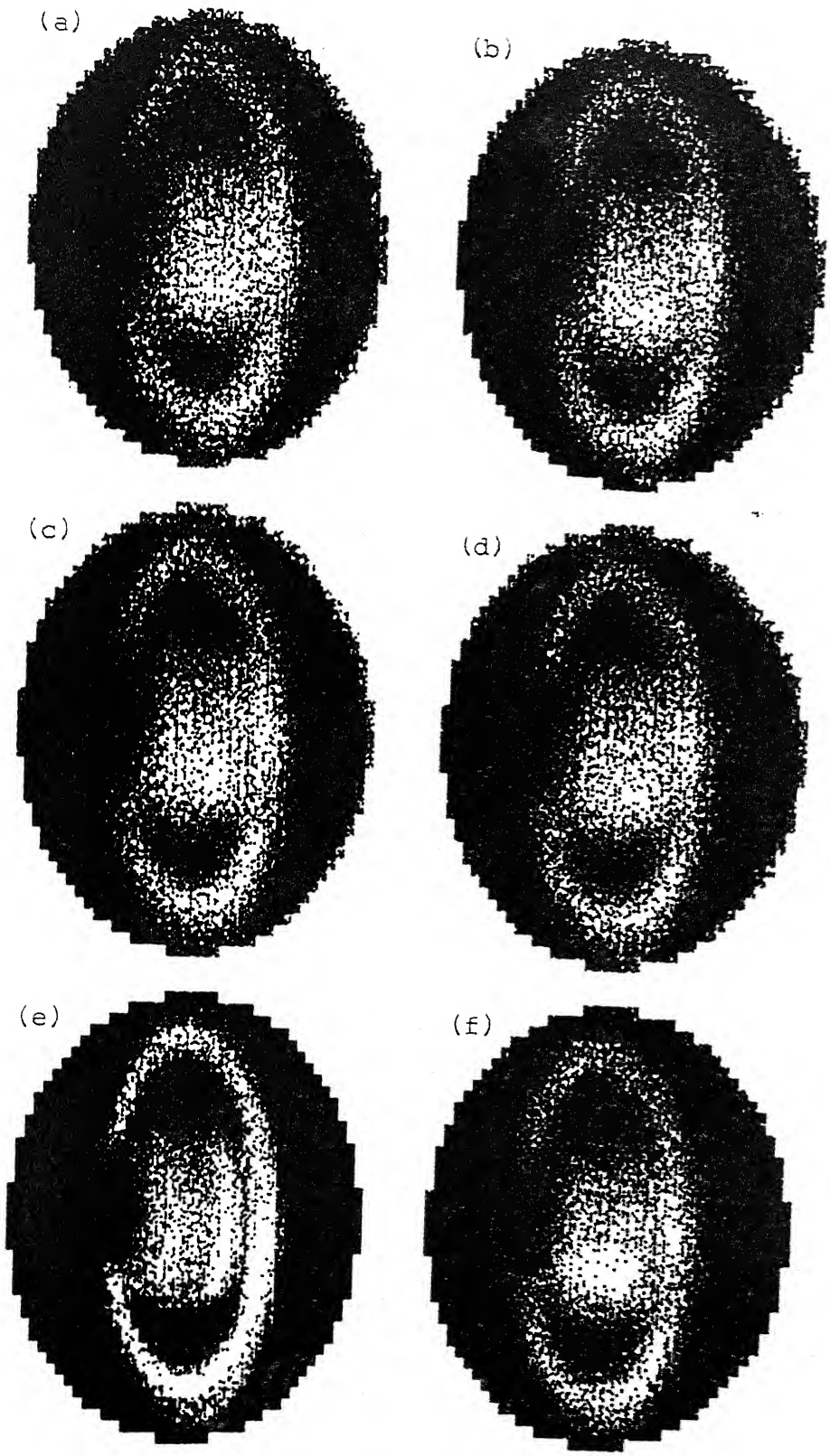

Fig. 6.60 Reconstruction of Saturn in PET line integral noisy case (a) CSI filter, (b) RAM filter, (c) RKS filter, (d) Shepp filter, (e) original picture, (f) optimal filter.

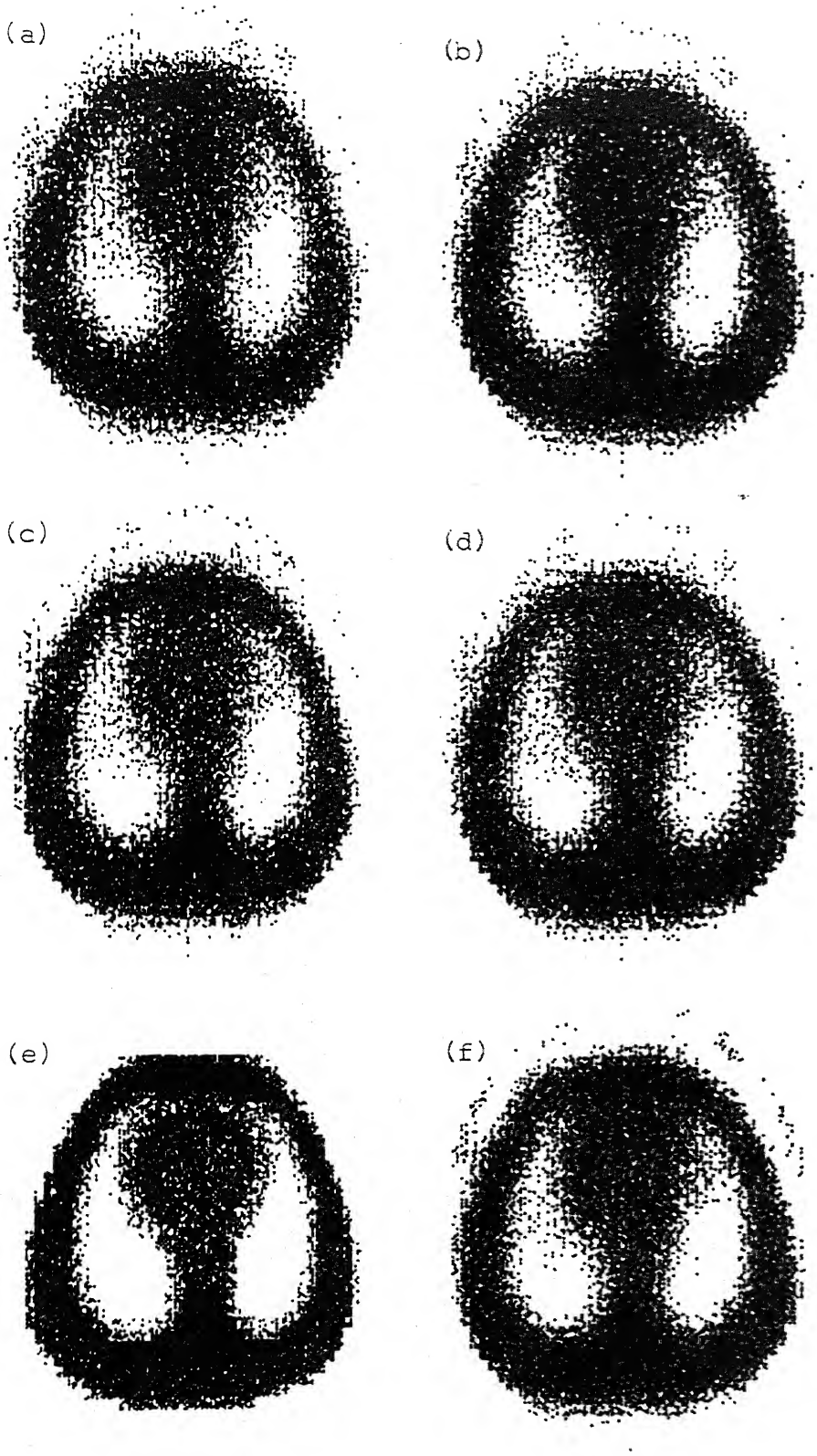

Fig. 6.61 Reconstruction of Thorax in PET line integral noisy case (a) CSI filter, (b) RAM filter, (c) RKS filter, (d) Shepp filter, (e) original picture, (f) optimal filter.

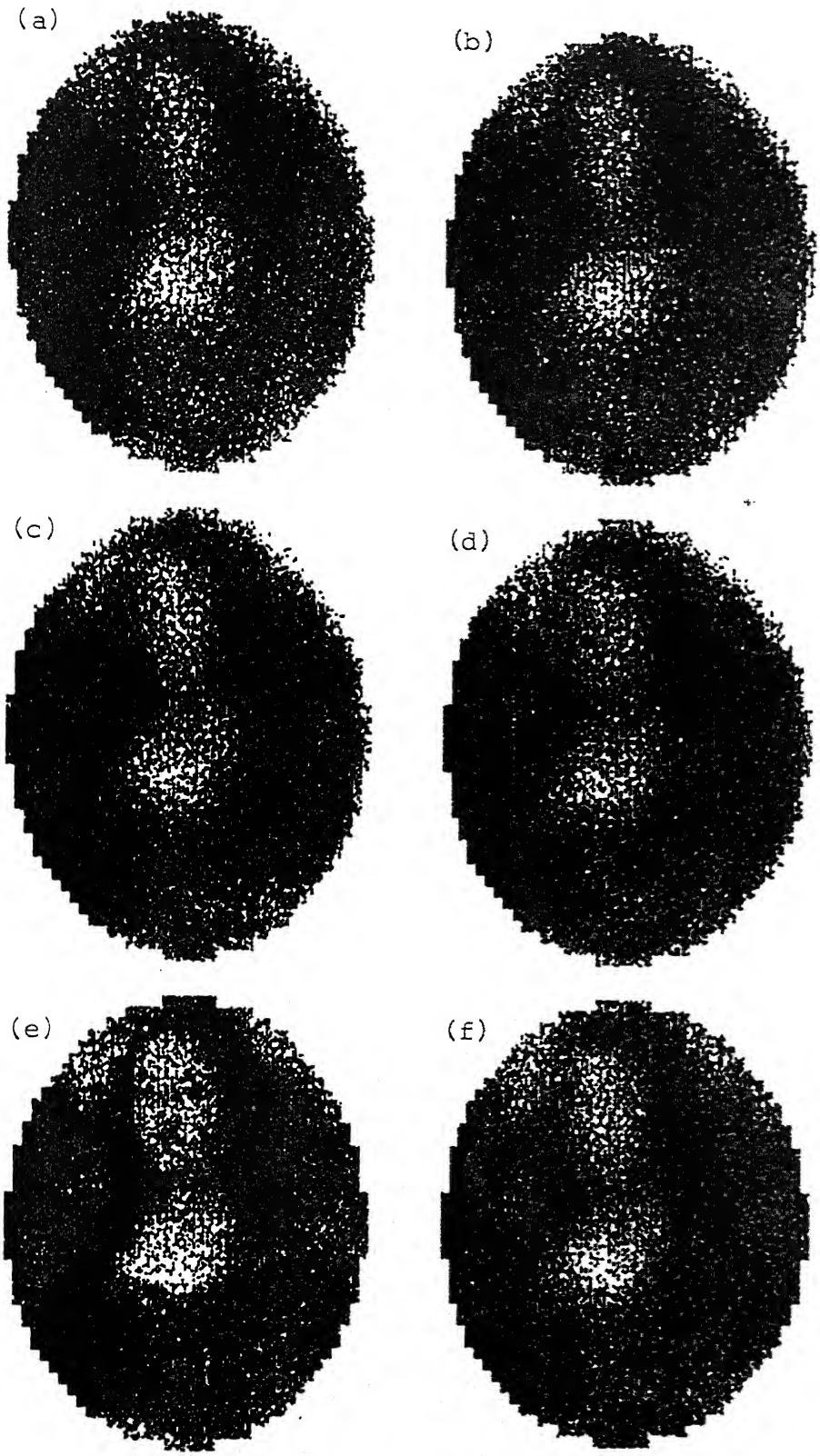

Fig. 6.62 Reconstruction of MonaLisa in PET line integral noisy case (a) CSI filter, (b) RAM filter, (c) RKS filter, (d) Shepp filter, (e) original picture, (f) optimal filter.

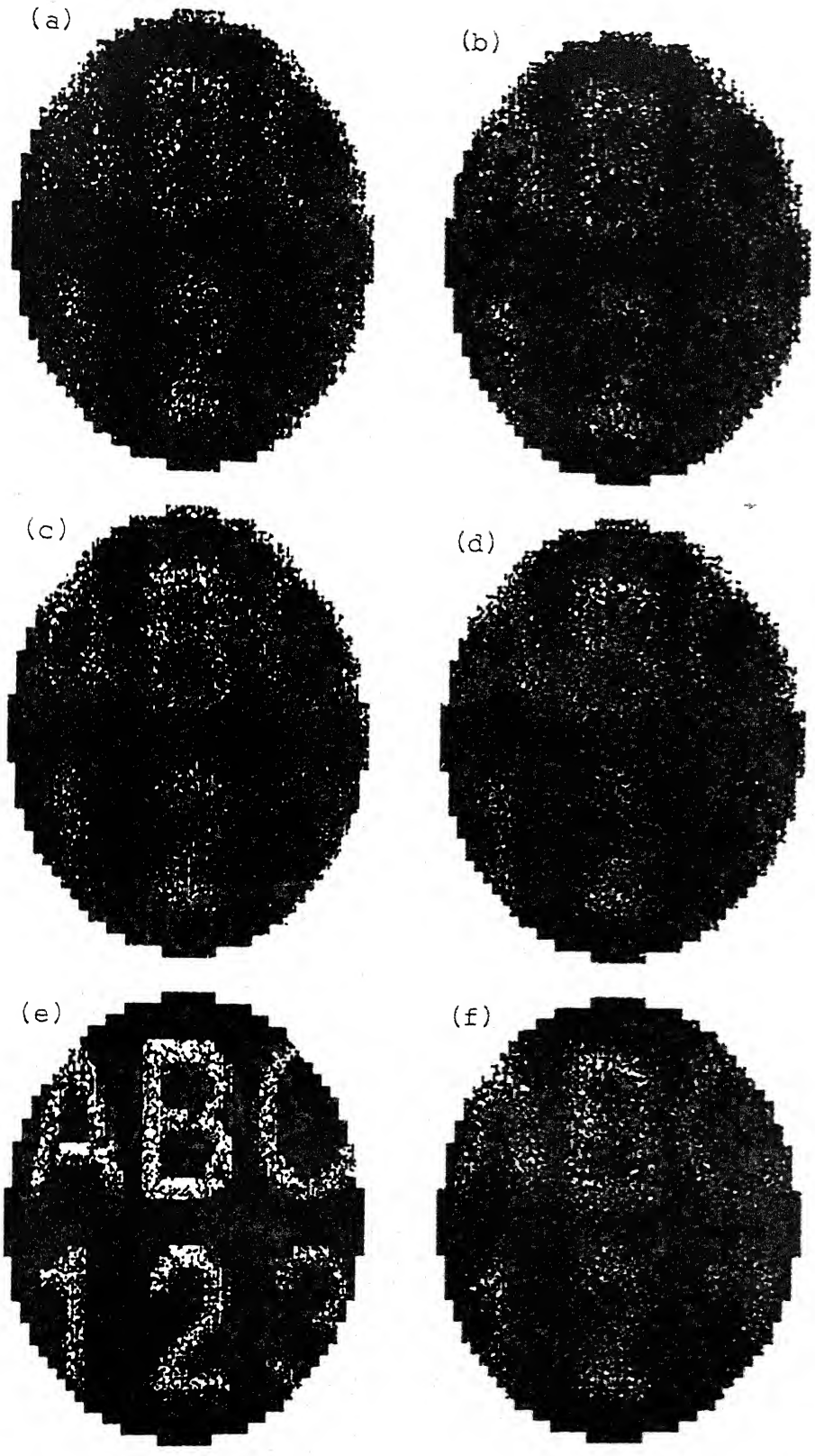

Fig. 6.63 Reconstruction of Characters in PET line integral noisy case (a) CSI filter, (b) RAM filter, (c) RKS filter, (d) Shepp filter, (e) original picture, (f) optimal filter.

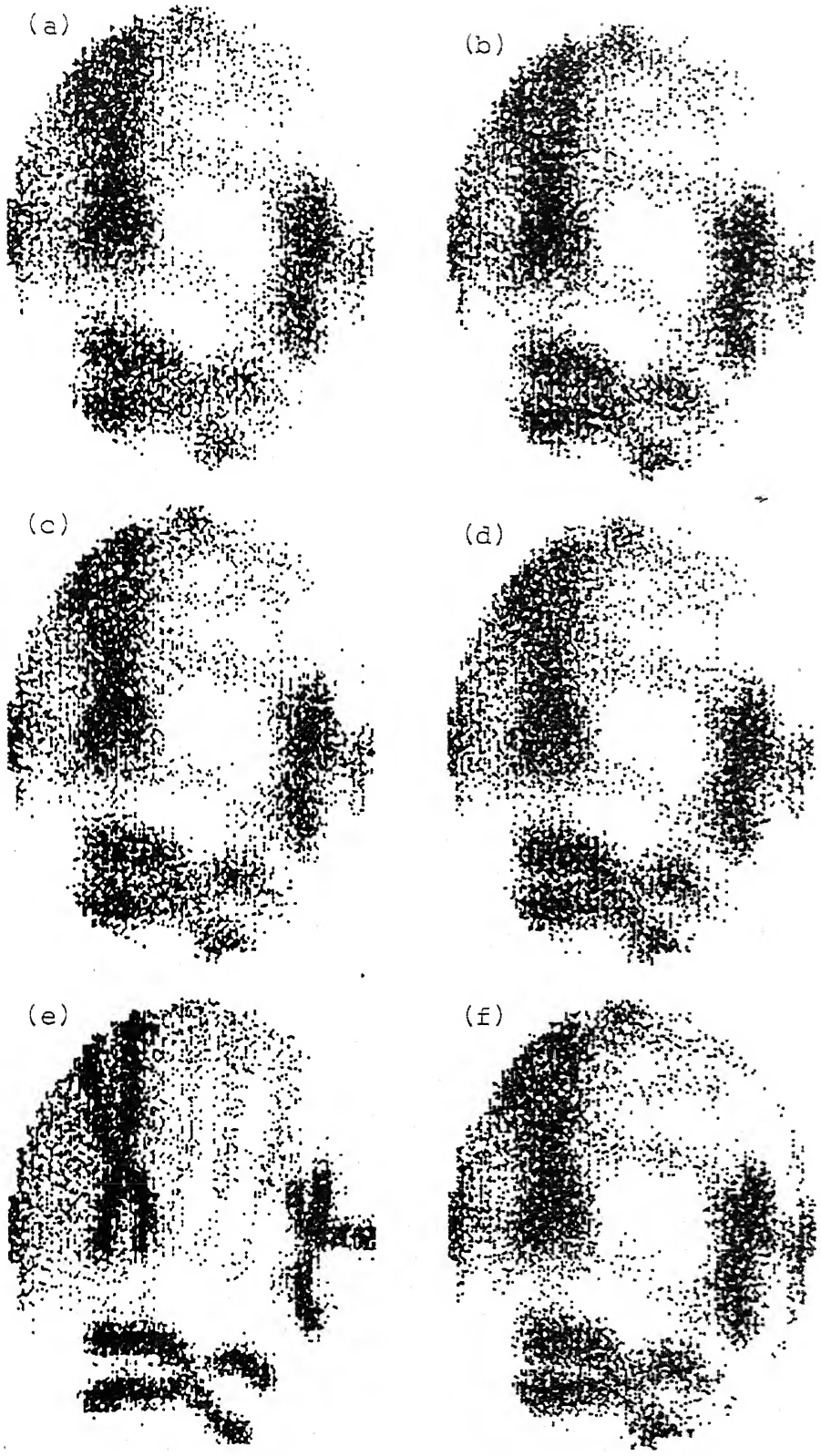
(a)
(b)
(c)
(d)
(e)
(f)

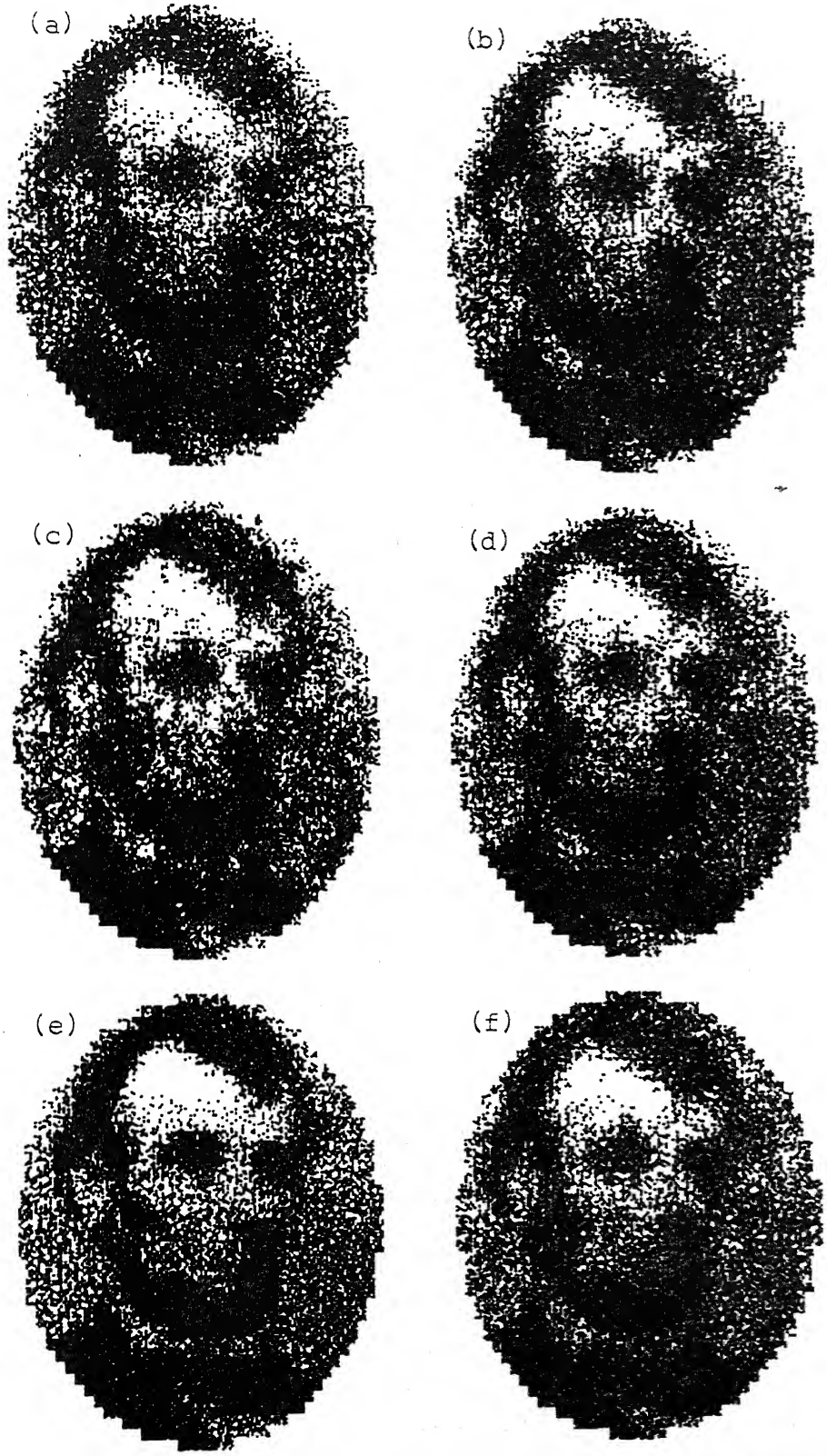

Fig. 6.65 Reconstruction of Lincoln in PET strip integral noisy case (a) CSI filter, (b) RAM filter, (c) RKS filter, (d) Shepp filter, (e) original picture, (f) optimal filter.

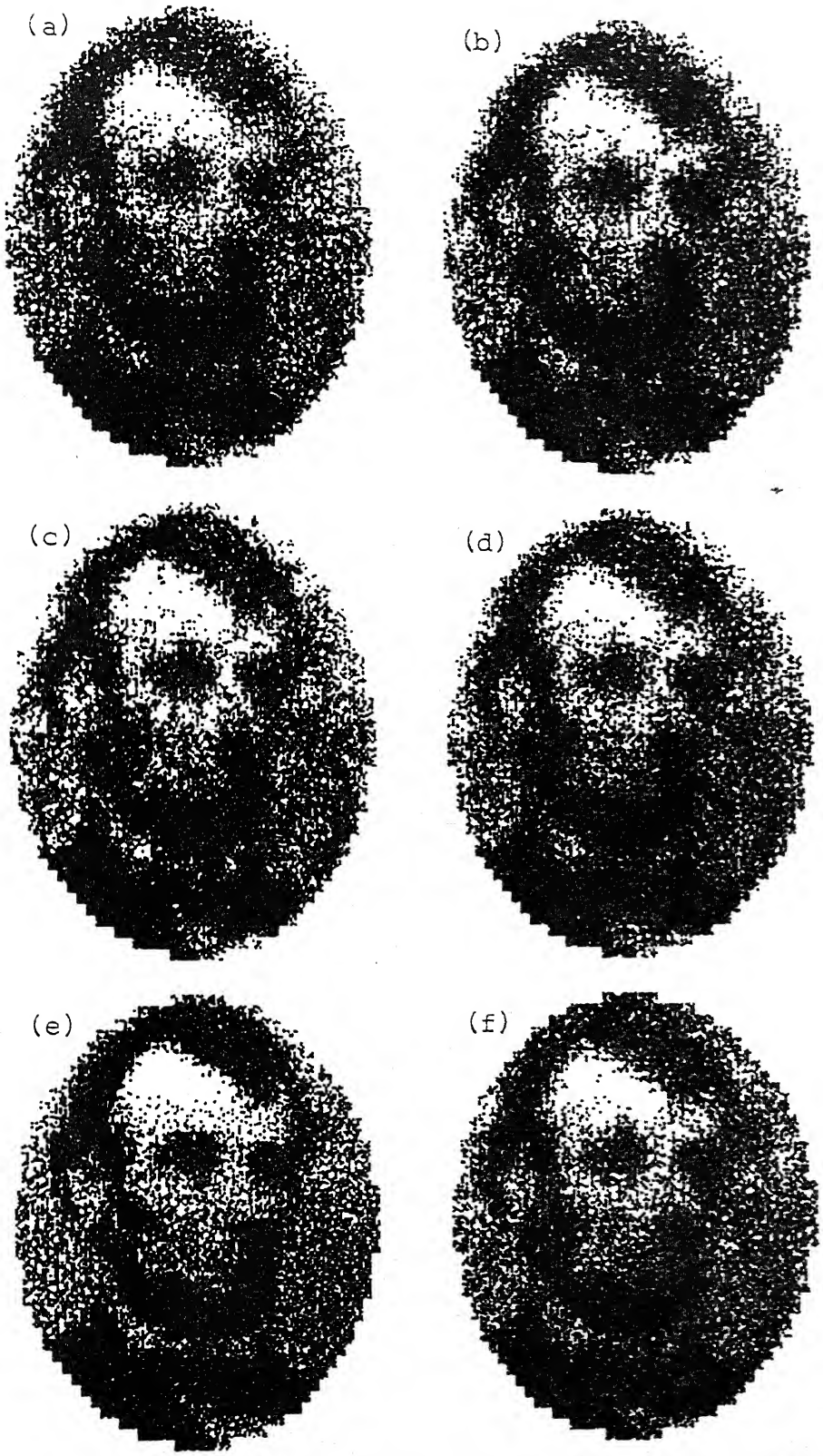

Fig. 6.65 Reconstruction of Lincoln in PET strip integral noisy case (a) CSI filter, (b) RAM filter, (c) RKS filter, (d) Shepp filter, (e) original picture, (f) optimal filter.

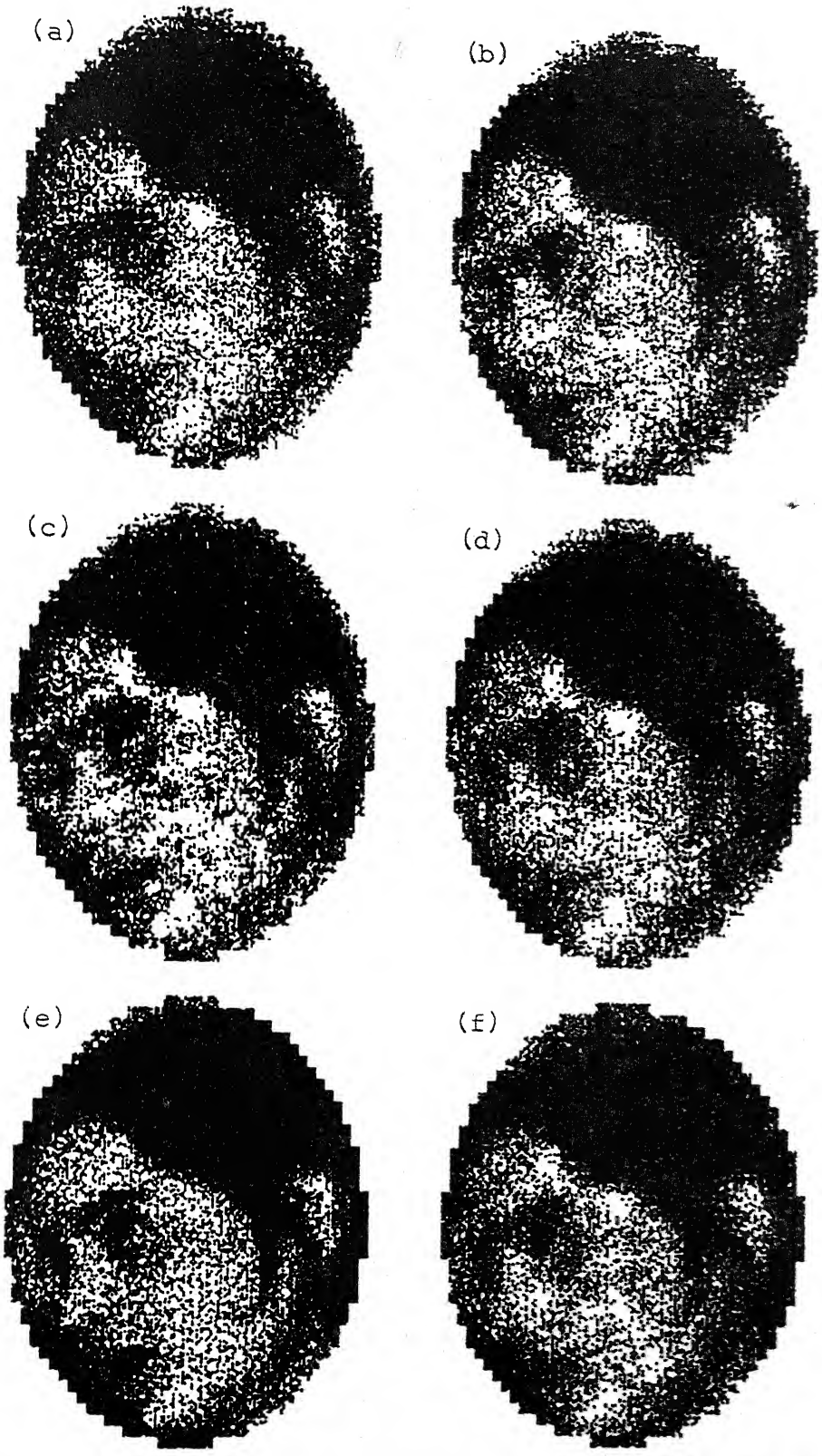

Fig. 6.66 Reconstruction of Face of a girl in PET strip integral noisy case (a) CSI filter, (b) RAM filter, (c) RKS integral, (d) Shepp filter, (e) original picture, (f) optimal filter.

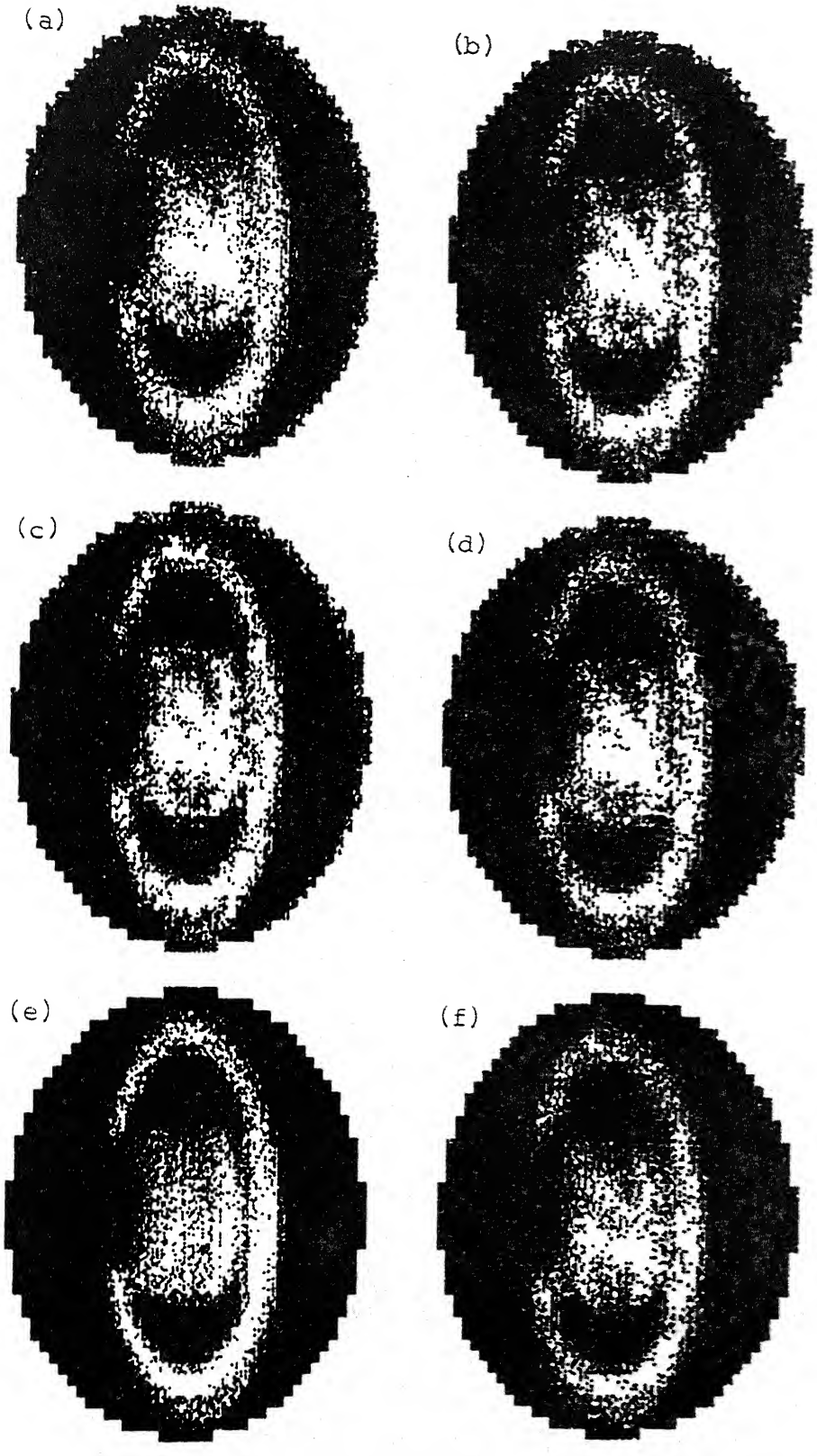

Fig. 6.69 Reconstruction of Saturn in PET strip integral noisy case (a) CSI filter, (b) RAM filter, (c) RKS filter, (d) Shepp filter, (e) original picture, (f) optimal filter.

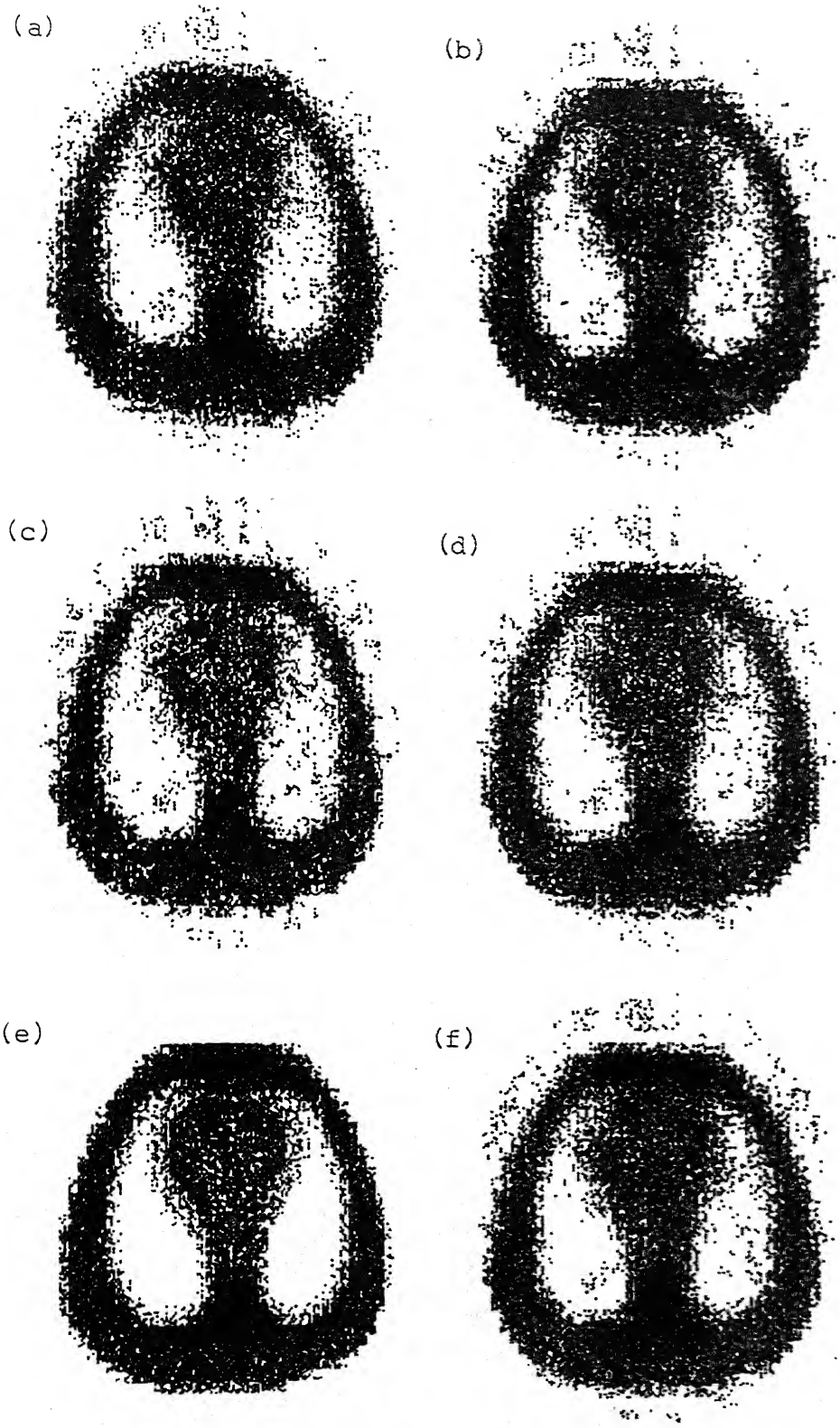

Fig. 6.70 Reconstruction of Thorax in PET strip integral noisy case (a) CSI filter, (b) RAM filter, (c) RKS filter, (d) Shepp filter, (e) original picture, (f) optimal filter.

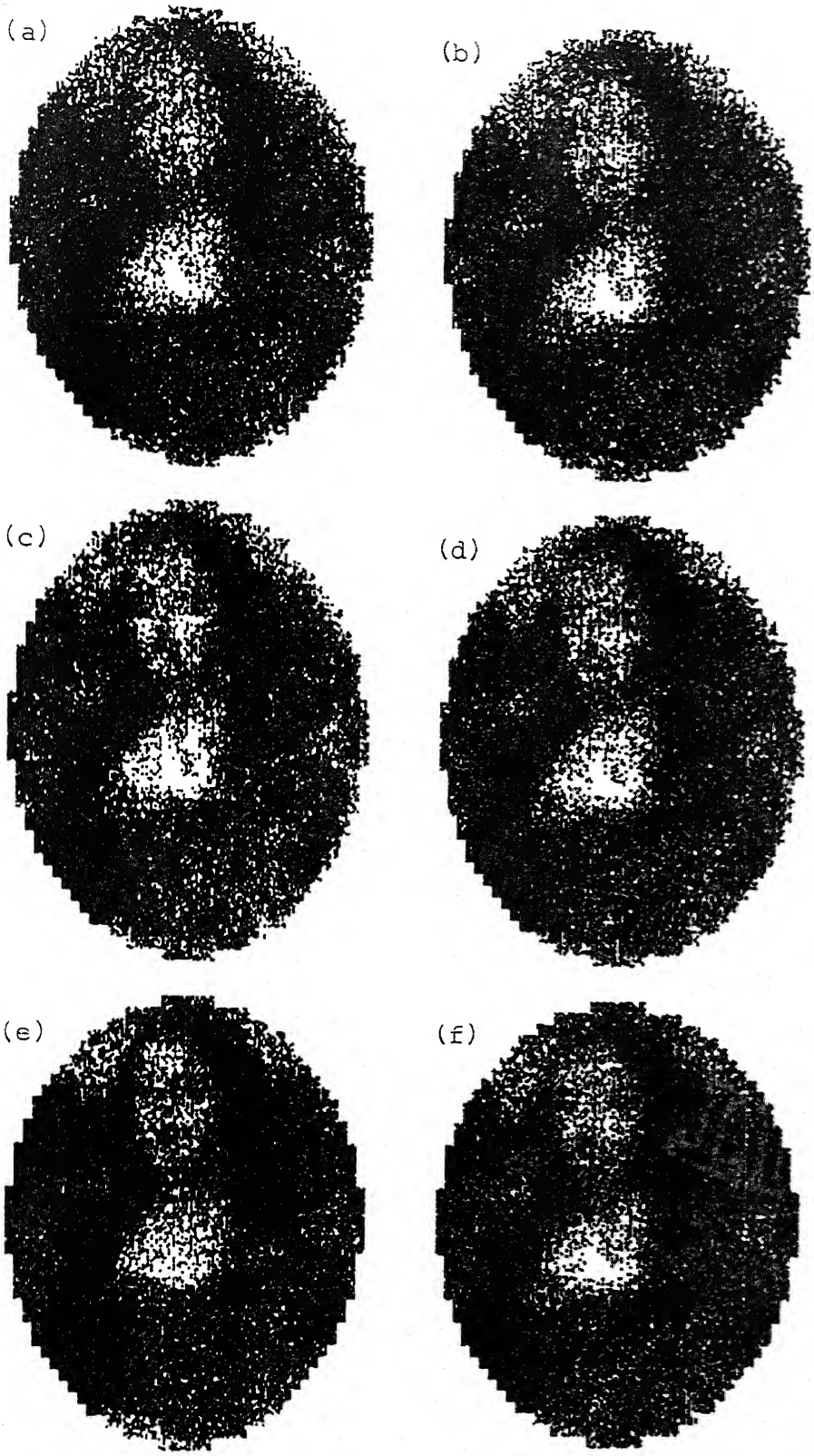

Fig. 6.71 Reconstruction of MonaLisa in PET strip integral noisy case (a) CSI filter, (b) RAM filter, (c) RKS filter, (d) Shepp filter, (e) original picture, (f) optimal filter.

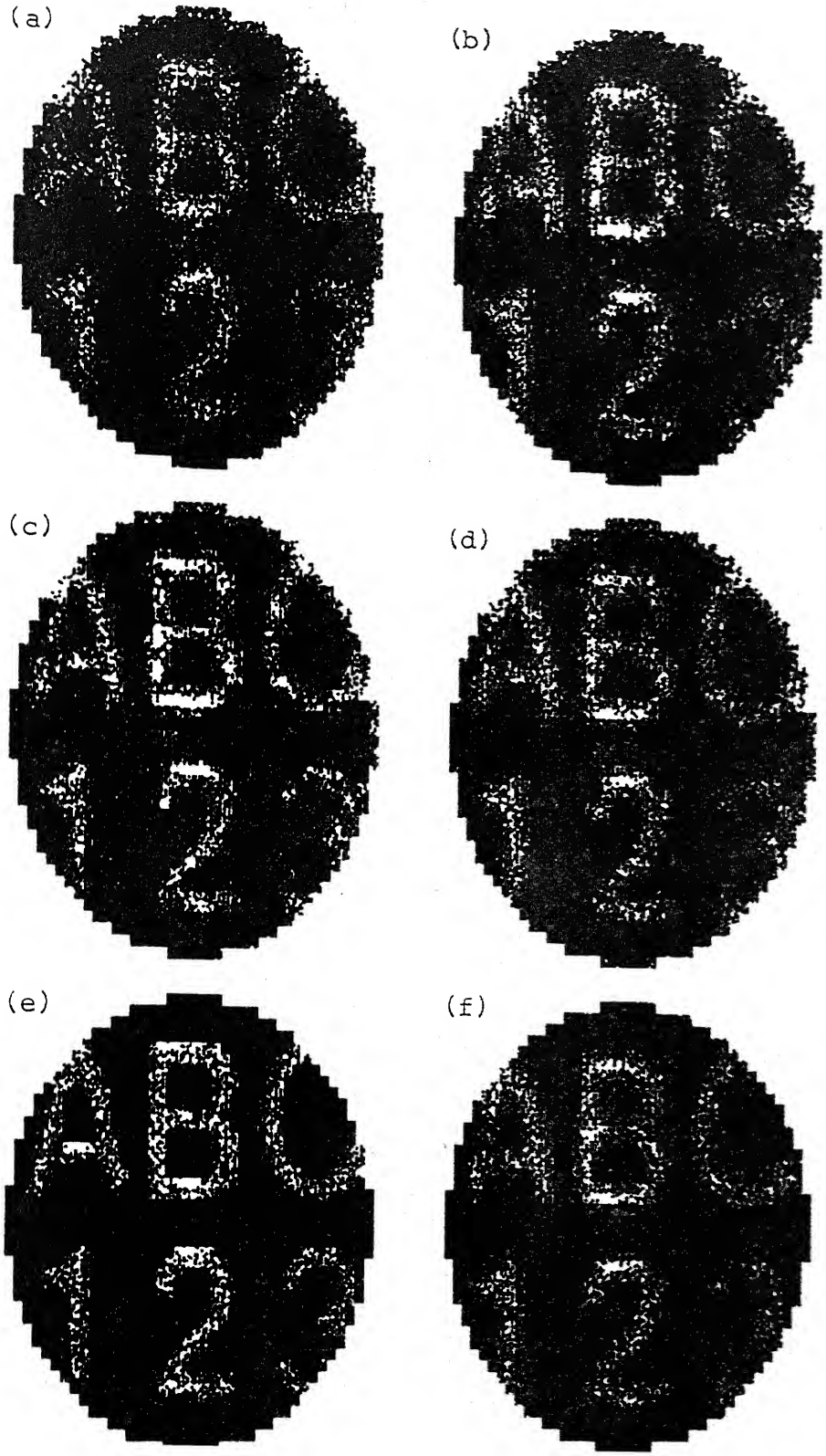
(a)
(b)
(c)
(d)
(e)
(f)

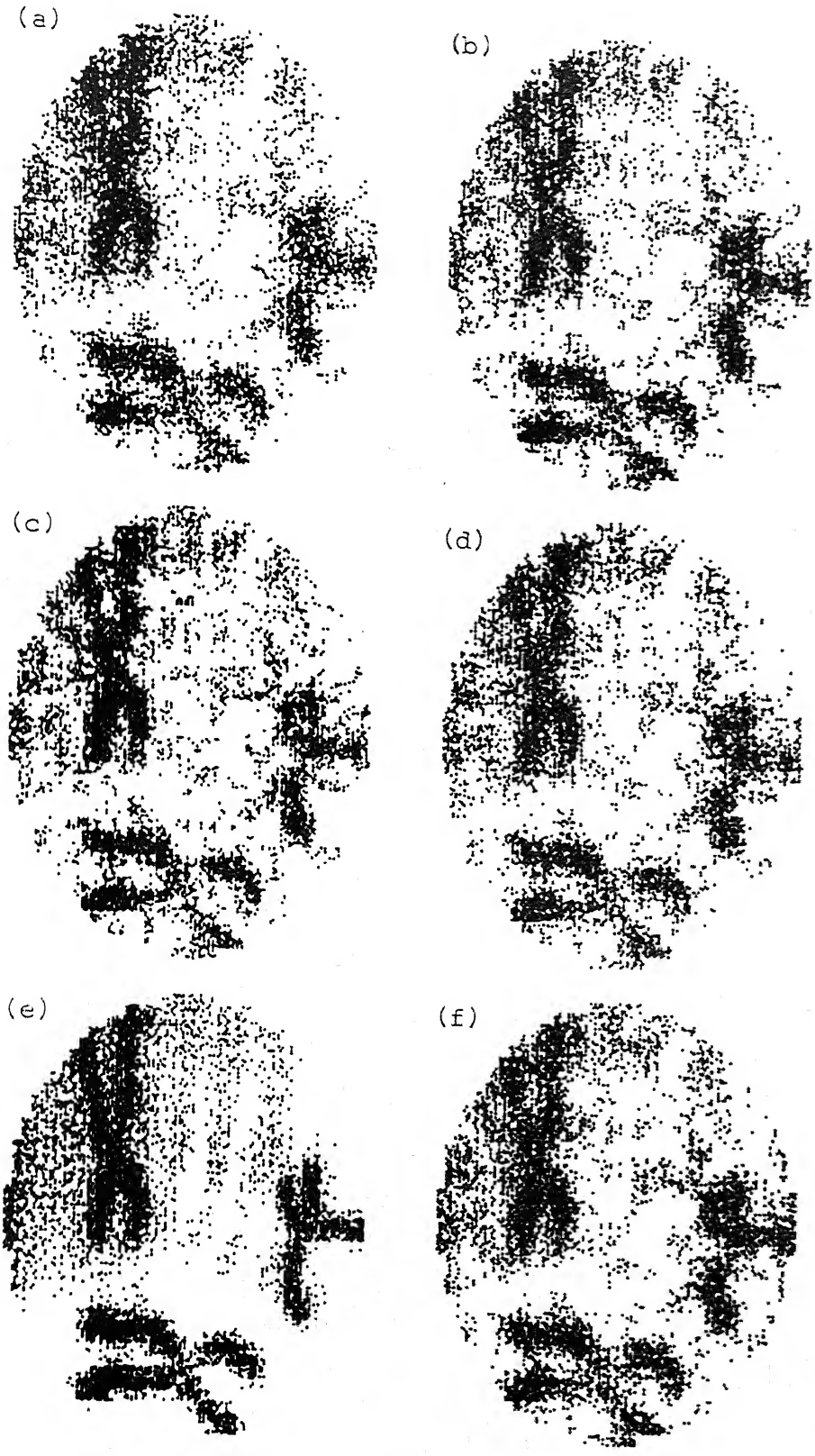

Fig. 6.73 Reconstruction of Chromosomes in PET strip integral noisy case (a) CSI filter, (b) RAM filter, (c) RKS filter, (d) Shepp filter, (e) original picture, (f) optimal filter.

REFERENCES

Becker, M. and Nessel, R.J.(1978): An elementry approach to inverse approximation theorems, *Journal of Approximation Theory*, 23, pp. 93-103.

Bertero, M.; DeMol, C.;and Viano, G.A.(1980) : The stability of inverse problem in *Inverse Scattering Problems in Optics* Ed. by H.P.Baltes, Springer-Verlag, Berlin, pp. 161-214.

Bracewell, R.N.(1956): Strip integral in radio astronomy. *Australian Journal of Physics*, 9, pp. 198-217.

Bracewell, R.N., Riddle, A.C.(1967): Inversion of fan beam scans in radio astronomy, *Astrophysical Journal*, **150**, pp.427-434

Bracewell, R.N.(1979): Image reconstruction in radio astronomy in *Image Reconstruction from Projections: Implementation and applications*, Ed. by G.T.Herman, Springar-verlag, Berlin, pp. 81-104.

Censor, Y.(1983): Finite series-expansion reconstruction methods, *Proceedings of the IEEE*, 71, pp. 409-419.

Censor, Y., Eggerment, P.P.B. and Gordon, D.(1983): Strong under relaxation in Kaczmarz's method for inconsistent systems, *Numerische Mathematik*, **41**, pp. 83-92.

Crowther, R.A., DeRosier, D.J. and Klug, A.(1970): The reconstruction of a three dimensional structure from projections and its application to electron microscopy, *Proceedings of the Royal Society of London, ser A*, **317**. pp. 319-340.

Deans, S.R.(1983): *Radon Transform and some of its Applications*, John Wiley and Sons, New York.

Dempster, A.P., Laird, N.M. and Rubin, D.B.(1977): Maximum likelihood from incomplete data via the EM algorithm, *Journal of the Royal Statistical Society, ser.B*, **39**, pp. 1-38.

Eggerment, P.P.B., Herman, G.T. and Lent, A.(1981): Iterative algorithm for large partitioned linear systems with applications to image reconstruction, *Linear Algebra and Its Applications*, **40**, pp. 37-67.

Gilbert, P.(1972): Iterative methods for three-dimensional reconstruction of an object from projections, *Journal of Theoretical Biology*, **36**, pp. 105-117.

Goldberg, S.(1966): *Unbounded Linear Operators*, McGraw Hill.

Gonzalez, R.C. and Wintz, P.(1977): *Digital Image Processing*, Addison-Wesley Publishing Co., Massachusetts.

Gordon, R., Bender, R. and Herman G.T.(1970): Algebraic reconstruction techniques (ART) fir three dimensional electron microscopy and X-ray photography, *Journal of Theoretical Biology*, **29**, pp. 471-481.

Gordon, R.(1974): A tutorial on ART, *IEEE Transactions on Nuclear Science*, **NS-21**, pp. 78-83.

Guenther, R.B., Kerber, C.W., Killian, E.K., Smith K.T. and Wagner, S.L.(1974): Reconstruction of objects from radiograph and the location of the brain tumors, *Proceedings of the National Academy of Scinces U.S.A.*, **71**, pp. 4884-4886.

Hanson, K.M. (1987): Bayesian and related methods in image reconstruction from incomplete data in *Image Recovery: Theory and Application*, Ed. by H.Stark, Academic Press pp.79-127.

Herman, G.T. and Lent, A.(1976): A computer implementation of bayesian analysis of image reconstruction, *Information and Control*, **31**, pp. 364-384.

Herman, G.T. and Neparstek, A.(1977): Fast image reconstruction based on a Radon inversion formula

appropriate for rapidly collected data, *SIAM Journal on Applied Mathematics*, **33**, pp. 511-533.

Herman, G.T., Hurwitz, H., Lent, A. and Lung, H.(1979): On the baysian approach to image reconstruction, *Information and Control*, **42**, pp. 60-70

Herman, G.T.(1980): *Image Reconstruction from Projections: The Fundamental of Computerized Tomography*, Academic Press.

Herman, G.T. and Natterer, F.(1981)(eds): Mathematical aspects of computerized tomography, *Proceedings*, Oberwolfach 1980, Springer.

Hounsfeild, G.N.(1973): Computerizes trnsverse axial scaning tomography part I, Description of the system, *British Journal of Radiology*, **46**, pp. 1016-1022.

Hunt, B.R.(1977): Bayesian methods in non-linear digital image restoration, *IEEE Transactions on Computers*, **C-26**, pp. 219-229.

Inouye, T.(1979): Image reconstruction with limited angle projection data, *IEEE Transactions on Nuclear Science*, **NS-26**, pp. 2666-2669.

Jerry, A. J.(1977): The Shannon sampling theorem and applications: A tutorial review, *Proceedings of the IEEE*, **65**, pp. 1565-1596.

Kaczmarz, S.(1937): Angenäherte Auflösung von System Linearer Gleichungen, Bull. Acad. Polon, Sci. Lett., **A35**, pp. 355-357.

Lakshminarayanan, A.V.(1975): Reconstruction from divergent ray data, Technical report, No, 92, Department of Computer Science , State University of New York.

Lakshminarayanan, A.V. and Lent, A.(1979): Method of least squares and SIRT in reconstruction, *Journal of Theoretical Biology*, **76**, pp. 267-295.

Rockmore, A.J. and Macovaski, A.(1977): A maximum likelihood approach to transmission image reconstruction from projections, *IEEE Transactions on Nuclear Scince*, **NS-24**, pp. 1929-1935.

Shepp, L.A. and Logan, B.F.(1974): The Fourier reconstruction of a head section, *IEEE Transactions on Nuclear Scince*, **NS-21**, pp. 21-43.

Shepp, L.A. and Vardi, Y.(1982): Maximum Likelihood recontruction for emission tomography, *IEEE Transactions on Medical Imaging*, **MI-1**, pp. 113-122.

Stark, H.(1987)(Ed.): *Image Recovery: Theory and Application*, Academic press New York.

Stark, H., Woods, J.W., Paul, I. and Hingorani,R.(1981a): Direct Fourier reconstructions in computer tomography, *IEEE Transactions on Acoustics, Speech and Signal Processing*, **ASSP-29**, pp. 237-245.

Stark, H., Woods, J.W., Paul, I. and Hingorani,R.(1981b): An investigation of computerized tomography by direct Fourier inversion and optimum interpolation, *IEEE Transactions on Biomedical Engineering*, **BME-28**, pp. 496-505.

Tanabe, K.(1971): Projection method for solving a singular system of linear equations and its applications, *Numerische Mathematik*, **17**, pp. 203-214.

Trussel, H.J. and Hunt, B.R.(9179): Improved method of maximum *a poseriori* restoration, *IEEE transactions on Computers*, **C-27**, pp. 57-62.

Vardi, Y., Shepp, L.A. and Kaufman, L.(1985): A statistical model for Positran emission tomography, *Journal of the American Statistical Association*, **80**, pp. 8-37.

Wernecke, S.J. and D'Addario, L.R.(1977): Maximum entropy image reconstruction, *IEEE Transactions on Computers*, **C-26**, pp. 351-364.

Wood, S.L. and More, M.(1981): A fast implementation of a minimum variance estimator for computerized tomography image reconstruction, *IEEE Transactions on Biomedical Engineering*, BME-28, pp. 56-68.

Zhuang, X., Ostevold, F. and Harlic, R.M.(1987): A differential equation approach to maximum entropy image reconstruction, *IEEE Transactions on Acoustics, Speech and Signal Processing* , ASSP-35, pp. 208-218.

Natterer, F.(1980): A sobolev space analysis of picture reconstruction, *SIAM Journal on Applied Mathematics*, **39**, pp. 402-411

Natterer, F.(1985): Fourier reconstruction in tomogarphy, *Numerische Mathematik*, **47**, pp. 343-353.

Natterer, F.(1986): *The Mathematics of Computerized Tomography*, John Wiley and Sons, New York.

Radon, J.(1917): Über die Bestimmung von Funktionen durch ihre Integralwerte Längs gewisser Mannigfaltigkeiten. Berichte Sächsische Akademie der Wissenschaften, Leipzig, *Math Phys. Kl* **69** pp. 262-267.

Ramachandran, G.N. and Lakshminarayanan(1971): Three dimensional reconstruction from radiographs and electron microscops: Application of convolution instesd of Fourier transforms, *Proceedings of the National Academy of Scinces U.S.A.*, **68**, pp. 2236-2240.

Ramakrishna, R.S., Mullick, S.K. and Rathore, R.K.S.(1985): A new iterative algorithm for image restoration, *Computer Vision, Graphics, and Image Processing*, **30**, pp. 47-55.

Rastogi, R.(1988): A study of performance of the EM-algorithm in positran emission tomography model, M.Tech. thesis, Indian Institute of Technology Kanpur, India.

Rathore, R.K.S.(1987): Non Fourier filters, Technical Report, NET programe Indian Institute of Technology Kanpur.

Rathore, R.K.S., Munshi,P., Jarwal, R.K. and Dhariyal, I.D. (1988): Investigation of the bubbly air/water flow using chord segment algorithm, *Nuclear Technology*, **82**, pp. 27-234.

Rockmore, A.J. and Macovaski, A.(1976): A maximum likelihood approach to emission image reconstruction from projections, *IEEE Transactions on Nuclear Science*, **NS-23**, pp. 1428-1432.

$$= \frac{1}{2\pi} \int_0^{2\pi} \iint_{\mathbb{R}^2\mathbb{R}^2} C_{\mathcal{Z},r,\phi}\,(y_1+(u_1-v_1)/A,\ y_2+(u_2-v_2)/A\,).$$

$$K(\underline{u})\,K(\underline{v})\,d\phi\,d\underline{u}\,d\underline{v}\ .$$

Since $K(\underline{x}) \in L^1[0,\infty)$, Fubini's theorem is applicable and thus,

$$C_{\mathcal{Z}_A,r,\bar{\phi}}(\underline{y}) = \iint_{\mathbb{R}^2\,\mathbb{R}^2} C_{\mathcal{Z},r,\bar{\phi}}(\underline{y} + (\underline{u} - \underline{v})/A)\,K(\underline{u})\,K(\underline{v})\,d\underline{u}\,d\underline{v}$$

and

$$D^{4p}_{r,\bar{\phi}}\,C_{\mathcal{Z}_A}(\underline{y}) = \iint_{\mathbb{R}^2\,\mathbb{R}^2} D^{4p}_{r,\bar{\phi}}\,C_{\mathcal{Z}}(\underline{y} + (\underline{u}- \underline{v})/A)\,K(\underline{u})\,K(\underline{v})\,d\underline{u}\,d\underline{v}\ .$$

Hence,

$$|\,D^{4p}_{r,\bar{\phi}}\,C_{\mathcal{Z}_A}(\underline{y})\,| \le \iint_{\mathbb{R}^2\,\mathbb{R}^2} |\,D^{4p}_{r,\bar{\phi}}\,C_{\mathcal{Z}}(\underline{y} + (\underline{u} - \underline{v})/A\,)\,|\cdot$$

$$|\,K(\underline{u})\,|\,|\,K(\underline{v})\,|\,d\underline{u}\,d\underline{v}$$

$$\le \|\,D^{4p}_{r,\bar{\phi}}\,C_{\mathcal{Z}}\,\|_0 \cdot \Big(\int_{\mathbb{R}^2} |\,K(\underline{u})\,|\,d\underline{u}\Big)^2$$

implying that,

$$\|\,D^{4p}_{r,\bar{\phi}}\,C_{\mathcal{Z}_A}\,\|_0 \le M_3^2\,\|\,D^{4p}_{r,\bar{\phi}}\,C_{\mathcal{Z}}\,\|_0 .$$

$$+ M_3^2 A^{4p} \| C_{(\mathcal{Z} - \mathcal{Z}_B)} \|_0 + M_3 L \| C_{\mathcal{Z}_B} \|_{4p}$$

the rhs of the above equation $= (2M_4 + M_3^2) \| C_{\mathcal{Z}_B} \|_{4p}$, so that which on using Lemma 4.2.3 gives

$$\| C_{\mathcal{Z}_A} \|_{4p} = \| C_{\mathcal{Z}_A} \|_0 + \| D^{4p}_{r,\bar{\phi}} C_{\mathcal{Z}_A} \|_0$$

$$= \| C_{(\mathcal{Z} - \mathcal{Z}_B)_A + (\mathcal{Z}_B)_A} \|_0 + \| D^{4p}_{r,\bar{\phi}} C_{\mathcal{Z}_A} \|_0$$

$$\leq 2 \left(\| C_{(\mathcal{Z} - \mathcal{Z}_B)_A} \|_0 + \| C_{(\mathcal{Z}_B)_A} \|_0 \right)$$

$$+ \| D^{4p}_{r,\bar{\phi}} C_{(\mathcal{Z} - \mathcal{Z}_B)_A} \|_0 + \| D^{4p}_{r,\bar{\phi}} C_{(\mathcal{Z}_B)_A} \|_0$$

$$+ M_3^2 A^{4p} \| C_{\mathcal{Z} - \mathcal{Z}_B} \|_0 + L M_3 \| C_{\mathcal{Z}_B} \|_{4p}$$

$$\leq 2 \left(\| C_{(\mathcal{Z} - \mathcal{Z}_B)_A} \|_{4p} + \| C_{(\mathcal{Z}_B)_A} \|_{4p} \right)$$

$$+ M_3^2 A^{4p} \| C_{\mathcal{Z} - \mathcal{Z}_B} \|_0 + L M_3 \| C_{\mathcal{Z}_B} \|_{4p} .$$

Using Lemma 4.2.5 and Lemma 4.2.6

$$\| C_{\mathcal{Z}_A} \|_{4p} \leq 2 M_4 A^{4p} \| C_{\mathcal{Z} - \mathcal{Z}_B} \|_0 + M_3^2 \| C_{\mathcal{Z}_B} \|_{4p}$$

$$+ M_3^2 A^{4p} \| C_{\mathcal{Z} - \mathcal{Z}_B} \|_0 + L M_3 \| C_{\mathcal{Z}_B} \|_{4p}$$

object function (respectively reconstructed function) value at i,j-th pixel, and MP is the total number of pixels used in summation. The first 50 images of sample 1 were used to estimate α_i's. From (5.1.2) we see that the estimation problem reduces to that of finding a solution of the following system of linear equation

$$\underline{e} = \underline{A}\ \underline{\alpha} \qquad \ldots.(5.3.1)$$

where

$\underline{e}_{50x1} = (e_1, \ldots\ldots, e_{50})$, e_k = ESE in k-th image.

$\underline{A}_{50x42} = (C_1' \ldots\ldots C_{50}')$, a matrix consisting of covariance vectors as it's rows and $\underline{\alpha}_{42x1}$ is the vector of co-efficients to be estimated. Next to illustrate the case of unknown covariance kernel, the covariances were estimated from reconstructed images at the same 42 distances. These estimated covariance vectors $\hat{C}_i$'s substituted for C_i's in (5.3.1) give rise to the system of linear equations

$$\underline{e} = \hat{\underline{A}}\ \underline{\beta} \qquad \ldots..(5.3.2)$$

where $\underline{\beta}$ is the 42x1 vector of co-efficients to be estimated.

In order to solve the sysytem (5.3.1) [or (5.3.2)] of linear equations the Residual Projection method was employed. This is because the columns of $\underline{A}$ are as such not independent, and so usual least square method to estimate the parameters is not applicable whereas the Residual Projection method gives a least squares solution. A brief description of the

TABLE 5.4 : SUMMARY OF ERRORS IN RECONSTRUCTION OF RANDOM IMAGES FROM SAMPLE 2

PIC	R_c	ER1	ERS	ERMax	$\tilde{E}$
1	16	1.36925	3.58375	12.76621	3.68718
	32	0.49455	0.39314	6.19933	0.59691
2	16	1.37991	3.78235	16.52750	9.55461
	32	0.49257	0.39152	5.52099	0.57670
3	16	1.31931	3.30063	11.82067	3.40341
	32	0.47929	0.36455	6.39629	0.55997
4	16	1.33757	3.39126	11.37459	3.48169
	32	0.48486	0.36446	5.67514	0.56092
5	16	1.32848	3.41509	10.49149	3.47412
	32	0.48738	0.37286	5.40592	0.56061
6	16	1.36158	3.47953	12.34249	3.55429
	32	0.48446	0.37690	6.15375	0.57260
7	16	1.34214	3.40325	11.06725	3.49621
	32	0.47869	0.36821	5.88351	0.54924
8	16	1.31688	3.33913	11.12923	3.42109
	32	0.46504	0.34267	5.62610	0.51768

TABLE 5.12 : SUMMARY OF NORMALIZED ERRORS IN RECONSTRUCTION OF RANDOM IMAGES FROM SAMPLE 2

PIC	R_c	ER1N	ERSN	$\tilde{E}N$
1	16	0.08940	0.12034	0.24074
	32	0.03229	0.04532	0.03897
2	16	0.08917	0.12239	0.61742
	32	0.03183	0.04477	0.03727
3	16	0.08390	0.11284	0.21644
	32	0.03048	0.04264	0.03561
4	16	0.08687	0.11672	0.22612
	32	0.03149	0.04351	0.03643
5	16	0.08578	0.11629	0.22432
	32	0.03147	0.04369	0.03620
6	16	0.08825	0.11756	0.23037
	32	0.03140	0.04399	0.03711
7	16	0.08731	0.11692	0.22744
	32	0.03114	0.04373	0.03573
8	16	0.08736	0.11819	0.22695
	32	0.03085	0.04305	0.03434

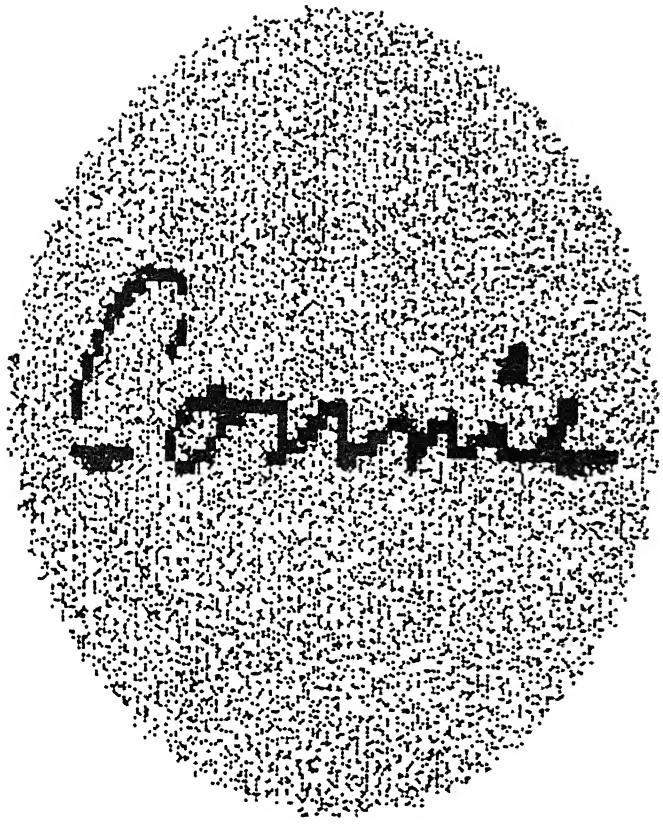

Fig. 5.1 Original simulated random picture of sample 1.

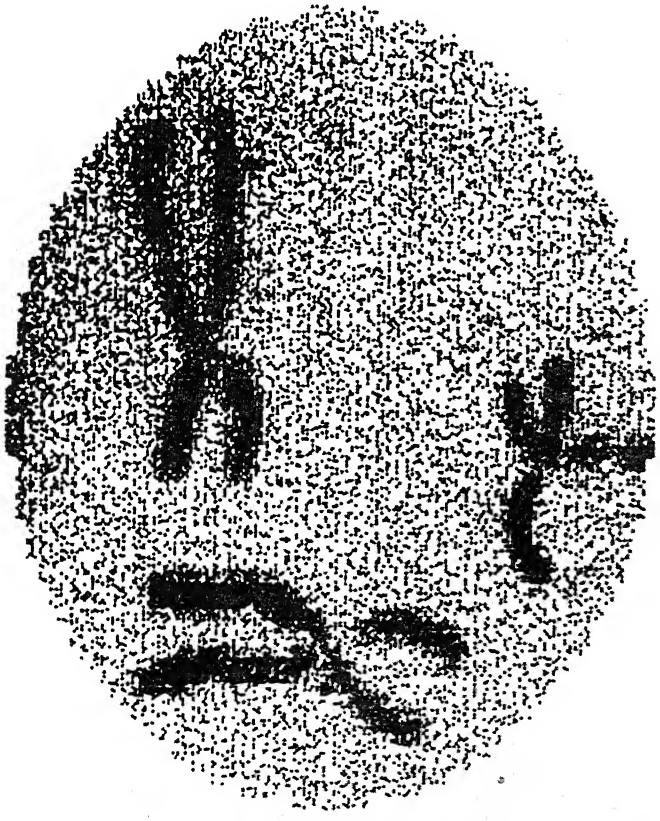

Fig. 5.2 Original simulated random picture of sample 2.

Then the estimate q_n of q_{opt} is given by

$$q_n = \tilde{Q}_n R_n$$

PROPOSITION: $q_n \longrightarrow q_{opt}$ w.p.1 where $q_{opt} = Q^+ R$ and Q^+ is the Moore-Penrose g-inverse of Q.

PROOF: We note that, at least along a subsequence of unitary matrices,

$$U_n \longrightarrow U \quad \text{and} \quad V_n \longrightarrow V, \quad n \longrightarrow \infty \qquad \ldots. \quad (6.3.2)$$

where U and V are unitary. Since

$$\lambda_i^{(n)} \longrightarrow \begin{cases} \lambda_i & \text{w.p.1} \quad i = 1..,r \\ 0 & \text{w.p.1} \quad i = r+1,\ldots,N_y \end{cases}$$

where λ_i's are singular values of Q, we have w.p.1

$$\tilde{Q}_n \longrightarrow Q^+ \qquad \text{w.p.1}$$

where the Moore-Penrose g-inverse Q^+ is

$$Q^+ = V \begin{bmatrix} \frac{1}{\lambda_1} & & & 0 \\ & \ddots & & \vdots \\ & & \frac{1}{\lambda_r} & \\ 0 & \cdots & 0 & 0 \end{bmatrix} U^* ,$$

This implies that along the subsequence,

TABLE 6.5: L_2 ERROR IN CAT LINE INTEGRAL (NOISY) CASE

PIC/FILTER	OPT	RAM	RKS	SHE	CSI
LIN	4.199	4.876	5.399	4.625	4.509
FAC	3.847	5.520	5.999	5.260	5.194
BRA	5.052	5.426	5.995	5.177	5.035
STA	3.735	4.371	4.911	4.095	3.903
COR	13.924	14.290	15.000	14.038	14.038
SAT	4.320	6.104	6.606	5.878	5.853
THO	4.402	4.938	5.506	4.662	4.532
SMO	1.982	3.094	3.764	2.694	2.324
PLA	3.475	4.247	4.844	3.931	3.721
BOY	4.336	4.492	5.039	4.238	4.101
MON	3.221	4.382	4.886	4.119	3.988
WOR	3.639	4.127	4.657	3.867	3.670
CHA	5.896	7.150	7.711	6.910	6.884
FIN	3.327	4.537	5.021	4.315	4.215
CRO	4.083	4.617	5.133	4.367	4.195
JET	4.479	5.023	5.510	4.760	4.666
GEO	3.178	4.230	4.743	3.985	3.887
AVERAGE	4.535	5.378	5.925	5.113	4.983

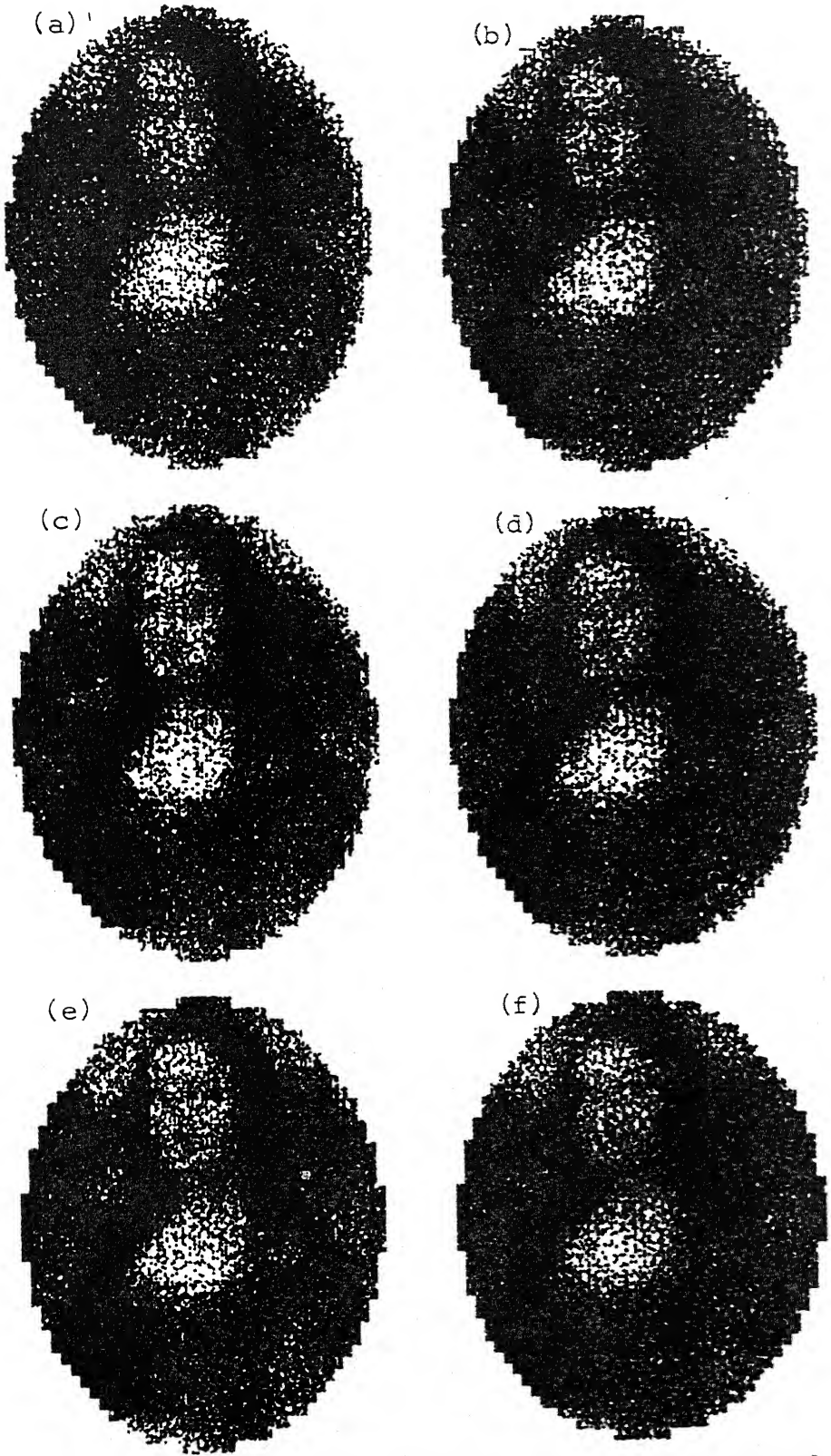

Fig. 6.8 Reconstruction of Monalisa in CAT line integral noise-free case (a) CSI filter, (b) RAM filter, (c) RKS filte (d) Shepp filter, (e) original picture, (f) optimal filter.

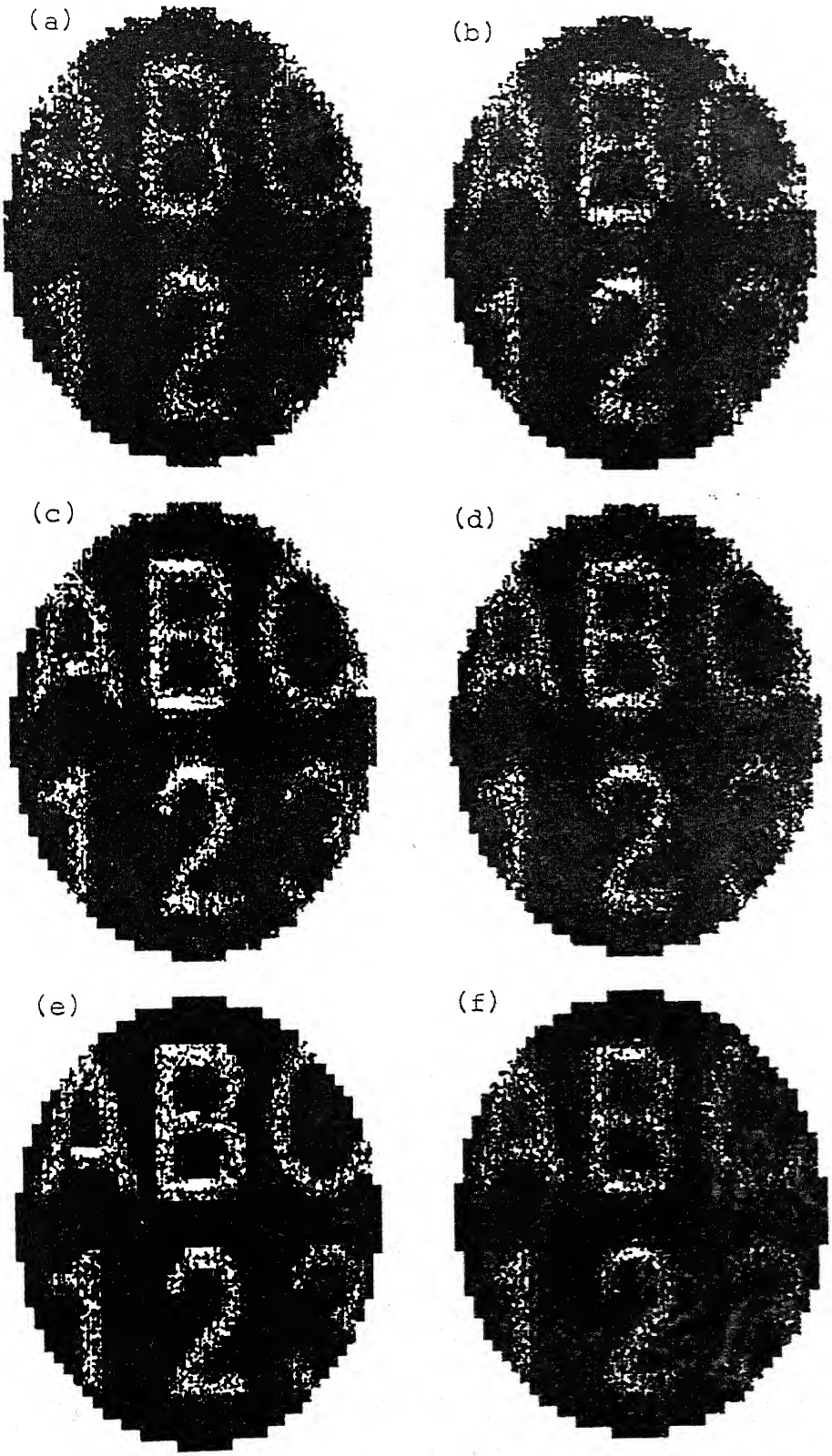

Fig. 6.18 Reconstruction of Characters in CAT strip integral noise-free case (a) CSI filter, (b) RAM filter, (c) RKS filter, (d) Shepp filter, (e) original picture, (f) optimal filter.

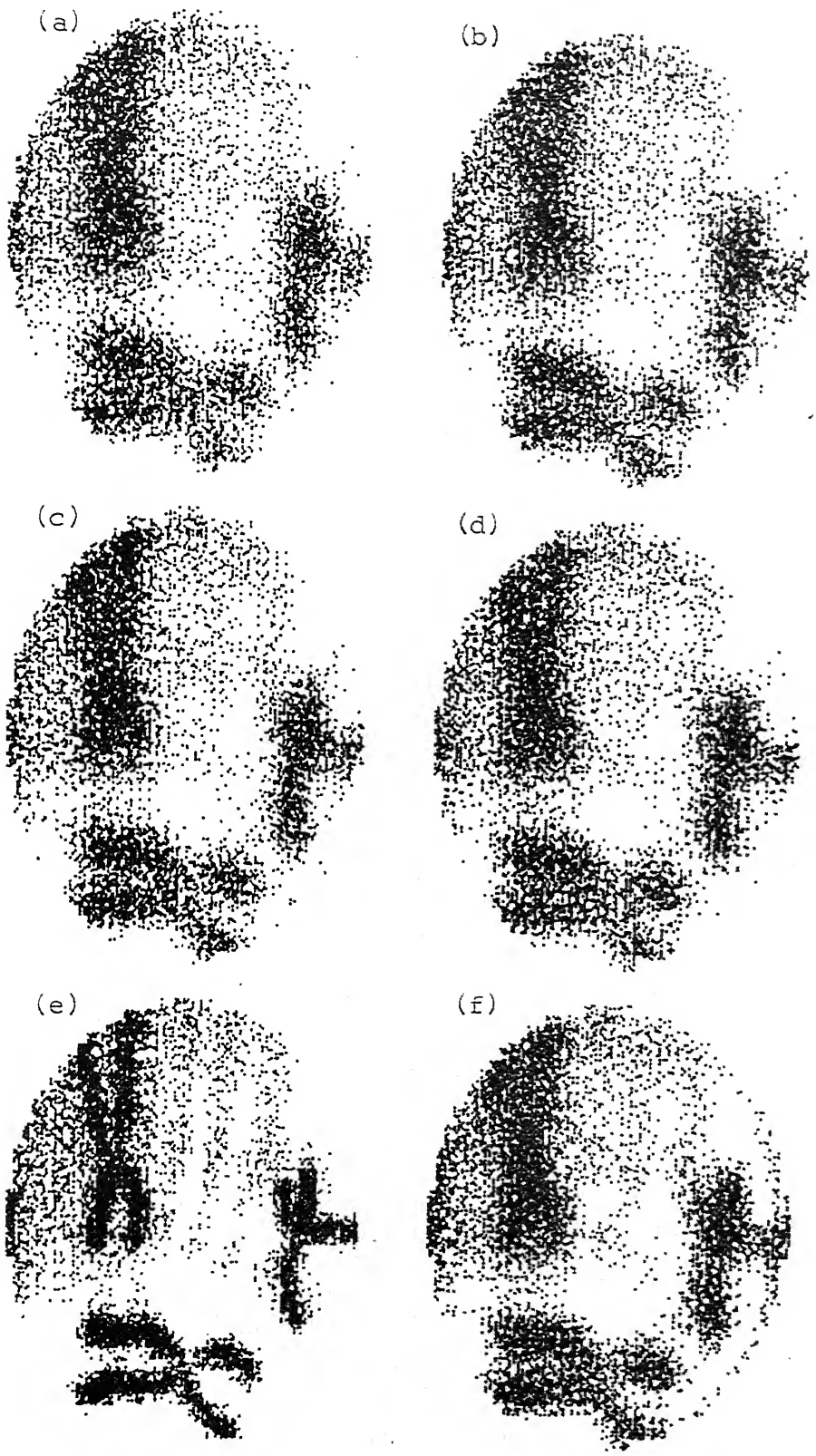

Fig. 6.28 Reconstruction of Chromosomes in PET line integral noise-free case (a) CSI filter, (b) RAM filter, (c) RKS filter, (d) Shepp filter, (e) original picture, (f) optimal filter.

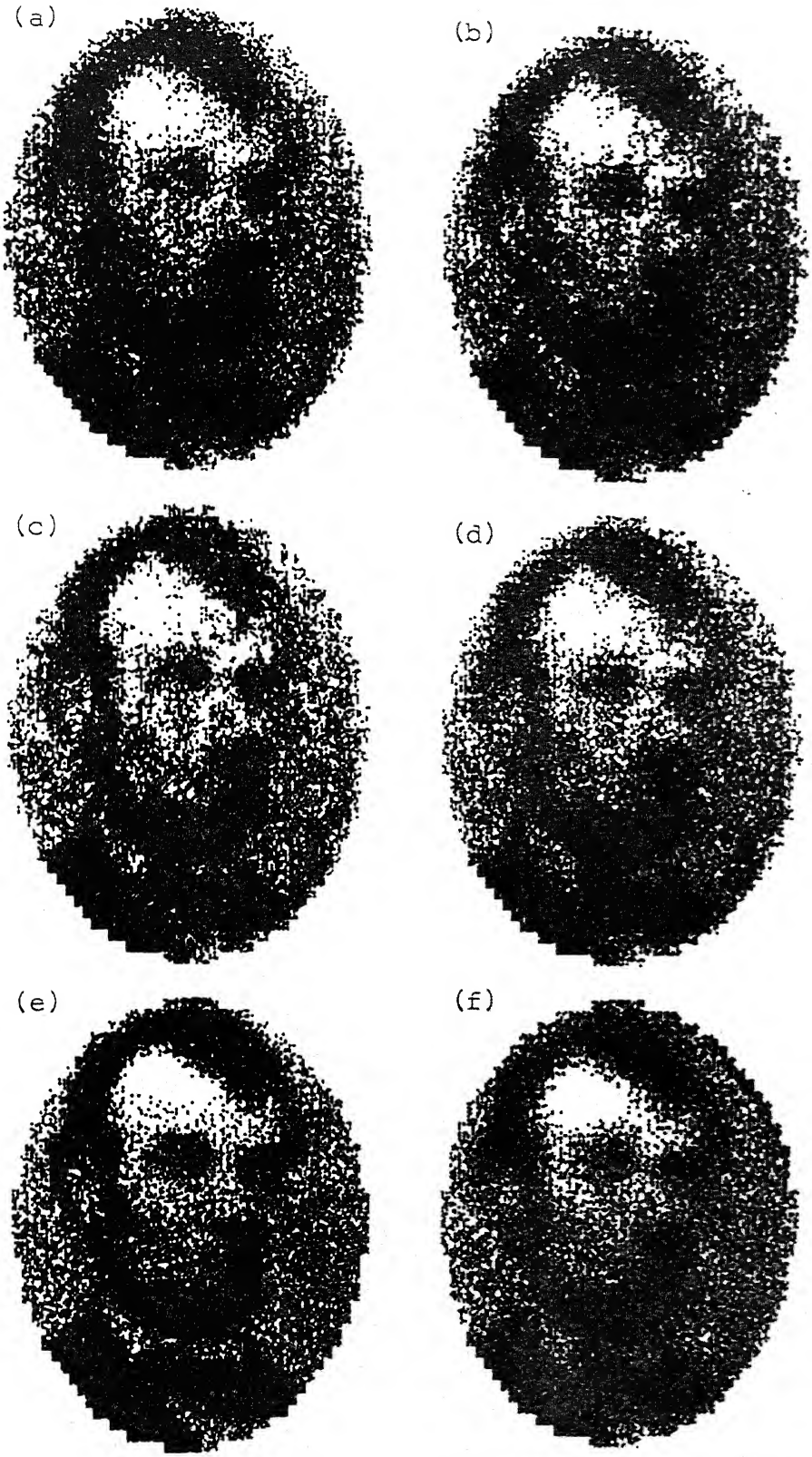

Fig. 6.38 Reconstruction of Lincoln in CAT line integral noisy case (a) CSI filter, (b) RAM filter, (c) RKS filter, (d) Shepp filter, (e) original picture, (f) optimal filter.

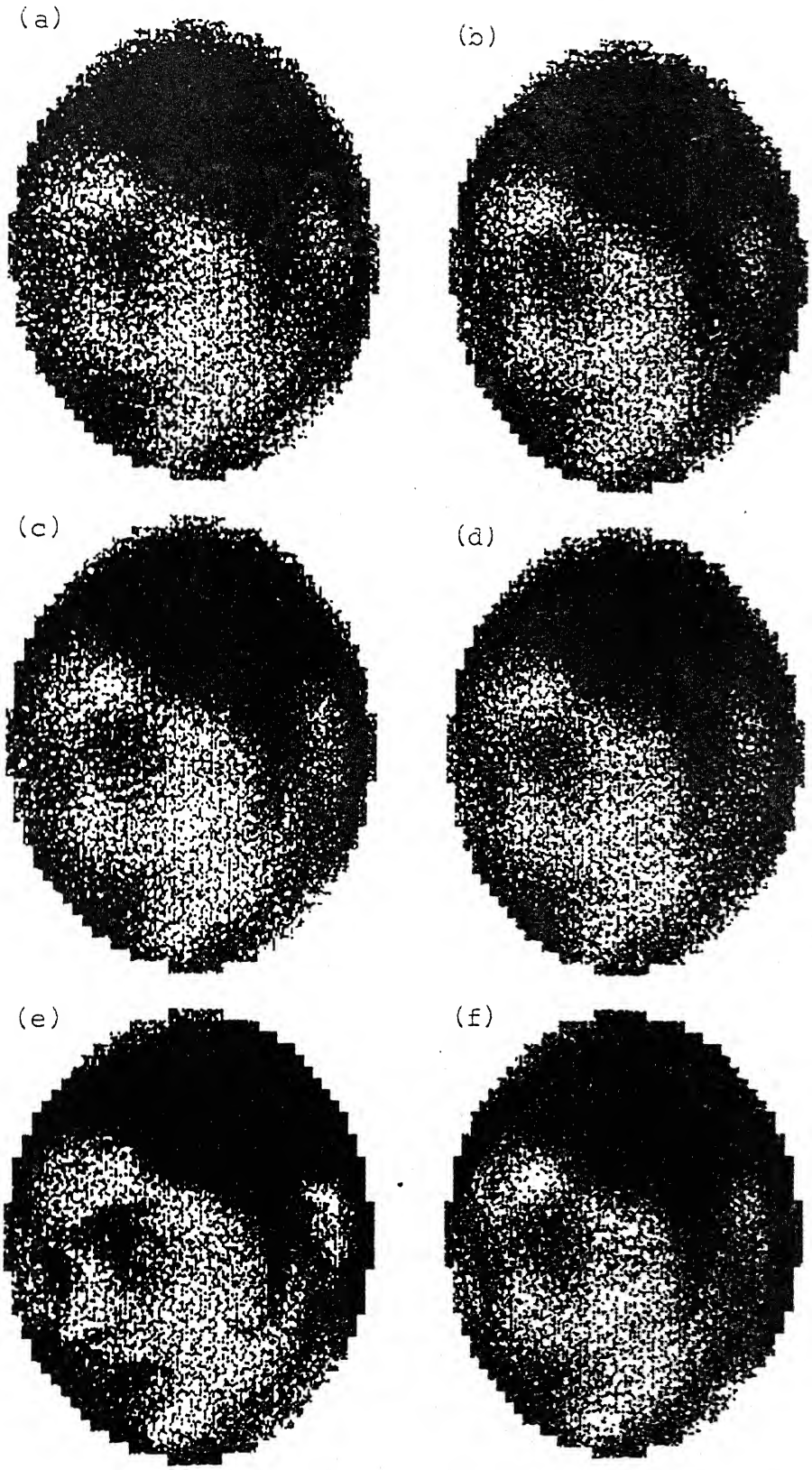

Fig. 6.48 Reconstruction of Face of a girl in CAT strip integral noisy case (a) CSI filter, (b) RAM filter, (c) RKS filter, (d) Shepp filter, (e) original picture, (f) optimal filter.

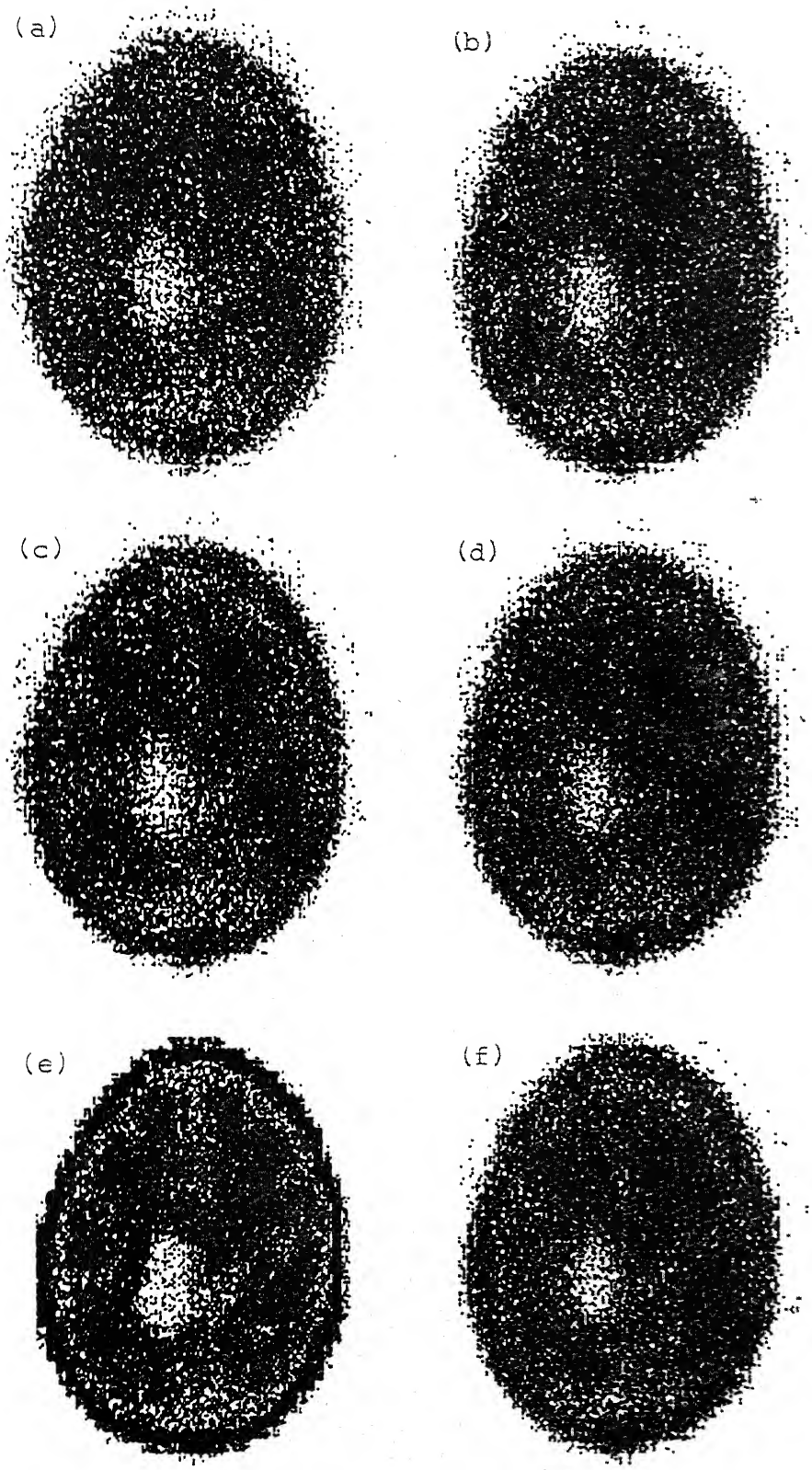

Fig. 6.58 Reconstruction of Brain in PET line integral noisy case (a) CSI filter, (b) RAM filter, (c) RKS filter, (d) Shepp filter, (e) original picture, (f) optimal filter.

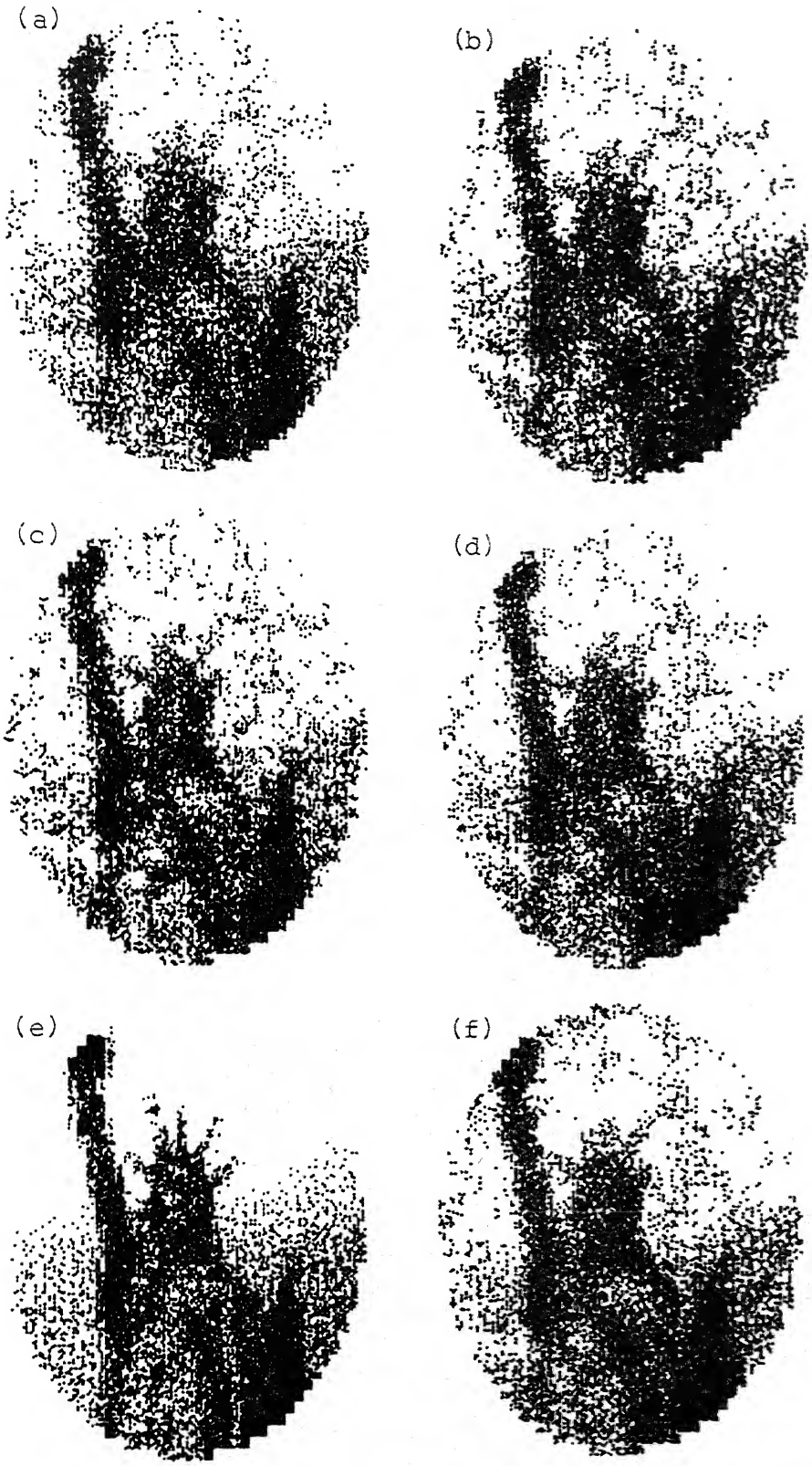

Fig. 6.68 Reconstruction of Statue of Liberty in PET strip integral noisy case (a) CSI filter, (b) RAM filter, (c) RKS filter, (d) Shepp filter, (e) original picture, (f) optimal filter.